ES&T

Pesticides of the future

464A

ONE INSTRUMENT FOR ALL TYPES OF WATER POLLUTION CONTROL

TCM 480

For Total Organic Carbon (T.O.C.) determination in drinkable, industrial and sea water

☐ Only 5 min. for direct measurement of T.O.C.
☐ High temperature catalytic oxidation and G.C. finish
☐ Wide range 0.1 — 1000 ppm
☐ Fully automatic
☐ Suitable for lab and/or on-line monitoring
☐ Low cost for analysis

CARLO ERBA STRUMENTAZIONE

FARMITALIA CARLO ERBA SUBSIDIARY ⚡ montedison GROUP

CIRCLE 5 ON READER SERVICE CARD

ES&T

CONTENTS

Volume 17, Number 10, October 1983

* To whom correspondence should be addressed.

This issue contains no papers for which there is supplementary material in microform.

DEPARTMENTS

GUEST EDITORIAL

Groundwater's future shines bright

I have the feeling that two apparently unrelated trends are going to be helpful to the future of groundwater protection. First, the frequent and in many cases careless reports of groundwater contamination problems have focused public concern on the quality of the nation's groundwater.

Second, the backsliding events of the past two years at EPA may have produced a countervailing result, i.e., increased national commitment to avoid environmental slippage. This new resolve, coupled with the new administrative leadership of the agency, may be a fortuitous combination for preventing groundwater degradation.

You may have heard or read in a variety of sources that only a fraction of 1% of the nation's groundwater supply is polluted. It's absolutely true. If all our actions that pollute groundwater were concentrated into 200 000 sources oozing into the ground for the past 40 years at a rate of 4 in. a day, producing contaminant plumes 1000 ft wide, 100 ft thick, and a mile long in aquifers with 25% porosity, we would have 200 trillion gal of polluted groundwater. Recent conservative U.S. Geological Survey estimates place groundwater availability in the U.S. in excess of 50 quadrillion gal. Thus, comparing these two numbers yields an estimate that $4/10$ of 1% of our groundwater may be polluted. It is clearly the correct order of magnitude.

But we have polluted the groundwater unevenly and concentrated our misdeeds where our dependence on water is greatest. The industrial sections of New York, New Jersey, and New England have indeed polluted more than 1% of their supply. Their problems are serious, but a considerable amount of unpolluted groundwater is still available, and cleanup technologies are advancing. Time is on our side as the glacially slow movement of groundwater allows us the luxury of well-reasoned remedies without the need for crisis management. In the next 10 years our new public morality against pollution, along with the aid of laws such as RCRA, CWA, SMCRA, SWDA, and TSCA, will eliminate new sources of pollution leaving us only the task of cleaning up the old.

The Comprehensive Environmental Response Compensation and Liability Act (CERCLA) should enable us to do that. It has thus far been hampered by the inappropriate nickname hung on it—Superfund.

CERCLA did establish a fund of 1.6 billion dollars to be used for cleanup as a last resort, but knee-jerk environmentalists and political opportunists were wrong in jumping all over Superfund for being grossly inadequate. The fund was only intended as ready cash to begin work on sites where the guilty parties could not be brought to their knees for past crimes against the populace. The emphasis and intention of the legislation were to persuade (through treble damages) liable parties to act independently of the government in a proper and timely manner.

It's time to stop calling it Superfund; this name implies a mountain of money with which to bury a national problem. It is time to see it as a politically innovative and effective tool to initiate cleanup activities by responsible parties. The new EPA administrator is determined to make it work, and I believe he will.

William Ruckelshaus, who has returned to head EPA after a 10-year hiatus, offers America an opportunity to move out of the garbage pits of our past into a clean, safe future. It will take us 10 to 20 years, and he will be long gone before the task is completed. But he will lead us in a direction that will not be significantly altered by any future, monstrously misguided bureaucratic repetition of our plight of the past two years. The people simply will not stand for it, and the politicians will never so badly misjudge the mood of the public again.

Jay H. Lehr

Jay H. Lehr *is executive director of the National Water Well Association, a research- and education-oriented organization dedicated to the protection of groundwater resources. He is a professor of hydrogeology at The Ohio State University and editor of the journals* Ground Water, Water Well Journal, *and* Ground Water Monitoring Review.

ES&T
CURRENTS

INTERNATIONAL

Turkey has passed its first environmental law. This law provides penalties for industrial and other establishments that cause air or marine pollution. First offenders could be fined $750 to $1500, and if they continue to pollute, they will be closed down by Turkey's Office of Environmental Protection (OEP), which is attached to the Prime Ministry. The OEP would allow the plant to resume activities only after necessary antipollution measures were taken. Other provisions will require special filters for motor vehicles, preservation of agricultural land, and designation of industrial areas.

A six-week experiment to study the flow of long-range transport of air pollution, conducted jointly by the U.S. and Canada, began in mid-September. Canadian scientists plan to release about 200 kg of an inert nontoxic tracer, perfluoromonomethyl-cyclohexane from the Sudbury, Ontario, area at one-week intervals. U.S. scientists will make three similar releases from Dayton, Ohio. Using seven aircraft and a network of 85 sampling stations on the ground, the movement of the tracer will be tracked across eastern North America for 1000 km. It is hoped that the project will help to improve the atmospheric models that are used in designing emission control strategies in both the U.S. and Canada.

WASHINGTON

The Reagan administration has apparently reversed its policy on hazardous waste exports, under the lead of EPA. Sources say that the Office of Management and Budget has agreed with EPA to support an amendment to the Resource Conservation and Recovery Act (RCRA) that would require written consent from an importing country before hazardous wastes listed under RCRA could be sent

there. The amendment, introduced by Sen. George Mitchell (D-Maine), authorizes EPA to prevent hazardous wastes from being shipped if the country has not consented to receiving them.

EPA officials announced that the amount of hazardous waste being generated in the U.S. is almost four times higher than previously estimated. From information supplied

Stafford: RCRA should be amended

by waste producers and handlers, they have determined that 150 million metric tons of hazardous waste are generated annually in the U.S. compared to a previous estimate of 40 million tons. Furthermore, an additional 300 million tons is being "managed" by the industry producing it. Most of this waste is handled by two methods—underground injection and surface impoundments. Sen. Robert T. Stafford (R-Vt.) said that the EPA survey "underscores" the need to amend the Resource Conservation and Recovery Act.

The Reagan administration has overturned the ban on urea formaldehyde foam insulation. Last year the Consumer Product Safety Commission (CPSC) decided to ban the product, saying that it "poses an unreasonable risk of injury to consumers." This spring the U.S. Court of Appeals for the Fifth Circuit set the ban aside. It said that the CPSC had based its decision on inadequate evidence but also warned that consumer com-

plaints "do identify a real problem." The CPSC asked the Justice Department to appeal the decision to the Supreme Court, but in August the Justice Department announced that it had decided against appeal. This decision prompted an angry response from Nancy H. Steorts, chairman of the CPSC, who said: "This is a problem product . . . which can be very harmful to consumers."

The Veterans Administration reports that no adverse health effects clearly related to Agent Orange have been found in medical examinations and laboratory tests of 85 000 Vietnam veterans who believe they were exposed to the defoliant. A wide variety of health problems were observed, but none could be definitely related to Agent Orange or dioxin exposure. The study revealed a slight increase in one form of cancer known as lymphomas, but it is too early to tell whether the increase in lymphomas is significant. The incidence of soft tissue sarcomas was actually lower than might be expected in a comparable population. However, Alvin L. Young, an Agent Orange expert at the Veterans Administration, said that the study was not a true epidemiologic study because the veterans were not compared to a carefully matched control group that had not been exposed to the herbicide.

PCBs in electrical transformers and capacitors were called a "medical time bomb" by Arnold Schecter, professor of preventive medicine at the Upstate Medical Center of the State University of New York at Binghamton, at the recent meeting of the American Chemical Society. He said that PCBs were a far greater hazard than Agent Orange or the dioxin at Times Beach, Mo. He showed the initial findings of medical tests performed on 10 people who entered a building in Binghamton after a fire had contaminated it with toxic soot from burning PCBs. The tests showed that

three of these individuals have liver damage whose only probable cause was the toxic soot. Other persons exposed to the toxic soot had skin rashes, skin cancer, and other problems, but not all of these could be definitely attributed to exposure to the soot.

STATES

The Atlantic Richfield Company plans to build a major oil exploration staging base on Alaska's St. Matthew Island, 250 miles from the Alaskan mainland. At present the island provides a home for 1.5–5 million seabirds, and 22 species of marine mammals feed along its shores. It has been a wildlife refuge for nearly 75 years and a wilderness area since 1970. The Department of the Interior has agreed to withdraw refuge and wilderness protection for 4000 acres of the island. The oil company intends to build living quarters for 250 people and two mile-long runways on the island as well as constructing a deep-sea harbor. The National Audubon Society and a coalition of conservationists, fishermen, and Alaskan natives have filed a suit against the action taken by the Interior Department.

Extensive monitoring took place in the Adirondacks (N.Y.) over a two-week period in August. Analyses for pH, conductivity, and calcium were carried out for 155 remote lakes and ponds, 91 of which had not been tested in the past eight years. About 40 of the lakes are "control" waters that are checked on an annual basis. Henry G. Williams, New York State Commissioner of Environmental Conservation, said that 1047 Adirondack lakes and ponds have been sampled since 1975 and that 19% of these waters "are critically acidified with a pH below 5." Most of these either lack fish populations or have greatly reduced numbers and diversity of fish.

A $3.4-million study of contamination in the New Bedford, Mass., area has been initiated by EPA under the Superfund program. The New Bedford area "is like no other hazardous waste site in our country, and extensive complex studies are needed before final remedies can be developed," said Michael R. Deland, regional EPA administra-

tor for Region I. An accelerated study will be undertaken of PCB hot spots in the Acushnet River Estuary, monitoring of PCBs and other pollutants will be carried out near Sullivans Ledge (a former quarry used as a dump site for unknown materials), and the quarry and the New Bedford landfill will be characterized hydrogeologically. Also, the sediment water and organisms in New Bedford Harbor and Buzzards Bay will be studied.

The state of Florida has passed a strict law to protect water quality, the Water Quality Assurance Act of 1983. A large part of the expenses incurred by the act will be financed by a trust fund. When the fund falls below $3 million, an automatic 2¢-per-barrel tax on pollutants will be levied to build up the fund to $12 million. The water act has several provisions that are unusual in state law. It prohibits hazardous waste landfills, requires construction of a multipurpose hazardous waste facility, and directs the Florida Department of Environmental Regulation to set up a monitoring network for groundwater quality.

SCIENCE

"There have been no confirmed human deaths from dioxin [2,3,7,8-tetrachlorodibenzo-*para*-dioxin]. Nor has it been shown to cause cancer, birth defects, or spontaneous abortions," says Fred Tschirley, a toxicologist at Michigan State University. He adds that the characterization of TCDD as "the most toxic substance ever made" is "correct for guinea pigs, not humans." He chided the popular press for not having made distinctions between effects on guinea pigs (or other small mammals) and on humans. Tschirley maintains that TCDD is produced by wood burning as well as by herbicide making, has been around "for centuries," and is detected now because of modern, sophisticated analytical instruments.

A new toxicology building has been opened by Battelle—New England at its oceanfront complex at Duxbury, Mass. This will enable Battelle to expand activities in aquatic toxicology and marine geochemistry to meet growing industrial and government needs. Analytical and

environmental chemists will use the facility to isolate, identify, and quantify potentially toxic and hazardous chemicals in marine, estuarine, and freshwater environments. Researchers will be able to expose aquatic organisms to various pollutants under natural conditions and then analyze the effects. A special feature is an ultraclean laboratory for analyzing trace metals.

Frost resistance may be improved

For the first time in a controlled experiment outside the laboratory, genetically engineered bacteria will be released to the environment. As soon as potato plants sprout above the ground, they will be sprayed with genetically altered bacteria. The experiment will take place at Tulelake Field Station in California. The leader in this research, Steven E. Lindow of the University of California at Berkeley, found that frost nuclei are produced primarily by *Pseudomonas syringae*, an otherwise harmless bacterium. When the gene that is the key to frost nuclei is removed from this bacterium, it prevents frost from forming. Researchers hope that spraying the potato plants with these altered bacteria will enable them to resist frost damage down to 21 °F.

What hazardous components might there be in geothermal wastes? EPA (Cincinnati, Ohio) engaged Acurex Corporation to find out. Samples were collected at The Geysers and Imperial Valley in California and in northwestern Nevada. About 20 were analyzed for anions, cations, moisture content, priority pollutants, and trace metals in leachate. Samples from The Geysers and Nevada were not classified as hazardous, according to RCRA regulations of May 19,

1980 (*Federal Register*). However, some samples from Imperial Valley were hazardous with respect to pH, "extract procedure" toxicity, radio-activity, and bioaccumulation—perhaps associated with the high salinity of geothermal fluids from that part of California.

TECHNOLOGY

Computer modeling can help to protect groundwater, says Donald Reddell of the Texas Agricultural Experiment Station and Texas A&M University. One important model simulates the movement of pollutants underground and is known as the saturated–unsaturated dispersion simulator (SUDS). SUDS can include the movement of air as well as water in analyzing the infiltration process. It can also describe the movement of a pollutant in groundwater and determine potential impacts on an aquifer by different types of pollutants. Among possible uses for SUDS are predictions of effects of saltwater intrusion, underground injection, and infiltration of surface pollutants.

One way to recover valuable unsaturated hydrocarbons from biomass could be through ablative (very rapid) oxygen-deficient pyrolysis, according to the Solar Energy Research Institute (SERI, Golden, Colo.). Normal slow pyrolysis produces about equal amounts of tarry liquids and char. Rapid pyrolysis seems to make almost entirely gaseous products, with "significant" amounts of ethylene, propylene,

and other unsaturated hydrocarbons, SERI says. The mechanism seems to be a heat transfer across a very thin film, from a metal surface at about 1000 °C. Biomass depolymerizes and vaporizes under a very high heat flux. SERI estimates that this method could make 35 gal of high-octane fuel/ton of biomass.

A process to remove some acid-rain-forming substances from smoke and combine them with flue gas in effect moves the acid rain reaction from the atmosphere to a controlled area. So say Richard Martinez and John Herron of the National Bureau of Standards, who patented the process. They combine the smoke and flue gas in a chamber in a way that they believe is similar to that in which acid rain is formed by SO_2 and NO_x in air. The inventors believe that the acids so produced could be safely and easily removed and possibly converted into fertilizers.

INDUSTRY

Federal acid rain legislation should be passed, and it should be based on a nationwide emissions tax to finance controls, says the American Public Power Association (APPA, Washington, D.C.). This legislation should apply to *all* fossil-fueled sources, according to APPA. Among points APPA advocates are applying funds to capital costs of control measures chosen, taxing actual, rather than allowable, emissions, and monitoring adequately. No requirements for new facility

offsets should be included in the emission reduction program, and utilities should have discretion to place their contributions to the emissions tax as a line item on a ratepayer's bill, APPA says.

An alternative funding plan for completing the Clinch River Breeder Reactor (CRBR) was forwarded to Congress by Energy Secretary Don Hodel. The Reagan administration is said to endorse the plan fully. Investment banking firms would arrange for $675 million to be raised through a bond issue. This sum plus interest would be paid from revenues from electricity generated by the CRBR at market prices for new generating capacity. An additional $150 million would be raised from private investors.

"There is 'unmistakable evidence' that the Toxic Substances Control Act** [TSCA] is working and that the purposes of the law are being met." Jerry Smith, director of toxicology for Rohm & Haas Company made this statement to a Senate subcommittee on behalf of the Chemical Manufacturers Association (Washington, D.C.). Smith cited six years of experience with TSCA. Still, he called for certain changes, such as exemptions from full premanufacture review for low-risk chemicals, more flexible testing guidelines, effective priority setting for testing, and greater selectivity in collecting information. Smith noted that EPA has taken steps to protect the public when health or environmental questions arose and that "extensive testing of existing chemicals is under way."

Three projects concerning polychlorinated biphenyls (PCBs) are being conducted under the aegis of the Electric Power Research Institute (EPRI, Palo Alto, Calif.). The first is to develop alternative scenarios for PCB removal and to outline research directions in this regard. The second is to develop methods for estimating PCB exposure levels in the general public. The third is a "comprehensive" assessment of potential health risks of occupational exposure to PCBs. EPRI also seeks to allay public fears of health consequences of transformer fires and capacitor failures. EPRI will hold a PCB seminar at Atlanta, Ga., Dec. 6–8. For information, contact Narain G. Hingorani, EPRI, P.O. Box 10412, Palo Alto, Calif. 94303.

Ablative pyrolysis of biomass

Source: SERI

ห้องสมุดกรมวิทยาศาสตร์บริการ
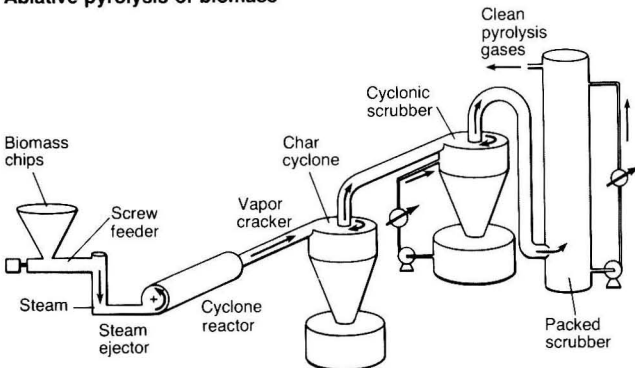
Can they ever be completely safe and environmentally harmless? Will they be broad spectrum or species specific? At a recent symposium, agricultural scientists looked at

Pesticides of the future
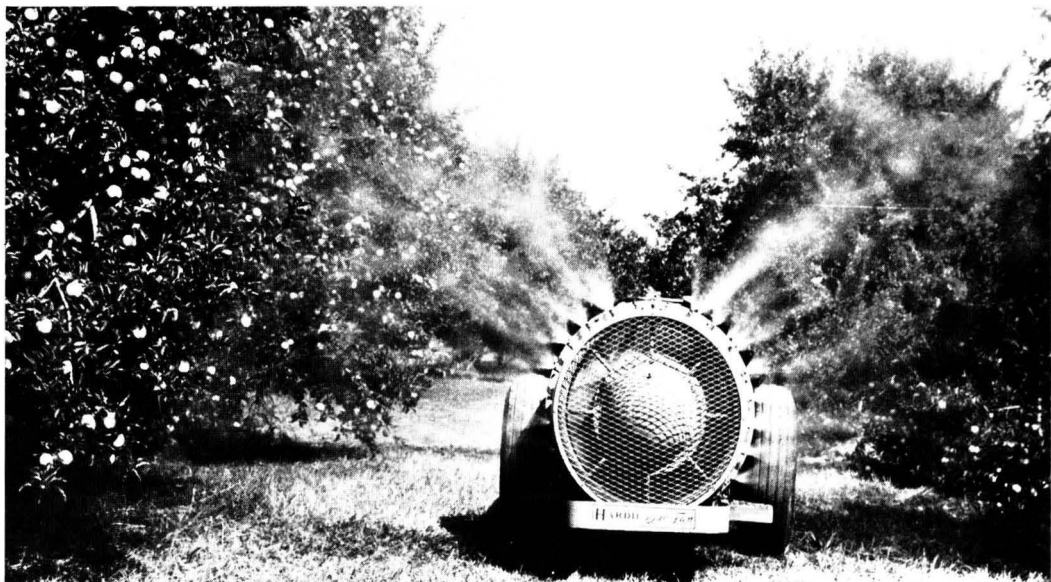
Agricultural chemicals, including pesticides, are needed to enhance crop production and to combat factors such as insects, weeds, and fungi that work against maximum crop production. Insects alone reduce potential crop yields in the U.S. by 13% and livestock productivity by 6%, and they destroy 5–10% of harvested commodities. Agricultural scientists and economists estimate that the combined cost of insect control and losses caused by insects is in excess of $23 billion/y.

The basic debate concerning the manufacture of agricultural chemicals of the future, especially pesticides, centers on whether they should be broad based or species specific.

Some say that these chemicals should be broad spectrum and that they should be applied to the environment carefully and in the smallest

possible amounts. Even given the difficulties of developing and registering candidate pesticides, such broad-based pesticides could command markets large enough to make them affordable, while at the same time, thanks to newer technology, they would cause the least harm to beneficial insects, other species, and the environment.

Others say that these chemicals should be as specific to one species as possible; this way, harm to other species and to the environment would be virtually impossible. A potential problem is that the high costs of developing and registering such substances, and the small markets and sales that would follow, could make it impossible to recover the expenses involved.

Until recently, the trend has been to develop broad-spectrum pesticides;

lately, however, increasing attention has been paid to their health and environmental effects. The future may bring further development of more species-specific and less environmentally harmful materials, if technical and economic barriers can be surmounted.

J. B. Kendrick, Jr., vice-president for agriculture and university services of the University of California State-wide Administration, acknowledged that emphasis on production enhancement "has sometimes led to adverse impacts by agricultural chemicals on health, safety, and the environment. Even under the best regulatory systems in the U.S., human illnesses related to the use of agricultural chemicals are still too commonplace . . . and environmental problems [such as soil and groundwater contamina-

tion, and bioaccumulation] caused by these chemicals continue to occur." But although such chemicals will never be environmentally neutral or 100% safe for humans, efforts are being made to minimize harm attributable to these substances.

One path to this objective is scientific research in the laboratory and field. But Kendrick suggested that basing regulations concerning agricultural chemicals on a goal of totally safe materials "may well prove to be counterproductive."

From the administrative standpoint, well-thought-out regulations could make a material contribution toward reducing harmful effects. Possible technical strategies include developing narrower-spectrum insecticides and devising chemicals that affect pests by means other than immediate, direct lethal toxicity, such as sex attractants and growth and reproduction disruptors. Parallel approaches may be considered for herbicides and fungicides. These possibilities were discussed at the Beltsville Symposium VIII on Agricultural Chemicals of the Future, sponsored by the U.S. Department of Agriculture's Agricultural Research Service (ARS), and held at Beltsville, Md., in May.

Efficacy and safety

John Todhunter, formerly EPA's assistant administrator for pesticides and toxic substances, and now an independent consultant in Silver Spring, Md., defined the efficacy of a pesticide as:

$$EI = \frac{D_A}{D_T}$$

where EI is the efficacy index; D_A is the dose or amount of pesticide required to produce an adverse effect on humans, mammals, or nontarget species; and D_T is the dose per acre, or amount required to provide effective pesticide treatment.

Todhunter observed that pesticide efficacy is often favored by factors such as high selectivity for a target pest, which reduces damage to beneficials; reasonable half-life of activity, which provides for postapplication residual activity; and ease and timing of application, which increases the probability of correct (least harmful) use.

The safety of an insecticide is also generally enhanced by high selectivity, as well as a low tendency to migrate from the site of its application and biodegradability, Todhunter said. He added that the same basic considerations apply to herbicides.

For the future, Todhunter sees in-

creasing use of integrated pest management (IPM), which makes use of biological as well as toxic chemical materials to control insects. Examples of IPM are use of *Bacillus thuringiensis* against the gypsy moth and of "milky spore disease" against the Japanese beetle. As for weed control, Todhunter looks to pathogens that could affect unwanted plants, provided safety measures, such as screening for mutants that could produce undesired effects, are carried out. Another possibility for the future is use of allelopathic agents against insects, fungi, and weeds—if the drawback of absence of selectivity can be overcome. These agents are natural chemicals that allow a plant making them to weaken, repel, or kill certain neighboring plants or attacking pests.

Narrow vs. broad spectrum

"For decades, broad-spectrum materials have dominated the pesticide [insecticide] market," Walter Zeck of Mobay Chemical Corporation (Vero Beach, Fla.) observed. But "since the 1960s and 1970s, increasingly more sophisticated chemicals show up with the claim to mitigate specific problems with a high degree of specificity and little environmental impact." While chemicals will certainly continue to play a major role in insect pest control, Zeck forecasts that the question will be "which chemicals and how?"

High on the "want list," especially for IPM practitioners, are insecticides that are truly selective, that act on a single pest, says Zeck (6). He quotes Metcalf who observed that the chemist and toxicologist "are capable of tailoring individual molecules, incorporating almost any combination of desirable selective properties" (7). Zeck comments, "A great challenge. Why is industry so coy about it?"

One major reason is economic. For instance, the chances of successfully screening a "conventional type" of insecticide are about 1 in 12 000 (8, 9). This means that for every 12 000 compounds synthesized and screened, one will get to market. One expert estimated that R & D costs for each successful chemical are about $25 million. For a highly selective compound, the chances of successful screening could be as low as 1 in 40 000–80 000, Zeck explains. (During the 1950s the success ratio was generally one in 1800 candidate chemicals.) Moreover, the screen itself would have to be changed from straight target-pest orientation to consideration of harmlessness to various other species.

At present, screening for harmless-

Insecticide spectra and selectivity

Zeck characterizes insecticide *spectra* as follows (1):

• monotoxic substances, to which only one species responds,

• oligotoxic substances, which act on a limited, often related number of species, such as a family or order of insects, and

• polytoxic substances, which exhibit a broad spectrum over many types of insects, including beneficials, since they act on a vital principle common to many insects (stomach poisoning, nervous system disabling, and others).

On the other hand, "*selectivity* is the measure of the capacity of a treatment to spare natural enemies while destroying pests" (2). Two modes of selectivity have been defined (3):

• ecological selectivity, by which a larger portion of the applied toxicant reaches the target, and little, if any, the predators or beneficials, and

• physiological selectivity, which is based on the intrinsic property of the chemical to be more toxic to the target species than to nonharmful organisms.

Zeck lists ways by which ecological selectivity might be achieved (4, 5):

• timing and application (when few beneficials or bees are present and insect pests are in their most vulnerable stages),

• method of application (in spot treatment, for example, rather than broadcast),

• lower application rates (to reduce harmful populations and allow beneficials to do the rest),

• use of systemic insecticides, especially in soil,

• microencapsulation, baiting, or use of feeding or sex attractants, and

• change in formulation, e.g., granules rather than spray.

Zeck points out that ecological selectivity may be achieved with a chemical which, by itself, is actually a broad-spectrum material. The aim is to avoid harm to nonharmful and, especially, beneficial organisms. In contrast, spectrum refers to a certain number of insects intrinsically sensitive to a particular material. Thus, the physiological, as compared with the ecological selectivity of the chemical is, to a large extent, identical to the spectrum of insecticidal activity.

A pest management aim for future agrochemicals. The idea is to control pests such as these . . .
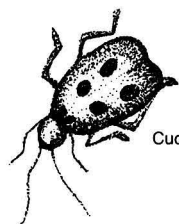
Cucumber beetle

Mexican bean beetle
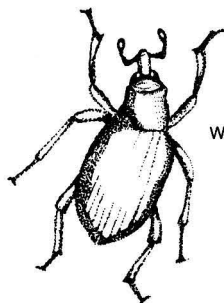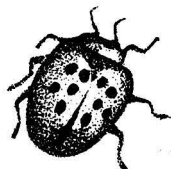
Weevil

. . . while preserving beneficials such as these

Honey bee
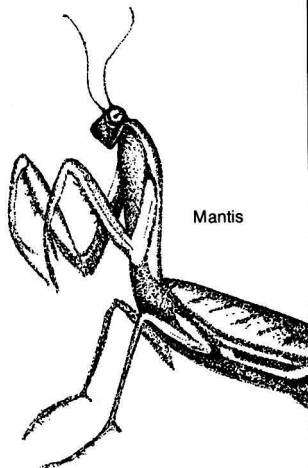
Mantis

Natural pyrethroid[a]
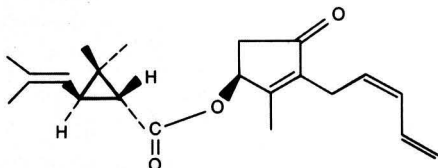
Pyrethrin I

[a] Extracted from certain species of genus *Chrysanthemum*

. . . and two synthetic pyrethroids
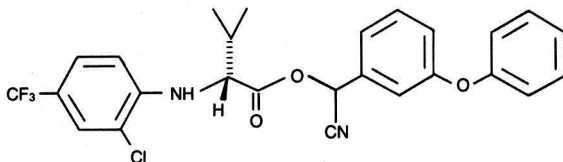
Fluvalinate
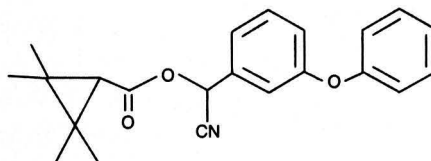
Fenpropathrin

Source: Symposium papers by John Todhunter and Julius Menn

ness and selectivity is done only after candidate chemicals pass initial screening tests for effectiveness against target pests, Zeck points out. To try to incorporate all screening objectives in the early phases is "absolutely unrealistic" and could raise screening costs by perhaps a factor of 10. Moreover, the market for the chemical could become so small that development costs could never be recovered. Zeck described several examples of market problems (*4, 10*). Other problems of species-specific insecticides might involve food chain disruption through the total removal of a single species (*5*).

Also, if several species need to be controlled, a "cocktail" of chemicals could be required. Zeck warns that this could mean loading the environment with solvents, surfactants, and other materials, possible adverse interactions between the chemicals, and, perhaps, additional effects. He favors broad-spectrum pesticides applied to the minimum extent possible and with the least environmental impact. He also urges that greater emphasis be placed on biodegradability and systemic materials and that screening take into account delayed effects of toxicants and changes in insect behavior.

Newer insecticides

Two principal factors stimulated the search for alternative means of pest management, both chemical and otherwise. One was a growing awareness of problems, such as human health effects and food chain magnification associated with some chemicals. "The other was the 'relentless' development of insect resistance to certain classes of insecticidal chemicals," says Julius Menn of Zoecon Corporation (Palo Alto, Calif.).

Among the newer materials in the pesticide arsenal are insecticides based on recent discoveries in natural product chemistry and in insect endocrinology. Materials in the former category may themselves be synthetic, but they are closely related structurally to various natural products and have many similar effects.

An example of natural-product-based insecticide chemistry are the photostable pyrethroids, which Menn says act against a range of pests but are relatively safe to mammals. The nat-

ural pyrethroids are extracted from certain species of the genus *Chrysanthemum*. Pyrethroids presently on the market have certain limitations, however. They are poor soil insecticides. Many are very toxic to fish and bees and lack systemic action; most do not control plant-eating mites (but could kill mite-eating predators and actually help to increase the mite population). But some new pyrethroids, such as fluvalinate, are less toxic to bees and certain beneficials, and others, like Fenpropathrin and fluvalinate, are reported to be effective miticides. A still-unresolved question concerns the potential for the development of insect resistance to such compounds.

Another newer class consists of Avermectins, isolated from the soil organism *Streptomyces avermitilis* (*11*). They are derivatives of pentacyclic 16-membered lactones. One example is Avermectin B_{1a} which reportedly works well against plant-eating mites and many insects under field conditions. It also seems to inhibit reproduction in queens of the imported red fire ant *Solenopsis invicta*. Its mode of action is to cause paralysis by inhibiting signal transmission at the neuromuscular junctions of arthropods (the biological phylum comprised of insects, crustaceans, spiders, etc.).

Among chemicals that disrupt insect endocrine functions are juvenile hormone (JH) antagonists. They cause premature changes from larval to chrysalis to adult stages and do not seem to have adverse environmental effects. One substance of this type, fluoromevalonate (FMev) (*12*, *13*), reportedly has this effect on lepidopterous (moths, and the like) larvae. However, although Menn believes that JH antagonists show promise for the future, no commercial product has yet been introduced.

Pheromones are specific chemical signals used by insects; sex attractants are one example. Jerome Klun of ARS observes that they are neither toxic nor persistent, nor are they expected to present any environmental hazard. On the other hand, they are highly specific and effective at extremely low concentrations. Synthetic sex pheromones could be used to disrupt the mating communications of target insects— and could thus help reduce pest populations.

For example, Klun pointed out that synthetic pheromones have been used experimentally against *Heliothis zea* and *H. virescens* (corn earworm and tobacco budworm). Researchers were able to induce interspecific matings of the two species, and cause the deaths

Avermectin B_{1a}

Source: Symposium paper by Julius Menn

A juvenile hormone . . .

JH I

. . . and a chitin synthesis inhibitor

CONHCONH

Diflubenzuron

Source: Symposium paper by Alexej Borkovec
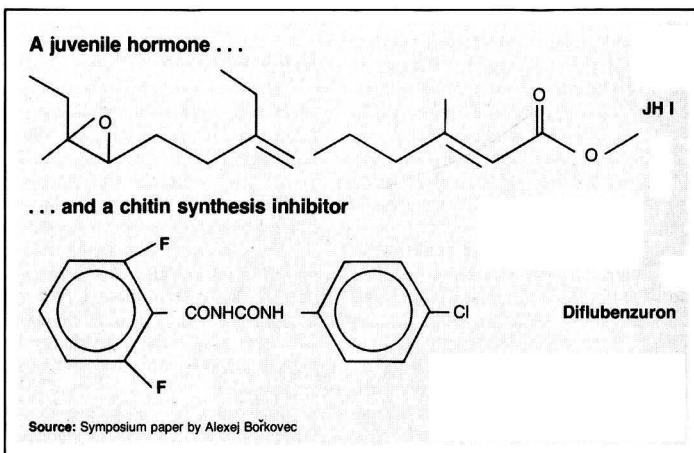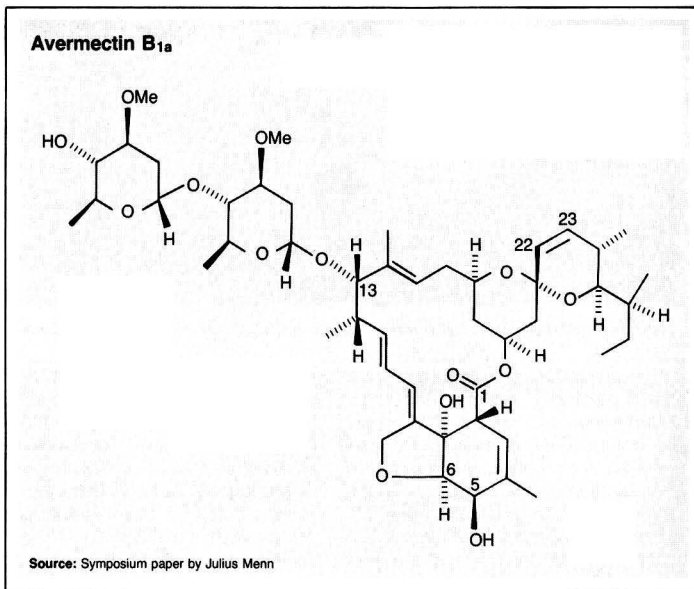
Pesticide test. *Juvenile hormones are being tried out on target insect larvae; if successful, they could disrupt larva–pupa–adult changeovers.*

Herbicide spraying. New weed killers might be required in much lower amounts.

of both partners, because they were morphologically incompatible. This result serves as evidence that sexual communications of insects are susceptible to disruption, and that in the future, pheromones may be useful for suppressing the reproductive potentials of pest populations. However, Klun notes that additional research in this area will be required to bring this concept of pest suppression to fruition.

Klun said that pheromones will be used increasingly in agriculture to detect and monitor pests and to forewarn growers of imminent pest infestations. Mathematical models are being developed for many of agriculture's most devastating insect pests. These models will allow translation of the rate of insect captures in pheromone-baited traps into quantitative estimates of adult population densities and predict subsequent egg laying and larval density in crops. Such quantitative data will aid pest management strategy decisions, Klun believes.

Other classes of pesticide chemicals will be aimed at controlling actual insect reproduction. Such control is achieved through the sterile insect release method (SIRM) and the field sterilization method (FSM). SIRM is limited to only a few insect species because of economic considerations; an example of its use has been the release of sterilized male cattle screwworm flies to mate with females and thus reduce the population of this cattle killer.

Alexej Bořkovec of ARS says that FSM is presently limited because of the lack of suitable chemical sterilants. But he adds that recent advances in insect reproduction physiology indicate that insects' reproduction regulators have multiple functions. Thus, interference with these regulators could produce sterilization, as well as lethal effects. Examples of chemicals that might work in this way include juvenoids (structural analogs of insect

juvenile hormones that regulate metamorphosis), chitin synthesis inhibitors, and certain other materials. Chitin is the hard polysaccharide covering that an insect "synthesizes" to give its body its hard outer covering. An example of a chitin synthesis inhibitor with sterilizing activity is diflubenzuron. Chemicals of this type are expected to he highly specific and not to cause adverse environmental effects.

Herbicides and fungicides

Control of weeds with chemicals will remain the method of choice for the future, predicts Edwin Alder of Lilly Research Laboratories (Greenfield, Ind.). But selectivity of herbicides might be enhanced through biotechnology. For example, crops tolerant to highly active short-residual herbicides could be developed through tissue culture and recombinant DNA techniques, Alder says. Biological control of weeds might come about through rDNA and advanced fermentation technology.

Herbicides of the future may be based more on heterocyclic structures, thus interacting with naturally occurring materials. This emphasis could lead to sharper selectivity in weed removers and preventers, Alder believes.

Examples of herbicides requiring lower amounts to be applied are sethoxydim (BASF), requiring 250 g/ha, and chlorsulfuron (Du Pont), needing as little as 25 g/ha. In contrast, during the 1950s and 1960s, herbicides sometimes had to be applied in quantities as high as 6 kg/ha.

Alder expects new fungicides to be developed that would also require lower rates of application and would attack specific biochemical sites in fungal pathogens. If a target fungus develops resistance to the chemical, perhaps slight molecular modifications could be made in the fungitoxicant. What Alder also hopes to see are fun-

gicides that can be applied to leaves and translocated downward to lower stems, crown, and roots; presently, systemic fungicides are translocated upward and are not as efficient.

Future plans

Efforts that will continue to be supported by ARS over the next several years include research on analytical methods and human exposure to pesticides. As to chemicals of the future, ARS will, if possible, implement a "new research effort" on ways to retard resistance of insects to insecticides and will maintain "a strong" program on attractants, repellents, and other behavior-modifying chemicals, ARS's Waldemar Klassen told the symposium. He added that his organization hopes to be able to target some research on the development of bioassays to determine effects of candidate insect control chemicals at cellular and subcellular levels.

Dale Wolf of Du Pont concurs with the importance of crop research at the cellular and subcellular levels. "A major opportunity for productivity increases appears to lie in areas of emerging technology, including molecular biology with emphasis on genetic engineering," he said. This type of research would also apply to pest control. He calls for a continuation of the tradition of cooperative research among government, industry, and academia for progress in improving crop protection chemicals.

—Julian Josephson

References

(1) Unterstenhoefer, G. *Pflanzenschütz Nachrichten* **1970**, *23*, 264–72.
(2) Bartlett, B. R. "Biological Control of Insect Pests and Needs"; Reinhold Publishing Co.: New York, 1964; Chapter 17.
(3) Ripper, W.E. et al. *J. Econ. Entomol.* **1951**, *44*, 448–58.
(4) Graham-Bryce, I. J. "Integrated Control in Orchards"; 5th Symposium, Bözen (Bolzano), Italy, 1974; pp. 315–26.
(5) Watson, J. C., Ed.; Marcel Dekker: New York, 1975; pp. 47–65.
(6) Metcalf, R. L. *Ann. Rev. Entomol.* **1980**, *25*, 219–56.
(7) Metcalf, R. L. "Requirements for Insecticides of the Future"; In "Proc. FAO Symposium of Integrated Pest Control"; Rome, Italy," 1966; pp. 115–33.
(8) Gasser, R. *Z. Angew. Entom.* **1975**, *78*, 20–27.
(9) Hoffmann, H. *Pflanzenschütz Nachrichten Bayer.* **1976**, *29*, 46–53.
(10) Kohn, G. K. In "Pesticide Selectivity"; Street, J. C., Ed. Marcel Dekker: New York, 1975; pp. 113–33.
(11) Albers-Schönberg, G. et al. *J. Am. Chem. Soc.* **1981**, *103*, 4216–21.
(12) Quistad, G. B. et al. *Nature* **1981**, *289*, 176–77.
(13) Quistad, G. B. et al. *J. Agric. Food Chem.* **1982**, *30*, 1151–54.

Indoor air pollution

*Radon levels in some Maine houses exceed the OSHA standard
for uranium mines. Such findings have been partly responsible
for a change in EPA policy on indoor air pollution.*

The common attitude toward indoor air quality is nonchalance. Generally, we believe that it is an aspect of our lives that is no problem and is under our control. We have a feeling that we can sense when indoor air deteriorates and that we can do something such as limiting smoking by occupants or opening windows to improve the air. Some of us may believe that the air quality in an office building or public building is less subject to personal control, but even about this, we are not usually greatly concerned, unless we are working in a building where many of the employees seem to be feeling sick for no apparent reason.

Witnesses at an August hearing held by two subcommittees of the House Committee on Science and Technology gave evidence that the air quality in some buildings is definitely dangerous to health. They said that high levels of certain pollutants such as radon and nitrogen dioxide would be entirely undetectable to the occupants without special instruments for measuring air pollution, but agreed that they could not assess the overall magnitude of the problem for the country without a concerted research effort.

Demetrios Moschandreas, research director at the Research Institute of the Illinois Institute of Technology, said, "Presently, using anecdotal research, we have sufficient data to suspect a potential problem." But he also noted that the overall quality of indoor air in U.S. housing is unknown. Anthony Nero of Lawrence Berkeley Laboratory believes that the problem is definitely serious: "Exposure to some indoor pollutants has the potential to cause thousands of extra deaths each year.... Our studies of health effects indicate that even average levels of some pollutants are reason for substantial concern, while in some buildings, levels of some pollutants are of great concern."

Outdoors, the average concentrations of most of the priority pollutants
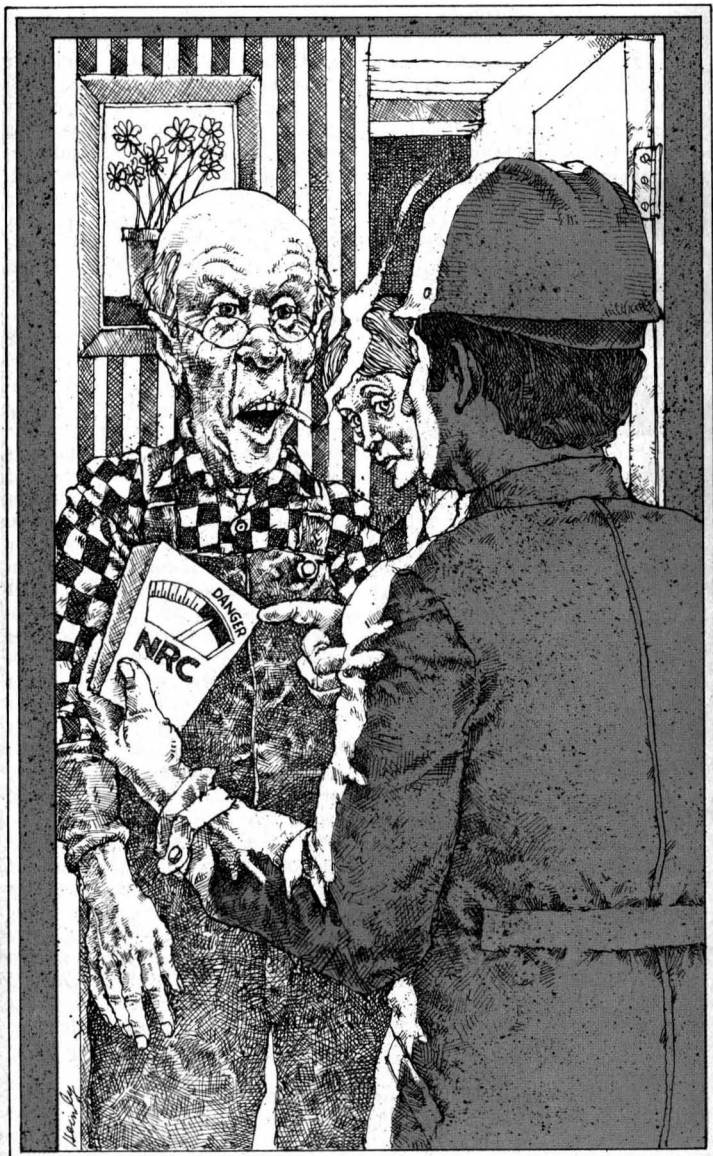
"Whadya mean there's a reactor in my basement!"

have decreased in the past 10 years. Of the six criteria pollutants, only NO_2 levels have increased recently in several urban areas. In contrast, the average indoor air has probably become less pure in the past decade.

This is primarily because electricity and fuel have become more expensive and, to save energy, we have reduced the ventilation rates in many new and older structures by insulating them and sealing them up. Also, more people live in mobile homes, which generally have lower ventilation rates than conventional houses. Another factor causing a decline in indoor air quality is that a large fraction of the population has begun to heat their houses with wood stoves and unvented kerosene heaters. Both of these can cause problems for indoor air. Sales of wood-burning stoves in the U.S. increased from fewer than 200 000 in 1972 to approximately 1.5 million in 1981. About three million kerosene heaters were being operated during the winter of 1981–82. A third factor is the increased use of synthetic building materials, some of which emit rather large amounts of formaldehyde.

Because of these developments and because the typical American spends 80–90% of his or her time indoors, the average air that each person breathes over the course of a day may be less pure than it was 10 years ago, despite the improvement in outdoor air quality. Peter Preuss of the Consumer Product Safety Commission testified that outdoors there were 241 million person days of exposure to unhealthy levels of NO_2 in 1981, most of which occurred in the Los Angeles basin, but that indoors there were one to one and a half billion person days of exposure to unhealthy concentrations of NO_2 in 1982 from the use of unvented gas heaters and kerosene heaters.

Natural radon

A number of pollutants are sometimes found in rather high concentrations in indoor air. John D. Spengler, associate professor at the Harvard University School of Public Health, said that some of the more important indoor contaminants are tobacco smoke, radon, carbon monoxide, nitrogen dioxide, asbestos fibers, formaldehyde, chlordane, microorganisms, and aeroallergens. From the perspective of those familiar with the indoor air quality issue, the testimony about radon at the August hearing was probably the newest and most startling information. Data about the high levels of indoor radon that have been found in recent measurements have not

been widely publicized.

As is the case with most indoor contaminants, not enough measurements of radon have been made to give an accurate picture of how extensive overall exposure is throughout the country. However, radon is different from most indoor contaminants in that its health effects are well-known compared to those of other pollutants. Spengler testified that the health effects of radon are the clearest of all indoor contaminants and that the risk of these effects is also comparatively well defined from studies of uranium miners and other hard-rock miners who were exposed to radon in poorly ventilated mines.

Radon gas is one of the radioactive elements evolved as uranium decays. Some areas of the country, especially granitic regions and phosphate-mining regions, have high levels of both uranium and radium in the soil and rock. These areas are located primarily in the New England states (especially Maine), along the eastern side of the Appalachian Mountains in Pennsylvania and Virginia, in Florida, and in granitic, uranium, or other mineral-bearing areas of the West. In such regions high concentrations of radon in indoor air can result from two pathways—soil and groundwater. Radon diffuses out of the soil through cracks and other entrances into buildings where it is trapped by the structural shell. The groundwater in such regions may also contain high levels of radon, and if it is used as the water supply from a well, it can cause high levels of airborne radon. The radon gas builds up in the water pipes and outgasses to the air when the water is used. Sprayer devices such as showers and dishwashers are likely to give the user a larger radon dose. Radon can also be emitted from building materials. At first these were considered the primary source, but recent investigations have shown that they are not the usual cause.

The principal ways of keeping radon out of a structure are aerating the water or filtering it with charcoal if radon-rich water is used, and filling any cracks or other openings where radon might enter into the basement and living quarters. Also, increasing ventilation rates by opening windows or using air-to-air heat exchangers prevents radon from building up to high levels.

Radon decays to radioactive daughter elements that attach themselves to particles in the air and may then be deposited in the walls of the lung. Because radon is an inert gas, the

primary health risk is not from radon itself but from the radon decay products such as polonium-218, lead-214, and bismuth-214. The major health effects from these seem to be lung cancer and some nasal cancers. There is a risk of stomach cancer from drinking water containing radon, but the risk is much smaller than that of the lung cancer that might result from airborne radon daughters.

University of Maine researchers estimate that a person drinking water with 20 000 pico-Curies/L (pCi/L) of radon for 60 years would have one chance in 500 of dying from stomach cancer. In contrast, the risk of dying from lung cancer is 1% for each 4 pCi/L of lifetime exposure to airborne radon. The one existing nonoccupational federal standard for indoor radon is applicable only to structures built in contaminated areas around inactive uranium mill tailings sites. Published by EPA in January 1983, it states that the indoor air must contain less than about 3 pCi/L (Table 1).

The Terradex Corporation (Walnut Creek, Calif.) has measured radon in a number of houses in the U.S. H. Ward Alter, president of the corporation, testified that a substantial fraction of the houses his company monitored exceed the EPA standard (Table 2). Although the number of houses tested is a very small portion of the total number of dwellings in high-risk areas, the results indicate that there are many houses, especially in Pennsylvania, Maine, and other areas of the Northeast, that exceed the EPA 3-pCi/L standard. (None of these buildings are located close to uranium mill tailings.)

In Pennsylvania, Terradex found that the radon levels in 15% of the houses measured exceed 20 pCi/L. If a family is exposed for a lifetime to this level of radiation, their total exposure lies in the range known to cause lung cancer in uranium miners. Alter stated that "these statistics imply that thousands of radon-related lung cancer cases may occur in Pennsylvania [over the course of 50 years] unless appropriate measurement and remedial action are undertaken." By contrast, calculations show that less than one cancer death in 50 years might result from the radiation released during the Three Mile Island accident. Another way to look at the problem is to observe that a person living in a house with 3 pCi/L of airborne radon is exposed to about 3000 millirems of radiation each year, in contrast to the average annual exposure of 0.3 millirems that a person receives from nuclear power plants.

Radon can enter a building in a variety of ways
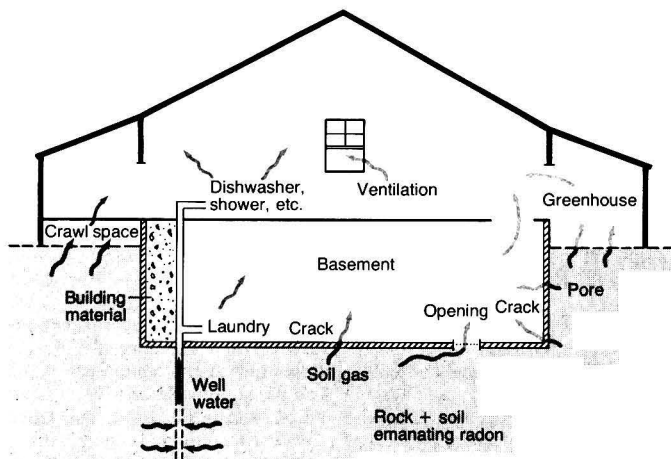
Source: University of Maine, February 1983

TABLE I
Airborne radon standards for buildings

Houses built on uranium mine wastes in U.S.	<3 pCi/L
Phosphate mining regions in Florida	4 pCi/L: remedial action required
	2 pCi/L: reduction to a reasonably feasible level required
Uranium mining regions in Canada	30 pCi/L: prompt remedial action required 4 pCi/L: remedial action required 2 pCi/L: investigation recommended
Sweden (maximum levels permitted)	11 pCi/L (existing buildings) 5 pCi/L (houses undergoing remodeling) 2 pCi/L (new houses)
Union of Concerned Scientists	>5 pCi/L: remedial action indicated 2–5 pCi/L: remedial action suggested

---

TABLE 2
Indoor radon results in the U.S.

Location	Number of measurements	Highest reading (pCi/L)	Percent> 4 pCi/L
Northern California	80	7.4	15
Midwest	64	7.4	20
South	304	2.7	0
Northeast	133	77	20
New York	413	50	15
Pennsylvania	249	91	42
Maine	427	133	21
Other U.S.	826	...	...
Total	**2496**		

Source: Testimony of H. Ward Alter, President, Terradex Corporation, August 1983

Charles T. Hess, professor of physics at the University of Maine (Orono) has been studying indoor radon for a number of years. At the hearing, he testified that "in granitic areas [of Maine], some of the [indoor] air concentrations exceed the OSHA standard for radon in uranium mines [>66 pCi/L]." He said that the radon levels in certain drilled wells in Maine are very high (up to 700 000 pCi/L) and that the average well has a concentration of 10 000 pCi/L. Generally, 10 000 pCi/L in the well water will produce 1.0 pCi/L in the indoor air. He stated that University of Maine researchers estimate that the risk of dying from lung cancer would be 1% for each 4 pCi/L of lifetime exposure to airborne radon and that this level is not at all unusual in Maine houses. According to his calculations, 88 excess lung cancer deaths could result annually in Maine from exposure to high levels of radon from well water. Rough estimates he has made of radon exposure throughout the U.S. show that 5000–20 000 excess lung cancers could result each year from indoor radon. Hess also stated that radon in indoor air is the largest single source of ionizing radiation for the public—"larger than medical radiation, other natural radiation, occupational radiation, or nuclear fallout" (Table 3).

Passive smoking

Tobacco smoke is another indoor contaminant that was emphasized at the hearing. Jan Solwijk, chairman of the Department of Epidemiology and Public Health at the Yale University School of Medicine, testified that the evidence about passive smoking is not altogether conclusive. He noted, however, that "there is a clear indication that on sensitive individuals the effects of [sidestream] tobacco smoke can be quite disabling." Spengler said that "the evidence is becoming more clear that children who live with parents who smoke have a higher rate of respiratory disease." He observed that more than half the population, 60%, live in houses where there is at least one smoker.

The average nonsmoker is a passive smoker of about three cigarettes a day, according to a witness from EPA, James Repace. He has made a rough calculation that about 5000 people die from passive smoking each year. This estimate should be viewed with caution because scientists agree that insufficient research has been done to make accurate estimates of mortality from passive smoking. Only one person at

TABLE 3
Annual radiation exposure from all sources [a]

Source	Millirems
Radon decay products [b]	80
Medical irradiation	50
Terrestrial gamma rays [b]	38
Internal irradiation [b]	37
Cosmic radiation [b]	31
Fallout	1
Occupational exposure	0.9
Miscellaneous sources	0.8
Nuclear power	0.3

[a] Data from U.K. NRPB Bulletin 39
[b] "Natural" radiation

EPA, Repace, worked on passive smoking during the past year.

Coordinated research effort

Although the data collected in the past several years give scientists some understanding of indoor air quality, the witnesses at the hearing, including the EPA witness, Donald Ehreth, generally agreed that a concerted interagency effort is needed to assess the magnitude of the problem and devise additional ways to combat it. Spengler said that "an overall strategy should be developed to investigate indoor exposures, health effects, control options, and public policy alternatives." He proposed a national survey of exposure to indoor air pollutants as one of the first steps in the process because thus far indoor air quality has been measured in only a small sample, about 3000 out of 80 million U.S. residences. The witnesses said that a number of agencies, including EPA, the Department of Energy (DOE), and the Department of Health and Human Services (HHS), should be involved since many different federal agencies have research responsibilities for indoor air quality. There was general agreement that EPA should lead such an interagency effort, with DOE, HHS, and CPSC (the Consumer Product Safety Commission) sharing some of the leadership responsibility.

An interagency group for indoor air quality research was established in 1979. It was cochaired by DOE and EPA. It met regularly and helped coordinate research between federal agencies until Anne Gorsuch became EPA administrator. At that time, the EPA leadership lost interest in indoor air and the group met rarely if ever.

Indoor air research probably reached its lowest point at EPA in late 1982 when zero funding was requested for this effort for FY 1984. At that time agency officials repeatedly stated that EPA has no regulatory authority over indoor air quality, and thus had no need to perform indoor air research. DOE's Office of Conservation and Renewable Energy followed in EPA's footsteps and requested no funds at all for indoor air research for FY 1984. Congress negated the decisions of both agencies by appropriating $2 million for indoor air research at EPA and $1.6 million for the Office of Conservation and Renewable Energy at DOE.

Therefore, EPA's strong plea at the hearing for a coordinated interagency research effort was strikingly different from previous statements made during the Reagan administration. It is alleged that the way in which this testimony was approved was a significant departure from normal practice. Policy changes for federal agencies are usually developed long before they are presented at a hearing. In this case, the policy was apparently made in the process of approving the testimony.

All agency testimony must be approved by the Office of Management and Budget (OMB) before it is presented to a Congressional committee. According to several EPA sources and members of the staffs of the congressional subcommittees involved, OMB initially rejected the testimony. It wanted the following sentence stricken from the statement: "EPA has the statutory authority to protect public health from indoor air pollution and other airborne contaminants, as required by the Clean Air Act; the Toxic Substances Control Act; the Safe Drinking Water Act; the Federal Insecticide, Fungicide, and Rodenticide Act; and the Uranium Mill Tailings Act." In place of this, sources say, OMB wanted EPA to justify indoor air research by saying that Congress had appropriated money for it. OMB apparently preferred that statutory authority for such research not be given.

After the testimony had been rejected by OMB and on the day before the hearing, sources allege that Deputy Administrator Alvin L. Alm personally took the testimony to the White House and obtained approval there. This seems to be another instance in which EPA Administrator William Ruckelshaus has been able to change EPA policy almost 180 degrees from what it was under Gorsuch–Burford. At the hearing, congressmen expressed delight and approval over the reversal. Rep. James H. Scheuer (D-N.Y.),

chairman of the Subcommittee on Natural Resources, Agriculture Research and Environment, said, "It's hard to believe that the same agency that produced this testimony asked for zero funding in FY 1984." EPA's Ehreth answered, "I can only say there has been a change."

Attack on DOE

On the second day of hearings, a major part of the time was spent questioning Joseph J. Tribble, then DOE assistant secretary of Conservation and Renewable Energy. Apparently, he had canceled three-quarters of the indoor air research projects DOE had with Lawrence Berkeley Laboratory, even though enough funds had been appropriated to carry on with all of them in FY 1984. The projects that were terminated concerned radon measurements, passive particle samplers, building materials emissions, and heat exchangers.

Tribble said he had canceled the projects because he had not been able to find out their details, so was unable to approve them, and because he felt other agencies or the private sector were better equipped to do them. When asked what scientific basis he had for his decisions, he admitted, "None." Reps. Don Fuqua (D-Fla.) and Richard L. Ottinger (D-N.Y.) were highly dissatisfied with Tribble's explanation. Ottinger had in his possession a March 1983 internal memorandum that he had obtained from a member of Tribble's staff which explained many reasons why DOE was most suited to carry on these projects and why they were needed. Members of Tribble's staff allege that his first assistant had the details of the projects since March, long before they were canceled. Ottinger concluded his questioning of Tribble by saying, "I don't think you've demonstrated to us that you have back up for the decision that you've made." Two weeks after the hearing, Tribble, who has been under attack for months from the public and members of Congress for allegedly dismantling the government's conservation programs, resigned his position at DOE.

EPA's policy in regard to indoor air has changed. It remains to be seen whether DOE's policy will undergo a similar transformation. As in many other areas, DOE seems far more determined than EPA to carry on with the original policy laid down at the beginning of the Reagan administration, rather than reappraise what is required to reflect the public's interest.

—Bette Hileman

Effluent guidelines for organic chemicals, plastics, and synthetic fibers

Richard M. Dowd

More than 4000 pages of comments were submitted by over 100 industrial, environmental, and individual interests by the close of EPA's comment period on the proposed organic chemicals, plastics, and synthetic fibers (OCPSF) effluent limitations guidelines (ELGs) and standards. The proposed regulation is the most recent agency attempt to establish limits and standards for OCPSF sources under the 1977 Clean Water Act and the terms of the 1976 Consent Decree in *Natural Resources Defense Council (NRDC) v. Train.*

The agency's proposal (*Fed. Regist.* March 21, 1983, *48*, 11827) would require Best Available Treatment Economically Achievable (BAT), Best Conventional Treatment, and Best Practical Treatment of industrial wastewater. EPA would also establish New Source Performance Standards for new and existing point sources and the pretreatment of indirect discharges. The proposed ELGs cover numerous facilities having total 1980 annual sales in excess of $75 billion. The proposed limitations cover a large variety of plants with highly varied effluent characteristics. A thorough review of the comments submitted on the proposed regulation will be undertaken by EPA and other interested parties. Pending EPA's summary remarks, the following provides an informal survey of the comments submitted to date.

Diversity of sources

Many commenters challenged EPA's ability to regulate such a diversity of industrial discharges. Until recently, the agency's data-gathering efforts and earlier regulatory programs involved fewer than 600 OCPSF plants and concentrated on effluents related primarily to high-volume products and processes at larger plants. However, EPA's proposal affects an estimated 1200–1500 plants, including almost every OCPSF plant engaged in chemical synthesis. The Synthetic Organic Chemical Manufacturers Association commented that the agency has not generated sufficient data on the expanded number of plants (especially small, specialty product plants) to warrant the inclusion of many of them.

Data base for specific ELGs

Many commenters questioned the data the agency used in establishing the various effluent and influent limitations. They criticized the representativeness of plant-specific data, the techniques used to develop various data bases, and the agency's data interpretation.

In March 1983, EPA's Science Advisory Board Environmental Engineering Committee (SAB/EEC) reported that the choice of analytical and quality assurance and quality control methods applied in the agency's data verification program limits the practical value of EPA's data base. The SAB/EEC stated: "The decision to use Gas Chromatography/Conventional Detectors methods in lieu of Gas Chromatography Mass Spectroscopy in the verification phase does not seem justified." To gather basic data to establish its BAT guidelines, EPA carried out four major sampling and analysis programs related to OCPSF point sources: a screening program, a verification program, a long-term sampling of some physical chemical systems, and a five-plant long-term sampling of biological treatment systems (with the Chemical Manufacturers Association).

In its *Federal Register* notice, EPA concluded that the practical limit for measuring organic priority pollutants is about 10 µg/L, although some pollutants can be detected at lower concentrations with careful application of certain methods. This detection limit of 10 µg/L, combined with data variability problems (e.g., false positives or measurements above 10 µg/L when, in fact, the concentration is not above 10 µg/L) led EPA to propose a limit of no less than 50 µg/L for the organics that were tested. Several industrial groups have commented that this proposal improperly leads to setting guidelines based on detectability limits rather than on water quality problems. Environmental groups and state and local agencies commented that this leads to unreasonably high limitations because many limitations could be set lower. In fact, the NRDC has recommended setting the lower limit not at 50 µg/L but closer to 10 µg/L.

Other commenters took issue with the subcategorization scheme applied to the BPT guidelines and the economic and regulatory impact assessments that accompanied the rulemaking.

One interesting aspect of this rule making is that it fully draws the science of analytical chemistry and the art of quality assurance and quality control into the regulatory arena. Many of the concerns raised in the comments are, in fact, scientific questions that deserve rigorous peer review.

EPA has notified the U.S. District Court that it will not meet the June 1984 deadline (imposed by the 1976 Consent Decree) for promulgating these regulations. According to Elwood Forsht, of the EPA's Effluent Guidelines Division, no alternative date has yet been proposed.

Richard M. Dowd, PhD, manages the Washington, D.C., office of Environmental Research & Technology, Inc.

Selected strategies to reduce acidic deposition in the U.S.

Several SO$_2$ emission reduction strategies are examined and their attributes clarified. The effectiveness of each method is measured by the changes it produces in total sulfur deposition.

David G. Streets
Duane A. Knudson
Jack D. Shannon
Argonne National Laboratory
Argonne, Ill. 60439
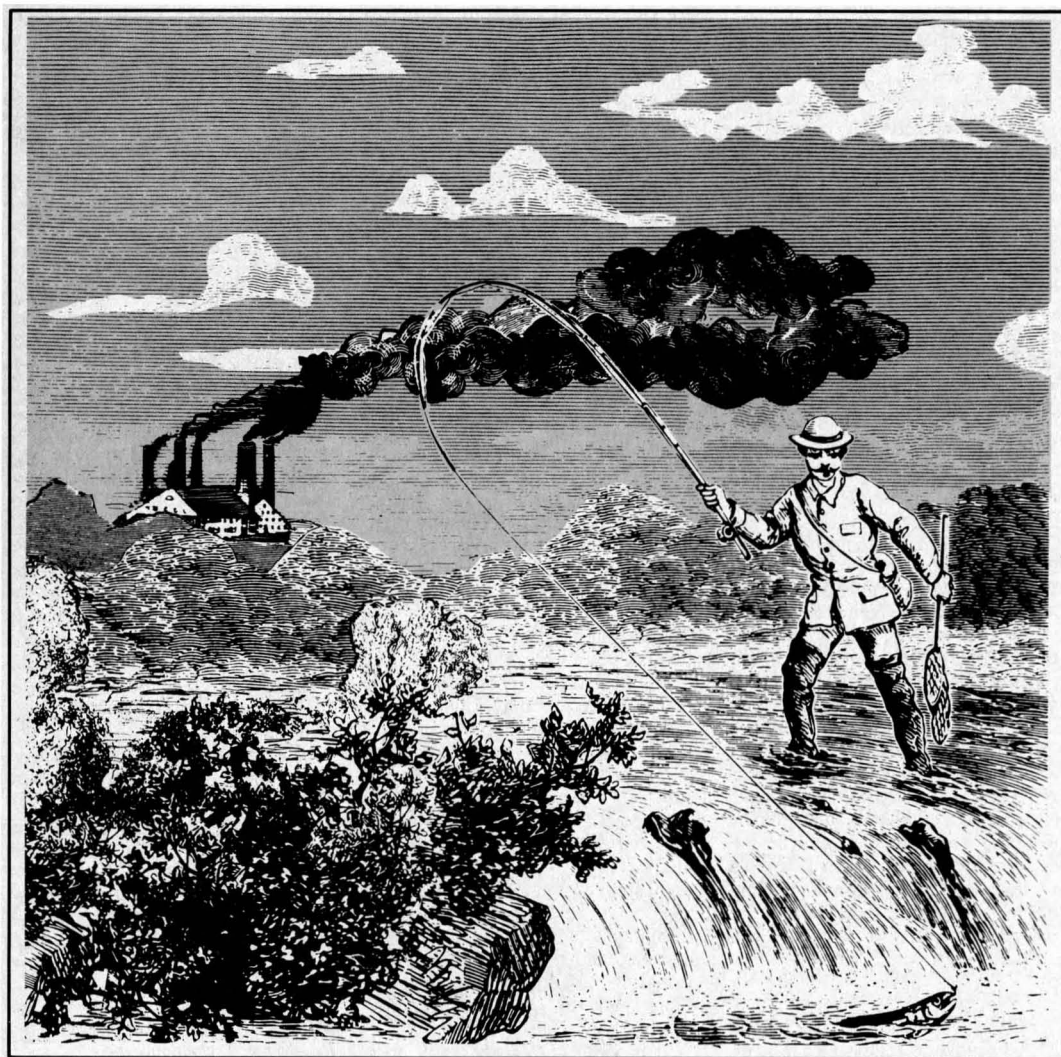
Although the research needed to fully characterize acidic deposition and its range of effects is many years from completion, political initiatives are being taken today to formulate control programs aimed at reducing the emissions of atmospheric pollutants believed to be responsible for environmental damage. Information on what effects such emission reductions would have on acidic deposition is incomplete, and there is no certainty that decreases in emissions would significantly reduce the adverse effects of acidic deposition. Nevertheless, the political process is moving ahead rapidly at both national and international levels and may be outrunning the pace of scientific research.

This article is an attempt to shed light on this controversial policy issue by examining the attributes of several plausible acid deposition control strategies for the U.S. It discusses the costs of these strategies, the emission reductions that would be obtained, and certain secondary effects they would have on selected regions of the country. Rather than attempting to complete the cost-benefit equation—which is arguably impossible given the current state of knowledge—this study provides some measure of the potential effectiveness of these strategies by estimating consequent reductions in sulfur deposition. It describes a systematic approach to portions of an organized cost-benefit analysis of acid rain legislation, but it is not intended to provide the definitive answer to the problem. (Ecological benefits are not even addressed here.) Many of the components necessary for a complete assessment are being developed in various government and utility studies.

Despite the fact that acidic deposition and its effects are not fully understood, it is clear that certain types of strategies could be implemented to reduce precursor emissions or otherwise mitigate effects. This article emphasizes the approach that has the greatest chance of being implemented in the U.S.: continuous reduction in emissions of sulfur dioxide from electric utility power plants. While this is the most likely approach, other options are also discussed briefly: a decrease in nitrogen oxide emissions, a reduction

in industrial or transportation emissions, intermittent fuel switching, and receptor mitigation (lake liming). The study examines several hypothetical sulfur dioxide control strategies, as well as other strategies that are currently being debated by congressional committees. Results are presented for the year 1995, based on the expected outcome of a 10-year program instituted in 1985. It is hoped that this analysis will contribute to the establishment of economically and environmentally sound policies for dealing with acidic deposition.

Analytical approach

To accomplish the objectives of this analysis, projections are made of the effects of various emission reduction strategies, each of which is implemented in the coal-fired electric utility power plant sector. The year 1980 is used as a base year; against this base are compared certain effects the following five alternative approaches would have in the year 1995:

- no specific acidic deposition control strategy (B95),
- a mandatory coal washing program (CWM),
- a ceiling on allowable SO_2 emissions of 2 lb $SO_2/10^6$ Btu (CP2),
- the Stafford bill, S. 3041 (STF), and
- the D'Amours bill, H.R. 4816 (DAM).

These approaches were chosen for close examination because they represent different conceptual approaches to a control program and because they cover a wide range of emission reductions. Other hypothetical approaches and congressional bills are discussed at appropriate points in the text.

The first three of these strategies—B95, CWM, and CP2—were analyzed in a joint study performed for the EPA, the Department of Energy (DOE), and Argonne National Laboratory by Teknekron Research, Inc. (*1*). In the Teknekron study, the Utility Simulation Model (USM) was used to project the effects of several control strategies for electric utilities (*2, 3*).

The USM consists of a number of interconnected computer modules and data sets that simulate decisions involved in utility system planning and operation and the impact of these decisions on utility finances and the environment. The model is driven by a set of exogenous parameters that include electricity demand, financial market conditions, fuel characteristics and availability, the use of advanced technologies, and environmental reg-

ulations. It simulates the joint operation of the various types of generating units and various capacity classes owned by all the utilities within a state. Output from the model includes fuel use, electricity generation, capital and equipment requirements, releases of environmental pollutants, financial statistics for utility firms, and average electricity prices.

The results of some of these control strategies were published earlier (*4*), and this article draws on these results for costs and secondary impacts (*1, 4*). State-level emission reductions for B95, CWM, and CP2 were calculated separately for use in long-range transport modeling (*5*). The USM results were obtained in 1980 and 1981 using the original version of the model employed by Teknekron Research, Inc., for EPA and DOE. The Universities Research Group on Energy (URGE), based at the University of Illinois at Urbana–Champaign, is currently designing an improved version of the USM called the Advanced Utility Simulation Model (AUSM). The values of the exogenous parameters reflect views of the future that were appropriate in 1980. Nevertheless, the results presented here are the best projections currently available, and improvements must await development of the AUSM.

The other two strategies—STF and DAM—are analyzed in a recent report, together with the other major acid rain control bills that were introduced into the 97th Congress: Mitchell (S. 1706), Moynihan (S. 1709), and Moffett (H.R. 4829) (*6*). It is difficult to project with any accuracy the costs of implementing each of these bills because of the many options they give the states for achieving the required emission reductions. In this study, therefore, only approximate cost estimates for the bills are provided, with no attempt to project secondary impacts. The Congressional Research Service has summarized analyses of the acid rain control bills that have been performed to date (*7*). The cost estimates in these analyses are in general agreement with those presented here.

The analysis in this article is restricted to the so-called acid rain mitigation study (ARMS) region, which covers the 31 states east of and bordering the Mississippi River and the District of Columbia (see, for example, Figure 1). This is the region addressed in the bills considered here and commonly used in technical analyses of the acid rain issue.

After discussing the regional costs

and emission reductions associated with each strategy, this article goes on to examine what effect each has on the following parameters:

- state-level emission reductions and costs,
- regional electricity prices,
- regional coal markets, and
- sulfur deposition.

The reductions in sulfur deposition resulting from emission changes are modeled using the advanced statistical trajectory regional air pollution (ASTRAP) model (8). Finally, the implications of the various strategies are discussed and compared with other approaches to reducing the potentially adverse effects of acidic deposition.

Specifications of each strategy

B95. The 1980 base case (B80) is compiled from a unit-level inventory created from DOE and EPA sources (9). Utility emissions are calculated from data on actual fuel use in the DOE/Federal Energy Regulatory Commission Form 67. The 1995 base case (B95) projects the emissions from utility sources in 1995 in the absence of any acid deposition control legislation. It includes new growth and retirement of older units and assumes that compliance with state implementation plans (SIPs) is achieved by 1985. Older units that were on-line prior to 1950 and smaller units with a generating capacity <100 MW are not required to meet the more stringent SIPs. In a sense, B95 represents a do-nothing strategy.

The emission reduction strategies are defined as follows:

CWM. This hypothetical approach consists of a mandatory requirement that all coal with sulfur content greater than 1.5% be cleaned by physical methods (1). The level of physical coal cleaning assumed in this analysis involves crushing the coal to a maximum diameter of 1.5 in. and flotation in a solution with a specific gravity of 1.6. The potential SO_2 emissions from the cleaned coal must be at least 10% lower than those from the raw coal.

CP2. This is the same as B95 except that a ceiling of 2 lb $SO_2/10^6$ Btu is placed on the allowable emissions from units meeting SIP limits. The advantage of such a ceiling is that emission reductions can generally be achieved by the use of low-sulfur or cleaned coal alone, without retrofitting the units with flue gas desulfurization systems.

STF. This strategy consists of implementing the Stafford bill, S. 3041 (a modified version of the Mitchell bill, S. 1706), approved by the Senate

FIGURE 1
State-level distribution of 1980 utility emissions in the ARMS region

Key
Emissions in 10^3 tons/y
- ☐ <50
- ▦ 50–250
- ▨ 250–500
- ▧ 500–1000
- ■ >1000
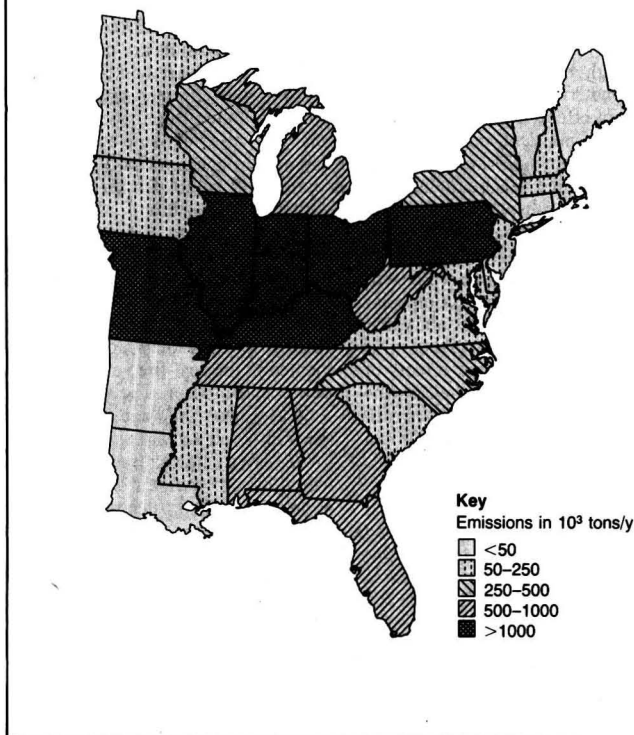
Committee on Environment and Public Works in July 1982 and introduced into the 97th Congress in November 1982. The Stafford bill sets a target SO_2 reduction of 8 million tons/y to be achieved in the ARMS region within 12 years of enactment. The decrease amounts to approximately 50% of the SO_2 emissions from the utilities in the 31-state region and 35% of the total SO_2 emissions in the region. State shares of the required reduction are to be determined in proportion to the ratio of the state's actual utility emissions in excess of 1.5 lb $SO_2/10^6$ Btu to the actual utility emissions in excess of 1.5 lb $SO_2/10^6$ Btu in the ARMS region. In addition, further reductions in SO_2 emissions from existing sources must be achieved to offset growth in SO_2 emissions from new sources. The growth offset has been analyzed elsewhere and is not addressed here (6).

The rationale behind the Stafford bill is to mandate a total level of reduction and then allow the states the flexibility of choosing their own methods of achieving it. Regional

trading, energy conservation, early retirement, and least emissions dispatching are all permissible methods.

DAM. This approach entails implementation of the D'Amours bill, H.R. 4816, which was introduced into the 97th Congress in October 1981. The D'Amours bill is considered here because it attempts to focus the control strategy on the reductions that could be achieved by retrofitting flue gas desulfurization units on the power plants with the largest SO_2 emissions. The bill calls for a reduction equivalent to an 85% decrease in the SO_2 emissions from the 50 largest SO_2 emitters in the ARMS region. In addition, a ceiling of 1.2 lb $SO_2/10^6$ Btu is placed on the emissions from all other SIP units larger than 100 MW. Although the bill addresses the 50 largest power plant emitters in calculating the *magnitude* of the reduction, the *source* of the reduction can be any stationary source of SO_2 in the region. Alternative methods are allowed as under the Stafford bill.

It can be seen that these strategies

represent a range of possible approaches to the acid rain problem. The remainder of this article examines the relative merits of these strategies, assuming implementation by the year 1995. It is difficult to ascertain the uncertainties of the results presented here. To the best of our knowledge, no formal uncertainty analysis has yet been performed for the USM. Analysis of the two congressional bills is greatly hindered by the fact that it is impossible to predict which of several methods of reducing emissions or combinations thereof would be adopted by the states. The results should, therefore, be viewed as indicators of the relative effects of alternative strategies and not as accurate projections of the future. From our perspective in 1983, we believe that the growth in electricity demand used in the USM represents an unrealistically high forecast.

Since this analysis was performed, the acid rain issue has been taken up by the 98th Congress. In March 1983, Senator Stafford introduced S. 768, which is identical to S. 3041, the bill analyzed here. Simultaneously, he introduced a more restrictive bill, S. 769, mandating a 12 million tons/y reduction with offsets for new growth in SO_2 and NO_x emissions. Notable among other initiatives of the 98th Congress is the proposal by Representatives Sikorski, Waxman, and Gregg (H.R. 3400) to achieve a total reduction of about 14 million tons/y by retrofitting scrubbers on the 50 power plants with the highest SO_2 emissions and instituting other measures to decrease SO_2 and NO_x emissions from stationary and mobile sources. This bill is in many ways similar to the D'Amours bill. Work is under way to analyze these latest proposals in detail.

Regional impacts

In 1980, the actual SO_2 emissions from electric utility power plants in the ARMS region amounted to 15.9 million English short tons, most of which was from coal-fired units (6). This can be compared with an estimated 21.8 million tons/y from all sources in the ARMS region and 26.5 million tons/y from all sources of SO_2 nationwide (10). It is clear, based on economic, geographic, and feasibility criteria, that coal-fired power plants in the ARMS region represent the most likely target for major SO_2 emission reduction strategies. Figure 1 shows the state-level distribution of SO_2 emissions from utilities in the ARMS region in 1980. Table 1 summarizes the regional effects of the five control strategies.

Compared to the level of emissions in B80, the do-nothing strategy (B95) results in a modest decrease in annual emissions of approximately 0.3 million tons at no added cost. New growth in SO_2 emissions from stationary sources in the region is estimated to be about 1.9 million tons/y; a reduction of about 1.1 million tons/y would result from compliance with SIPs (6). The small decrease in emissions is a combination of these two factors, together with decreases resulting from the projected retirement of a number of older coal-fired units by 1995.

The coal-washing strategy (CWM) results in an overall annual reduction in emissions, relative to B80, of 1.7 million tons at a cost of approximately \$820 million/y by 1995. At \$470 per ton of SO_2 removed, this strategy is not very cost-effective. Also, it is unlikely that the limited SO_2 reductions obtained with this method would be large enough to substantially affect the amount of sulfur deposition.

The imposition of a 2 lb $SO_2/10^6$ Btu ceiling on allowable SO_2 emissions (CP2) yields an annual reduction of about 5.7 million tons at a cost of about \$1.7 billion/y. This strategy costs \$300/ton of SO_2 removed and is therefore more cost-effective than coal washing.

The two bills (STF and DAM) yield larger annual emission reductions of 8 and 9.9 million tons, respectively. Costs are difficult to determine for these two strategies because of the range of methods that can be used to implement them. The USM has not been used to project the effects of these bills. Cost estimates for STF performed by other groups are \$3.1 bil-

lion/y (11) and \$3.6 billion/y (12) in 1980 dollars. The D'Amours bill has not been analyzed elsewhere, but its cost is estimated at approximately \$4.0 billion/y (6), using a value of \$400/ton of SO_2 removed.

Under current regulations, the average price of electricity in the ARMS region is projected to rise from 5.1¢/kWh in 1985 (after SIP compliance has been achieved) to 5.37¢/kWh in 1995 (1980 dollars in both cases). The effect of both CWM and CP2 is to increase average prices by an additional 1% by 1995. The effects of STF and DAM would be more significant. ICF, Inc., estimates an increase by 1995 of 2.9% under STF (11).

The USM predicts that the generation capacity of power plants with scrubbers will increase from 70 GW (gigawatts) in 1985 to approximately 210 GW in 1995, with or without a coal-washing program (that is, with either B95 or CWM). Under CP2, about 65 GW of additional capacity would be scrubbed. Recent estimates of additional scrubbed capacity under STF vary widely from only 7 GW (11), to 22 GW (12), to a high of 89 GW (13).

Emission reductions and costs

Because sulfur dioxide emissions are currently greatest in the industrialized Midwest (Figure 1), the midwestern states would bear the brunt of the reduction requirement. Unfortunately, these same midwestern states are currently experiencing the worst of the economic recession and are consequently the least able to absorb any additional costs of pollution control. Table 2 lists the emission reductions

---

TABLE 1

Effects of the control strategies in the ARMS region

| | Control strategy | | | | | |
	B80	B95	CWM	CP2	STF	DAM
Regional SO_2 emissions (10^6 tons/y)	15.91	15.63	14.17	10.21	7.91	6.01
Reduction achieved[a] (10^6 tons/y)	—	0.28	1.74	5.70	8.00	9.90
Annual cost of control (10^9 1980 \$)	—	0	0.82	1.73	3.1–3.6	(3.97)[b]
Cost effectiveness of strategy (\$/ton reduced)	—	0	470	300	—	—
Average price of electricity (1980 ¢/kWh)	5.10[c]	5.37	5.41	5.44	—	—
Scrubbed capacity (GW)[d]	70.3[c]	212.1	211.2	276.0	—	—

[a] Relative to B80.
[b] Value estimated at \$400/ton SO_2 removed.
[c] Values given are for 1985, after SIP compliance has been achieved.
[d] Total capacity of units on which flue gas desulfurization systems are installed.

required under each strategy in Pennsylvania, in the four midwestern states with the highest current emissions, and, for comparison, the state of Florida.

In the absence of acid rain control initiatives, emissions in 1995 are projected to be greater than 1980 emissions in three of these six states. The strategies discussed here require emission reductions ranging as high as 80% of the current utility emissions in Missouri. Clearly, under DAM the majority of larger power plants would be forced to retrofit a flue gas desulfurization system. In contrast, emission reductions required in Florida are no higher than 44%, due to the lower emission rates in that state.

Table 3 indicates that by 1995 control costs may increase by as much as $660 million/y for the state of Ohio. In contrast, a maximum increase of $130 million/y is projected for Florida. Cost-effectiveness is greater in the midwestern states, however, because a portion of the reduction in emissions can be obtained by switching fuels, cleaning coals, or blending coals. These options, however, entail disruption of traditional coal markets, which may have important social and political ramifications (discussed later in this article). Generally, the most cost-effective option is CP2, and the least cost-effective option is CWM. Figure 2 shows the pattern of state-level reductions in the ARMS region required by the most stringent control strategy: implementation of the D'Amours bill. It illustrates clearly that this stringent control program would have a potentially large impact on the industrialized midwestern states.

Regional electricity prices

The USM has a detailed financial module that simulates the costs and revenue requirements of 86 hypothetical utility firms, obtained by treating all investor-owned utilities within a given state as a single aggregate utility, and similarly treating all municipally owned utilities (1). It contains an accounting structure that provides an annual income statement, balance sheet, and sources and uses of funds for each of these "state" firms. The module also projects year-by-year utility expenses, including capital, operation and maintenance, and fuel. This structure enables the USM to project changes in electricity prices as a function of the implementation of a control strategy, where the price of electricity is defined as the total utility revenue requirements divided by the total sales to consumers. In this article, the effect of a single control strategy, CP2, on the price of electricity in the ARMS region is examined. The effects of STF and DAM are anticipated to be greater.

The regional average price of electricity in 1985 is projected to be 5.10¢/kWh. In the absence of any acid rain control program, this price would increase to 5.37¢/kWh by 1995—a 5.3% increase over the 1985 price. (All prices are in constant 1980 dollars.) Imposition of a 2 lb $SO_2/10^6$ Btu ceiling on allowable emissions would further increase this price to 5.44¢/kWh by 1995—a 1.3% increase over the 1995 price otherwise expected.

The effect on individual states in the region is variable, as Figure 3 shows. On the one hand, electricity prices in Ohio would increase by 16.8% between 1985 and 1995 under the current regulatory framework and by 21.4% with CP2. On the other hand, prices in Florida would increase by 4.1% under present regulations and by 4.7% with CP2.

Against this must be balanced the fact that electricity prices in the Midwest today are significantly lower than prices in the Atlantic Coast states. (The 1985 electricity price projection for Ohio is 4.1¢/kWh and for Florida is 6.4¢/kWh.) The proponents of strict control measures maintain that consumers in the East are currently paying higher prices for electricity partly because of a strong environmental stance taken in earlier years that included stringent SIPs and switching to clean fuels. Therefore, the increases in electricity prices in the Midwest must be accepted, they would argue, to bring midwestern states in line with the rest of the country. The Midwest would prefer an approach by which all states would contribute in appropriate, as yet undefined, amounts to the total costs of additional pollution control. The Sikorski Waxman bill includes such an approach.

Regional coal markets

The effect of a particular control strategy on patterns of coal use can be important for determining the political viability of the strategy. The potential for major shifts in regional coal mar-

---

TABLE 2

Sulfur dioxide emissions under different strategies from utilities in selected industrialized states in the Midwest and Pennsylvania

State	Utility SO_2 emissions (10^3 tons/y)						Range of emission reductions [a] (%)
	B80	B95	CWM	CP2	STF	DAM	
Ohio	2240	1801	1465	890	819	583	20–74
Indiana	1522	1470	1315	807	527	589	3–65
Pennsylvania	1488	1243	1103	930	798	467	14–68
Missouri	1131	1158	1107	565	356	221	−2–80
Illinois	1115	1219	1136	637	464	363	−9–67
Florida [b]	705	779	739	634	459	393	−10–44

[a] Relative to B80. Negative values indicate B95 > B80.
[b] Southern state included for comparison purposes.

TABLE 3

Cost impacts of the four control strategies CWM, CP2, STF, and DAM on selected industrialized states of the Midwest and Pennsylvania [a]

State	Range of control cost increases (10^6/y) [b]	Range of cost effectiveness ($/ton) [b]
Ohio	180–660	400–520
Indiana	80–400	260–500
Pennsylvania	100–390	330–940
Missouri	30–360	220–610
Illinois	30–300	210–510
Florida [c]	30–130	400–680

[a] All costs in 1980 dollars.
[b] Covering the four control strategies, relative to B80.
[c] Southern state included for comparison purposes.

FIGURE 2
State-level distribution of emission reductions required by the DAM strategy

Key
Emission reductions
in 10³ tons/y
☐ <50
▦ 50–250
◩ 250–500
▨ 500–1000
■ >1000
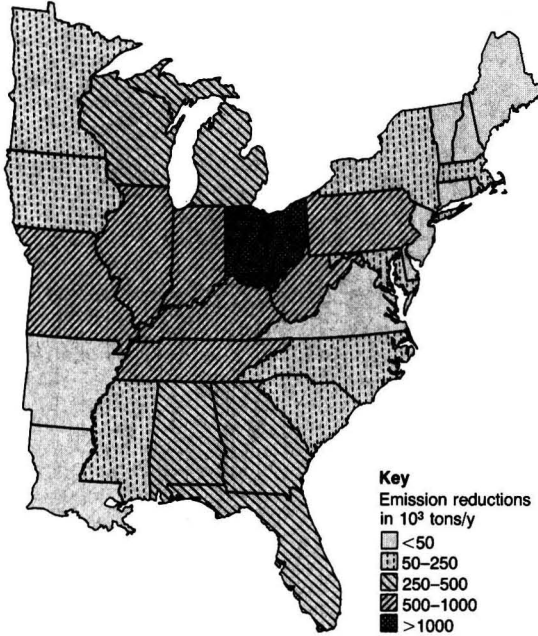
FIGURE 3
Changes in electricity prices in selected states in the ARMS region over the period 1985-95 under the CP2 strategy

Without CP2
With CP2

Regional average with CP2

Regional average without CP2

Change in electricity prices (%)

Ohio   Indiana   Pennsylvania   Missouri   Illinois   Florida
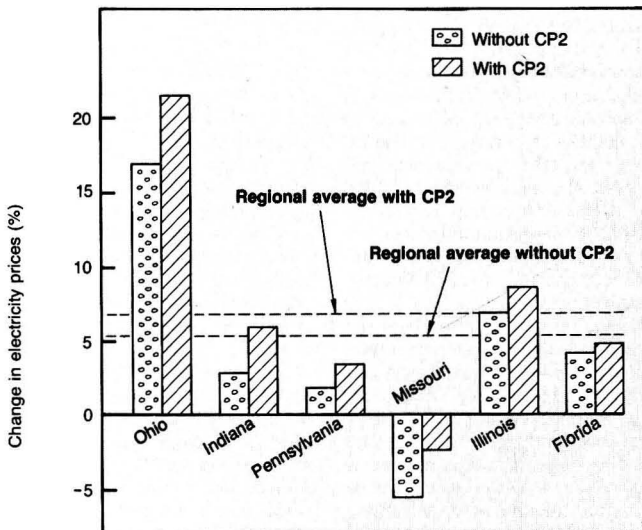
kets can induce vigorous opposition to new initiatives in the states affected, which in turn can lead to powerful resistance in congressional committees and Congress itself. The protection of local coal industry production and jobs is a strong political force.

Implementation of emission reduction programs can force utility owners to switch fuels in order to comply with regulations at minimum cost. This may act to the detriment of traditional, local coal sources. Figure 4 shows projected patterns of utility coal consumption in the six states discussed previously, for the year 1995. For each state, the first bar represents the B95 strategy and the second bar represents the control strategy, CP2. B95 was chosen in preference to B80 in order to eliminate confounding factors arising from growth in coal use (that is, in Figure 4, the total coal consumption is approximately the same for the two strategies). CP2 was selected because it is the control scenario with the greatest potential for coal market disruption. This is because under a ceiling of 2 lb $SO_2/10^6$ Btu the optimum (least-cost) compliance strategy for the majority of plants would involve switching to a low-sulfur coal or blending an existing coal with lower-sulfur coals.

The more restrictive strategies, particularly DAM, are so stringent that flue gas desulfurization would probably be a requirement for many plants irrespective of coal sulfur content. Local midwestern coals, with high sulfur content, would therefore be preferred because of their lower cost.

Figure 4 reveals several interesting things. First, several states, exemplified by Pennsylvania and Florida, are relatively immune to coal market shifts, either because they have in-state low-sulfur coal supplies or because they are too far removed from alternative coal sources. It is interesting to find, however, that under CP2 in 1995, a certain amount of Powder River coal from Montana is projected to penetrate the Florida market, in spite of the large transportation costs involved. Second, several states in the center of the nation, typified by Missouri, currently use a number of different coal sources and are therefore quite flexible when control programs involving changes in emission limits are introduced.

The states most vulnerable to coal market disruptions are those midwestern states such as Ohio, Indiana, and Illinois that currently rely heavily on relatively high-sulfur coals from in-state or from neighboring states. If a ceiling on emissions were imposed,

low-sulfur coals from Central Appalachia (in the case of Ohio) and from the Powder River basin (in the cases of Indiana and Illinois) would penetrate the local markets in significant amounts to be used as compliance coals. The projected reductions in local coal use are 28% for Ohio, 28% for Illinois, and 13% for Indiana in 1995.

Therefore, control strategies such as the ones described here clearly present a conflict. The most cost-effective strategies cause the greatest disruption in coal markets, whereas the least cost-effective strategies tend to preserve local coal interests (see box).

To examine this phenomenon further, USM was used to project the effects of these same strategies with protection of local coal interests (*1*). A strategy was developed, CL2, which is identical to CP2 except that coal-switching options are limited to locally produced coals, for those states that are themselves major coal producers. Plants in the affected states were permitted only to switch to local, in-state coals or to install flue gas desulfurization systems. The effect of this constraint was to increase regional costs in 1995 by 6% ($1.84 billion/y as opposed to $1.73 billion/y) for the same reduction in emissions (5.7 million tons of SO_2/y). States potentially benefiting the most from local-coal protection provisions are Illinois, Indiana, and Ohio.

Sulfur deposition

The ASTRAP model was used to convert the changes in SO_2 emissions that would be produced by these control strategies into projected changes in sulfur deposition patterns (*8*). ASTRAP and almost all other operational models of long-range transport and deposition assume a linear relationship between emissions and deposition for any single source and specified meteorological period; that is, if the emissions from source A are reduced by one-third, the deposition at receptor B associated with emissions from source A will be reduced by exactly one-third. This linearity assumption makes the deposition from different sources additive and allows the models to be used repeatedly in examining alternative strategies.

However, if source-receptor relationships are not linear, as some experts hold, the value of such simulations may be limited. Certainly, the relationship must be linear if integrated over sufficiently broad scales (e.g., globally and annually). The recent acid rain report prepared by the National Academy of Sciences concluded that there is no convincing evidence of significant nonlinearity in eastern North America if averaged on an annual basis over spatial scales of 1000 km or more (*14*).
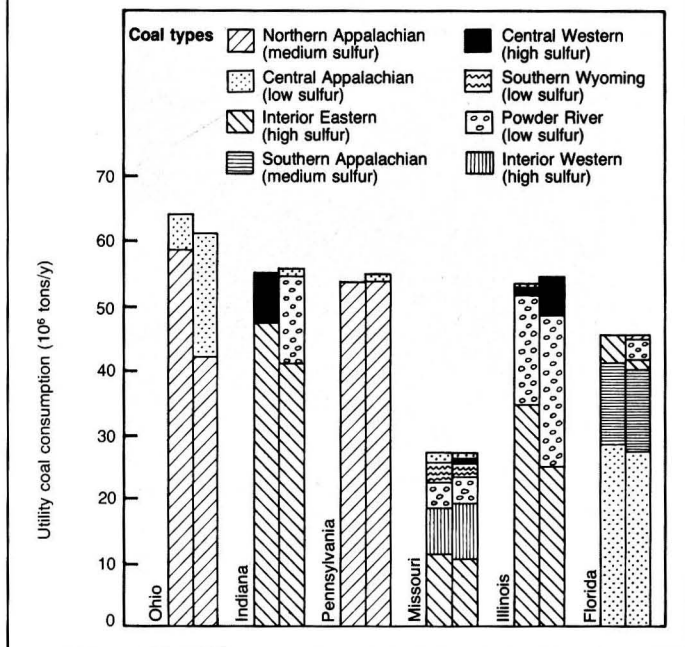
It is quite likely that some transformation and removal processes are nonlinear, as they would be if NO_2 and SO_2 are in competition for available oxidants. The crux of the linearity-nonlinearity question is whether marked nonlinearities exist over scales commensurate with either emissions decisions (on a statewide annual basis) or ecological, material, or health effects. (These effects are not examined here, but the most widely accepted view at this time is that they are a function of long-term total sulfur and nitrogen deposition, perhaps independent of speciation [*15*].) The answer is not yet known.

In addition to questions about the linearity assumption, general uncertainties in modeling of transport and deposition are ill-defined. Model sensitivity is an inadequate substitute for model uncertainty. The horizontal net mass flux of pollutants is not monitored, and dry deposition cannot yet be successfully monitored on a routine basis (*16*). Thus, in any model two of the three sink terms for pollutants cannot be compared with observed data. In addition, wet deposition measurements integrate the contribution of all sources and do not directly measure the effect of a single source.

In preliminary comparisons with measurements of annual wet deposition of sulfur in four U.S. and Canadian networks, ASTRAP simulations explained 75% of the observed variance in 1980. This is not offered as proof that ASTRAP correctly simulates the sulfur deposition changes that would be associated with these proposed emission changes, but it is encouraging. These simulations do not consider changes in emissions from nonutility or Canadian sources, nor emissions of other acidifying pollutants, oxidizing agents, or neutralizing agents, because that is beyond the scope of the proposed legislation examined here, and in part beyond the capability of the model.

For this exercise, it was considered appropriate to examine the changes in deposition associated with changes in utility emissions resulting from all U.S. and Canadian anthropogenic sulfur sources. All simulations are for one three-month summer season (June–August, 1980).

It is recognized that deposition

FIGURE 4
Patterns of utility coal consumption in selected states in the ARMS region in 1995, by supply region, for the strategies B95 (first bar) and CP2 (second bar)

Coal types:
Northern Appalachian (medium sulfur)
Central Appalachian (low sulfur)
Interior Eastern (high sulfur)
Southern Appalachian (medium sulfur)
Central Western (high sulfur)
Southern Wyoming (low sulfur)
Powder River (low sulfur)
Interior Western (high sulfur)

Utility coal consumption (10^6 tons/y)

States: Ohio, Indiana, Pennsylvania, Missouri, Illinois, Florida

varies considerably from year to year. Indeed, wet deposition of pollutants is much reduced when precipitation itself is decreased, as in a drought, for example. To some extent, dry deposition then increases since more pollutant is available for this form of deposition. The meteorological data—primarily upper air winds and precipitation observations—necessary for many models exist. However, the time-consuming job of having a computer reformat the meteorological data into a usable synoptic form has not yet been undertaken. Therefore, to describe a systematic approach, a single season is examined here.

All simulations are for total (wet plus dry) deposition of anthropogenic sulfur. The 1980 base case in Figure 5 is calculated from an inventory of 27.9 million tons of SO_x emissions (expressed as SO_2) for the U.S. and 4.5 million tons for Canada. This inventory is a minor modification of the 1978 emissions inventory produced by the working groups established under the U.S.–Canadian Memorandum of Intent on Transboundary Air Pollution, and has seasonal and about 100-km resolution (10). The meteorological data—gridded 1000-mb and 850-mb wind fields and 24-h precipi-

tation fields—were obtained from the Atmospheric Environment Service of Canada. The version of the model used here differs from that used in a recent report primarily because the wet removal parameters were adjusted according to a different resolution in the input precipitation data (17).

In the simulation using current total anthropogenic emissions, the maximum total sulfur seasonal deposition occurs in the upper Ohio River basin (Figure 5). It is in excess of 10 kg sulfur/ha. This simulation shows that almost all of the ARMS region and most of southeastern Canada have deposition rates greater than 2 kg sulfur/ha.

Table 4 shows how the sulfur deposition as calculated with the ASTRAP model (in kilotons of sulfur for the three-month period) varies with receptor region. The model predicts that approximately 60% of the total emissions are deposited on the North American continent. About 64% of that deposition occurs in the eastern U.S., and 17% occurs in eastern Canada.

The changes in deposition brought about by implementation of the five control strategies (B95, CWM, CP2, STF, and DAM) are simulated in the

ASTRAP model by appropriate emission reductions at the state level applied to the utility sector component of the total inventory of SO_2 sources. The minimum resolution of the 1995 simulations is therefore statewide.

Figures 6–10 show the reductions in sulfur deposition achieved for each of the emission reduction strategies examined. Isopleths are of changes in deposition, measured in kg of sulfur/ha for the same three-month period. Note that Table 4 gives the same information according to region and control strategy. Changes in nonutility emissions and Canadian emissions are not considered.

It is interesting to observe that in the do-nothing strategy (B95), deposition is projected to increase slightly in two regions (eastern Canada and the western U.S.), and total deposition is reduced slightly. At the extreme opposite end of the range, implementation of the D'Amours bill (DAM) is estimated to reduce sulfur deposition in eastern North America by 41%—a reduction of 33% in total North American deposition.

The deposition simulations shown in Figures 6–10 can be examined with respect to the possible effects of the strategies on deposition in an ecologi-

FIGURE 5
Current patterns of sulfur deposition in kg/ha in the eastern U.S. and Canada from all anthropogenic sources

FIGURE 6
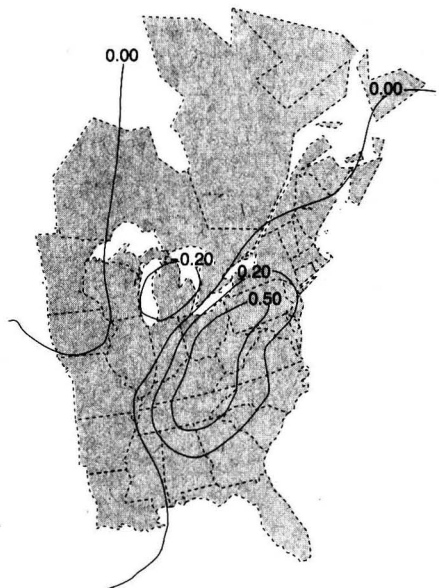**Sulfur deposition reduction in kg/ha in 1995 under the B95 strategy**

FIGURE 7
Sulfur deposition reduction in kg/ha in 1995 under the CWM strategy
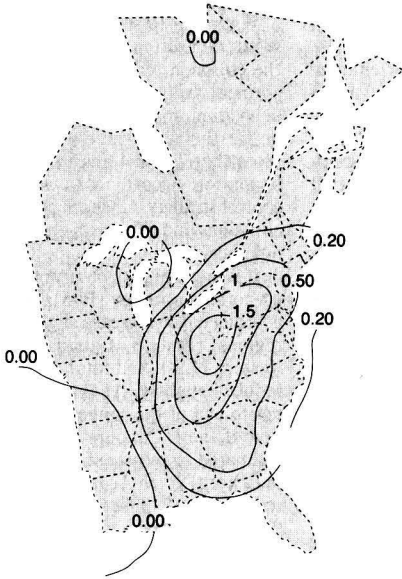
FIGURE 9
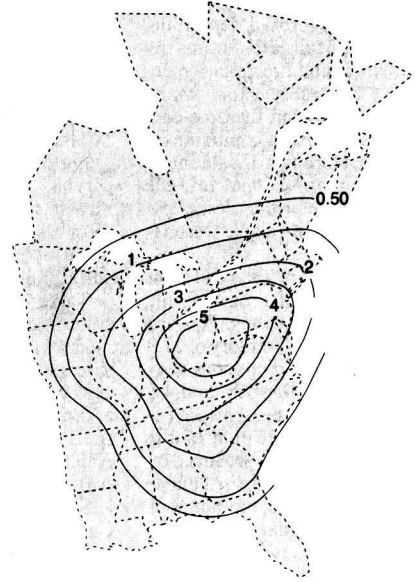**Sulfur deposition reduction in kg/ha in 1995 under the STF strategy**

FIGURE 8
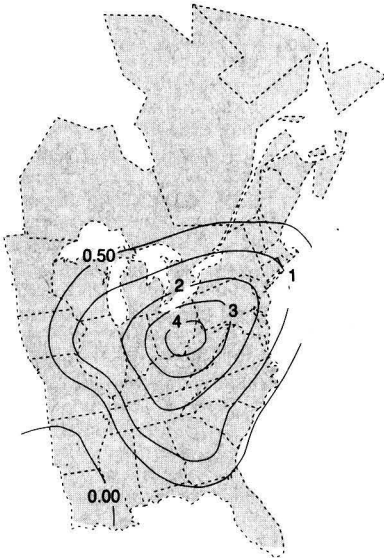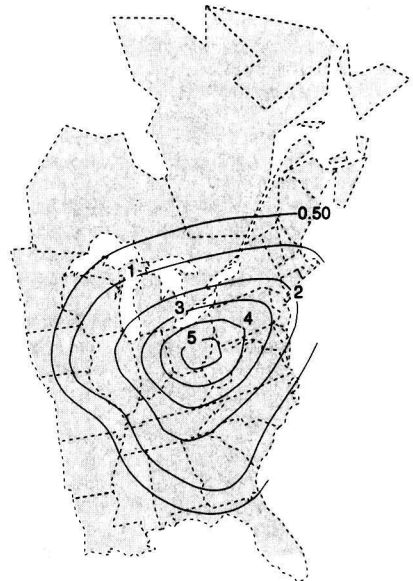**Sulfur deposition reduction in kg/ha in 1995 under the CP2 strategy**

FIGURE 10
Sulfur deposition reduction in kg/ha in 1995 under the DAM strategy

cally sensitive region, the Adirondacks in New York State. According to the simulation of current conditions, the seasonal deposition of total sulfur here is about 3.8 kg sulfur ha^{-1}. Both B95 and CWM, which reduce emissions most in Tennessee, Kentucky, and Ohio, result in a deposition reduction pattern oriented southwest–northeast and reduce seasonal deposition in the Adirondacks by about 0.1 and 0.3 kg sulfur ha^{-1} season^{-1}, respectively. On the other hand, the emission reductions in CP2, STF, and DAM significantly affect many more states, and the resulting patterns of deposition change appear much like scaled versions of the current pattern (Figure 5), except in Canada and in parts of the Northeast where Canadian emissions contribute a significant share to the current pattern. The deposition reductions in the Adirondacks are about 0.8, 1.1, and 1.4 kg sulfur ha^{-1} season^{-1}, respectively, very nearly the same as the ratios of the overall emission reductions would indicate.

It is not surprising that in a linear model, broadly based emission reductions result in broad deposition reductions. At this time, proven methods are not available to translate these predicted changes in sulfur deposition to changes in measurable ecological response.

Discussion

The acidic deposition issue is fraught with major uncertainties. It is not known with certainty how much reduction in atmospheric emissions is necessary to mitigate the deleterious effects of acidic deposition, nor how that reduction should be assigned to achieve the greatest benefits for the least cost. And it is not known how quickly emissions must be lowered to protect sensitive receptors.

On the one hand, views have been expressed that the causal link between atmospheric emissions and adverse effects is tenuous, or, at best, unquantifiable. On the other, categorical assertions have been made that the link has been sufficiently demonstrated to support immediate action. Proponents of control have called for decreases in sulfur oxide emissions in excess of 10 million tons/y, while others recommend the treatment of selected lakes with lime and no reduction in emissions. It has been postulated that immediate action is necessary to prevent irreversible, long-term losses to sensitive ecosystems. The opposing viewpoint is that the time scale for damage is on the order of decades or longer and that the gradual replacement of old,

uncontrolled plants by new, well-controlled plants is a sufficient strategy in itself.

This article has focused on a particular kind of strategy that would be favored if emission reductions are deemed necessary—a rollback in the emissions of SO_2 from coal-fired utility power plants in the eastern U.S. This kind of strategy has many advantages: The potential for the greatest absolute reduction exists in the utility sector in this region; it is almost certainly the most cost-effective strategy in terms of dollars per ton of pollutant removed; it is easy to implement; and it will have the minimum impact on the national economy per unit of pollution reduction. Arguably, it also addresses the actual cause of the problem, though the roles of local sources, oil-fired boilers, and non-SO_2 emissions are still being debated.

This article examines a range of SO_2 reduction strategies—a range both in terms of technical approach and in terms of the magnitude of SO_2 reduction (between 0 and 10 million tons/y). It does not advocate any particular approach because it is not known what magnitude and spatial configuration of reductions are necessary to alleviate adverse effects. Rather, an attempt is made to clarify the attributes of alternative types of strategies in order to facilitate the design of control programs that are efficient, equitable, and cause minimum disruption of other sectors of the economy. The "effectiveness" of a particular strategy is measured by the total amounts and regional patterns of changes in sulfur

deposition as projected by the ASTRAP model.

Several conclusions regarding utility control programs can be made from this study. The do-nothing and mandatory coal washing strategies would in all likelihood be ineffective in reducing emissions and sulfur deposition by significant amounts by 1995. Coal washing is also less cost-effective than might have been anticipated. The effects of the Stafford and D'Amours bills would be very significant. Deposition would be reduced considerably, but costs would be high. Several midwestern states would receive economic shocks, with significant increases in electricity prices. An important observation on these strategies is that the deposition reductions are largest in the Ohio River basin and surrounding areas where present indications are that ecosystems are quite resilient to acidic deposition. The deposition reductions in areas with sensitive ecosystems such as the Adirondacks and Great Smoky Mountains are significantly less, drawing into question the effectiveness of such measures.

A 2 lb SO_2/10^6 Btu ceiling on SIP emissions would be cost-effective and produce reasonable reductions in deposition in comparison with the two bills. Its main drawback is that it causes disruption of existing coal supply patterns. One advantage of a simple ceiling on emissions allowed under SIPs is that regulatory enforcement and implementation of the program would be quite straightforward. The disadvantage of the flexible approaches such as STF and DAM is

TABLE 4

Changes in sulfur deposition as a result of implementing the control strategies

Receptor region	Current [b]	ΔB95	ΔCWM	ΔCP2	ΔSTF	ΔDAM
	Deposition (10^3 tons S/season) [a]					
Eastern U.S.	1487	40	143	413	545	661
Eastern Canada	399	−6	10	57	85	100
Western U.S.	367	−1	−1	2	4	4
Western Canada	87	0	0	1	1	1
Total North America	2341	33	152	472	634	767
Percent of current eastern North American deposition	—	2	8	25	34	41
Percent of current total deposition	—	1	6	20	27	33
Emissions decrease [c]	3872 [d]	35	219	717	1005	1243

[a] Deposition calculated by the ASTRAP model using meteorology for the three-month period June–August 1980. Units are English short tons of sulfur for the three-month period.
[b] Current deposition from all U.S.–Canadian man-made sources. Strategy Δ's are calculated relative to this base. A positive value indicates a reduction in deposition; a negative value indicates an increase.
[c] Decreases in emissions converted to tons of sulfur for the same three-month period.
[d] Current U.S.–Canadian anthropogenic emissions in the same units.

that a variety of technical solutions, including conservation programs and emissions trading, may be proposed that would frustrate implementation and enforcement activities.

The question of equity among the states applies to all the reduction strategies. Whether the costs of reducing emissions should be borne entirely by the states in which the largest emitters are located or whether all states in the ARMS region, or in the continental 48 states perhaps, should contribute in some way to the costs of control is debatable. One solution might be to impose a levy on all 48 continental states in proportion to, say, quantity of electricity produced (as in the Sikorski–Waxman bill) or quantity of SO_2 currently emitted. The fund generated could then pay for controls in the states where the most effective reduction could be achieved (see box).

Other approaches

How do these strategies to control SO_2 emissions from utilities compare with other possible approaches to the problem? Although the control of nitrogen oxide emissions from power plants would produce a reduction in acidic deposition, even less is known about the source–deposition relationship for nitrogen oxides than for sulfur oxides. Also, nitrogen oxides are generally believed to be less harmful to ecosystems than sulfur oxides. Several of the congressional bills (Mitchell, Moynihan, and Moffett) allow credits for reductions in NO_x emissions on the basis of two units of NO_x for each unit of SO_2 emissions, by weight. The potential for NO_x emission reductions in the utility sector is not high nor is it likely to be particularly effective. Utility NO_x emissions in the ARMS region are expected to rise from about five million tons/y in 1980 to six million tons/y in 1995 (1). However, the potential for reductions in NO_x emissions at existing boilers is limited. Improved combustion techniques such as low-NO_x burners, burners-out-of-service, and overfire air can reduce NO_x emission levels by only 30–50%, while the more efficient flue gas treatment processes are still under development and expected to be expensive.

ICF, Inc. has estimated that NO_x control strategies for utility boilers will be limited to about a 25% reduction in emissions, with cost effectiveness ranging from $50 per ton (for simple combustion modification of tangentially fired boilers) to $290 per ton (for wall-fired boilers) (18). The new limestone injection/multistage burner (LIMB) technology is promising, but not expected to be widely used before 1990.

Strategies that address sulfur oxide emissions from industrial fuel combustion or industrial processes, or nitrogen oxide emissions from transportation sources, will probably be ineffective in the absence of other measures. Industrial SO_2 emissions in 1995 are projected to be five million tons/y, and NO_x emissions from transportation are also projected to be about five million tons/y (19). In both cases, significant reductions in these

levels would be cost-ineffective, difficult to implement and enforce, and potentially damaging to the economic well-being of specific industries. The utility sector is, in general, more robust in its ability to deal with price shocks than is the industrial sector, though it is certainly not as robust as it was in the past.

If it is determined that regional emission reductions are necessary or desirable, then it would seem reasonable to specify utility sources as the vehicle for reduction, or at least to calculate the required decrease on this basis, but to permit trading with other categories of sources at prescribed "exchange rates." If it is ultimately determined, however, that the goal of reducing acidic deposition is to protect relatively small receptor areas, and that local sources are the primary contributors to deposition, then the need for regional emission reductions might be obviated and specific emitters or specific states would be targeted for control irrespective of source category.

The possibility of an intermittent fuel switching strategy has been proposed (20) and its feasibility analyzed to a limited extent (21). The rationale for this approach is that the conversion of sulfur oxides to sulfate tends to be episodic, corresponding to periods of stagnating high pressure systems in the eastern U.S. during spring and summer. If a significant fraction of the total acidic deposition occurred during these relatively few episodes during the year, then intermittent fuel switching from coal to natural gas or other clean fuel during these periods might be effective in reducing total deposition.

The feasibility study of intermittent fuel switching does not support the effectiveness of such a strategy. Sulfate deposition was found to be somewhat episodic in the northeastern U.S., with typically about 30% of the annual deposition being contributed in eight episodes totaling about 50 days annually. However, a simulated reduction in SO_2 emissions of 50% at all coal-fired power plants in the upper Ohio River basin during a stagnation episode produced only a minor reduction in sulfur deposition in downwind areas. The technical and implementation problems of extending the reduction either in space, time, or magnitude further inhibit the attractiveness of the strategy. The need for meteorological forecasting, alert mechanisms, and compliance verification would create additional problems.

Finally, the possibility of "receptor mitigation," as opposed to "source

---

Update on pending acid rain legislation

Since this article was written, H.R. 4400 was introduced in the 98th Congress by Representatives Sikorski, Waxman, and Gregg. This bill requires a 10-million-ton reduction in SO_2 emissions and a 4-million-ton reduction in NO_x emissions. A large part of the SO_2 decrease is to be achieved by mandating that scrubbers be installed on the 50 power plants with the highest current SO_2 emissions. This requirement is included in the bill to minimize disruptions in the coal market (such as those discussed in this article). Because scrubbers are required on the 50 largest emitters, those plants would have no incentive to change to low-sulfur coal. Some smaller plants would probably switch fuels, causing certain changes in the coal markets but smaller disruptions than those projected under STF and DAM.

The Sikorski–Waxman bill establishes a 1 mill/kWh user fee on non-nuclear electricity generation throughout the 48 continental states. This money would be channeled into a trust fund to reimburse utilities for 90% of the capital cost of installing scrubbers. Thus, the cost of scrubbers, the major expense of acid rain control, would be spread throughout the nation. An analysis prepared by the Office of Technology Assessment projects that electricity rate increases under this bill would range from 1–10%, with an average of 3.2–3.7% during the most expensive years. The Sikorski–Waxman bill allows utilities less flexibility in choosing methods of SO_2 control than they would have under either STF or DAM, and the overall cost to the nation may be higher than that associated with either of the other two bills.

—Bette Hileman

mitigation" should be considered. Liming of acidified lakes has been suggested as a solution to a problem that may be limited in geographical extent to a relatively few lakes in only a handful of areas. The obvious drawback to this approach is that it does nothing to ameliorate impacts on other ecosystems or materials, whether currently known, suspected, or unsuspected. There are several other disadvantages. Liming is not a permanent solution. Lime must be added to a lake periodically in an amount appropriate to the watershed and the current pH. Also, lime is a very impure substance that adds other pollutants such as heavy metals to the lakes.

Crocker et al. have attempted to evaluate the costs of a lake-liming strategy on the basis of several assumptions about the extent of liming necessary and the resultant lake pH levels that are desirable (22). The estimates range between about $400 million/y and $8 billion/y (in 1978 dollars). These costs are of the same order of magnitude as the costs of the SO_2 reduction strategies reported here. Fraser et al., in a study for the Electric Power Research Institute, estimate a cost of $100/acre for a lake-liming program, cautioning that the cost may vary significantly depending on the accessibility of the lake and its proximity to the limestone source (23). These investigators do not attempt to estimate the total costs of such a program. It is clear that further research is needed to fully identify the extent of liming that would be necessary and thereby to narrow the range of cost estimates.

Acknowledgment

References

(1) "Electric Utility Emissions: Control Strategies and Costs," Report No. RK-80-2057; Teknekron Research Inc., Berkeley, Calif., April 1981.
(2) Silverman, B. G. *J. Air Pollut. Control Assoc.* **1982**, *32*, 1031.
(3) House, P.; Williams, T. *Energy Syst. Policy* **1981**, *5*, 1.
(4) Knudson, D. A.; Streets, D. G. *Env. Prog.* **1982**, *1*, 146.
(5) Van Horn, A., TERA Corporation, private communication, November 1982.
(6) Streets, D. G.; Conley, L. A.; Carter, L. D.; Vernet, J. E. "An Analysis of Proposed Legislation to Control Acid Rain," Argonne National Laboratory Report ANL/EES-TM-209, January 1983.
(7) Parker, L. "Summary and Analysis of Technical Hearings on Costs of Acid Rain Bills"; Congressional Research Service, July 26, 1982.
(8) Shannon, J. D. *Atmos. Environ.* **1981**, *15*, 689.
(9) Pechan, E. H. & Associates. "Estimates of Sulfur Oxide Emissions from the Electric Utility Industry"; Prepared for U.S. EPA; National Technical Information Service, September 1982.
(10) "Emissions, Costs and Engineering Assessment," final report of Work Group 3B of the U.S.–Canada Memorandum of Intent on Transboundary Air Pollution Study, June 1982.
(11) ICF, Inc. "Analysis of a Senate Emission Reduction Bill (S. 3041)"; Prepared for U.S. EPA, Washington, D.C., February 1983.
(12) Energy Information Administration. "Impacts of the Proposed Clean Air Act Amendments of 1982 on the Coal and Electric Utility Industries," DOE/EIA-0407, June 1983.
(13) Calculated by the Energy Information Administration from data reported in "A Report on the Results from the Edison Electric Institute Study of the Impacts of the Senate Committee on Environment and Public Works Bill on Acid Rain Legislation (S. 768)"; National Economic Research Associates, Inc., for Edison Electric Institute, June 1983.
(14) "Acid Deposition: Atmospheric Processes in Eastern North America"; National Academy Press: Washington, D.C., 1983.
(15) Cowling, E. B. Memorandum to members of the National Research Council Scientific Committee on Transport and Transformation Chemistry in Acid Deposition, "Biological Perspectives Regarding Acid Deposition and Its Effects"; North Carolina State University, Oct. 1, 1982.
(16) Hicks, B. B.; Wesely, M. L.; Durham, J. L. "Critique of Methods to Measure Dry Deposition, Workshop Summary," EPA-600/9-80-050, September 1980.
(17) Shannon, J. D.; Kleinman, L.; Benkovitz, C.; Berkowitz, C. "Intercomparison of MAP3S Models of Long-Range Transport and Deposition," preprint Volume of the Third Joint Conference on Applications of Air Pollution Meteorology; American Meteorological Society, Jan. 11-15, 1982; p. 29.
(18) "Alternative Strategies for Reducing Utility SO_2 and NO_x Emissions," draft report; ICF Incorporated, Washington, D.C., September 1981.
(19) MITRE Corporation. "National Environmental Impact Projection 80"; Prepared for the U.S. Department of Energy, Office of Environmental Assessment, February 1981.
(20) See *New York Times* review conducted by P. Shabecoff (Nov. 14, 1982) and letter by E. Altwicker (Nov. 24, 1982).
(21) Knudson, D. "Evaluation of the Feasibility of a Regional Intermittent Control Strategy for Sulfur Dioxide," Argonne National Laboratory Report ANL/EES-TM-193, June 1981.
(22) Crocker, T. D.; Tschirhart, J. T.; Adams, R. M.; Foster, B. "Methods Development for Environmental Control Benefits Assessment, Volume VII: Methods Development for Assessing Acid Deposition Control Benefits," draft report for U.S. Environmental Protection Agency, Office of Research and Development.
(23) Fraser, J.; Hinckley, D.; Burt, R.; Severn, R. R.; Wisniewski, J. "Feasibility Study to Utilize Liming as a Technique to Mitigate Surface Water Acidification," EPRI-EA-2362, April 1982.

David G. Streets is manager of the Policy Sciences Section of the Energy and Environmental Systems Division at Argonne National Laboratory. He received BSc and PhD degrees in physics from the University of London, England. He was a postdoctoral fellow under the sponsorship of the National Science Foundation in 1971–72 and Imperial Chemical Industries in 1972–74. He joined Argonne in 1975 and is presently responsible for management of an interdisciplinary group analyzing energy and environmental issues for the U.S. Department of Energy.
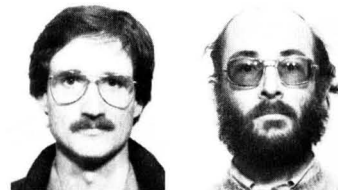
Duane A. Knudson (l.) is an environmental policy analyst in the Energy and Environmental Systems Division at Argonne National Laboratory. He graduated from Northern Illinois University in 1974 with a BS degree in meteorology. Graduate training at the University of Missouri—Columbia led to a MS in atmospheric science in 1976. He worked for three years in the Air Quality Branch of the Tennessee Valley Authority. He is involved in a variety of air quality policy assessment activities.

Jack D. Shannon (r.) is a meteorologist and deputy head of the Atmospheric Physics Section, Environmental Research Division, of Argonne National Laboratory. He received a PhD degree in meteorology from the University of Oklahoma. His primary research interests are modeling of long-range transport and deposition of air pollutants and optimal design of networks.

PCB replacements in dielectric fluids

Here is an assessment of the environmental behavior of these materials on the basis of their production, use and disposal patterns, environmental mobility, and biological effects

Richard F. Addison
Marine Ecology Laboratory
Bedford Institute of Oceanography
Dartmouth, Nova Scotia B2Y 4A2,
Canada

Polychlorinated biphenyls (PCBs) are mixtures obtained by fractional distillation of the products of the catalytic chlorination of biphenyl. Since the early 1930s, they have been used as components of dielectric fluids, flame-resistant plasticizers, and hydraulic fluids when chemically stable materials showing a range of physical properties were required. By 1970, PCBs were recognized as persistent and possibly hazardous environmental contaminants, and their only U.S. manufacturer voluntarily restricted their production. During the 1970s, national and international regulations further restricted their use. These events motivated the chemical industry to develop PCB replacements, particularly for electrical use.

The pattern of PCB production and use in the U.S. from 1965 to 1978 is shown in Figure 1. Data for 1965 to 1970 are from Reference 1; for 1971 and 1972, from Reference 2; and for 1973 onward, from Reference 3. PCB production in the U.S. reached a maximum by 1970. About half of the output was used in capacitor and transformer dielectric fluids; the remainder was used mainly as a flame-resistant plasticizer. By 1975, output had fallen to less than 50% of that in 1970, and almost all was used in dielectric fluids. At that time, there was also a shift toward production of the less chlorinated PCB mixtures. By 1978, PCB consumption in all manu-
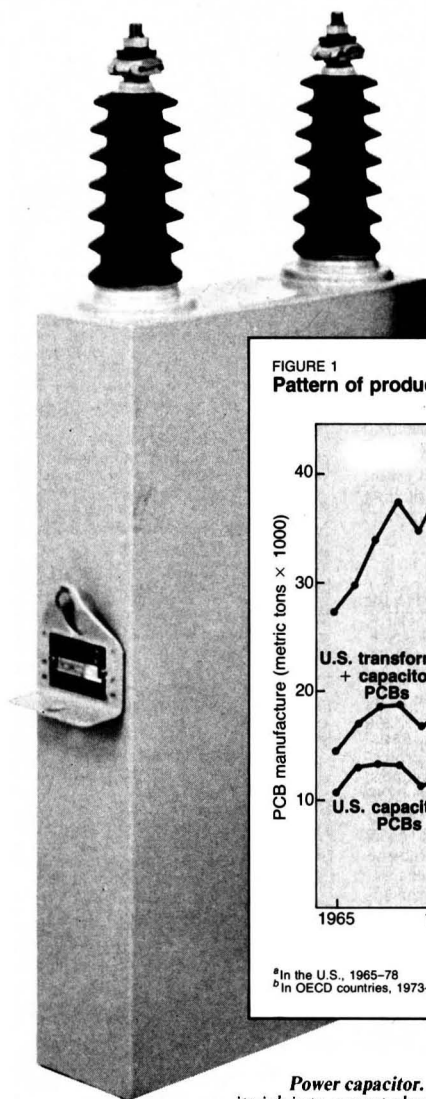
FIGURE 1
Pattern of production and use of PCBs[a, b]
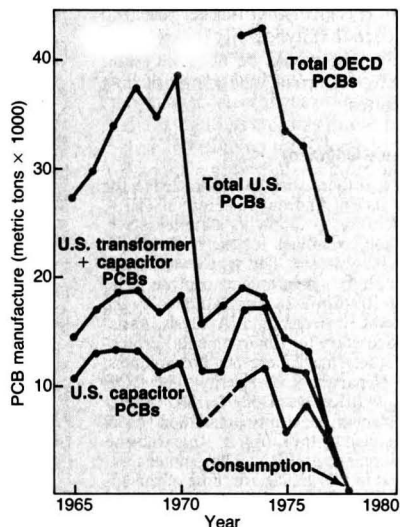
[a] In the U.S., 1965–78
[b] In OECD countries, 1973–77

Power capacitor. This one uses PCB replacements; its job is to correct phase on electrical transmission lines.

factured products had fallen to about 240 tonnes (metric tons), about 0.6% of the 1970 output.

These U.S. trends seem to have been typical of world PCB production. Before 1970, U.S. PCB manufacture was about one-third of world PCB production (4); after that, U.S. production represented about 40% of that reported in Organization for Economic Cooperation and Development (OECD) countries (3). The OECD data show that after 1970, PCBs were used mainly for electrical applications. World consumption of PCBs in dielectric fluids in 1970 would therefore have been around 50 000 tonnes/y. During the early 1970s, this demand and any increase caused by industrial growth would have been met by the lower-chlorinated PCB mixtures, but increasingly thereafter, by non-PCB replacements.

The removal of PCBs from plasticizers and hydraulic fluids seems not to have been so disruptive to industries using them as to the dielectric fluid industry. Presumably, this is because suitable alternatives (such as triaryl phosphate flame-retardant plasticiz-

ers) were already available, and in any case were under continuous modification and development (5). Finally, the use of PCBs as plasticizers was only a small fraction of total world production of plasticizers, which, in the early 1970s, was more than 1.1×10^6 tonnes (6).

Composition and analysis

Table 1 shows some examples of the range of PCB replacements proposed or used as dielectric fluids by late 1982. As new replacements are developed, the manufacture of older ones may cease, but products containing these older ones may still be used. The list is not comprehensive, but it contains examples from each major class of PCB replacements. Some of these materials, such as silicones, have been used previously for other purposes. Others, such as butylated monochlorodiphenyl ethers, have been prepared specifically as dielectric PCB substitutes. A description of the toxicology of some PCB substitutes appeared while this review was being prepared (7).

Paraffins. RTEmp is a high mo-

lecular weight (MW) purified paraffin (8). Occupational Safety and Health Administration information (manufacturer's technical literature) lists its boiling point as being above 427 °C, which corresponds to an *n*-alkane chain length of $>C_{26}$. RTEmp is prepared by hydrogenation of petroleum fractions; it is low in aromatics, but contains antioxidant additives. Its analysis has not been described, but it might be amenable to gas–liquid chromatography (GLC) at high temperatures.

PAO 13CE is a polyalphaolefin derived from 1-octene (9). It is described (manufacturer's technical literature) as being similar to PAO 60, which is also a poly(1-octene), and has an average MW of about 600. No analytical procedures have been described for PAO 13CE, but PAO 60 can be analyzed by gel permeation chromatography (10).

Ester-based materials. The Midels are described (manufacturer's technical literature) as esters of pentaerythritol with C_5-C_9 vegetable fatty acids mixed with aromatic triesters; the latter are shown as esters of ben-

TABLE 1

Sources, composition, and uses of some PCB replacement fluids

Material	Manufacturer	Composition	Uses
Paraffins			
RTEmp	RTE Corp. (U.S.)	High MW purified paraffin ⎱	Transformer dielectric
PAO 13CE	Uniroyal (U.S.)	Poly (1-octene) ⎰	
Ester-based materials			
Midel 7131 ⎱	Micanite & Insulators ⎱	Pentaerythritol aliphatic esters +	Capacitor dielectric
Midel 7211 ⎰	Co. (U.K.) ⎰	aromatic triesters	Transformer dielectric
Faradol 100	Asea (Sweden)	Benzyl neodecanoate	Capacitor dielectric
Dielektrol II	General Electric (U.S.)	Di-(2-ethylhexyl)phthalate + 1,2,4-trichlorobenzene	Capacitor dielectric; components have other uses
Aromatics			
Wemcol	Westinghouse (U.S.)	Isopropylbiphenyls	Capacitor dielectric
KMC-A	Kreha Co. (Japan)	Diisopropylnaphthalenes ⎱	Electrical uses and in pressure-
SAS-295 ⎱	Nisseki Co. (Japan)	Phenylxylylethanes ⎰	sensitive copying paper
SAS-296 ⎰			
C-4	Dow (U.S.)	Butylated monochlorodiphenyl ethers	Capacitor dielectric
Chloralkylene	Prodélec (France)	Isopropylchlorobiphenyls	Electrical uses
Silicones			
SF 97(50)	General Electric (U.S.) ⎱	Polydimethylsiloxanes	Transformer dielectrics; several
DC-561	Dow Corning (U.S.) ⎰		other uses

zene-1,3,5-tricarboxylic acid with medium-chain-length alcohols. The patent literature (*11*) describes very similar materials based on pentaerythritol esters mixed with trimellitates (benzene-1,2,4-tricarboxylates, themselves used as plasticizers), which are used as high-performance lubricants. Two Midel samples transesterified by conventional methods (*12*) and subjected to GLC and mass spectrometry (GLC/MS) on silicone-coated open-tubular columns contained about 60% of the total fatty acids as saturated straight-chain C_7 and C_8 acid; the balance consisted of highly branched C_8 acids. This identification was based on the comparison of retention times with those of standards, equivalent chain-length plots (*13*), and studies of MS fragmentation patterns (J. D. Leonard, personal communication). Since the Midels could be easily transesterified, the C_8 acids are presumably branched at some point beyond the α-carbon. This behavior is quite unlike that of benzyl neodecanoate, which is highly branched *at* the α-carbon. The Midels are amenable to GLC analysis with flame ionization detection (FID) (Figure 2).

Faradol 100 is benzyl neocaprate (manufacturer's technical literature). The structures of the synthetic neodecanoic (neocapric) acids, derived from branched nonenes, are shown by Fefer (*14*); all of the components are trialkylacetic acids, and most are α,α-dialkylpropionic acids. Faradol 100 can be analyzed conveniently by GLC (Figure 2).

Dielektrol II is a mixture of "a phthalate ester plasticizer mixed with a halocarbon widely used as a textile dye solvent" (manufacturer's technical literature). GLC/FID analysis showed three components. The most abundant corresponded to di-(2-ethylhexyl) phthalate (DEHP), and a second component corresponded to 1,2,4-trichlorobenzene (1,2,4-TCB). The third component, present in small amounts, was probably 1,2,3-TCB. Methods are available for the analysis of these materials in various samples (*15*, *16*).

Aromatics. Wemcol is described (*17*) as 4-isopropylbiphenyl. However, Tulp et al. (*18*) found that appreciable amounts of the 3-isomer were present, with traces of more highly substituted biphenyls; they describe a complete analysis by GLC and GLC/MS.

KMC-A is a mixture of alkyl naphthalenes of which the principal component (87%) is a diisopropylnaphthalene, presumably the 2,6-isomer, since the material is prepared by
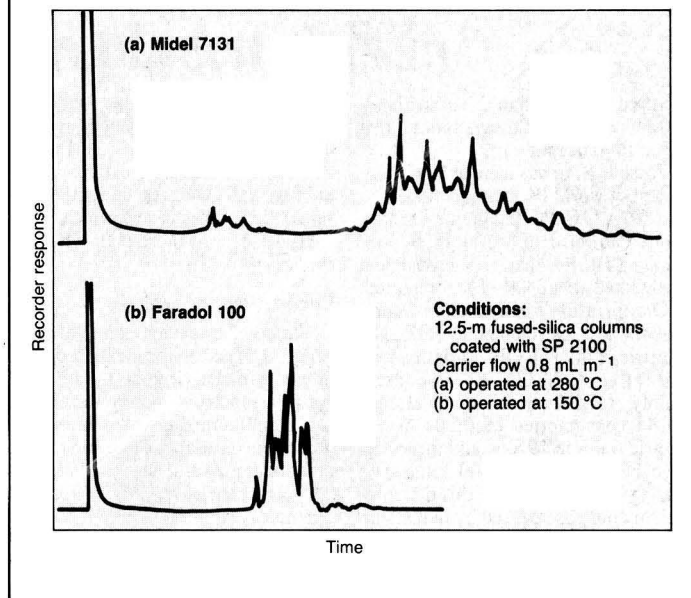
the Friedel-Crafts alkylation of naphthalene with propene. Some monoisopropyl naphthalenes and isopropyl methylnaphthalenes also are present (*19*). Extraction and cleanup procedures and GLC/FID analyses applicable to various samples have been described (*19*, *20*).

SAS-295 and -296 consist of phenylxylylethanes, principally the 1-phenyl-1-(3,4-xylyl)- and 1-phenyl-1-(2,4-xylyl)-isomers. Traces of related compounds also may be present. The composition of these mixtures has been described (*19*). They may be analyzed easily by GLC/FID, and methods for their extraction and cleanup from fish tissue have been reported (*19*, *20*).

Dielectric fluid C-4 is based on butylated monochlorodiphenyl ethers. The major components—which together represent about 70% of the total—of its precursor, XFS-4169L, are 4-chlorodiphenyl ether and 2-sec-butyl-4'-chloro- and 4-sec-butyl-4'-chlorodiphenyl ethers; miscellaneous dibutylated components make up the balance (*21*). The analysis of C-4 by GLC/FID in fish tissues has been described (*22*).

Chloralkylenes consist of isopropyl chlorobiphenyls. The two mixtures whose analyses are described, Chloralkylenes 9 and 12, contain mostly 2,4'-dichlorobiphenyl that has been alkylated with propene to yield mainly

di- (and traces of tri-) isopropyl derivatives (*23*, *24*). Full analyses of the mixtures are discussed in these references. The Chloralkylenes behave similarly to PCBs during normal residue analyses and may be extracted from soil and vegetables (*25*) and from animal tissues (*26–28*).

Silicones. Two silicone preparations, SF 97 (50) and DC 561, are proposed as PCB replacements. Both are polydimethyl siloxanes with viscosities of 50 centistokes (0.5 $cm^2 \cdot s^{-1}$) at 25 °C. From the relationship

$$\log \eta = 1.00 + 0.0123 M_n^{0.5} \quad (1)$$

where η is expressed in centistokes (cst) and M_n is the average molecular weight (*29*), their average MW should be about 3200. Silicone analysis has been reviewed (*30*); traces of silicones in environmental samples are probably best analyzed by extraction with an organic solvent, followed by atomic absorption determination of silicon (*31*). Silicones have a characteristic infrared band at 7.95 μm; this is probably not sensitive enough for trace analysis, although it may be useful as a confirmatory technique.

Scale of production

The world market for dielectric fluids appears to be on the order of

FIGURE 2
Chromatograms of some PCB replacements

(a) Midel 7131

(b) Faradol 100

Recorder response

Time

Conditions:
12.5-m fused-silica columns coated with SP 2100
Carrier flow 0.8 mL m⁻¹
(a) operated at 280 °C
(b) operated at 150 °C

50 000 tonnes/y, of which the U.S. market might represent 30–40% or about 15 000–20 000 tonnes/y. Since various materials may compete for that market, production capacity for any one material in the U.S. may be considerably less than this—perhaps 5000–10 000 tonnes/y. For example, Dow planned to produce as much as 5000 tonnes/y of its fluid C-4 in 1976 (32).

Products with uses other than as dielectric fluids may be manufactured in larger amounts. For example, phenylxylylethanes, which also are used in pressure-sensitive copying papers, were expected to be produced in Japan at a rate of 10 000 tonnes/y (33). Obviously, products such as silicones, which have many uses other than as dielectric fluids, are manufactured at a much greater rate. Table 2 summarizes the published production figures for some PCB replacements.

There seems to be some confusion about the extent to which PCBs were used as dielectrics. According to one report, in 1970, ". . . fewer than 5% of [transformers and capacitors] used PCBs . . ." (34), whereas Broadhurst (35) reports that in the early 1970s, more than 95% of capacitors contained PCBs. These statements could be reconciled by concluding that virtually none of the transformers used PCBs, but this would be inconsistent with PCB production data (Figure 1).

Use and disposal patterns

Some of the PCB substitutes listed in Table 1 are planned solely for specific dielectric applications. Usually contained in a relatively small number of large individual units, fluids used in this way would not be available to the general consumer market. In principle, it should be simple to control and monitor the use and disposal of these fluids. Examples include the Dow fluid C-4 and probably Faradol 100.

The only routes by which these materials are likely to reach the environment are deliberate disposal or accidental spillage, both of which can be recorded. Thus, Dow (manufacturer's technical literature) recommends landfill disposal or high-temperature incineration of waste or used C-4 fluid. The company states, however, that the "life" of a capacitor fluid is on the order of several years and that such materials do not present an immediate environmental problem. Nevertheless, there have been accidental spills of dielectric fluids (36), and these no doubt will recur. Although such events are infrequent, they represent a possible route of entry into the environment.

Some PCB replacements designed primarily as dielectric fluids may find other uses. The diisopropylnaphthalenes and the phenylxylylethanes, for example, have been used in Japan as solvents for microencapsulated inks in pressure-sensitive copying papers since the early 1970s. This widespread and uncontrolled "open" use has led to their becoming environmental contaminants (20). Isopropylbiphenyl has been patented as a component of solvents used in pressure-sensitive copying papers (37) and is being considered as an anti-inflammatory drug (38); it could enter the environment through both of those uses. The latter route would almost certainly be minor, especially since the compound is quite biodegradable. Materials similar to the Midels have been patented for use as high-performance lubricants (11).

A third group of PCB replacements includes materials already in widespread use. The prime examples are the silicone fluids; the use of these materials as PCB substitutes in the amounts assumed above may account for at most 5–10% of all silicone use (Figure 1 and Table 2). Since the 1940s, silicones have had many open uses such as in waxes, greases, and polishes and have been detected as trace environmental contaminants (31).

Similarly, the major components of Dielektrol II (DEHP and 1,2,4-TCB) have been in general use for some time. DEHP accounts for almost half of the total phthalate plasticizer used in consumer products based on polyvinyl chloride. Although DEHP comprises about 70% of Dielektrol II, this would represent only about 1–3% of total DEHP use on the basis of the data in Figure 1 and Table 2. 1,2,4-TCB has miscellaneous uses as a solvent, a dielectric, and a synthetic intermediate; it is currently produced at a rate of about 1000 tonnes/y (39). Use in Dielektrol II could therefore double current amounts.

Paraffinic products similar to RTEmp or PAO 13CE are already in widespread use or are almost indistinguishable from materials now widely used in products such as transmission fluids, greases, and creams. The use of these materials is so great that additional use as PCB replacements would be insignificant (Table 2).

Environmental distribution

The distribution and transport of a chemical in the environment depend on its physicochemical properties. The most important of these seem to be vapor pressure, water solubility, and lipid–water partition coefficient (measured in practice as an octanol–water partition coefficient, $K_{O/W}$). Vapor pressure will affect atmospheric distribution and transport. The other characteristics control distribution in water, adsorption to particulate material, and accumulation in biota. Several models have been developed to use these properties for predicting the distribution of chemicals. Table 3 summarizes the physicochemical properties of some PCB replacements.

One model (40) predicts that the phenylxylylethanes should resemble p,p'-DDE and a pentachlorobiphenyl

TABLE 2

Production of PCBs and of PCB replacements for which information is available

Material	Production (metric tons/y)	Reference
PAO 13CE	Not specified. Total polyalphaolefin production (all uses, U.S., late 1970s): 100 000	(74)
KMC-A	Several thousand	(20)
SAS-295 SAS-296	3000–5000 (Japan, 1975) Capacity 10 000 (Japan, 1979)	(33)
C-4	5000 (capacity, U.S., 1976)	(32)
Dielektrol II components:		
Di-(2-ethylhexyl)-phthalate	116 762 (all uses, U.S., 1980)	(75)
1,2,4-trichloro-benzene	1000 (all uses, U.S., 1975)	(39)
SF 97(50) DC 561	Not specified. Total silicone production (all uses, U.S., 1980): 104 537	(75)
PCBs	46 865 (all uses, U.S., 1970)	text

in being readily adsorbed to particulate material, whereas KMC-A and C-4 should tend to partition much more to the atmosphere (41). This model is simplistic in that it takes no account of dynamic processes of transport or degradation, because the relevant information is rarely available. Its value, however, is that it identifies the major reservoirs into which a chemical may partition, and so suggests processes that should be important in the eventual degradation of the chemicals. In the examples cited, atmospheric photolysis may be important in the degradation of KMC-A and C-4, while soil and sediment microbial degradation may be important in the case of Wemcol and the phenylxylylethanes.

There are insufficient data to allow even the simplest modeling of the behavior of several PCB replacements. However, for materials to function successfully as dielectric fluids or as organic solvents, they must be relatively stable and nonpolar, and therefore, lipid soluble. Thus, most PCB replacements can be expected to have roughly similar properties of lipid and water solubility, but their vapor pressures may vary appreciably. One might therefore expect the behavior of PCB replacements to differ most in those features that depend on vapor pressure. The Midels, silicones, and paraffins—all of which are of relatively high MW and have low vapor pressures—should partition to the at-

mosphere to only a limited extent; adsorption to particulate material is the more probable fate of these materials.

Metabolism and other rates

The bioaccumulation, metabolism, and excretion of several PCB substitutes have been studied extensively, but rarely have the studies led to directly comparable data, because investigators have emphasized different aspects of their work. Some have dealt only with identifying metabolic products, while others have concentrated on overall mineralization rates. Table 4 summarizes microbial degradation rates. In Table 5, rates of accumulation and clearance are shown for some PCB replacements.

The degradation of hydrocarbons, especially by bacteria, has been studied in detail. There are at least three major degradative pathways, all involving oxidation. One leads through oxidation of a terminal methyl group to an alcohol, and then to a fatty acid, which can undergo the normal processes of fatty acid metabolism. In addition, the initial oxidation step may occur at some nonterminal point on the hydrocarbon chain, to yield secondary alcohols and acids (42). The ease of oxidation decreases in order from n-alkanes, to branched alkanes, to cycloalkanes, and finally to aromatics. Thus, RTEmp, a purified paraffin, is aerobically degraded 50% by bacteria

in 7.7 d at 20 °C (8). Structures such as PAO 13CE, which may be more highly branched, might be degraded more slowly. The uptake or clearance of the paraffinic PCB replacements by biota has not been described.

No information exists about the uptake or clearance of the Midels or of Faradol 100 by biota. The latter undergoes 100% primary degradation within 48 h in unacclimated urban polluted water (manufacturer's technical literature). Fatty acids are readily degradable, although by analogy with the hydrocarbons, one might expect branched structures to be more resistant than straight chains. Since Faradol 100 contains mostly trialkylacetic acids, it is presumably degraded only by ω-oxidation. The less branched C_8 structures in the Midels might be degraded more rapidly, since other processes including β-oxidation might occur, but no degradation rates are published.

Of the Dielektrol II components, DEHP is accumulated from water by fish and invertebrates. Its octanol–water partition coefficient is probably around 10^5 —since that of the shorter-chain di-n-butyl phthalate is also in that range (43). DEHP is accumulated by fish, but to a much lesser extent than would be expected from its high $K_{O/W}$; observed bioconcentration factors (BCF) range from 100 to 900 (44, 45). This low BCF is attributable to the easy degradation of DEHP; only about 60% of the DEHP-derived residue in fish existed as parent compound (44), and the whole-body half-life of DEHP and metabolites was approximately 12 d at 25 °C. Studies on other fish also suggest rapid degradation of DEHP, at least as far as the monoester (46), but it is not clear whether degradation is a requirement for excretion. Aquatic invertebrates accumulate DEHP more rapidly and to higher BCF values than do fish (44, 45), which implies less efficient degradation.

Dielektrol II's minor component, 1,2,4-TCB, is also rapidly accumulated from water by trout, and its BCF is in the range of 10^3 (16, 47). However, elimination is also relatively rapid, with whole-body half-lives (substrate plus metabolites) of around 30 d (47). Slightly lower BCF values (200) and shorter whole-body half-lives (<7 d) have been reported in sunfish (45). The large amount of radioactivity found in bile after exposure of trout to ^{14}C-1,2,4-TCB suggests some metabolism (47).

Although metabolites in fish have not been rigorously identified, by

TABLE 3
Physicochemical properties governing the environmental behavior of some PCB replacements and a component of PCB mixtures

Material	Vapor pressure (torr, 25 °C)	Water solubility (ppm)	Log₁₀Ko/w
Midel 7131	1×10^{-7}	NA[a]	NA
Faradol 100	3×10^{-4}	<3[b]	NA
Wemcol	5×10^{-4}	1	5.23
KMC-A	5×10^{-4}	0.8	5.00
SAS-295	8×10^{-4}	0.5	5.38
C-4	1.1×10^{-4} [c]	0.14[c]	4.21[c]
Dielektrol II Component: 1,2,4-TCB	0.25[d]	NA	3.97[e]
PCB Component: 2,4,5,4',5'-pentachlorobiphenyl	8×10^{-6} [f]	0.01[f]	6.11[f]

[a] NA: Not available
[b] Manufacturer's technical literature
[c] Reference 61
[d] From Antoine equation (76)
[e] Reference 77
[f] Summarized from various sources (41)

Source: R. F. Addison, unpublished data unless otherwise stated

TABLE 4
Microbial degradation of PCB replacements and of PCBs under comparable conditions

Material	System and rate of degradation	Reference
RTEmp	Bacterial cultures: 50% in 7.7 d at 20 °C	(8)
Midels	E. coli culture: complete (no conditions listed)	Manufacturer's literature
Faradol	Unacclimated bacteria: 100% in 2 d	Manufacturer's literature
Wemcol	River die-away: 80% in 2 d Sewage sludge: 60% in 1 d Sewage sludge: 100% in <7 d	(17)
KMC-A PCB (Unspecified)	Activated sludge: 30–80% in 28 d Activated sludge: <5% in 28 d	(58)
C-4	Activated sludge: BOD_{10} 62% theoretical	(61)
Dielektrol II Components: DEHP	Activated sludge: 91% in 2 d Pond water: 20% in 28 d	(15)
1,2,4-TCB	Wastewater: 44–100% in 135 d	(78)
Chloralkylene	Activated sludge: no rates quoted; products identified	(23)

TABLE 5
Bioaccumulation and clearance from vertebrates of PCB replacements and of PCBs under comparable conditions

Material	Bioaccumulation factor	Clearance half-life (or similar)	Reference
Wemcol (4-isopropylbiphenyl)	NA[a]	<20% residues in 48 h (rat)	(38)
KMC-A	NA	55–270 h (rat)	(53)
PCBs	NA	Variable with structure, up to 27 d (rat)	(79)
Dielektrol II Components: DEHP	150–900	12 d @ 25 °C (minnow)	(44)
1,2,4-TCB	≈1000	≈30 d @ 12 °C (trout)	(47)
C-4	≈300	33–44 h @ 12 °C (trout)	(59)
KMC-A	≈200	56 h @ 25 °C (carp)	(57)
Chloralkylene	≈1000	38 h @ 25 °C (carp)	(28)
PCB (Clophen A-50)	≈10^4	≈20 d @ 22 °C (goldfish)	(80)

[a] NA: Not available

analogy with other vertebrates, phenols are probably formed. 2,4,5-trichlorophenol is a metabolite of 1,2,4-TCB in the frog (48); in addition, 2,3,5-trichlorophenol is formed by the rabbit (49). Invertebrates such as Daphnia can accumulate ^{14}C-1,2,4-TCB from water, but may not degrade it (45). 1,2,4-TCB also can be used by microorganisms found in natural or industrial waters (50).

Wemcol is degraded rapidly in river water and by sewage sludge (Table 4). Metabolic studies in rats—undertaken partly because of the potential of this material as an anti-inflammatory agent—showed it to be metabolized fairly rapidly by side-chain oxidation (18, 38). Forty-eight hours after 4-isopropylbiphenyl was fed to rats, less than 20% remained in the carcasses (Table 5) and approximately equal amounts were excreted in urine and feces; urinary metabolites included some ring-hydroxylated products. Its uptake or clearance by aquatic biota has not been described.

The components of KMC-A also are relatively degradable. 2-isopropyl naphthalene (a minor component) was cleared rapidly from the bloodstream of rats after single oral doses, according to a two-component polyexponential curve that represented "compartments" with half-lives of approximately 2 and 6 h. Its clearance from rat adipose tissue after prolonged feeding followed a two-compartment model, with half-lives of approximately 30 and 100 h (51).

2,6-diisopropylnaphthalene, one of the major KMC-A components, was cleared less rapidly; plasma clearance half-lives were about 2 and 20 h (52), and adipose tissue clearance half-lives (from a two-compartment model) were around 55 and 270 h (53). 2,6-diisopropylnaphthalene was degraded exclusively through side-chain oxidation to a mixture of acids, alcohols, and their conjugates, which were excreted in urine; these represented about 23% of the total dose (54). Fecal excretion (studied elsewhere) (55) could account for another 70% of the dose. It therefore seems unlikely that these isopropyl naphthalenes would accumulate appreciably in biota.

A slightly different series of metabolites, again produced by side-chain oxidation, is found in excreted material from carp exposed to 2,6-diisopropyl naphthalene (56, 57). Metabolism also seems slower than in the rat, although the data were not directly comparable. In activated sludge, KMC-A was degraded rapidly by side-chain oxidation and ring cleavage, the latter process leading to salicylic acid derivatives. Depending on conditions, 20–80% of KMC-A was degraded to carbon dioxide (CO_2) (58). In general, KMC-A appears to be fairly biodegradable, although the occurrence of its residues in estuarine sediments (20) shows that degradation is incomplete. The kinetics of KMC-A accumulation or clearance in fish have not been described.

Less is known about the behavior of the phenylxylylethanes. By analogy with KMC-A and the remote structural similarity to the DDT group of insecticides, metabolism would be expected to proceed along three lines, probably in decreasing order of importance: side-chain oxidation, xylyl ring methyl function oxidation, and ring hydroxylation or cleavage. No experimental evidence for any of these processes is available, but it might be inferred from the observation that residues of phenylxylylethanes were absent from samples in which diisopropyl naphthalenes were present (20). This assumes, however, that the phenylxylylethanes were used and disposed of in the same way as was KMC-A.

A ^{14}C analogue of dielectric fluid

C-4 showed a BCF of approximately 300 in rainbow trout (Table 5) and the whole-body clearance half-life was approximately 35–40 h at 12 °C. Some thin-layer chromatography evidence suggested that metabolism to polar products took place; these were not identified, but would probably be side-chain oxidation products (59). Ring hydroxylation products are formed from nonalkylated chlorodiphenyl ethers by the rat (60). $^{14}CO_2$ production from C-4 by activated sludge was about 45 times faster than from a trichlorobiphenyl (61).

The metabolism of the Chloralkylenes has been studied, particularly in comparison with that of the PCBs. The Chloralkylenes are fairly readily accumulated by organisms, but to a lesser extent than PCBs. Fish, for example, accumulated Chloralkylenes to an equilibrium BCF of approximately 10^3, whereas the BCF for two chlorobiphenyls was around 10^4 (28) (Table 5). The Chloralkylenes were eliminated more rapidly (with half-lives of less than two days) than were the chlorobiphenyls. Rapid elimination is probably attributable partly to metabolism; in a separate experiment with other Chloralkylene components, goldfish produced metabolites (found only in ambient water and not in fish tissues) consisting of side-chain oxidation products (26). Similar metabolites are produced by the frog (26), the rat (62), and the monkey (27).

"Parent" Chloralkylenes as well as various metabolites were found in soil treated with Chloralkylene-9 and in carrots grown in the soil (25). Fungi can degrade Chloralkylenes to hydroxylated and ring cleavage products (26). Chloralkylenes are also degraded photolytically more rapidly than the corresponding PCBs (63).

The relatively high MW silicones appear not to be appreciably accumulated or metabolized. Hobbs et al. (64) could not find any consistent accumulation of ^{14}C in tissues of fish exposed to labeled 300-cst fluid (average MW approximately 14 000, based on Equation 1). However, high MW silicones may not form true solutions, and in any case, these molecules may be too large to be absorbed by fish or other organisms. Any ^{14}C found in the fish probably arose from adsorption to external surfaces.

High MW silicones are not metabolized by mammals, probably because of the difficulty of absorbing or transporting them in circulatory systems. However, such compounds are converted in soils (presumably by microbial activity) to lower MW cyclic

or silanol products; rates of conversion are relatively slow (65).

Biological effects

Table 6 lists the acute oral toxicities of some PCB replacements to the rat. Acute toxicity may vary with factors other than the chemistry of the test compound including the sex and the reproductive and nutritional status of the organism, its age, and general health. It is therefore difficult to compare toxicity data unless they have been obtained under identical conditions, which is rarely the case.

The acute oral lethal dose (LD_{50}) of PCBs for rats is in the range of 4 to 11 g/kg of body weight, depending on the mixture tested and on test conditions (66). The majority of PCB replace-

ments have roughly similar acute toxicities (Table 6); the high MW silicones, PAO 13CE, and Faradol 100 are appreciably less toxic. In the case of silicones, this may be because their high MW precludes absorption.

Table 7 summarizes the acute toxicity of PCB replacements to aquatic organisms. The same caveats apply here as to Table 6, with the additional reservation that the data quoted may refer to *added* concentrations that may far exceed the aqueous solubility of the materials tested. Such data describe the toxicity of saturated solutions, rather than of the concentrations quoted.

Short-term static tests show the lethal concentrations (LC_{50}) to be in the range of 1 to 60 ppm (66), with values

---

TABLE 6

Acute oral toxicity of PCB replacements and PCBs to rats

Material	LD_{50} ($g \cdot kg^{-1}$)	Reference
Paraffins		
PAO 13CE	>40	Manufacturer's literature
Esters		
Faradol 100	25	Manufacturer's literature
Dielektrol II	4	Manufacturer's literature
Aromatics		
Wemcol	8.5	(17)
Aroclor 1016	1.6	(17)
KMC-A	≈5	(81)
SAS Mixtures	1.8	(81)
C-4	>10	(61)
Unspecified PCB	1.6	(61)
Silicones		
Various high MW silicones	>30	(71)

TABLE 7

Acute toxicity of PCB replacements and PCBs to aquatic organisms

Material	Organism	96-h LC_{50} (ppm)	Reference
Esters:			
Midel	Rainbow trout	1×10^5	Manufacturer's literature
Faradol 100	Unspecified fish	Moderately toxic	Manufacturer's literature
Dielektrol II	Bluegill	11	Manufacturer's literature
	Minnow	16	
Aroclor 1254	Minnow	1	
Aromatics:			
Wemcol	Bluegill	4	(17)
	Trout	2.5	
KMC-A	Yellowtail	2 $g \cdot kg^{-1}$ LD_{50}, intraperitoneal	(73)
C-4	Minnow	15.4	(61)
Silicones	Bluegill	>10 000	(64)

depending on the species of the test organism and the PCB mixture tested; the higher value exceeds the solubility of some PCB mixtures. The acute toxicities of the PCB substitutes are within this range, except those of the Midels and silicones, both of which are nontoxic at (presumably) saturated solutions. In a few cases, noted in Table 7, direct comparisons with PCBs have been made, and in such cases, the substitutes are less toxic than are the PCBs.

The value of acute toxicity as a criterion of environmental acceptability is debatable. Obviously, acutely toxic materials are undesirable, but the PCBs and their replacements can hardly be considered acutely toxic. There have been cases of acute toxicity attributed to PCBs—the Yusho incident (67) is the best known—but these have been the exceptions rather than the rule. In this instance, toxicity may have been caused, or aggravated, by polychlorinated dibenzofurans and polychlorinated quaterphenyls formed from PCBs (67, 68)—although to the victims, this distinction must appear academic. However, considering the concentrations at which PCBs usually occur in adventitiously contaminated samples, and at which PCB replacements are likely to be found, the detection and assessment of sublethal effects as early warnings of subtle or insidious long-term effects are probably more important.

Only a few studies have been made of such chronic or sublethal effects. Among the most detailed was a study of the effects of C-4 on rats. Up to 90 mg·kg^{-1}·d^{-1} of C-4 was fed to rats for 156 d. Only at the highest dose were any effects detected; these consisted of a slight swelling of the kidney and liver, which, in the case of the kidney, was rapidly reversible. In both cases, the effects were judged to be mild (69). Residues of C-4 accumulated in tissues, principally fat.

In another detailed study, KMC-A and the phenylxylylethane mixtures—each material at two levels—were fed to pregnant mice. No effects on body weight, reproductive success, infant survival, or infant growth up to 42 d after birth were detected (70). Thus, neither material appears to be chronically toxic.

In a study that was not as well documented, Wemcol was fed at various levels, up to 0.1% of their diet, to rats over a 28-d period, and no adverse effects were found (17). Also, high MW silicones (350 cst) were reported to have no teratogenic, reproductive, or mutagenic effects when fed to rabbits

and rats for an unspecified period (71). When fed to rabbits for 7 d at approximately 3 mL·kg^{-1}·d^{-1}, these materials had no effect on body or testis weights (72).

In addition to these gross and histopathological observations, some biochemical responses have been investigated. One well-established sublethal effect of PCBs is to induce the activity of liver microsomal mixed-function oxidases (MFOs) in various organisms. The induction of MFO enzymes may represent some diversion of normal metabolic activity to extra protein synthesis and presumably has some adaptive significance in inducing detoxification systems.

Although PCBs are powerful MFO inducers, their replacements studied so far have not been as effective. In trout, C-4 was inactive as an MFO inducer, in comparison with Aroclor 1254, when fed at the same dietary level (22), but KMC-A, SAS-295, and SAS-296 all induced MFO activity, though not as much as did Aroclor 1254 (19). Among other biochemical effects, diisopropylnaphthalenes administered to fish at relatively high doses affect serum enzymes in a way that suggests liver and kidney damage (73).

Impact assessment

It is possible to make some assessments of the probable environmental impact of PCB replacements. For instance, some materials, such as the Dow fluid C-4, are or will be produced on a relatively small scale and used under closely controlled conditions. The chance of their escaping to the environment is slim and, in any case, their properties are such that they would probably not be as persistent as the PCBs. Faradol 100 may be another example of such a material, but there is not enough information at present about production or use patterns to make this judgment.

Several PCB replacements are produced on a slightly larger scale, and in addition to closed uses, such as power capacitor dielectrics, they may have open uses. For instance, KMC-A and the phenylxylylethanes are used as ink solvents in pressure-sensitive copying papers, Wemcol is patented for this use, and the Midels closely resemble some specialty lubricants. Such materials are likely to reach the environment, but no information exists from which to estimate release rates. On the basis of limited information, these replacement materials are probably less persistent and hazardous than PCBs.

Some materials, such as (probably) the paraffins and (definitely) the polyalphaolefins, silicones, and DEHP, are chemicals now in heavy use, and the additional consumption arising from their employment as PCB replacements will be negligible. This does not mean that their possible environmental impact should be ignored; in fact, there has already been considerable interest in the possible environmental behavior of DEHP. On the basis of relatively limited data, it seems likely that most of the heavily used PCB replacements would be less persistent and hazardous than PCBs. Although the silicones persist, they seem to have negligible biological effects.

Unfortunately, these assessments are based on very few hard facts. The basic physicochemical data that would allow even rudimentary modeling of the possible environmental distribution of PCB replacements are rarely available. There is little of the more advanced information, such as degradation rates in different environmental compartments, to allow any comparison between replacement materials.

In view of the known partitioning of PCBs and the expected partitioning of PCB replacements to the atmosphere, it is surprising that almost nothing is known about how atmospheric photochemical processes will affect these materials. Finally, with the exception of C-4, possibly KMC-A and the phenylxylylethanes, and of the silicones, the chronic or sublethal biological effects of most of these materials remain unknown. In short, much less is known about PCB replacements—whose production and use are apparently accepted—than about the PCBs themselves, which are banned.

References

(1) *Chem. Eng. News*, Dec. 6, 1971, p. 15.
(2) Durfee, R. L.; Contos, G.; Whitmore, F. C.; Barden, J. D.; Hackman, E. E.; Westin, R. A. "PCBs in the United States: Industrial Use and Environmental Distributions," EPA Report 560/76-005, available as NTIS PB 252 012; 1976.
(3) OECD Environment Directorate Report,

Env. (82)5, Paris; 1982.

(4) Hutzinger, O.; Safe, S.; Zitko, V. "The Chemistry of PCBs"; CRC Press: Cleveland, Ohio, 1971.

(5) *Plast. Eng.*, April 1980, pp. 35–37.

(6) Krauskopf, L. B. "Plasticizers"; In "Modern Plastics Encyclopedia"; 1971–1972; pp. 270–73.

(7) Saperstein, M. D.; Faeder, E. J. *Regul. Toxicol. Pharmacol.* **1982**, *2*, 238–46.

(8) Piotrowski, M. "Toxicity, Transport and Mechanisms of Environmental Impact of Dielectric Fluids," RTE Report 78F1AE, RTE Corporation, Waukesha, Wis., 1978.

(9) *Can. Chem. Proces.*, Aug. 1977, p. 10.

(10) Onsuka, F. I. *J. Chromatogr.* **1977**, *186*, 259–71.

(11) *Chem. Abstr.* **1976**, *85*, 65533a; **1977**, *87*, 70816r.

(12) Addison, R. F.; Ackman, R. G.; Hingley, J. H. *J. Fish. Res. Board Can.* **1968**, *25*, 2083–90.

(13) Ackman, R. G.; Burgher R. D. *J. Am. Oil Chem. Soc.* **1965**, *42*, 38–42.

(14) Fefer, M. *J. Am. Oil Chem. Soc.* **1978**, *55*, 342A–45A.

(15) Pierce, R. C.; Mathur, S. P.; Williams, D. T.; Boddington, M. J. "Phthalate Esters in the Aquatic Environment," National Research Council of Canada Publication NRCC 17583, 1980.

(16) Smith, A. D.; Griffith, T. J.; Orr, D. E.; Ozburn, G. W. "Assimilation Efficiency and Clearance of Trichlorobenzenes in Rainbow Trout"; In "Aquatic Toxicology"; Eaton, J. G.; Parrish, P. R.; Hendricks, A. C., Eds.; STP 707; American Society for Testing and Materials: Philadelphia, 1980; pp. 216–23.

(17) Mercier, G. E. *Proc. Am. Power Conf.* **1977**, *39*, 1043–51.

(18) Tulp, M.T.M.; van Stein, G. C.; Hutzinger, O. *Chemosphere* **1978**, *7*, 747–59.

(19) Addison R. F.; Zinck, M. E.; Willis, D. E.; Wrench, J. J. *Toxicol. Appl. Pharmacol.* **1982**, *63*, 166–72.

(20) Sumino, K. *Arch. Environ. Contam. Toxicol.* **1977**, *6*, 365–69.

(21) Willis, D. E.; Zinck, M. E.; Addison, R. F. *Chemosphere* **1978**, *7*, 787–90.

(22) Addison, R. F.; Zinck, M. E.; Willis, D. E.; Darrow, D. C. *Toxicol. Appl. Pharmacol.* **1979**, *49*, 245–48.

(23) Sundstrom, G.; Hutzinger, O.; Karasek, F. W.; Michnowicz, J. *J. Assoc. Off. Anal. Chem.* **1976**, *59*, 982–88.

(24) Klesse, C.; Parlar, H.; Hustert, K.; Korte, F. *Chemosphere* **1981**, *10*, 1293–1305.

(25) Moza, P. N.; Scheunert, I.; Korte, F. *Arch. Environ. Contam. Toxicol.* **1979**, *8*, 183–89.

(26) Tulp, M.T.M.; Tillmans, G. M.; Hutzinger, O. *Chemosphere* **1977**, *6*, 223–30.

(27) Muller, W. F.; McMurray, T.; Coulston, F.; Korte, F. *Chemosphere* **1979**, *8*, 21–24.

(28) Sugiura, K.; Mase, T.; Imasaki, K.; Goto, M. *Bull. Environ. Contam. Toxicol.* **1981**, *26*, 46–53.

(29) Meals, R. "Silicones"; In "Kirk-Othmer Encyclopedia of Chemical Technology," 2nd ed.; Interscience: New York, 1969; Vol. 18, pp. 221–60.

(30) Smith, A. L. "Analysis for Traces of Silicones"; In "Analysis of Silicones"; Smith, A. L., Ed.; Wiley: New York, 1974; pp. 73–82.

(31) Pellenbarg, R. *Environ. Sci. Technol.* **1979**, *13*, 565–69.

(32) *Chem. Eng. News*, Dec. 8, 1975, p. 7.

(33) *Jpn. Chem. Week*, Dec. 27, 1979, pp. 1–2.

(34) *Chem. Mark. Rep.*, Oct. 20, 1980, p. 26.

(35) Broadhurst, M. G. *Environ. Health Persp.* **1972**, *2*, 81–102.

(36) National Research Council of Canada, Associate Committee on Scientific Criteria for Environmental Quality. "A Case Study of a Spill of Industrial Chemicals—Polychlorinated Biphenyls and Chlorinated Benzenes," NRCC 17586; Ottawa, Ontario, 1980.

(37) *Chem. Abstr.* **1979**, *90*, 191615t; **1981**, *94*, 23001f.

(38) Sullivan, H. R.; McMahon, R. E.; Roffey, P.; Hoffman, D. G.; Marshall, F. J.; Billings, R. E.; Benslay, D. N.; Marshall, W. S. *Xenobiotica* **1978**, *8*, 333–40.

(39) Robinson, K. S.; Kavlock, R. J.; Chernoff, N.; Gray, L. E. *J. Toxicol Environ. Health* **1981**, *8*, 489–500.

(40) Mackay, D.; Paterson, S. *Environ. Sci. Technol.* **1981**, *15*, 1006–14.

(41) Addison, R. F.; Paterson, S.; Mackay, D. *Chemosphere* **1983**, *12*, 827–34.

(42) Ratledge, C. "Degradation of Aliphatic Hydrocarbons"; In "Developments in the Biodegradation of Hydrocarbons—1"; Watkinson, R. J., Ed.; Applied Science Publishers: U.K., 1978; pp. 1–46.

(43) Renberg, L.; Sundstrom, G.; Sundh-Nygard, K. *Chemosphere* **1980**, *9*, 683–91.

(44) Mayer, F. L. *J. Fish. Res. Board Can.* **1976**, *33*, 2610–13.

(45) Macek, K. J.; Petrocelli, S. R.; Sleight, B. H. "Considerations in Assessing the Potential for, and Significance of, Biomagnification of Chemical Residues in Aquatic Food Chains"; In "Aquatic Toxicology"; Marking, L. L.; Kimerle, R. A., Eds.; STP667; American Society for Testing and Materials: Philadelphia, 1979; pp. 251–68.

(46) Stalling, D. L.; Hogan, J. W.; Johnson, J. L. *Environ. Health Persp.* **1973**, *3*, 159–73.

(47) Lech, J.; Melancon, M. "Uptake, Metabolism and Disposition of Xenobiotic Chemicals in Fish," EPA Report 600/3-80-082, available as NTIS PB 81-135329, 1980.

(48) Safe, S.; Jones, D.; Kohli, J.; Ruzo, L. O.; Hutzinger, O.; Sundstrom, G. *Can. J. Zool.* **1976**, *54*, 1818–23.

(49) Kohli, J.; Jones, D.; Safe, S. *Can. J. Biochem.* **1976**, *54*, 203–8.

(50) Pfaender, F. K.; Bartholomew, G. W. *Appl. Env. Microbiol.* **1982**, *44*, 159–64.

(51) Kojima, S.; Maruyama, K. *Eisei Kagaku* **1979**, *25*, 327–33.

(52) Kojima, S.; Nakagawa, M.; Suzuki, R.; Horio, M.; Tanaka, Y. *Chem. Pharm. Bull.* **1978**, *26*, 3007–9.

(53) Kojima, S.; Nakagawa, M.; Suzuki, R.; Horio, M.; Taniguchi, Y.; Tanaka, Y. *Eisei Kagaku* **1979**, *25*, 221–24.

(54) Kojima, S.; Honda, T.; Nakagawa, M.; Kiyozumi, M.; Takadate, A. *Drug Metab. Dispos.* **1982**, *10*, 429–33.

(55) Iwahara, S. *Boei Eisei* **1974**, *21*, 273–90.

(56) Kojima, H.; Saito, H.; Yoshida, T. *Chemosphere* **1982**, *11*, 1003–10.

(57) Yoshida, T.; Kojima, H. *Chemosphere* **1978**, *7*, 491–96.

(58) Yoshida, T.; Kojima, H. *Chemosphere* **1978**, *7*, 497–501.

(59) Blanchard, F. A.; Takahashi, I.; Alexander, H. C.; Bartlett, E. A. "Uptake, Clearance and Bioconcentration of ^{14}C-*sec*-butyl-4-chlorodiphenyl Oxide in Rainbow Trout"; In "Aquatic Toxicology and Hazard Evaluation"; Mayer, F. L.; Hamelink, J. L., Eds.; STP634; American Society for Testing and Materials: Philadelphia, 1977; pp. 162–77.

(60) Tulp, M.T.M.; Sundstrom, G.; Martron, L.B.J.M.; Hutzinger, O. *Xenobiotica* **1979**, *9*, 65–77.

(61) Branson, D. R. "A New Capacitor Fluid—A Case Study in Product Stewardship"; In "Aquatic Toxicology and Hazard Evaluation"; Mayer, F. L.; Hamelink, J. L., Eds.; STP634; American Society for Testing and Materials: Philadelphia, 1977; pp. 44–61.

(62) Tulp, M. T. M.; Sundstrom, G.; de Graaff, J. C.; Hutzinger, O. *Chemosphere* **1977**, *6*, 109–16.

(63) Ruzo, L. O.; Sundstrom, G.; Hutzinger, O.; Safe, S. *Chemosphere* **1976**, *5*, 71–76.

(64) Hobbs, E. J.; Keplinger, M. L.; Calandra, J. C. *Environ. Res.* **1975**, *10*, 397–406.

(65) Buch, R. R.; Ingebrigtson, D. N. *Environ. Sci. Technol.* **1979**, *13*, 676–79.

(66) World Health Organization. "Environmental Health Criteria 2: Polychlorinated Biphenyls and Terphenyls"; WHO: Geneva, 1976.

(67) Kuratsune, M. "Yusho"; In "Halogenated Biphenyls, Terphenyls, Naphthalenes, Dibenzodioxins and Related Products"; Kimbrough, R. D., Ed.; Elsevier: Amsterdam, 1980; pp. 287–302.

(68) Kashimoto, T.; Miyata, H.; Kunita, S.; Tung, T.-C.; Hsu, S.-T.; Chang, K.-J.; Tang, S.-Y.; Ohi, G.; Nakagawa, J.; Yamamoto, S.-I. *Arch. Environ. Health* **1981**, *36*, 321.

(69) Branson, D. R.; Humiston, C. G.; Jersey, G. C.; Boggs, G. U.; Schwetz, B. A. *Toxicol. Appl. Pharmacol.* **1978**, *45*, 245.

(70) Kawai, M.; Maruta, H.; Ueda, K.; Tojyo, K. *Nippon Eiseigaku Zasshi* **1977**, *31*, 637–43.

(71) Calandra, J. C.; Keplinger, M. L.; Hobbs, E. J.; Tyler, L. J. *Polym. Prepr.* **1976**, *17*, 14.

(72) Hobbs, E. J.; Fancher, O. E.; Calandra, J. C. *Toxicol. Appl. Pharmacol.* **1972**, *21*, 45–54.

(73) Ozaki, H.; Ikeda, Y. *J. Tokyo Univ. Fish.* **1976**, *62*, 147–57.

(74) Demianiw, D. G. "Higher Olefins"; In "Kirk-Othmer Encyclopedia of Chemical Technology", 3rd. ed.; Interscience: New York, 1981; Vol. 16, pp. 480–99.

(75) U.S. International Trade Commission. "Synthetic Organic Chemicals, U.S. Production and Sales, 1980," USITC Publication 1183; U.S. GPO: Washington, D.C., 1981.

(76) Kao, C.-I.; Poffenberger, N. "Chlorinated Benzenes"; In "Kirk-Othmer Encyclopedia of Chemical Technology," 3rd ed.; Interscience: New York, 1979; Vol. 5, pp. 797–808.

(77) Chiou, C. T.; Freed, V. H.; Schmedding, D. W.; Kohnert, R. L. *Environ. Sci. Technol.* **1977**, *11*, 475–78.

(78) Gaffney, P. E. *J. Water Pollut. Control Fed.* **1976**, *48*, 2731–37.

(79) Roberts, J. R.; Rodgers, D. W.; Bailey, J. R.; Rorke, M. A. "Polychlorinated Biphenyls: Biological Criteria for an Assessment of Their Effects on Environmental Quality," National Research Council of Canada Publication NRCC 16077, 1978.

(80) Hattula, M. J.; Karlog, O. *Acta Pharmacol. Toxicol.* **1973**, *32*, 237–45.

(81) Hasegawa, H.; Sato, M.; Tsurata, H. "Special Report on the Effects on Human Health and Chronic Toxicity of PCB and Other Pollutants to Prevent the Pollution from Them"; Science and Technology Agency of Japan: Tokyo, 1973; pp. 139–211.

Richard F. Addison has degrees in chemistry and agricultural chemistry from Queen's University, Belfast, Northern Ireland. Since 1975 he has been head of the Environmental Quality Division at Marine Ecology Laboratory, Bedford Institute of Oceanography. His research interests are in the distribution, metabolism, and sublethal effects of marine pollutants. He is currently chairman of the Environment Division of the Chemical Institute of Canada.

ES&T
PRODUCTS

Digital thermometer

Hand-held device has a resolution of ±0.1 °C over the temperature range −50–200 °C. An auto-ranging feature permits resolution of 1 °C over the range 200–650 °C, with a system accuracy of ±1 °C. Its full range is −100–650 °C. Hart Scientific **101**

Gas chromatograph

This chromatograph has a double oven and a valveless "live" column switching system. With this system, multidimensional chromatographic procedures such as backflushing the precolumn can improve resolution and save time. ES Industries **102**

HPLC internal standard kit

Each kit contains 1g each of nine alkylphenones. These are a family of neutral compounds whose retention value is not affected by solvent modifiers or buffers. Because of their wide solubility range, both polar and nonpolar solvent systems can be used. A common ultraviolet detector can measure nanogram quantities. Pierce Chemical **103**
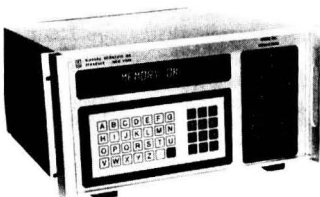

Data collection system

Microcomputer-based system automatically retrieves ambient air, water, or meteorological data from the field. The unit reduces and stores raw data, performs statistical computations, and telemeters them back to the central station. Many options are available including expanded storage, automatic calibration control, and special meteorological reduction software. Niagara Scientific **104**

Need more information about any items? If so, just circle the appropriate numbers on one of the reader service cards bound into this issue and mail in the card. No stamp is necessary.

Water-filtering system

Unit removes sediment and foul tastes and odors as well as several potentially hazardous organic chemical contaminants from the water supply. Twin filter housings contain carbon granules that take out up to 96% of trihalomethanes and substantially reduce traces of pesticides, dichloroethane, carbon tetrachloride, and several other compounds. A smaller cartridge removes sediment down to 20 μm in size. Ametek **105**
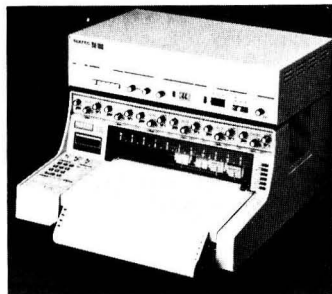
Transient recorders

Four-and six-pen recorders have an LED readout and keyboard entry operation. The pen speed is greater than 750 mm/s, and the programmable chart speeds range from 1000 cm/s to 100 cm/min in almost 3000 steps. This recorder also has a standard pen offset correction so that all channels are recorded with no offset error. SOLTEC **106**

Filter paper tape samplers

The samplers' flexible design permits a single instrument to sample particles or H_2S gas with only minor field modifications. They are designed for automatic, sequential sampling. Systems are available to evaluate sample spots continuously during the sampling period and provide an output signal to an integral or remote recorder. Andersen Samplers **107**

Fixed-wavelength detector

Differential light absorbance detector continuously and quantitatively monitors the absorbance of one liquid stream or the differential absorbance between two streams. High sensitivity with a small cell volume is achieved by

the combination of a full 10-mm absorption pathlength and a cell chamber diameter of only 1 mm. LDC/Milton Roy **108**

Vent adsorber

Constructed of polyvinyl chloride pipe and endcaps, stainless steel hardware, and a waterproof filter body, this unit treats vapors that are generated when a tank is filling. The filter does not require frequent replacement because it is cleaned by inlet air stripping while the tank is emptying. Adsorbent Products **109**

Recording system

System records up to six channels of analog input signal at frequencies from dc to 50 kHz. Each amplifier–signal digitizer channel operates as a 50-mV to 500-V, full-scale dc preamplifier, feeding directly into a recorder channel. When in the storage mode, this signal digitizer records higher frequencies by sampling analog signals and then stores these signals as 8-bit digital words in each channel's 8K memory. Gould **110**
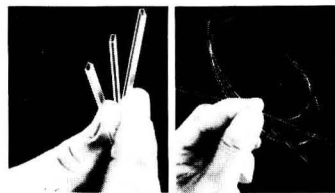
Small-diameter glass tubing

This tubing is available in circular, multibore, square, rectangular, and oval shapes as well as a wide variety of other irregular shapes with light and heavy wall weights. Friedrich & Dimmock **111**

Cleaning furnaces

Controlled pyrolysis is used to remove large amounts (up to 200 lb) of plastics, waxes, resins, hot-melt adhesives,

Companies interested in a listing in this department should send their releases directly to Environmental Science & Technology, Attn: Products, 1155 16th St., N.W., Washington, D.C. 20036

or other organic material from extruder hardware and other processing equipment. Automated cleaning cycle uses heat at 800–900 °F to safely decompose plastics and other organic residues to volatile pyrolysis smoke and gases in an oxygen-deficient atmosphere. The pyrolysis smoke and gases are consumed by pollution control equipment. Pollution Control Products **112**

Stack-sampling train
System determines organic compounds in stack gases, including principal organic hazardous constituents in hazardous waste incinerators. It conforms to the requirements of EPA Method 5. The train may be used for either stack gas sampling or combustion zone sampling, depending on the type of probe selected. Andersen Samplers **113**

Calibration gas generator
Portable instrument is designed for calibrating and checking chlorine or bromine gas detectors. It provides gas in air concentrations from 0 to 10 ppm, and the meter is calibrated for direct full-scale readings of 1.0, 3.0, or 10.0 ppm. SKC **114**

Fume exhaust hoods
Made of vinylester resin fiberglass for resistance to either acid or caustic vapors, these hoods are available in three standard sizes—$4 \times 4 \times 3$ ft, $4 \times 4 \times 5$ ft, and $4 \times 4 \times 10$ ft. Transparent front doors cover the full face of each unit. Fibrenetics **115**

Electronic balances
Two balances are available with 500-g and 5000-g capacities. They have large weighing pans, a vacuum fluorescent display, and are portable with an optional rechargeable battery. Both parallel BCD and serial RS232 outputs can be used to interface to a variety of computers and other devices. Printers specifically designed for these balances are also offered. Arbor Laboratories **116**

Formaldehyde dosimeter
In 1–4 h, this device monitors formaldehyde vapors in homes, offices, and work areas, measuring concentrations from 0.03 ppm to 1.0 ppm. The user returns the dosimeter after exposure to Envirotech Services for laboratory analysis. Envirotech Services **117**

Expanded software
Expanded software is now available for the IR/80 and IR/90 series FT–IR spectrometers. The software package uses the Gram–Schmidt thresholding technique to record and display the FT–IR trace in a format similar to that of the gas chromatographic detector. This provides an easy way of comparing peaks via retention times. Extensive postrun data manipulation capabilities are also available. IBM Instruments **118**

Oxygen probe
This uses a heated zirconia element at the probe end to measure percent oxygen in a smokestack, duct, or furnace. The concentration range is from 1 ppm to 100%, and the temperature range goes to 2850 °F. The heater element maintains a constant temperature regardless of the flue gas temperature. Datatest **119**

In-stack cascade cyclone
This device collects up to 1000 times more than typical cascade impactors because each stage has a 10-g capacity. Up to six stages are available. Each cyclone includes sampling nozzles, a backup filter, and attachments for EPA Method No. 5 or other stack samplers. Sierra Instruments **120**

High-voltage test instrument
High-voltage power supplies may be tested with this unit, which is suitable for laboratory use. It measures the load regulation and ripple and dynamic response of power supplies delivering up to 25 kV at 3 mA. The remote programming and monitoring features allow the unit to be integrated into automatic test equipment systems. Bertan **121**

Freeze dryer
Designed for laboratories handling moderate quantities of material, this dryer has a front panel with a "constant reading" electronic gauge. The gauge is accessible through the front panel for calibration. A built-in condenser temperature gauge continuously indicates both degrees Fahrenheit and Celsius. Labconco **122**

Safety bottle cover
This is designed for safer handling and storage of solvents and hazardous liquids in glass bottles. Made of chemically resistant polyethylene, the two-piece bottle cover fits securely around glass bottles to provide three-way protection. Burdick & Jackson Laboratories **123**

Digital colorimeter
Two concentration ranges as well as absorbance and percent transmittance can be read directly on the high-contrast liquid crystal display. The universal cuvette holder permits the use of square cuvettes up to 12.5 mm and round tubes up to 19-mm diameter. Chemtrix **124**

Gas analyzer
This quadrupole analyzer is very easy to use, according to the manufacturer. "Soft keys" can be operated by anyone without programming experience. A library of cracking patterns, including all common semiconductor processing gases, is built in. NGS Associates **125**

Micro dispensers
Designed for fast, repetitive dispensing of microliter volumes directly from small vials and bottles, these dispensers are available in both fixed and adjustable volume models covering the range 10–1000 μL. Reagent bottles or vials attach to the dispenser, allowing direct dispensing into test tubes or other vessels. Brinkmann Instruments **126**

Dry ice keeper
Rugged dry ice storage container has 2-in.-thick walls of insulation enclosed by a heavy-duty polyethylene inner and outer case. In this container, 75 lb of dry ice last up to six days. Polyfoam Packers **127**

ES&T
LITERATURE

Aerosol sampling. Brochure describes the FASTAC II sampler, said to be the only atomic absorption (AA) autosampler that uses aerosol deposition of the sample for furnace atomization. It is 10 times more efficient than the previous model. Instrumentation Laboratory **151**

Environmental analysis. Brochure describes complete hazardous waste analyses, priority pollutant analyses, water analyses, and air scans. It describes a fully instrumented and computerized laboratory. Crippen Laboratories **152**

Gas analyzer. Bulletin TI 612-106 describes an analyzer that meets needs for carbon monoxide (CO), carbon dioxide (CO_2), and methane (CH_4) analysis. It has applictions in ambient air and stacks and uses nondispersive infrared radiation. Foxboro **153**

Toxic chemical handling. Wall chart gives information on handling, storage, and disposal of more than 300 toxic and hazardous chemicals found in industry. Lab Safety Supply **154**

Toxic organic gas monitors. Catalog describes portable and stationary monitors for organic vapors in industrial environments and gives related information. Analytical Instrument Development **155**

Laboratory microcomputers. Bulletin 679 features selected microcomputer hardware and software for laboratory and other requirements. Printer terminal is included. Fisher Scientific **156**

Freeze drying. Catalog contains information on and complete specifications for freeze-drying apparatus. Sample preservation is one of many possible applications. Labconco **157**

Pipe linings. Brochure AB-72 describes a line of abrasion-resistant pipe and equipment linings with a Mohs hardness of 8. Abresist **158**

Closed-loop cooling. Bulletin describes proper protection of closed-loop cool-

ing and heating systems and lists four factors that can cause severe damage. Mogul **159**

Catalytic emission control. Brochure, "Torvex Catalytic Reactor," explains how catalysts enhance air pollution control, incineration, and solvent vapor, visible emission, and odor abatement. Engelhard **160**

Sewer conductivity cell. Catalog sheet 221-02 describes an electrodeless conductivity cell for detecting solutions in industrial sewer lines that may cause fouling because of suspended solids or fibers. Beckman Instruments **161**

Biological research. Catalog describes multiple-diffusion chambers for the study of mixed-culture interactions and biological air samplers. Cellular interactions in many environments can be studied. New Brunswick Scientific **162**

Water test kits. "1983 Water Test Kit Directory" lists portable test kits for measurement of water and wastewater quality, with applications to many specific types of analysis. LaMotte Chemical Products **163**

Continuous-process mixer. Brochure describes Polycoated Inliner stationary mixer, which prevents particle cling, is abrasion resistant, and is impervious to many corrosive environments up to 300 °C. Lightnin **164**

Respirators. Wall chart shows all 17 recent NIOSH/OSHA approvals granted to HSC's cartridge-filter combinations for respirators. Air-cleaning cartridge is properly matched up with contaminant. HSC **165**

pH measurement. Brochure introduces the injection flow electrode concept to pH measurement. Free-flowing liquid junction does not clog. Hach **166**

Water clarifier. Catalog covers sloped-plate clarifiers, designed as alternatives to conventional bowl-type thickeners for removing suspended solids from wash water for recycling or discharge. Eagle Iron Works **167**

Microbial growth study. Reprint by E. S. Littmann explains how to monitor microbial growth by adenosine triphosphate assay with the Model 20 photometer and luminescence purity reagents. Turner Designs **168**

Hazardous materials. Catalog lists products, supplies, and forms necessary for compliance with government specifications concerning hazardous materials handling. J. J. Keller & Associates **169**

Meteorological instruments. Product portfolio lists meteorological instruments, including those for measuring wind and temperature. Many have environmental monitoring applications. R. M. Young **170**

Home solar power. Brochure announces photovoltaic (solar-electric) equipment that can be used to power certain appliances in homes, boats, and campers. It can charge batteries and drive 12-VDC equipment. Solar Power **171**

Density measurement. Brochure announces Mettler/Paar DPR2000 in-line density measuring system for quality and process control and purity measurements. Mettler Instrument **172**

Industrial gases. Brochure describes company's capabilities in the field of industrial gases for wastewater treatment, oil recovery, and many other applications. ANSUTECH **173**

Micro pipets. Catalog lists line of micro pipets and dispensers for research, industry, and clinical testing. Monoject Scientific **174**

Aerosol monitor. Releases announce the APS-33 Aerodynamic Particle Sizer data sheet and the piezoelectric respirable aerosol mass monitor. Faster, more precise measurement is possible. TSI **175**

HPLC columns. Brochure lists empty HPLC columns, fittings, connectors,

and fitting kits. Precut tubing kits are also listed. Alltech **176**

pH electrodes. Bulletin 7732 tells how to choose pH electrodes, buffers, and accessories for specific applications. A step-by-step decision sequence is presented. Beckman Instruments **177**

HPLC components. Catalog lists HPLC items such as injectors, valves, fittings, and syringes. Some are made of Teflon, for applications in which contact with metals is not wanted. Rheodyne **178**

Continuing education. Brochure announces availability of cassettes for continuing education in 18 engineering disciplines. Included are air pollution, solar energy, and phase behavior in oil recovery processes. Association for Media-Based Continuing Education for Engineers, Inc., 225 North Ave., Atlanta, Ga. 30332 (write direct)

Renewable-resource chemicals. Announcement No. 460/X lists publications on chemical feedstocks from renewable resources. D. W. Jared, Oak Ridge National Laboratory, Union Carbide Corp., Nuclear Division, P.O. Box X, Oak Ridge, Tenn. 37830 (write direct)

Nuclear power. Brochures list numerous publications on nuclear power and related topics. American Nuclear Society, 555 N. Kensington Ave., La-Grange Park, Ill. 60525 (write direct)

Cyanides from minerals. Report from a workshop focuses on all chemical aspects of cyanides as they relate to the gold and silver mining industry and froth flotation. Ferron A. Olson, Director, Utah MMRRI, University of Utah, 209 W. C. Browning Bldg., Salt Lake City, Utah 84112 (write direct)

Potentially toxic chemicals. "IRPTC Bulletin" is the "International Register of Potentially Toxic Chemicals," published by the United Nations Environment Programme. Director, IRPTC/UNEP, Palais des Nations, 1211 Geneva 10, Switzerland (write direct)

Available wastes. What is waste for some is useful material for others. Whole listing. Issue No. 9, August 1983, Northeast Industrial Waste Exchange, 700 E. Water St., Room 711, Syracuse, N.Y. 13210 (write direct)

ES&T
BOOKS

Hazardous Materials Emergencies. John R. Cashman. 400 pages. Technomic Publishing Co., Inc., Box 3535, Lancaster, Pa. 17604. 1983. $45, hardcover.

This book discusses types of emergencies, response teams, equipment, strategies, techniques, and case histories. References are provided.

Flow Phenomena in Porous Media. Robert A. Greenkorn. ix + 550 pages. Marcel Dekker Inc., 270 Madison Ave., New York, N.Y. 10016. 1983. $75, hardcover.

This book is concerned mainly with fundamentals and applications of petroleum production, water recovery, and crop growth. Conducting these endeavors in an environmentally safe manner requires knowledge of the nature of macroscopic and microscopic porous media and their relations to mechanistic flow phenomena.

Siting Hazardous Waste Management Facilities. xii + 71 pages. National Audubon Society, 115 Indian Mound Trail, Tavernier, Fla. 33070. 1983. $3, paper.

This work addresses such issues as how human health and the environment can be protected; accidents and failures; and how chances of failures can be reduced. The problem of obtaining new public revenue from a site and effects on attraction of new industry and on local property values are discussed.

Pest Resistance to Pesticides. George P. Georghiou, Tetsuo Saito, Eds. xi + 809 pages. Plenum Press, 233 Spring St., New York, N.Y. 10013. 1983. $89.50, hardcover.

This book examines the origins and dynamics of insect, fungal, bacterial, and other resistance to pesticides, mechanisms of resistance development, and suppression and management of resistance that may develop. Insecticides, fungicides, and herbicides are covered.

Resource Recovery Guide. James G. Abert, Ed. xi + 593 pages. Van Nostrand Reinhold Co., 135 W. 50th St., New York, N.Y. 10020. 1983. $44.50, hardcover.

This work discusses waste as a source of raw materials and energy. It covers recycling of many materials and financial and economic aspects. Also examined is energy recovery through direct combustion, pyrolysis, and other means.

Carcinogenicity and Toxicity of Benzene. Myron A. Mehlman, Ed. viii + 128 pages. Princeton Scientific Publishers Inc., P.O. Box 3159, Princeton, N.J. 08540. 1982. $42, hardcover.

This book is Vol. IV of the series "Advances in Modern Environmental Toxicology." It reviews myths and facts of benzene carcinogenicity, relationships between the toxicity and metabolism of benzene, immune system and blood effects, benzene in ambient water, and worker protection.

Proceedings, Seminar on Groundwater and Petroleum Hydrocarbons: Protection, Detection, Restoration. Petroleum Association for Conservation of the Canadian Environment, 1202-275 Slater St., Ottawa, Ontario K1P 5H9, Canada. Inquire as to price. Paper.

The seminar was held in Toronto in June. Its basic aim was to convey the petroleum industry's recognition that it has a great responsibility to conserve vulnerable groundwater resources. Various strategies are discussed.

Too Hot to Handle? Social and Policy Issues in the Management of Radioactive Wastes. Charles A. Walker et al., Eds. xiii + 209 pages. Yale University Press, 82A Yale Station, New Haven, Conn. 06520. 1983. $5.95, paper.

Chapters cover topics such as the history of radioactive waste management in the U.S., public health risks, public attitudes about nuclear wastes, the science and technology of processes that make these wastes and methods proposed for handling them, and political issues involved.

Remedial Action for Waste Disposal Sites. P. J. Rogoshewski et al. xii + 497 pages. Noyes Data Corp., Mill Road at Grand Avenue, Park Ridge, N.J. 07656. 1983. $36, hardcover.

This book presents the latest advances in managing wastes disposed of improperly on land. Such advances entail newer methods of surface controls, groundwater and leachate controls, contaminated sediment removal, direct treatment of wastes, and controls on gas migration.

Nonconventional Energy Resources. Philip R. Pryde. xv + 270 pages. Wiley-Interscience, John Wiley & Sons, Inc., 605 Third Ave., New York, N.Y. 10016. 1983. $19.95, hardcover.

Fossil fuels are certainly finite, and nuclear power is fraught with political and perhaps technical problems. Which way should we go? One possibility is small- and large-scale hydroelectricity; another is ocean energy. Still other alternatives include solar, wind, and geothermal energy, biomass, and hydrogen.

Environmental Radioanalysis. H. A. Das et al. vi + 298 pages. Elsevier Science Publishing Co., Inc., 52 Vanderbilt Ave., New York, N.Y. 10017. 1983. $83, hardcover.

This book deals explicitly with radioanalysis. Chapters include neutron activation analysis, radiotracer measurements for environmental studies, analytical criteria, radioanalysis of water, and practices in environmental radioanalysis.

Catalytic Processing in Petroleum Refining. Esber I. Shaheen, 264 pages. PennWell Publishing Co., P.O. Box 1260, Tulsa, Okla. 74101. 1983. $45.95, hardcover.

This book covers many aspects of refining, including cracking operations, reforming, alkylation, and polymerization. One important chapter discusses typical processes for removing major air pollutants. The author is president of the International Institute of Technology, Inc., Joplin, Mo.

Atmospheric Deposition. 476 pages. Publications Department, Air Pollution Control Association, P.O. Box 2861, Pittsburgh, Pa. 15230. 1983. $30 ($25 for APCA members), hardcover.

This book presents 33 papers from a specialty conference on atmospheric deposition. It discusses global and regional deposition sources, models and receptors, nonacidic deposition effects on organics and metals, and deposition control costs and benefits. Source–receptor relationships and control strategies also are considered.

Seasonal Variations in the Nature and Removability of Reservoir THM Precursors. Bulletin 127. Robert C. Hochn et al. xi + 128 pages. Virginia Water Resources Research Center, 617 N. Main St., Blacksburg, Va. 24060-3397. 1983. $6, paper ($8 if billed; free to residents and organizations in Virginia).

This study emphasizes the importance of biological activity in altering the nature of dissolved organic carbon (DOC) in a reservoir, especially that portion that can become trihalomethanes (THMs). Studies and their results are presented.

Natural Levels of Lead in Humans. Clair C. Patterson. 58 pages. Institute for Environmental Studies, University of North Carolina, 311 Pittsboro St.,

256 H, Chapel Hill, N.C. 27514. $3, paper.

This essay is based on a lecture that Patterson presented March 22, 1982, at Chapel Hill. It represents a synthesis of his more than 20 years of research on this subject.

Pest Control with Nature's Chemicals. Elroy L. Rice. 240 pages. University of Oklahoma Press, 1005 Asp Ave., Norman, Okla. 73019. 1983. $28.50.

Nonnutritional chemicals with which plants influence other plants and animals are known as *allelochemics;* chemical messengers between animals are *pheromones.* This book explains how allelochemics and pheromones help to carry out functions such as pest killing or repulsion, and how these features might be put to use in pest management.

Compilation of Water Resources Computer Program Abstracts. Charles A. Kohlhaas, Ed. 188 pages. Abstracts, 50 Broad St., 19th Floor, New York, N.Y. 10004. 1983. $50, paper.

This compilation contains abstracts that document nonproprietary com-

puter programs in the water resources and water quality fields.

Groundwater Monitoring Technology. Robert D. Morrison. 132 pages. Timco Mfg., Inc., 851 15th St., Prairie du Sac, Wis. 53578. 1983. $31 (+$2 for shipping; outside U.S., add $12).

This book covers three major topics: monitoring in the vadose (unsaturated) zone; monitoring in the saturated zone; and sampling equipment. Sampling site selection and site preparation, equipment calibration, sample and site contamination, collection methods, and many other pertinent subjects are discussed.

20 Simple Solar Projects. Elizabeth Calhoun. 256 pages. Rodale Press, Inc., 33 E. Minor St., Emmaus, Pa. 18049. 1983. $16.95, hardcover.

This book offers a variety of solar "do-it-yourself" projects. Examples consist of cookers, a flat-plate collector, a window greenhouse, a small irrigation system, and a battery charger. Proponents of solar energy maintain that the use of such energy reduces the need for forms they say harm the environment.

Oct. 12–13 Gaithersburg, Md.
Workshop on the Analysis of Volatile Organic Chemicals in Water. Chemical Manufacturers Association
Write: William Gulledge, Chemical Manufacturers Association, 2501 M St., N.W., Washington, D.C. 20037; 202-887-1188

Oct. 16–18 Wildwood Crest, N.J.
21st Annual Fall Water Resources Conference: "The Delaware—A Basin in Transition." Water Resources Association of the Delaware River Basin
Write: Bruce E. Stewart, Executive Director, WRA/DRB, Box 867, Davis Rd., Valley Forge, Pa. 19481; 215-783-0634

Oct. 26–28 Columbus, Ohio
8th International Symposium on Polynuclear Aromatic Hydrocarbons. Battelle's Columbus Laboratories
Write: Denise Sheppard, Battelle's Columbus Laboratories, 505 King Ave., Columbus, Ohio 43201; 614-424-5532

Oct. 27–28 San Diego, Calif.
Groundwater Investigations at Hazardous Waste Sites: Safety and Liability Considerations. National Water Well Association
Write: Kathy Butcher, National Water Well Association, 500 W. Wilson Bridge Rd., Worthington, Ohio 43085; 614-846-9355

Oct. 31–Nov. 1 Philadelphia, Pa.
Symposium on Rationale for Sampling and Interpretation of Ecological Data in Assessment of Fresh Water Ecosystems. American Society for Testing and Materials
Write: Earl Sullivan, ASTM, 1916 Race St., Philadelphia, Pa. 19103; 215-299-5514

Nov. 1–4 New Orleans, La.
EPA/EPRI Symposium on Flue Gas Desulfurization. EPA and Electric Power Research Institute
Fee: $80. *Write:* Tasia Toombs, Electric Power Research Institute, P.O. Box 10412, Palo Alto, Calif. 94303; 415-855-8973

Nov. 1–4 New Orleans, La.
Joint Conference on Occupational Health. American Academy of Occupational Medicine and American Academy of Industrial Hygiene
Fee: $105 ($95 for AAOM and AAIH members). *Write:* Donald L. Hoops or Elizabeth Cameron, 2340 S. Arlington Heights Rd., Arlington Heights, Ill. 60005; 312-228-6850

Nov. 2–3 New Orleans, La.
4th ASTM Symposium on Pesticide Applications. ASTM Committee E-35 on Pesticides
Write: Thomas M. Kaneko, BASF Wyandotte Corp., Wyandotte Mich. 48192; 800-521-9100 or 313-282-3300

Nov. 3–4 Arlington, Va.
Hazardous Waste Regulations, 1983 Update. Government Institutes Inc.
Write: Brooke C. Larsen, Government Institutes, Inc., 966 Hungerford Dr., No. 24, Rockville, Md. 20850; 301-251-9250

Nov. 6–9 Arlington, Va.
4th Annual Meeting of the Society of Environmental Toxicology and Chemistry. Society of Environmental Toxicology and Chemistry
Write: SETAC, P.O. Box 352, Rockville, Md. 20850; 301-468-6704

Nov. 9–11 Orlando, Fla.
Regional Workshop on Composting and Land Application. *BioCycle* magazine and Florida Department of Environmental Regulation
Fee. $175. *Write:* Mildred Lalik, *BioCycle*, Box 351, Emmaus, Pa. 18049; 215-967-4135

Nov. 13–16 Lexington, Ky.
1983 Eastern Oil Shale Symposium. Kentucky Energy Cabinet and University of Kentucky
Write: Connie Blakemore, University of Kentucky, Institute for Mining and Minerals Research, P.O. Box 13015, Lexington, Ky. 40512; 606-252-5535

Nov. 14–17 Las Vegas, Nev.
5th International Conference on Used Oil Recovery and Reuse: "Theory to Reality." Association of Petroleum Re-refiners and other sponsors
Write: Association of Petroleum Re-refiners, 2025 Pennsylvania Ave., N.W., Suite 1111, Washington, D.C. 20006; 202-833-2694; Telex: 904059 WSH

Nov. 15–17 Houston, Tex.
6th International Coal and Lignite Utilization Conference: "Coal Technology '83."
Write: Coal Technology '83, P.O. Box 721948, Houston, Tex. 77272; 713-879-8929; Telex: 790-821 INDPRES HOU

Nov. 29–30 Toronto, Ontario
Technology Transfer Conference No. 4. Ontario Ministry of the Environment
Write: M. Moselhy, MOE Policy and Planning Branch, 135 St. Clair Ave. W., Toronto, Ontario M4V 1P5, Canada; 416-965-5788

Nov. 29–Dec. 2 Atlanta, Ga.
6th World Energy Engineering Congress. Association of Energy Engineers
Write: 6th World Energy Engineering Congress, 4025 Pleasantdale Rd., Suite 340, Atlanta, Ga. 30340; 404-447-5083

Dec. 4–7 Norfolk, Va.
11th Annual Water Quality Technology Conference. American Water Works Association
Fee: $225. *Write:* American Water Works Association, 6666 W. Quincy Ave., Denver, Colo. 80235; 303-794-7711

Dec. 6–8 Atlanta, Ga.
EPRI PCB Seminar. Electric Power Research Institute
Write: Gil Addis or Ralph Komai, EPRI, P.O. Box 10412, Palo Alto, Calif. 94303; 415-855-2286 or 415-855-2463

Dec. 6–9 East Lansing, Mich.
Dioxins in the Environment. Michigan State University and other sponsors
Fee: $50. *Write:* R. W. Leader or Michael Kamrin, C-231 Holden Hall, Michigan State University, East Lansing, Mich. 48824; 517-353-6469

Jan. 30–Feb. 3 Lake Buena Vista, Fla.
8th Annual Meeting on Energy from Biomass and Wastes. Institute of Gas Technology
Write: Maryann Manrot, Institute of Gas Technology, 3424 S. State St., Chicago, Ill. 60616; 312-567-3881; Telex: 25-6189

COURSES

Oct. 20–21 Hartford, Conn.
EPA Stationary Source Dispersion Models: Theory and Application. Air Pollution Control Association
Fee: $330 ($300 for APCA members). *Write:* John McGovern, Air Pollution Control Association, P.O. Box 2861, Pittsburgh, Pa. 15230; 412-621-1090

Oct. 27–28 Park Ridge, Ill.
Gas Analysis Techniques in GC. Varian Instrument Group
Fee: $320. *Write:* Training Department, Varian Instrument Group, P.O. Box 9020, Walnut Creek, Calif. 94598; 415-939-2400, ext. 2533

Nov. 3–4 Washington, D.C.
Hazardous Wastes Regulations Course. Government Institutes, Inc.
Fee: $595 with handbook; $515 without. *Write:* Government Institutes, Inc., 966 Hungerford Dr., No. 24, Rockville, Md. 20850; 301-251-9250

Nov. 7–11 Austin, Tex.
Advanced Water Pollution Control: Physical and Chemical Waste Treatment. The University of Texas at Austin
Fee: Inquire. *Write:* Continuing Engineering Studies, College of Engineering, Cockrell Hall 2.102, University of Texas, Austin, Tex. 78712; 512-471-3506 or 512-471-3396

INTERNATIONAL

Nov. 8–11 Hiroshima, Japan
5th International Conference on Boundary Elements. Hiroshima Institute of Technology
Fee: $350. *Write:* Conference Secretary, Computational Mechanics Centre, Ashurst Lodge, Ashurst, Southampton SO4 2AA, U.K.

Nov. 23–25 Noordwijkerhout, The Netherlands
Anaerobic Wastewater Treatment, European Symposium
Write: Symposium Secretariat, The Congress Bureau of TNO Communication Department, P.O. Box 297, 2501 BD, The Hague, The Netherlands; Phone: (070) 81 44 81, ext. 411 or 458; Telex: 31660 TNOGV NL

CALL FOR PAPERS

Nov. 15 deadline (abstracts)
20th Annual American Water Resources Association Conference and Symposium. American Water Resources Association
The conference will be Aug. 13–16, 1984, in Washington, D.C. *Write:* Warren Viessman, Jr., A. P. Black Hall, University of Florida, Gainesville, Fla. 32611; 904-392-0834

Nov. 15 deadline
IAWPR's Biennial International Conference on Water Pollution. International Association on Water Pollution Research
The conference will be Sept. 17–20, 1984, in Amsterdam, The Netherlands. *Write:* IAWPR, Alliance House, 29/30 High Holborn, London WC1V 6BA, U.K.

professional consulting services directory

CLASSIFIED SECTION ■ POSITIONS OPEN

USE THE CLASSIFIED SECTION

INDEX TO THE ADVERTISERS IN THIS ISSUE

ES&T RESEARCH

Optimization of Purging Efficiency and Quantification of Organic Contaminants from Water Using a 1-L Closed-Loop-Stripping Apparatus and Computerized Capillary Column GC/MS

W. Emile Coleman, * **Jean W. Munch, Robert W. Slater, Robert G. Melton, and Frederick C. Kopfler**

Health Effects Research Laboratory (HERL), U.S. Environmental Protection Agency, Cincinnati, Ohio 45268

■ Optimization of a HERL-designed 1-L closed-loop-stripping (CLS) system, using variations of sample water bath temperatures and purging times, was accomplished by spiking five 1-chloroalkanes (C_6, C_8, C_{12}, C_{16}, and C_{18}) into low organic Milli-Q reagent water to determine the recovery efficiency of each. Average recovery of the C_6, C_8, C_{12}, and C_{16} chloroalkanes exceeded 97% after CLS of water samples for 2 h at a sample bath temperature of 40 °C; the C_{18} chloroalkane's average recovery was 63% under the same conditions. Once operating conditions of purging time and water bath temperature were determined, on the basis of optimum recovery of the 1-chloroalkanes, recovery studies of a 22-compound standard mixture of organics were initiated by using two 1-L CLS devices of different design.

Introduction

CLS and computer-assisted capillary column GC/MS have been used routinely in this laboratory for the past 5 years to analyze organic compounds at the parts per trillion (nanograms per liter) level. Most of the compounds detected were in the 50–400 molecular weight range. Validation and applications of CLS as described by Grob (*1*) were discussed previously (*2–4*). In these previous studies (*2, 3*) a CLS device consisting of a 3.8-L (1 gallon) jug and computer-assisted glass capillary GC/MS and automatic quantitation procedures based on single mass ion quantification were used to provide results from repetitive CLS of standard compounds in water at the 10–100 ng/L level for statistical evaluation. Single ion quantification was used to resolve the effects of overlapping and coeluting GC peaks. Quantification is based on the ion current area of a single selected mass ion in a given mass spectrum, instead of the area produced by the summation of all ions in the mass spectrum. This ion is usually unique to a compound that may coelute with one or more compounds to produce ambiguous mass spectra. Statistical results (*3*) using the 1-gallon CLS device showed relatively low recovery efficiencies for many of the test compounds (average 45%) with an average relative standard deviation (RSD) of 30%. It was thought that the observed low recovery of higher molecular weight compounds and the imprecision of the 1-gallon CLS device could be improved by (1) purging a smaller volume with the same system, (2) better controlling the temperature of the gas entering the filter and of the filter itself, (3) increasing the temperature

of the sample water bath, and (4) eliminating as much metal as possible in the closed loop between the sample bottle and the activated carbon trap. Figure 1 shows the 1-L CLS system currently in use in this laboratory. This paper discusses the optimization of the 1-L CLS system using variations of the four experimental parameters above as determined by optimum recovery of 1-chloroalkanes. Results from a commercial CLS system are also discussed and compared with the HERL 1-L CLS system. All accuracy and precision data in this report involve the use of the total analytical method, including all operations from the stripping of test compounds in water to the automatic computerized quantification of these compounds by the capillary GC/MS data system.

Experimental Section

Description of the 1-L CLS System. We have taken the CLS system discussed by Coleman (*2, 3*) and rebuilt and modified the apparatus so that it measures purgeable organics in 1-L samples instead of 1-gallon samples (see Figure 1). Air is continually recirculated through the closed-loop system by means of a pump (Metal Bellows Corp. Model MB-21). Air flows from the pump, through $^1/_8$-in. (3 mm) stainless steel tubing and a metal frit, and bubbles through the water sample which is immersed in a thermostatically controlled water bath (MGW–Lauda Model T1). To accomodate the inlet and exit lines, the poly(tetrafluorethylene) (PTFE) liner is removed from the sample bottle (1-L Wheaton/Kimler graduated culture media bottle) cap and a $^3/_4$-in. (20 mm) hole is drilled through it. The $^1/_8$-in. stainless steel inlet and exit lines are silver soldered to a stainless steel disk of the same inside diameter as the bottle cap. The disk with air lines attached is placed into the bottle cap; the bottom of the disk is covered with a PTFE washer; and the cap is screwed firmly onto the 1-L bottle. The sparging device, which includes the inlet and exit lines, bottle cap, frit, disk, and washer, is very similar to the one reported by Coleman (*2*). The $^1/_8$-in. stainless steel tube exiting the bottle is just long enough to allow it to be connected to the bottom of a Graham condenser (Corning) modified by attaching a $^1/_4$-in. glass tube. A $^1/_4$-$^1/_8$-in. stainless steel Swagelok reducing union with PTFE ferrules is used to make this connection. The condenser is heated with 95 °C water from a recirculating bath (Haake Model FJ). The top portion of the condenser is also modified by removing 2.5 in. of glass tubing beyond the water jacket, replacing it with
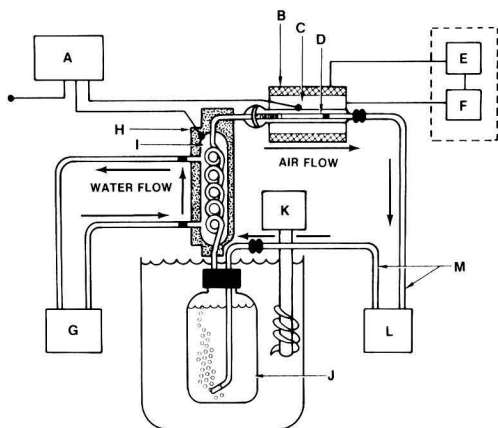
Figure 1. HERL closed-loop-stripping apparatus (Aug 1980). Key: (A) temperature monitor; (B) heater block insulation; (C) aluminum heating block with cartridge heater; (D) glass filter holder with carbon filter; (E and F) temperature controller (maintains 50 °C); (G) thermostatically controlled water circulator for I (set at 95 °C); (H) foam insulation; (I) glass condensing column; (J) 1-L sample bottle; (K) thermostatically controlled water bath circulator (set at 40 °C); (L) Metal Bellows air pump; (M) $^1/_8$-in. stainless steel tubing.

the male half of the glass filter holder, and making a 90° bend. The activated carbon filter is placed in the female half of the filter holder, and the two halves of the holder are joined with spring clips. The filter and filter holder rest in an aluminum block $3 \times 3^1/_2 \times 1^3/_4$ in. (7.6 × 9 × 4.5 cm) heated and monitored by an Omega Model 4001 JC temperature controller. The $^1/_4$-in. (6 mm) glass exit end of the filter holder is connected to the stainless steel tubing leading to the pump with a Swagelok reducing union as previously described.

Optimization of the 1-L CLS system was accomplished by performing replicate CLS GC/MS analyses of five 1-chloroalkanes (C_6, C_8, C_{12}, C_{16}, and C_{18}) at sample water bath temperatures of 30–50 °C in increments of 5 °C. The condenser recirculating water temperature was maintained at 95 °C. The temperature of the carbon filter was maintained at 10 °C above the selected temperature of the sample bath water. The reference amount of each of the first four 1-chloroalkane standards, from which recovery efficiencies were determined, was 52 ng. The amount of C_{18} was 104 ng. The quantitation reference internal standard was 1-chlorododecane. Quantification was based on selected single ion areas relative to the selected single ion area of 1-chlorododecane (2, 3). The percent recovery of each standard was then determined by comparing the computer quantitated amount from the purged water samples to the amount in the spiked water, according to the following formula:

$$\% \text{ recovery} = \frac{\text{amount calculated (ng)}}{\text{amount spiked (ng)}} \times 100 \quad (1)$$

Recovery Studies. Once optimum purging conditions were determined as described in the above study, recovery studies were conducted by using a mixture of 22 reference compounds spiked in water. Since all organic compounds have varying vapor pressures and solubilities in water and since all compounds are not 100% purged from the water by CLS, experimental response factors, which include GC/MS response and CLS recovery factors, must be determined in order to measure levels of organic compounds in environmental samples.

Seven repetitive GC/MS analyses of the direct injections of a 22-compound standard mixture of organics were performed to establish sets of average relative retention times (RRTs) and GC/MS reponse factors (RFs) for each compound. These values were entered into a computerized quantitation library. The use of the quantitation library to measure organics in water has been previously described (2, 3). Six repetitive CLS GC/MS analyses of water spiked with a 22-compound standard mixture were performed by using both CLS systems. RRT and RF values established in the above direct injection measurements were used to quantify and determine the recovery efficiency of each of the 22 compounds from water. The recovery of each compound was determined by using eq 1 above.

Reagents and Equipment. All solvents and chemicals used for the preparation of standard solutions were reagent grade.

Preparation of Standard Solutions. Stock solutions of the 22 test compounds and of the 1-chloroalkane standards were prepared in acetone. Aliquots of the acetone stock solutions were diluted with carbon disulfide to prepare the direct injection standards for GC/MS RRT and RF determinations. Standards and internal standards for spiking reagent water were diluted with acetone. An aliquot containing the five 1-chloroalkanes was added to each direct injection standard solution and to each water sample before CLS. The reference amounts for the 1-chloroalkanes including the quantitation reference standard, 1-chlorododecane, were the same as in the optimization study, above; the reference amounts of the direct injection and CLS standards were in the 20–30-ng range. Detailed preparation of standard solutions has been previously reported by Coleman (3).

Closed-Loop-Stripping Analysis. CLS analyses were performed at optimized temperatures on 1-L samples of water. Temperatures of 40, 50, and 95 °C were maintained for the sample bath water, carbon filter, and the recirculating condenser water, respectively, and for all analyses in the recovery studies. CLS was initiated by filling a sample container to capacity with Milli-Q water, decanting a small amount of the water down to the 1-L mark, adding 2 μL each of the acetone standard solution and the internal standard solution, and then assembling the purging apparatus. After placing the assembled purging apparatus and activated carbon trap in the closed loop, the pump was started and the sample was stripped of organics by recirculating the head space gas through the water sample and the carbon filter for 2 h. Sampling, stripping, and carbon filter extraction procedures, as used in this laboratory, are similar to the procedures described by Grob (1) and Coleman (2). Two microliters of the approximate 8 μL of collected carbon disulfide extract was used for GC/MS analysis. The amounts determined in this 2-μL sample were compared to the reference amounts of individual standards to calculate their recovery.

Computerized Fused Silica Capillary GC/MS System. GC/MS analyses and quantification results were performed on a Finnigan Model 3300 quadrupole mass spectrometer equipped with an Incos Model 2300 data system computer. A Carlo-Erba Fractovap 4160 gas chromatograph was equipped with a Grob-designed splitless injector and a 60 m long × 0.25 mm i.d. wall-coated-open-tubular fused silica SE-30 column. One end of the column was inserted into the MS ion source chamber just to the edge of the ion beam, by way of a transfer oven, the temperature of which was held at 270 °C.

Two microliters of each CLS extract was injected with the column vent of the splitless injector closed. The

column vent (20:1 ratio) was opened 30 s after injection. Grob's (5) hot needle injection technique was used for all analyses. The helium carrier gas flow rate was about 3 mL/min at 25 °C; the linear velocity through the GC column was 25 cm/s with a helium head pressure of 1.2 kg/cm^2 (17 psi) without a flow controller. The injector temperature was maintained at 260 °C. Samples were injected at 20 °C by cooling the GC oven with liquid nitrogen. After a 6-min hold at 20 °C, the oven temperature was programmed to 250 °C at a rate of 2 °C/min. Mass spectra were acquired from 14 to 450 amu at the rate of one scan per 2 s. The 20 °C initial column temperature and the 2 °C/min temperature program rate sufficiently retarded the elution of very volatile compounds to allow a 2-s scan rate. A total of 95% of all GC peaks had minimum elution times of 12 s, thus guaranteeing good ion distribution and representative mass spectra for identification and quantification. Experience in this laboratory has shown that the statistical variations for peak areas at faster scan times (i.e., 1 s) are not that different from a 2-s scan time when at least six samples of the GC peak are acquired by the data system. Peak area measurements and variations have been discussed previously (2, 3). The electron energy was 70 eV, and the source temperature was 90 °C. Source pressure was approximately 5×10^{-6} torr when the GC column temperature was 25 °C. Data acquisition was terminated after 3900 mass spectra (130 min) were obtained.

Quantification. Automatic computerized quantification procedures (3) based on selected single ions of a mass spectrum and the internal standard (IS) method of quantification were used to calculate the level of organics in direct injection standards and in CLS extracts. A computer quantitation library containing reference mass spectra of the 22 standard compounds and of 1-chlorododecane as the quantitation reference standard was established. In addition, the library contained RRT values, single ion RFs (relative to 1-chlorododecane), and reference amounts for each compound. The reference amount of 1-chlorododecane was 52 ng; its quantitation mass was m/z 91. Quantitation formulas used by the computer are shown in eq 2–4

$$\text{amount } Z = \frac{\text{single ion area } Z \times \text{IS amount}}{\text{single ion area IS} \times \text{RF(L)}} \quad (2)$$

(L) = library RF for Z

amount Z in water =

$$\frac{\text{single ion area } Z \times \text{IS amount}}{\text{single ion area IS} \times [\text{RF(L)} \times \text{RE}]} \quad (3)$$

where RE is the recovery efficiency of Z and RE = % recovered/100 or

amount Z in water =

$$\frac{\text{single ion area } Z \times \text{IS amount}}{\text{single ion area IS} \times \text{RF(L)}} \times \text{U1} \quad (4)$$

where U1 is a user parameter stored in the quantitation library as an amount multiplier equal to 1/RE. U1 may vary depending on the sample matrix. Therefore, recovery efficiencies must be determined for each sample matrix. Equation 4 is preferred when quantifying compounds in water samples, since U1 can be removed from the computer quantitation statement when direct injection standards are analyzed.

Previous studies (2, 3) have shown that the accuracy and precision of single ion quantification depend mainly on the stability of the MS when the data system is set to acquire

Table I. Mean Percent Recovery^a of 1-Chloroalkanes after CLS of 1 L of Water

	sample water bath temp, °C^b	closed-loop-stripping time, h			
		0.5	1.0	1.5	2.0
1-chlorohexane	30	72	78	83	87
	35	77	72	81	86
	40	97	97	97	98
1-chlorooctane	30	62	74	81	86
	35	81	72	77	88
	40	97	97	98	98
1-chlorododecane^c	30	53	67	80	83
	35	82	74	90	99
	40	98	98	99	99
1-chlorohexadecane	30	7	11	30	40
	35	27	46	73	98
	40	28	63	84	98
1-chlorooctadecane	30	2	2	6	10
	35	6	9	18	29
	40	8	15	27	63

^{a} Based on triplicate analysis. ^{b} In each case, the filter holder temperature was adjusted to 10 °C above the water bath temperature; the condenser water temperature was maintained at 95 °C. ^{c} Quantitation reference standard. At 40 °C and 2-h stripping time, the RSD was ±6% on the basis of six determinations.

a minimum of six samplings of a GC peak. The fact that the RFs are based on a single ion from the internal standard (m/z 91 of 1-chlorododecane) relative to a single ion in the mass spectrum of the compounds to be measured (ranging from m/z 91 to 284 in this study) mandates that the relative intensities of mass ions in a given spectrum should remain consistent in order to obtain reproducible RFs. There was generally a lower degree of accuracy and precision for those compounds quantified on mass ions above m/z 180. Such was the case for the polychlorinated benzenes and biphenyls, whose spectra have ions predominately from m/z 150 to 365.

Blanks. Procedural blanks were incorporated into the analytical scheme. Before analysis of actual samples, carbon filter blanks and CLS blanks of Milli-Q reagent water containing the five 1-chloroalkane standards were determined. All reported quantities were corrected for contaminants in the blanks.

Results and Discussion

Results of the 1-L optimization study based on the recovery of 1-chloroalkanes are shown in Table I. The data indicate that >95% of C$_6$, C$_8$ and C$_{12}$ were recovered in the first 0.5 h of stripping and that >95% of C$_{16}$ was recovered in 2 h of gas stripping of water samples at 40 °C. The recovery of C$_{18}$ averaged 63% at 40 °C. Attempts were made to improve the recovery of C$_{18}$ by increasing the sample water bath temperature to 45 and 50 °C (carbon filter at 55 and 60 °C, respectively). In both cases, the increase in stripping temperatures caused water vapor to condense in the trap. In viewing all parameters, a 40 °C bath temperature and a 2-h stripping time were considered to be optimum in order to recover these 1-chloroalkane standards with the greatest efficiency. We recognize that the CLS system could not be optimized for all compounds under a single set of conditions when doing broad spectrum analyses. However, the group of 1-chloroalkanes (C$_6$–C$_{18}$) represented a range of molecular weights from 120 to 288 and boiling points from 134 to 348 °C. It is conceivable that longer stripping times at 40 °C would improve the recovery of the C$_{18}$ chloroalkane and of higher molecular weight compounds, but increased analysis time would also

Table II. Precision of Repetitive Direct Injection Study

compound	quantitation mass m/z	amt injected, ng	mean[a] GC/MS response factor	RSD, %
thiophene	84	25.4	2.416	5.9
dibromochloromethane	129	29.4	0.847	4.7
styrene	104	21.8	2.884	5.5
isopropylbenzene	105	24.2	3.923	4.9
2-chlorotoluene	91	25.9	2.932	4.2
bis(2-chloroethyl) ether	93	24.4	1.871	3.7
α-methylstyrene	118	21.6	2.003	6.0
1,4-dichlorobenzene	146	19.8	1.950	7.1
2-ethyl-1,3-dimethylbenzene	119	24.1	4.410	4.6
4-chloro-o-xylene	105	25.7	2.516	4.6
1,1-dimethylindan	131	21.7	3.512	4.6
p-methylphenol	107	26.6	2.323	3.4
tetrahydronaphthalene	104	23.4	2.428	4.7
1,2,4-trichlorobenzene	180	23.2	1.178	7.3
hexachloro-1,3-butadiene	225	26.9	0.347	10.1
2-methylbiphenyl	168	24.4	1.635	7.0
1,6-dimethylnaphthalene	156	24.2	1.953	5.8
2-isopropylnaphthalene	155	22.7	3.562	5.7
pentachlorobenzene	250	26.1	0.400	12.0
hexachlorobenzene	284	20.1	0.265	11.3
2,2',4,4',6,6'-hexachlorobiphenyl	145	27.0	0.202	6.0
2,2',4,5,5'-pentachlorobiphenyl	254	28.2	0.141	11.3
1-chlorododecane[b]	91	52.2	1.000	

[a] Based on seven determinations.   [b] Quantitation reference standard.

Table III. Recovery and Precision Data for Repetitive Purge Study—HERL 1-L CLS System

compound	std amt, ng	mean[a] recovered amt, ng	range	recovery efficiency, %	RSD, %
thiophene	25.4	8.8	7.2–10.9	34.6	15.9
dibromochloromethane	29.4	16.6	13.3–21.0	56.5	12.6
styrene	21.8	17.4	15.9–19.6	79.8	6.9
isopropylbenzene	24.2	25.9	23.8–28.7	107.0	7.7
2-chlorotoluene	25.9	23.3	21.6–26.9	90.0	7.7
bis(2-chloroethyl) ether	24.4	2.8	2.6–3.5	11.6	10.7
α-methylstyrene	21.6	19.4	18.1–21.6	89.9	6.2
1,4-dichlorobenzene	19.8	18.3	16.4–20.6	92.5	8.2
2-ethyl-1,3-dimethylbenzene	24.1	22.3	20.8–24.7	92.4	5.8
4-chloro-o-xylene	25.7	21.8	20.2–26.0	84.8	9.2
1,1-dimethylindan	21.7	23.8	21.6–26.2	109.5	7.1
p-methylphenol	26.6	ND[b]			
tetrahydronaphthalene	23.4	23.1	20.2–26.3	98.6	10.4
1,2,4-trichlorobenzene	23.2	19.2	17.6–20.9	82.9	7.3
hexachloro-1,3-butadiene	26.9	30.9	27.4–34.3	113.8	9.2
2-methylbiphenyl	24.4	24.8	22.0–27.1	101.4	7.7
1,6-dimethylnaphthalene	24.2	9.5	7.6–11.2	39.3	11.6
2-isopropylnaphthalene	22.7	20.6	18.8–22.3	90.8	6.3
pentachlorobenzene	26.1	12.4	10.7–14.3	47.7	11.3
hexachlorobenzene	20.1	6.2	5.0–7.4	31.1	12.9
2,2',4,4',6,6'-hexachlorobiphenyl	27.1	28.2	26.1–32.3	104.3	7.1
2,2',4,5,5'-pentachlorobiphenyl	28.2	23.0	17.8–27.6	81.5	14.3

[a] Based on six purging analyses using single ion quantification.   [b] ND = not detected.

be impractical in most laboratories where several samples are analyzed daily.

The standard deviations around the norm were calculated for the RFs, amounts, and recovery efficiencies by using data from both CLS systems. Table II shows the precision of the repetitive direct injection study. The individual RFs obtained by single ion quantification of the listed masses in Table II had RSDs ranging from 3.4% to 12.0%. Compounds quantified on m/z ions 84–168 had RSDs of 3.4–7.1%; those quantified on m/z ions 180–284 had RSDs of 7.3–12.0%. The average RSD for RFs of all compounds in the direct injection study was 6.4%. Previous studies (2, 3), where standard deviations were calculated for GC/MS peak areas of these standards, showed that single ion areas had RSDs of 13%. However, and most importantly, the internal standard method of quantitation compensated for these variations when the

amounts were calculated by the computer.

Recovery and precision data from the 1-L CLS systems are shown in Tables III and IV. Table V summarizes the data in Tables III and IV and compares it to the recovery data from the 1-gallon CLS system (3). In general, Table V shows that the two 1-L CLS systems were about equal in performance, with the HERL system having a slight edge in overall method precision. Mean recovery efficiencies (percent) and RSDs, for 20 compounds that were common to each study, were 48% (28% RSD), 80% (9% RSD), and 83% (13% RSD), respectively, for the 1-gallon, 1-L HERL, and 1-L commercial CLS systems.

This laboratory recently participated in two collaborative studies using closed-loop stripping. One study involved the analysis of purgeable aromatics at the 7–65 ng/L level, and the other was for the analysis of organic compounds causing taste and odor at the 3–35 ng/L level.

Table IV. Recovery and Precision Data for Repetitive Purge Study—Commercial 1-L CLS System

compound	std amt, ng	mean[a] recovered amt, ng	range	recovery efficiency, %	RSD, %
thiophene	25.4	13.5	10.0–15.8	53.7	14.1
dibromochloromethane	29.4	23.3	18.1–26.9	79.3	12.4
styrene	21.8	17.9	13.8–22.7	82.1	15.1
isopropylbenzene	24.2	25.2	20.9–30.9	104.3	13.5
2-chlorotoluene	25.9	23.2	18.9–27.8	89.4	12.1
bis(2-chloroethyl) ether	24.4	4.4	3.5–4.8	18.0	9.1
α-methylstyrene	21.6	18.3	14.8–22.6	84.8	13.7
1,4-dichlorobenzene	19.8	18.2	14.8–20.7	91.7	11.5
2-ethyl-1,3-dimethylbenzene	24.1	22.2	18.4–25.6	92.0	10.8
4-chloro-o-xylene	25.7	21.1	17.4–25.6	85.9	12.2
1,1-dimethylindan	21.7	23.1	19.3–27.1	106.0	11.7
p-methylphenol	26.6	ND[b]			
tetrahydronaphthalene	23.4	22.9	17.8–27.1	97.7	12.2
1,2,4-trichlorobenzene	23.2	19.9	16.3–23.9	85.9	11.0
hexachloro-1,3-butadiene	26.9	29.7	24.4–35.2	110.5	12.1
2-methylbiphenyl	24.4	25.4	22.8–27.8	104.2	7.5
1,6-dimethylnaphthalene	24.2	12.2	9.6–15.7	50.4	18.9
2-isopropylnaphthalene	22.7	21.7	19.8–24.7	95.8	7.8
pentachlorobenzene	26.1	13.4	9.9–20.2	51.5	25.4
hexachlorobenzene	20.1	7.3	4.9–12.1	36.5	32.9
2,2',4,4'6,6'-hexachlorobiphenyl	27.0	31.6	28.5–37.3	117.0	8.9
2,2',4,5,5'-pentachlorobiphenyl	28.2	24.8	17.9–30.2	88.0	21.0

[a] Based on six purging analyses using single ion quantification. [b] ND = not detected.

Table V. Recovery Efficiency Comparisons of CLS Devices

compound	1 gallon		HERL 1 L		commercial 1 L	
	recovery efficiency,[a] %	RSD, %	recovery efficiency,[b] %	RSD, %	recovery efficiency,[b] %	RSD, %
thiophene	NA[c]		34.6	15.9	53.3	14.1
dibromochloromethane	15.7	71.3	56.5	12.6	79.3	12.4
styrene	53.7	22.0	79.8	6.9	82.1	15.1
isopropylbenzene	72.2	26.9	107.0	7.7	104.3	13.5
2-chlorotoluene	54.3	22.3	90.0	7.7	89.4	12.1
bis(2-chloroethyl) ether	0.4	75.0	11.6	10.7	18.0	9.1
α-methylstyrene	56.4	22.7	89.8	6.2	84.8	13.7
1,4-dichlorobenzene	71.2	26.5	92.5	8.2	91.7	11.5
2-ethyl-1,3-dimethylbenzene	NA		92.4	5.8	92.0	10.8
4-chloro-o-xylene	52.5	23.4	84.8	9.2	85.9	12.2
1,1-dimethylindan	73.4	25.6	109.5	7.1	106.0	11.7
p-methylphenol	ND[d]		ND		ND	
tetrahydronaphthalene	53.6	23.1	98.6	10.4	97.7	12.2
1,2,4-trichlorobenzene	55.1	25.4	82.9	7.3	85.9	11.0
hexachloro-1,3-butadiene	89.4	28.7	113.8	9.2	110.5	12.1
2-methylbiphenyl	51.9	28.3	101.4	7.7	104.2	7.5
1,6-dimethylnaphthalene	12.3	36.6	39.3	11.6	50.4	18.9
2-isopropylnaphthalene	49.1	26.7	90.8	6.3	95.8	7.8
pentachlorobenzene	26.0	37.7	47.7	11.3	51.5	25.4
hexachlorobenzene	11.9	65.5	31.1	12.9	36.5	32.9
2,2',4,4',6,6'-hexachlorobiphenyl	58.7	30.5	104.3	7.1	117.0	8.9
2,2',4,5,5'-pentachlorobiphenyl	18.8	39.9	81.5	14.3	88.0	21.0

[a] Average of 16 determinations. [b] Average of six determinations. [c] NA = not analyzed. 2-Methylthiophene and 2-ethyl-1,4-dimethylbenzene were in the 1-gallon study. [d] ND = not detected.

The reported results from both studies were all acceptable and within 95% confidence limits. It is obvious from these studies that truly low concentrations of organic compounds can be accurately measured by CLS.

Summary and Conclusions

A redesigned and modified 1-L CLS system was optimized for maximum purging efficiency of 1-chloroalkane standards spiked in water. The optimum conditions established to recover all 1-chloroalkanes with the greatest efficiency were 40 °C for the sample bath water, 50 °C for the activated carbon trap, 95 °C for the Graham condenser, and 2 h for the stripping time. Under these sets of conditions, >95% of 1-chlorohexane, 1-chlorooctane, 1-chlorododecane, 1-chlorohexadecane, and 63% of 1-

chlorooctadecane were recovered from replicate CLS analyses.

The above optimized conditions were used for CLS of 1-L water samples spiked with a 22-compound standard mixture in order to determine recovery efficiency factors from two different 1-L CLS systems. The CLS carbon extracts were analyzed by fused silica capillary column GC/MS. Quantification procedures, using single ion quantification and the internal standard method of analysis, were used to determine recovery results.

Quantification and recovery results from the two 1-L and the previously reported 1-gallon CLS systems were compared. The two 1-L CLS systems were about equal in overall method recovery efficiency for the test compounds. The average recovery efficiency for all compounds using

the 1-gallon CLS system was about half that of the 1-L systems. Comparing the results from the 1-gallon CLS study to the optimized 1-L CLS study, the mean recovery efficiency (percent) and RSD were 48% (28% RSD) and 80% (9% RSD), respectively. Of the 22 compounds tested with the optimized 1-L CLS system, 10 had recoveries >90% including a hexachlorobiphenyl isomer (M_r 358).

This report supports previous CLS applications papers (2–4) demonstrating that CLS–capillary column GC/MS is an excellent method to measure many toxic organics in drinking water and in groundwater. For quantitative results, recovery efficiencies of individual compounds must be determined in the same matrix as the sample matrix.

Literature Cited

(1) Grob, K.; Zurcher, F. *J. Chromatogr.* **1976**, *117*, 285–294.
(2) Coleman, W. E.; Melton, R. G.; Slater, R. W.; Kopfler, F. C.; Voto, S. J.; Allen, W. K.; Aurand, T. A. *J.—Am. Water Works Assoc.* **1981**, *73*, 119–125.
(3) Coleman, W. E.; Allen, W. K.; Slater, R. W.; Voto, S. J.; Melton, R. G.; Kopfler, F. C.; Aurand, T. A. In "Advances in the Identification and Analysis of Organic Pollutants in Water"; Keith, L. H.; Ed.; Ann Arbor Science: Ann Arbor, MI, 1981; Vol. 2, Chapter 37, pp 675–688.
(4) Melton, R. G.; Coleman, W. E.; Slater, R. W.; Kopfler, F. C.; Allen, W. K.; Aurand, T. A.; Mitchell, D. E.; Voto, S. J.; Lucas, S. V.; Watson, S. C. In ref 3, Chapter 36, pp 597–673.
(5) Grob, K.; Grob, G. *HRC CC, J. High Resolut. Chromatogr. Chromatogr. Commun.* **1979**, *2*, 109–117.

Statistical Approach for Deciding If Mussels (*Mytilus edulis*) Have Been Collected from a Water Body Polluted with Trace Metals

J. David Popham† and **John M. D'Auria***

Department of Chemistry, Simon Fraser University, Burnaby, British Columbia, Canada V5A 1S6

■ A statistical approach is developed to decide whether specimens of *Mytilus edulis* (mussels), a sentinel organism for heavy metals, are inhabiting a water body that can be classified as polluted. Principal component analysis was applied to the correlation matrix of variates (Mn, Fe, Cu, Zn, and Pb concentrations, dry weight, wet weight, shell length, day/season of collection) measured in specimens collected monthly over a 12-month period from an unpolluted location in an estuary of southwestern British Columbia. Using the principal component scores determined for this set as a reference, a procedure is developed to decide whether similarly measured variates and related principal component scores for mussels collected from other locations indicate if these other water bodies were "polluted" with heavy metals.

Introduction

Mytilus edulis (mussels) are well recognized as a valuable monitor of trace-metal pollution of estuarine waters (1–3). However, a necessary part of monitoring environments is deciding whether or not they are polluted on the basis of trace-metal body burdens in the mussels. Goldberg et al. (1) have suggested that concentrations 10 times those found in base-line studies of mussels collected from nonpollutant waters may be a suitable criterion to denote a polluted water body, but this hypothesis should be tested. In a previous study (4), we have suggested that a statistical

approach could be used to resolve such issues by using what is known as a generalized distance function (5). For a study in which the concentration of only one element is of interest in deciding if a water body is polluted or not, the square of the standard score, z^2, can be used:

$$z^2 = (x - m)^2/s^2 \qquad (1)$$

where x is the measured value of the concentration of the element of interest in the specimen selected from a habitat of unknown quality and m and s^2 are, respectively, the mean and variance of the concentration of the element in specimens from a reference habitat having an acceptably low trace-metal concentration. The χ-square distance function is equal to z^2, and the probability, P, for a given χ-square can be calculated in order to estimate the proportion of organisms of the reference sample that reside as close to or closer to the mean than organisms collected from the habitats of unknown quality (5). Obviously, large positive differences between x and m results in large z scores. These, in turn, yield large χ-square distances, resulting in low probabilities that the sample in question is representative of the reference population used to derive m and s^2 (5).

Unfortunately, many physiological functions in bivalves are related to their size, their state of the gametogenic cycle, or both. Bayne et al. (6) have recently discussed this phenomenon with respect to selecting the required number of animals in order to use an analysis of covariance for detecting differences among populations with respect to oxygen consumption in the bivalve *Scrobicularia plana*. Metal concentrations in mussels are also well correlated

with size and state of the gametogenic cycle (7, 8), the salinity of the surrounding seawater (9, 10), and possibly, even the concentration of other metals (11, 12). For these instances in which there are many variates, covariate analyses may not be most appropriate statistical procedure since many observations are required in order to obtain stable regression coefficients (5).

While multivariate discriminate analysis of the data resulting in composite variates (i.e., canonical variates) for maximum separation of samples could be used, it is doubtful that this statistical procedure would be appropriate since there is only one way to be unpolluted (that is, to have low values for every pollutant) but many ways to be polluted. As a result, it would be highly improbable that samples from all types of polluted environments could be obtained in order to derive the meaningful canonical variates or discriminate functions applicable for all monitoring programs.

Finally, the question still remains as to whether a "pollution effect" can be detected in one, two, or many samples of mussels. In other words, we are suggesting that, for maximum utility, a program of "pollutant monitoring" should be independent of sample size. For this reason, we propose that a generalized distance function (χ^2) resembling that for the inverse of the variance–covariance matrix ($\mathbf{D}^{-1}$) be used; i.e. (5)

$$\chi_{ji}{}^2 = x_{ji}{}^1 \cdot \mathbf{D}^{-1} \cdot x_{ji} \qquad (2)$$

This distance function

$$\chi_{ji}{}^2 = x_{ji}{}^1 \cdot \mathbf{R}^{-1} \cdot x_{ji} \qquad (3)$$

where $\mathbf{R}^{-1}$ is the inverse of the correlation matrix and is based upon what are known as the principal component scores of an individual, which are calculated by using the inverse of the correlation matrix. χ-Square values (χ^2) for these principal scores can be easily obtained for samples of organisms collected from environments of unknown quality following principal component analysis of the correlation matrix (thereby removing the effects of scale associated with variance–covariance matrices) of the data for the reference sample (5). The χ-square value of an individual from the habitat of unknown quality then determines how well its principal component scores resemble the scores for organisms collected from an "acceptable" environment. We are using the expression "acceptable" to denote that decisions for setting standards of environmental quality are also based on criteria outside the realm of science, namely, political and socioeconomic factors.

Principal components are linear combinations of the original variables; e.g.

$$PC = b_1 V_1 + b_2 V_2 + ... + b_n V_n \qquad (4)$$

where PC is the principal component, b_1–b_n are the principal component coefficients, and V_1–V_n are the standardized variates. The first principal component accounts for the highest proportion of the variance of the data set, and each succeeding component accounts for successively smaller proportions of the total variance. Further, each principal component is uncorrelated with every other principal component. Generally, only a few principal components are necessary to account for most of the variance of a data set, resulting in a parsimonious explanation of the data. Second, since the principal components are uncorrelated with one another, they can be drawn at right angles to one another and the location or coordinates of any one specimen (its principal component scores) with respect to the origin is a simple Euclidean distance. As previously mentioned, the correlation matrix was used in

this study rather than the variance–covariance matrix on account of the problems of scale. For example, the body weight of mussels and trace-metal concentrations are expressed by numbers of much different magnitudes. By use of the correlation matrix, the effect of differences due to magnitude is removed so that each variable is given the same relative importance.

Materials and Methods

For slightly over 1 year, mussels were obtained at monthly intervals from Rocky Point (49°17′ N, 122°51′ W), a location in Burrard Inlet, British Columbia, previously shown to be relatively unpolluted compared to other areas in Burrard Inlet (13–15). Mussels were collected from a floating wharf in order to avoid the possibility of the location of the mussels within the intertidal zone affecting results (16, 17). Specimens were also obtained occasionally from other locations in British Columbia waters, and all specimens were analyzed for trace-element (Mn, Fe, Cu, Zn, Pb) concentrations by X-ray energy spectroscopy (XES). Further details of specimen preparation and analytical procedure are described elsewhere (3, 13–15).

The data were log-transformed (7) and then analyzed by using the statistical package BMDP 4M (factor and principal component analyses) (18). A statistical summary of the data is presented in Appendix Table A1 of ref 14 while the complete set of data is available on request.

Although the effect of season could be taken into account in several ways, e.g., water temperature, hours of daylight, or the Julian day of the year mussels were collected, we decided to use a mathematical function to statistically simulate annual seasonal changes; namely

day' = sin (Julian day − 364) + cos (Julian day − 364)

where Julian day is the day of the year of the collection (e.g., Jan 1, 1979 = day 1). This function then approximately reproduces the oscillating behavior of a possible seasonal effect against which the variates can be compared mathematically.

Results

The matrix of correlations among the variates measured in this study for the 103 mussel samples collected from Rocky Point is listed in Table I. Three principal components with eigenvalues greater than one were extracted from this matrix and accounted for slightly less than 71% of the total variance. The correlations between these principal components and the original variates after Varimax rotation are listed in Table II, while Table III lists the means and standard deviations of the variates so that the normalized scores can be derived. Table IV lists the value of the component score coefficients so that the component scores of specimens of mussels not collected from Rocky Point can be calculated (refer to Appendix). As discussed later, Figure 1 is a scatter plot of the scores of the first and third principal component scores for half the total number of mussels collected from Rocky Point (lower numbers representing order of collection; e.g., 1 collected before 2) and other areas in southwest British Columbia (circled numbers). The subscript beside the circled number indicates whether the mussels used in the analysis were larger than 46 mm (large: L) long or smaller than 21 mm (small: S) long. As can be seen in the figure, the plot is divided into four quadrants. Note that the sequence of numbers roughly follows a counter-clockwise pattern with the first [1, 2] and the last samples [13, 14] of mussels (winter collections) being located in the lower right quadrant and the middle samples [6, 7] in the upper left quadrant. Such a pattern would be expected if sea-

Table I. Correlation Matrix of the Variates Used in Determining Water Quality[a]

	dry wt	day'	Mn	Fe	Cu	Zn	Pb	H₂O	length
dry wt	1.000								
day'	−0.189	1.000							
Mn	−0.356	0.535	1.000						
Fe	−0.428	0.674	0.673	1.000					
Cu	−0.298	0.393	0.498	0.609	1.000				
Zn	0.077	0.329	0.243	0.404	0.195	1.000			
Pb	−0.010	0.132	0.138	0.214	0.224	0.262	1.000		
H₂O	−0.258	0.257	0.044	0.433	0.251	0.301	0.189	1.000	
length	0.909	−0.123	−0.378	−0.308	−0.248	0.180	0.051	−0.011	1.000

[a] The definition of the variates in this table are as follows: (1) dry wt = dry weight of the meats; (2) day' = function reflecting season of collection in mussels; (3) Mn to Pb = log-transformed concentrations of the elements in mussels (mass of metal − unit dry mass of mussel⁻¹); (4) H₂O = relative proportion of water in the mussels = (1 − dry weight/wet weight); (5) length = length of the right valve of the mussels (mm).

Table II. Correlations (after Varimax Rotation) between the Original Variates (Symbols as in Table I) and the First Three Principal Components Extracted from the Correlation Matrix and the Communalites of the Variates

| | principal components | | | commu- |
	1	2	3	nalities[b]
dry wt	−0.206	0.942[a]	−0.119	0.944
day'	0.795[a]	0.015	0.160	0.658
Mn	0.857[a]	−0.216	−0.087	0.789
Fe	0.808[a]	−0.246	0.362	0.844
Cu	0.647[a]	−0.216	0.229	0.518
Zn	0.426[a]	0.338	0.524[a]	0.570
Pb	0.134	0.087	0.580[a]	0.362
H₂O	0.058	−0.198	0.848[a]	0.762
length	−0.200	0.929[a]	0.123	0.918

[a] Values used in interpretation of the PC's. [b] Communalities represent the proportion of variate accounted for by the three principal components.

Table III. Statistics (Mean (x), and Standard Deviation (s)) of Transformed Variates Necessary for Deriving Standardized Scores (Z)

variates[a]	mean	std dev
dry wt	−0.806 94	0.429 21
shell length	1.517 87	0.135 46
day'	0.066 56	1.070 38
metal concn		
Mn[b]	0.654 90	0.553 95
Fe	2.539 77	0.228 79
Cu	0.932 94	0.124 01
Zn	2.711 74	0.187 13
Pb[b]	0.397 42	0.286 76
water content[c]	−0.084 40	0.014 06

[a] Variate = log variate. [b] Pb = log (Pb + 1); Mn = log (Mn + 1). [c] Water content = log (1 − dry weight/wet weight).

Table IV. Principal Component Coefficients for Deriving Scores for the First and Third Principal Components of the Mussels Collected from Rocky Point

| variates | coefficients | |
	PC1	PC3
dry wt	0.090 91	−0.107 41
shell length	0.029 07	0.078 56
day'	0.354 27	−0.083 37
metal concn		
Mn	0.409 20	−0.273 23
Fe	0.263 38	0.088 26
Cu	0.223 71	0.024 01
Zn	0.133 19	0.268 93
Pb	−0.068 56	0.405 61
water content	−0.224 52	0.652 59
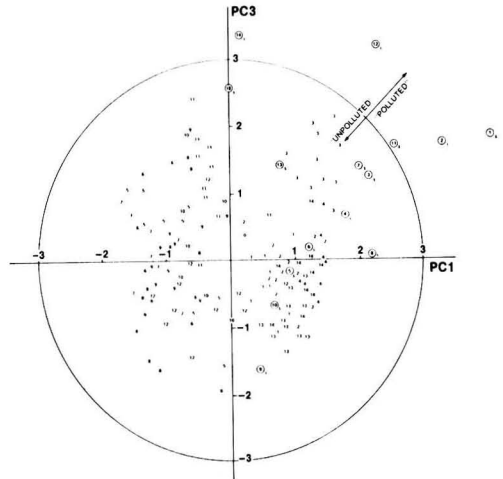
Figure 1. Plot of the first and third principal component scores of half the number of mussels collected from Rocky Point. Each number represents one mussel specimen. The value of the numbers indicates the order of the sample in which the mussels were collected. For example, all the 8's represent mussels of the eighth collection sample. The circled numbers are the index numbers (see Table V) of mussels collected from other areas in British Columbia. The letters (L, S) indicate whether or not the mussel was longer than 46 mm or shorter than 21 mm.

sonal effects were playing a role in determining the body burdens of trace metals.

Tables V and VI list, respectively, data for mussels collected in other waters of British Columbia and the normalized scores. These data are used to determine whether or not the waters from which these mussels are collected are polluted relative to the water at Rocky Point.

Discussion

Interpretation of the biological significance of the principal components (PC) is difficult if interpretation is based on the values of the correlations between the first three "unrotated" PC's and the original variates. This is because many of the correlations are in the midrange between 0 and (the absolute value remain 1. For example, the correlations between the original, unrotated PC's 1–3 and dry weight are, respectively, −0.626, 0.678, and −0.303, which are midrange values. If the combined variance of the remaining six variates (accounting for less than 30% of the total variance) is considered, then the principal components can be rotated once more so as to maximize (or minimize, as the case may be) the correlations between

Table V. Data for Mussels Collected from Various Locations in Southwest British Columbia (1979)

location	index identi- fication	dry wt, g	day of collection	μg g⁻¹, dry weight Mn	Fe	Cu	Zn	Pb	H₂O concn, g g⁻¹	shell length, mm
				Mn	Fe	Cu	Zn	Pb		
Brittania Beach	1	0.009	119	67	1973	288	734	12	0.845	13
Brittania Beach	2	0.631	119	38	1476	87	966	4	0.868	47
Caulfield Cove	3	0.023	83	45	1429	28	574	5	0.790	16
Caulfield Cove	4	0.396	83	23	430	29	439	9	0.834	50
Grief Point	5	0.038	91	17	240	25	272	3	0.834	20
Grief Point	6	0.411	91	15	405	20	322	2	0.854	53
Seaspan Wharf	7	0.094	93	32	633	49	415	12	0.855	27
Seaspan Wharf	8	0.474	93	19	516	46	333	7	0.817	47
Montague Harbour	9	0.564	176	22	519	11	127	nd[a]	0.822	60
Montague Harbour	10	0.029	176	27	629	19	244	nd	0.842	19
Seven Seas Wharf	11	0.072	121	31	1212	55	616	31	0.831	16
Seven Seas Wharf	12	1.029	121	30	710	38	1418	169	0.832	59
Crofton Wharf	13	0.012	147	19	455	23	617	25	0.824	13
Crofton Wharf	14	0.172	147	nd	344	29	1541	14	0.869	48
Seabus Wharf	19	0.021	177	nd	540	32	590	81	0.810	19

[a] Not detected.

Table VI. Normalized Scores $[(x_j - m_j)/s]$ of the Variates for the Various Specimens, the Resulting Scores for These First and Third Principal Components, and the Euclidean Distances (D) of the Specimens from the Centroids (Results Are Plotted in Figure 1)

index ID	dry wt	day'	Mn	Fe	Cu	Zn	Pb	H₂O	length	PC1	PC3	D
1	-2.886	0.390	2.126	3.302	12.301	0.823	2.499	0.801	-2.989	4.04	1.81	4.43
2	1.414	0.390	1.690	2.751	8.117	1.460	1.052	1.620	1.132	3.29	1.77	3.73
3	-1.937	1.033	1.819	2.689	4.147	0.252	1.328	-1.278	-2.323	2.15	1.25	2.49
4	0.942	1.033	1.309	0.410	4.269	-0.370	2.101	0.396	1.330	1.81	0.71	1.94
5	-1.429	0.920	1.084	-0.697	3.750	-1.481	0.714	0.396	-1.407	0.91	-0.17	0.93
6	0.980	0.920	0.991	0.296	2.968	-1.090	0.278	1.128	1.517	1.19	0.32	1.23
7	-0.512	0.888	1.559	1.144	6.106	-0.501	2.499	1.164	-0.645	2.06	1.39	2.48
8	1.125	0.888	1.166	0.756	5.885	1.012	1.763	-0.240	1.132	2.24	0.07	2.24
9	1.301	-0.857	1.276	0.767	0.875	-3.249	-1.386	0.052	1.915	0.46	-1.65	1.71
10	1.702	-0.857	1.430	1.131	2.789	-1.733	-1.386	0.691	-1.772	0.71	-0.69	0.98
11	0.782	0.346	1.535	2.377	6.511	0.416	3.863	0.285	-2.323	2.42	1.69	2.95
12	1.909	0.346	1.510	1.361	5.216	2.351	6.392	0.322	1.861	2.30	3.18	3.93
13	2.595	-0.246	1.166	0.517	3.408	0.420	3.548	0.023	-2.989	0.78	1.44	1.64
14	0.099	-0.246	-1.182	-0.014	4.269	2.544	2.715	1.666	1.199	0.20	3.40	3.41
19	2.029	-0.876	-1.102	0.842	4.614	0.316	5.288	-0.506	-1.772	0.02	2.56	2.56

the PC's and the original variates. Once rotation, using the Varimax criterion, has occurred, the correlations between the PC's are either near 0 or 1, thereby facilitating interpretation of the biological significance of each PC.

As a matter of interest, changes in the rotation of the axes result in changes of the positions of the individuals but do not change the absolute positions of the specimens in the multivariate space. The distance of only two specimens to the centroid and the angle made by these three points remain constant.

The biological significance of the "rotated" PC's is based on interpretation of the values of the correlations between the PC's and the original variates (Table II). For example, the only high values occurring in the vector of correlations for the second PC are those between this PC and the original variates, dry weight and shell length. Since this PC is not highly correlated with any other variables, its total can be interpreted as "a component" accounting for that part of the total variance of the data describing that feature of the mussels known as body size. This does not mean mussel size and metal concentrations are not correlated, but the PC provides a "measure" of that part of the total variance contributed by mussel size, "independent" of any other relationships. Variations in metal concentrations in the mussels also contribute to the total variance, and the PC representing them can be considered also to be independent. Now, since we are only interested in variance of metal concentrations per se, we can ignore the second PC when we come to determining

water quality based on the values of metal concentrations found in mussels. We will not lose any important information regarding the quality of water in which the mussels are living because this component tells us nothing about water quality, only mussel size. Hence, addition of the second PC to Figure 1 will add only a dimension accounting for size and essentially will do nothing to help account for variations in trace-metal concentrations in the environment.

However, we must emphasize that our data set includes only a very limited amount of variables and does not include all those variables describing the organic compounds in seawater. If these had been included and if these variables were not correlated with any other variables except mussel size, then it could well be that it would have been necessary to include it in the measure of distance. At the moment, with these data, however, it is not necessary.

The interpretation of the first PC is slightly more difficult than it is for the second. First, note that the variate day' is highly correlated with this PC but not with the other two. Hence, this PC can be interpreted, at least in part, as a variable accounting for seasonal changes in mussels. Concentrations of Mn and Fe in mussels also are highly correlated with the first PC and only modestly correlated or poorly correlated with the other two PC's. Hence, the first PC can also be interpreted as a variate accounting for much of the change in Mn and Fe concentrations in the mussels. (Note that these two variables

have the highest correlations with day'.) Concentrations of Cu and Zn in mussels are also well correlated with the PC. This combination of the high correlation of variate, day', and the modest to high correlations of the trace metals, excluding Pb, with the first PC leads us to conclude that this artificial variate is accounting for the seasonal changes in Mn, Fe, Cu, and Zn in mussels. As previously noted, inspection of the correlation matrix (Table I) shows that all metals except for Pb are well correlated with day' and supports this interpretation and previously published results (e.g., ref 19–21). Independent of this seasonal effect component is another, represented by the third PC, which shows moderately high correlations between it and the concentrations of Zn and Pb as well as with the concentration of body water in the mussel. Since the correlations all have the same sign, the component can be interpreted as indicating that those mussels with high body burdens of lead and zinc also tend to have high concentrations of body water. That is to say, these mussels have a high wet weight to dry weight ratio. One possible hypothesis for this phenomenon could be that biologically available lead and zinc are being introduced into the seawater surrounding the mussels when water is draining from the surrounding land. As a result of this drainage, there is a decrease in the salinity of the surrounding seawater and a corresponding increase in Zn and Pb concentrations. We had previously found that the concentration of iron in seawater was well correlated with the amount of rainfall recorded for a 96-h period prior to sampling (11), suggesting that levels of Zn and Pb could be introduced by surface runoff. An alternative hypothesis is that mussels with high body burdens of lead and zinc are less able to regulate water levels and are not as well equipped to prevent flooding of the tissues and cells, compared with those with low body burdens of these metals. At present we have no data to support either hypothesis.

The results show that two principal components, the first and the third, account for most of the variance in the measured trace-metal concentrations in the mussels collected from Rocky Point. The question now remains as to how these two principal components can be of value in determining trace-metal pollution in estuarine waters. For such a determination, we first calculated the scores for the first and third principal components for the mussels by using the regression coefficients (listed by the BMDP 4M program), as shown by ref 5 (see also Appendix), and then plotted them in Figure 1. With respect to monitoring other locations within British Columbia waters, it no longer matters whether or not the size of the mussels that were collected from other sites varies among samples. This is because the effect of size on trace-metal concentrations is mostly accounted for by the second component, and this component has been removed from the analysis, thereby rendering the relationships of samples on an easily interpretable plane. The principal component score (regression) coefficients for deriving the values of the scores for the first and third principal components are listed in Table III. The circle about the origin of Figure 1 is the isopleth of the third standard deviation unit from the origin and therefore also is the isopleth of the 99th centile. This centile is equivalent to a probability and displays the similarity of any one individual to the group of mussels used for deriving the correlation matrix and principal component scores. For example, in this study specimens of mussels whose PC scores fall between 1 and 2 have a probability of between 23% and 5% of having been drawn from the same population as those mussels from Rocky Point, while any mussels outside the third standard deviation isopleth

have less than a 1% change of having been drawn from a population of mussels resembling those from Rocky Point. Further, on account of the high values of the regression coefficients of the equations describing the PC scores, mussels having high body burdens of trace metals will be located in the upper right quadrant.

If scores for mussels had been found outside the isopleth of the third standard deviation unit and in the lower left quadrant, they would have been interpreted as indicating the mussels had been collected from an environment with extremely low concentrations of trace metals. It is for this reason that we have inserted the "unpolluted–polluted" axis.

We can take, as an example, the illustration of the use of the statistical procedure shown in the Appendix. Note that specimen 7 has high positive standardized scores for the trace metals (especially Cu), resulting in a high score for PC1. The PC1 coefficient for Pb is negative but small and, hence, does not contribute much to the final score. However, with respect to PC3, the coefficient is very high and, hence, would contribute a large positive value to the PC3 score. Two large positive values for PC1 and PC3 cause the specimen to be located in the upper right quadrant. Conversely, if a specimen had been used with very low concentrations of heavy metals (thus yielding negative standardized scores), the specimen would have two negative scores for the PC's. For the other two quadrants, the following conditions could arise. If a specimen has a very large negative standardized score for Mn and day' (e.g., collected late in the year) and a large positive standardized score for Pb and water content, it will be located in the upper left quadrant (a specimen collected during the seventh collection period shows this pattern, Figure 1). Conversely, specimens having high positive standardized scores for Mn and day' and high negative standardized scores for Pb and water content will be located in the lower right quadrant. If all variables have zero standardized scores, except for one of the variables for trace-metal concentrations that has a high positive standard score (e.g., resemble the reference area exactly except for the metal in question), it will be located in the lower right quadrant for Mn, the upper right quadrant for Fe, Cu, and Zn, and the upper left quadrant for Pb. The reader may notice that although one of the specimens, 12$_L$, has a very high concentration of Pb (169 ppm), it is not located in the upper left quadrant. This is because the other variables are also entered into the score.

The fundamental notion on which this project is based is that, since the body burden of trace metals in mussels has been shown to reflect the concentration of trace metals in the environment (14, 22, 23), we can conclude that the environments are also different with respect to the concentrations of trace elements in the seawater.

We now turn our attention to the application of the statistical procedure for sites other than Rocky Point (Figure 1) to see if any of them are "polluted". As described in preceding studies (14, 15), mussels were collected from other areas of British Columbia, namely, Brittania Beach, Caulfield Cove, Grief Point, and some locations in Burrard Inlet. The location of these sites and the raw data for some of the mussels collected from them are listed in Table V. (Note that mussels with large differences in size have been used to show that the effect of size makes no different in interpretation of water quality.) The normalized scores of these data, the resulting scores for the first and third principal component, and the Euclidean distances of the resulting coordinates from the centroid are listed in Table VI. The scores for the mussels are also

Table VII. Calculation of Score for PC1 Using Specimen 7 (Table V)

variate	raw data	transformed data	standardized[a] score	PC1[b] coeff	PC1[c]
dry wt	0.094	−1.027	−0.512	0.091	−0.047
day of collection	93	1.017	0.888	0.354	0.314
metal concn					
Mn	32 + 1	1.519	1.559	0.409	0.638
Fe	633	2.801	1.144	0.263	0.301
Cu	49	1.690	6.106	0.224	1.368
Zn	415	2.618	−0.501	0.130	−0.067
Pb	12 + 1	1.114	2.499	−0.069	−0.172
water content	0.855	−0.068	1.164	−0.225	−0.262
shell length	27	1.431	−0.645	0.029	−0.019
score for PC1 =					2.054[d]

[a] For example, for day of collection = (1.017 − 0.067)/1.070, where 0.067 and 1.070 are the mean and standard deviation of the variate from the reference area (cf. Table III and eq 1). [b] See Table IV. [c] PC1 = standardized score × PC1 coefficients. [d] Number differs from that shown in Table VI due to rounding off error.

plotted in Figure 1 but have been circled. The letters "S" and "L" indicate whether a small or large mussel was used. The values of the mussels from some of the sites in question are close to the centroid and indicate that the mussels from these sites resemble those mussels collected from the reference area, Rocky Point. The data for these mussels suggest that the waters in which they live contain approximately the same concentration of trace metals as those at Rocky Point. Although one of the distances for the mussel from Montague Harbour is high, it is due to the high negative value on the third principal component, which measures trace-metal body burdens independent of time of year. The large value is due primarily to the large negative scores for concentrations of lead and zinc in these mussels compared with those collected from Rocky Point. We can conclude that there is probably less lead and zinc in the waters at Montague Harbour than there is at Rocky Point, and hence, the area may represent an environment with a higher quality than that found at Rocky Point. In contrast to lead and zinc, the concentration of copper is higher in mussels from Montague Harbour than those collected from Rocky Point. These mussels were collected in the intertidal region bordering a provincial park. Further, Montague Harbour is situated in the Gulf Islands, which have virtually no industry and hardly a significantly high population. The area is virtually pristine. Hence, the data indicate that natural background concentrations of copper in seawater at Montague Harbour may be higher than those assessed for the reference area. The remaining mussels have scores that are sufficiently high that their coordinates on the figure lie outside the third standard deviation isopleth. This indicates that they have less than a 1% probability of resembling mussels collected from the reference site, and therefore, it can be inferred that the water quality is poorer than that found at Rocky Point. This is not surprising considering that some mussels were taken from near storm water outfalls (Seabus, Seven Seas) and others from near sites used for shipping or industrial use (Crofton Wharf, Seaspan Wharf).

Conclusion

Two necessary requirements of monitoring programs are to be able to detect pollution effects against the background of the natural variability found in sentinel organisms (6) and then to decide whether such an effect is sufficiently different from a reference population, i.e., represents a population of organisms from a polluted environment. This paper shows a statistical approach for resolving the "pollution signal" from the "noise" (6) and then deciding whether or not such a signal is significantly

different from that obtained for the reference area.

Only some of the known priority pollutants were considered due to the nature of the analytical technique. Nevertheless, we suggest that areas in which mussels are found to have very high concentrations of lead, zinc, copper, or iron are reflecting industrial pollution of the surrounding seawater. One aspect of our test showing the validity of the concept discussed in this paper is that we were able to locate an area having less Zn and Pb pollution than the reference area, as well as locating other areas with much higher levels. Further, these areas have been identified in spite of the fact that individual mussels of different sizes were analyzed and collected at different times of the year. Obviously, greater reliability of the data for new areas can be obtained if the data are obtained for mussels that have been pooled together so that the sample is representative of the population. Such pooling also permits analyses of single samples of many mussels from areas to be analyzed and, hence, reduces the cost of a monitoring program.

Appendix

Question: Is the seawater around Seaspan Wharf Polluted?

(1) Collect Specimens.

(2) Measure values for each of the variates and calculate PCs as in 3 below.

(3) Let us use specimens described in Table V and plotted in Figure 1 (see Table VII).

(4) Similarly the value for PC3 can be determined (PC3 = 1.39).

(5) Calculate distance of specimen from origin:

$$\sqrt{D^2} = \sqrt{2.054^2 + 1.39^2} = 2.48$$

(6) Since $D = 2.48$ is between 2 and 3 standard deviation units from the origin, we can conclude that the probability that the specimen in question resembles the specimens of the reference collection is between 5% and 1%.

(7) The exact probability value can be determined by using the χ-square value, e.g., $\chi^2 = D^2 = 6.151$.

(8) The probability of $\chi^2 = 6.151$ with one degree of freedom is 1.313%.

Literature Cited

(1) Goldberg, E. D.; Bowen, V. T.; Farrington, J. W.; Harvey, G.; Martin, J. H.; Parker, P. L.; Risebrough, R. W.; Ropertson, W.; Schneider, E.; Gamble, E. *Environ. Conserv.* **1978**, *5*, 101.
(2) Phillips, D. J. H. *Environ. Pollut.* **1977**, *13*, 281.
(3) Popham, J. D.; Johnson, D. J.; D'Auria, J. M. *Mar. Pollut. Bull.* **1980**, *11*, 261.
(4) Popham, J. D.; D'Auria, J. M. *Water, Air Soil Pollut.* **1980**, *14*, 115.
(5) Cooley, W. W.; Lohnes, P. R. In "Multivariate Data Analysis"; Wiley: Sons: New York, 1971; p 364.
(6) Bayne, B. L.; Clarke, K. R.; Moore, M. N. *Aquat. Toxicol.* **1981**, *1*, 159.
(7) Boyden, C. R. *J. Mar. Biol. Assoc. U.K.* **1977**, *57*, 675.
(8) Phillips, D. J. H. *Mar. Biol.* **1976**, *38*, 59.
(9) Davenport, J. *J. Mar. Biol. Assoc. U.K.* **1977**, *57*, 63.
(10) Phillips, D. J. H. *Mar. Biol.* **1977**, *41*, 79.
(11) Popham, J. D.; D'Auria, J. M. *Bull. Environm. Contam. Toxicol.* **1981**, *17*, 660.
(12) Sutherland, J.; Major, C. W. *Comp. Biochem. Physiol. C* **1981**, *68*, 63.
(13) Stump, I. G.; Kearney, J.; D'Auria, J. M.; Popham, J. D. *Mar. Pollut. Bull.* **1979**, *10*, 270.
(14) Popham, J. D.; D'Auria, J. M. *Arch. Environm. Contam. Toxicol.* **1982**, *11*, 273.
(15) Popham, J. D.; D'Auria, J. M. *Arch. Environm. Contam. Toxicol.* **1983**, *12*, 1.
(16) Graham, D. *Veliger* **1971**, *14*, 365.
(17) Nielson, S. A. *New Zealand J. Mar. Freshwater Res.* **1974**, *8*, 631.
(18) Dixon, W. J.; Brown, M. B. In "Biomedical Computer Programs, P-Series"; University of California Press: Berkeley, CA, 1979; p 880.
(19) Simpson, R. D. *Mar. Pollut. Bull.* **1979**, *10*, 74.
(20) Fowler, S. W.; Oregioni, B. *Mar. Pollut. Bull.* **1976**, *7*, 26.
(21) Dare, P. J.; Edwards, D. B. *J. Exp. Mar. Biol. Ecol.* **1975**, *18*, 89.
(22) Schultz-Baldes, M. *Mar. Biol.* **1973**, *21*, 98.
(23) Pentreath, R. J. *J. Mar. Biol. Assoc. U.K.* **1973**, *53*, 127.

Measurement and Prediction of Distribution Coefficients for Wastewater Aromatic Solutes

James R. Campbell and Richard G. Luthy*

Department of Civil Engineering, Carnegie-Mellon University, Pittsburgh, Pennsylvania 15213

Manuel J. T. Carrondo

Departamento de Ciencias do Ambiente, Universidade Nova De Lisboa, Lisboa, Portugal

■ Experiments were performed to evaluate distribution coefficients for aniline, naphthalene, naphthol, phenol, and pyridine between water and several organic solvents. The data for aniline, phenol, and pyridine have shown that distribution coefficients for these compounds in clean water, single solute systems are not statistically different from distribution coefficients determined in a complex coal conversion wastewater. Application of these and other data for distribution coefficient modeling techniques has shown that a regular solution theory model is accurate only for systems that do not include hydrogen bonding. However, this approach is suitable for a relative ranking of the solvents for extraction of phenolic solutes. For hydrogen-bonded solvent systems, the distribution coefficient appears to be well correlated with solute octanol–water partition coefficient data when compatible hydrogen-bonding solute–solvent systems are compared.

Introduction

Solvent extraction is a useful unit operation for separation of organic compounds from an aqueous phase. This process can be used to remove organic compounds from wastewater, and it may play a key role in processing of organic-laden condensates formed from the production of synthetic fuels in coal liquefaction and low-temperature gasification (1–6). An important parameter for evaluation and design of solvent extraction systems is the distribution coefficient, which describes the partitioning of an organic solute between water and the organic solvent. Therefore,

it is of interest to measure and predict distribution coefficients for specific organic compounds that may be present in a wastewater stream. This paper addresses techniques for evaluating the partitioning of representative wastewater aromatic solutes (4, 6–8) between water and several organic solvents. The solvents chosen for this study were selected in order to represent major classes of solvents; another consideration was to employ solvents that have been used in pilot or commercial solvent extraction facilities [9, 10].

Distribution Coefficient

The equilibrium partitioning of organic compounds (solute) between aqueous and organic solvent phases may be determined experimentally from the equilibrium ratio of solute mass concentration (C, mg/L) in each phase

$$K_D = C_s/C_w \qquad (1)$$

where the subscripts s and w identify the solvent and water phases, respectively. This ratio is referred to as the solute distribution coefficient.

By imposing the equilibrium condition that solute chemical potential is equal in each phase together with the assumption that for dilute solutions the solute mole fraction may be expressed as the product of solute molar concentration and solvent molar volume, we can express K_D as (11)

$$K_D = C_s/C_w = (\gamma_w^* V_w^*)/(\gamma_s^* V_s^*) \qquad (2)$$

where γ^* = solute mole fraction activity coefficient in each

phase at equilibrium and V^* = partial molar volume of each phase $(cm^3/(g \cdot mol))$.

For water–solvent systems that are immiscible, solute activity coefficients in mutually saturated phases (γ^*) are equal to those in the pure solvent (γ), and partial molar volumes (V^*) reduce to pure solvent molar volumes (V). Hence, pure component properties may be used.

Predictive Models

Regular Solutions. From eq 2 it can be seen that the distribution coefficient can be calculated from knowledge of the mole fraction activity coefficients of a given solute in both the aqueous and solvent phases. For organic compounds in water, various correlations have been developed that relate molecular properties and structural characteristics with the aqueous phase activity coefficient. For the compounds studied in this investigation, we have taken pure component infinite dilution aqueous phase activity coefficients from a compilation presented by Tsonopoulos and Prausnitz (12), and for pyridine we have calculated γ_w from the UNIFAC method described in ref 13.

The pure component solute mole fraction activity coefficient at infinite dilution in the extraction solvent phase may be predicted by using an extension of the regular solution concept (14). In a strict sense the regular solution concept applies only to nonpolar, reasonably symmetric solute and solvent molecules whose interactions are dominated by nonspecific dispersion forces. However, regular solutions can be used to describe systems that include some degree of polar interaction, so long as these forces do not result in specific orientation of solute and solvent molecules (14).

Weimer and Prausnitz (15) and Helpinstill and Van Winkle (16) expanded the regular solution concept to describe systems with polar components. The pure component infinite dilution solute mole fraction activity coefficient in the solvent phase may be expressed as (16)

$$\ln \gamma_s^\infty = [V_2/(RT)][(\lambda_1 - \lambda_2)^2 + (\tau_1 - \tau_2)^2 - 2\psi_{12}] + \ln (V_2/V_1) + 1 - (V_2/V_1) \quad (3)$$

where γ_s^∞ = mole fraction activity coefficient of solute at infinite dilution in the solvent phase, V = molar volume (cm^3/mol), λ = nonpolar solubility parameter $(cal/cm^3)^{1/2}$, τ = polar solubility parameter $(cal/cm^3)^{1/2}$, ψ_{12} = empirical correction term (cal/cm^3), R = universal gas constant $(cal/(K \cdot mol))$, T = absolute temperature (K), subscript 1 = solvent, and subscript 2 = solute.

The polar and nonpolar solubility parameters of a substance represent the energy required to remove it from its own pure liquid and may be calculated from enthalpy of vaporization data $(\Delta H_v, cal/mol)$ as the potential energy per unit volume (14–16):

$$\lambda^2 + \tau^2 = (\Delta H_v - RT)/V \quad (4)$$

The nonpolar solubility parameter may be computed separately from a correlation with refractive index (n) given by Karger et al. (17):

$$\lambda = 30.7(n^2 - 1)/(n^2 + 2) \quad (5)$$

Polar solubility parameters may thus be calculated from eq 4 and 5.

$$\tau = [[(\Delta H_v - RT)/V] - \lambda^2]^{1/2} \quad (6)$$

The empirical correction term (ψ_{12}) represents the interaction energy between solute and solvent molecules that is not symmetric. It is intended to account for interactions where the solvent and solute molecules play separate roles.

This includes induction effects where the permanent dipole of one molecule acts on the polarizability of the other and hydrogen-bonding forces where one molecule acts as proton donor and the other as proton acceptor. Weimer and Prausnitz (15) developed one expression for ψ_{12} based on correlations with the solvent polar solubility parameter by using experimental data for nonpolar solute–polar solvent pairs. The correction term for aromatic solutes was developed from data for polar solvent–benzene systems for which

$$\psi_{12} = 0.45\tau_1^2 \quad (7)$$

Helpinstill and Van Winkle (16) proposed a different correlation for the empirical correction term, referred to as ψ_{12}^*. They suggest using both solute and solvent polar solubility parameters to estimate the value of the correction term. The authors developed their correlation for aromatic solutes from data for hydrocarbon solute–polar solvent pairs as

$$\psi_{12}^* = 0.477(\tau_1 - \tau_2)^2 \quad (8)$$

Others (17–19) have utilized an expanded solubility parameter approach to compute γ_s^∞ for applications in chromatography where the empirical correction term (ψ_{12}) is replaced with solubility parameters which describe hydrogen-bonding and dipole induction effects. However, correlations for these solubility parameters do not escape empiricism and often the data needed for their calculation are not available. From a practical point of view, for the range of solutes and solvents of interest in this investigation, these expanded solubility parameter models are cumbersome and do not improve upon the results given by eq 3.

Linear Free Energy Relationships. When nonrandom molecular interactions are considered, the concept of regular solutions may not provide adequate estimates of solute activity coefficients. This is true whether one is dealing with pure components which self-associate (e.g., water) or with component mixtures which form strongly interactive pairs such as hydrogen-bonded systems (20). Hence, for hydrogen-bonded systems, another approach for estimation of the distribution coefficient is warranted. One such approach, termed linear free energy relationships (21), correlates distribution coefficients for a given solvent–solute–water system with a partition coefficient from a reference system.

Leo and Hansch (21) have shown that octanol is a particularly good choice as a reference solvent. Tabulations of various octanol–water partition coefficients (K_{ow}) are available for a wide variety of solutes (22, 23), and correlations with K_{ow} have been used in other applications including aqueous solubility (11, 24), bioaccumulation (25, 26), and sorption of organics on soil (27). No correlations with K_{ow} have been found for the solvents of practical interest for removal of aromatic solutes from wastewater.

The correlation between K_D for a given solvent–solute–water system and K_{ow} is (21)

$$\log K_D = a + b \log K_{ow} \quad (9)$$

where a and b are constants. The numerical values of the correlation coefficients a and b are dependent upon the solvent and solute sets being considered.

Materials and Methods

Reagents and Glassware. Distribution coefficients were experimentally determined for aniline, naphthalene, naphthol, phenol, and pyridine between water and five organic solvents. The solvents included methyl isobutyl

Table I. Summary of the Distribution Coefficients (K_D, (mg/L)/(mg/L)) for Liquid–Liquid Equilibrium between Single Solutes and Solvents

| solute | solvent | K, (mg/L)/(mg/L)[a] | | |
		mean ± SD	RSD %	range
aniline	DIPE	7.6 ± 0.4	5.3	6.9–8.2
	MIBK	31.4 ± 1.4	4.5	28.9–33.5
	NBA	23.1 ± 1.5	6.4	20.8–25.3
	tetradecane	0.74 ± 0.07	9.4	0.67–0.88
	toluene	8.4 ± 0.4	5.2	7.6–9.1
pyridine	DIPE	1.34 ± 0.10	7.7	1.21–1.51
	MIBK	2.9 ± 0.14	4.8	2.7–3.2
	NBA	2.8 ± 0.2	6.7	2.5–3.0
	tetradecane	0.46 ± 0.05	10.0	0.41–0.56
	toluene	2.5 ± 0.2	6.1	2.3–2.8
naphthalene	DIPE	3534 ± 577	16.3	2670–4446
	MIBK	5076 ± 442	8.7	4444–5726
	NBA	6398 ± 236	3.7	6226–6813
naphthol	DIPE	740 ± 101	13.6	603–893
	MIBK	1370 ± 192	14.0	1123–1691
	NBA	1360 ± 160	11.7	1163–1559

[a] Except relative standard deviation, %.

ketone (MIBK), *n*-butyl acetate (NBA), diisopropyl ether (DIPE), toluene, and tetradecane. K_D values were determined for these components in single and multiple solute clean water systems and in an actual coal gasification wastewater.

The raw gasification wastewater was obtained from the slagging fixed-bed gasifier at the Grand Forks Energy Technology Center during steady-state operation with a lignite coal. This wastewater was buffered by high levels of dissolved ammonia and carbon dioxide to pH 8.3 (*28*). The clean water samples were composed of distilled water buffered with 0.1 N sodium bicarbonate to pH 8.4; thus, pH was not a variable in these experiments. For phenol (pK_a = 9.98) the value of K_D is lowered by about 2% at pH 8.3 (*29*), which is within the experimental accuracy of these tests.

Extraction Experiments. Distribution coefficients for aniline, pyridine, and phenol were determined by batch extraction at ambient laboratory temperatures (23 ± 2 °C) by using glass separatory funnels. Duplicate tests were performed at solvent-to-water ratios of 0.2, 0.4, 0.6, 0.8, and 1.0. Water and solvent were mixed by conducting 50 sample inversions in approximately 90 s. This was followed by 30 min of separation after which the aqueous phase was placed in a tapered volumetric flask for further analysis. It was found in initial screening studies that the sample inversion and settling procedure provided sufficient contact time for equilibrium. Other workers (*30*) have also reported equilibrium to be achieved rapidly when extracting solutes from water to solvent.

Because naphthalene and naphthol have relatively low aqueous solubilities, a different technique was used to determine distribution coefficients for these solutes. Batch extractions were conducted in specially constructed Erlenmeyer flasks at ambient laboratory temperatures in the absence of light with no head space. The flasks were fitted with septum ports at the base in order that aqueous phase samples could be withdrawn for HPLC analysis. Teflonlined screw caps were fitted to the top of the flasks to prevent loss of solvent and solute by volatilization. The solutions were mixed on a magnetic stirrer for 24 h, as screening tests had shown that 24 h was required for equilibrium to be achieved under conditions in which solute was extracted from solvent to water. This was followed by 90 min of separation after which an aqueous sample was withdrawn with a microliter syringe for immediate analysis.

Analysis. Aqueous samples of aniline, phenol, and pyridine were analyzed on a temperature-programmable Varian 3700 gas chromatograph equipped with a flame ionization detector. Aniline and pyridine analyses were performed with a glass column (1.8 m × 2 mm i.d.) packed with a silicone phase on a support deactivated for basic compounds (Supelco, catlog no. 1-1896). Phenol was analyzed on a Tenex-GC glass column (1.8 m × 2 mm; Supelco, no. 1-3671). Naphthalene and naphthol determinations were accomplished with a Perkin-Elmer Series 3 high-pressure liquid chromatograph by using a constant flow gradient pumping system with acetonitrile and water, a reverse-phase column (Supelcosil LC-PAH, 4.6 mm × 250 mm), and a fluorescence detector.

Experimental Results

Single Solute Systems. Initial tests were conducted with single solute, clean water solutions of aniline or pyridine by using each of the five solvents. Table I summarizes the results of these tests for the systems considered, where each reported value of K_D represents the mean of 12 experimental values. Standard deviation (SD), relative standard deviation (RSD, %), and range (lower–higher experimental value) are also included in Table I. The relative standard deviation and range data show the reliability of experimental results. It was also noted that the water/solvent ratio did not affect the value of K_D for these systems. Table I also shows results of determination of distribution coefficients for naphthalene and naphthol with the polar solvents. Typically, 8–12 determinations were performed with each combination of naphthalene, naphthol, and solvent.

Experiments were also performed to determine the effect of pyridine and aniline concentration on the distribution coefficient with the most polar solvent, MIBK. Single solute aqueous solutions of 500, 2000, 10 000, and 20 000 mg/L aniline or pyridine were extracted with MIBK at two volume ratios (0.2 and 0.4); duplicate tests were performed. An analysis of variance using the F test (*31*) was performed on the 16 results, and this showed that solute concentration does not affect the value of the distribution coefficient for aniline or pyridine in MIBK up to concentrations of 20 000 mg/L.

Multiple Solute and Wastewater Systems. Because a wide range of organic and inorganic compounds will exist in wastewaters, it is of interest to investigate the possibility of antagonistic or synergistic effects on the equilibrium

Table II. Distribution Coefficients for Liquid–Liquid Equilibrium between Solutions Containing Aniline and Pyridine at 500 mg/L Each and Four Solvents

solute	solvent	K_D, (mg/L)/(mg/L), mean ± SD	t test[a] variances equal	assumed different
aniline	DIPE	7.6 ± 0.3	0.049, NS[b]	0.058, NS
	MIBK	30.0 ± 0.4	1.97, NS	3.15, 0.01[c]
	NBA	23.9 ± 1.5	0.92, NS	0.92, NS
	toluene	8.1 ± 0.2	1.17, NS	1.64, NS
pyridine	DIPE	1.41 ± 0.08	1.21, NS	1.38, NS
	MIBK	3.03 ± 0.03	1.95, NS	3.26, 0.01
	NBA	2.9 ± 0.1	1.11, NS	1.34, NS
	toluene	2.4 ± 0.1	1.26, NS	1.39, NS

[a] Comparison with the experimental values from the single solute tests (see text). [b] This mean and that reported in Table I are not significantly (NS) different at the 95% confidence level. [c] This mean and that reported in Table I are significantly different at the 99% confidence level ($\alpha = 0.01$).

Table III. Distribution Coefficients for Liquid–Liquid Equilibrium between Aniline, Pyridine, and Phenol in Filtered Coal Gasification Wastewater and Four Solvents

Aniline and Pyridine

solute	solvent	K_D, (mg/L)/(mg/L),[a] mean ± SD	t test[b] variances equal	assumed different
aniline	DIPE	7.3 ± 0.3	1.17, NS	1.47, NS
	MIBK	31.4 ± 1.8	0.01, NS	0.01, NS
	NBA	23.4 ± 1.4	0.40, NS	0.41, NS
	toluene	8.4 ± 0.4	0.10, NS	0.10, NS
pyridine	DIPE	1.34 ± 0.14	0.03, NS	0.02, NS
	MIBK	2.9 ± 0.2	0.21, NS	0.18, NS
	NBA	2.7 ± 0.1	0.42, NS	0.51, NS
	toluene	4.8 ± 0.6	13.0, 0.01	7.70, 0.01

Phenol

solvent	K_D, (mg/L)/(mg/L)	reported K_D[c]
DIPE	30 ± 1.0	29
MIBK	102 ± 4	100
NBA	69 ± 5	71
toluene	2.5 ± 0.2	2.0

[a] Initial concentrations were 500, 495, and 2020 mg/L for aniline, pyridine, and phenol, respectively. [b] For notation see Table II. [c] Ref 23.

distribution coefficient. To address this issue, K_D's were experimentally determined in clean water solutions with both aniline and pyridine and in an actual phenolic coal gasification wastewater.

The clean water tests were conducted with initial aniline and pyridine concentrations of 500 mg/L. Duplicate extractions were performed at water-to-solvent ratios of 0.2 and 0.4. These results were then compared statistically with results shown in Table I by performing a t test on differently sized populations. The t tests were performed by assuming sample variances to be equal and also considering them not necessarily equal (i.e., different) by using the Smith–Satterthwaite test (31).

Results of this statistical analysis are shown in Table II. It can be seen that for the NBA, DIPE, and toluene systems there are no apparent antagonistic/synergistic effects; that is, the sample means are not statistically different at the 95% confidence level. The MIBK systems show means that are different. However, because the difference was not significant when variances were assumed equal and because this small difference in mean values was not observed in tests conducted with the coal gasification wastewater, it was felt that this result was an anomaly.

Wastewater tests were conducted with a filtered sample of coal gasification condensate. Because the wastewater had low concentrations of aniline and pyridine (approximately 20 and 40 mg/L, respectively), it was spiked to a measured concentration of 500 and 495 mg/L, respectively. The phenol content after spiking was 2020 mg/L. Duplicate extractions were performed at solvent/water ratios of 0.2 and 0.4. These results were compared statistically with single solute distribution coefficient data for aniline and pyridine given in Table I. Wastewater samples were also analyzed for phenol content under the same conditions. As there were not adequate experimental results for a statistical comparison, the values reported in the literature for phenol in clean water are presented for straight comparison.

Results of the wastewater tests are summarized in Table III. For the aniline and pyridine systems the statistical analysis shows that for all cases except pyridine–toluene, the values of the distribution coefficients are not affected by the presence of other wastewater species. The toluene–pyridine system showed a sharply increased value for the distribution coefficient in the wastewater. This test was repeated under the same conditions, and similar results were obtained. To determine if some interaction between pyridine and phenol was responsible for this ef-

fect, a synthetic aqueous solution of pyridine and aniline at 500 mg/L each and phenol at 5000 mg/L was prepared and extracted at 0.2 and 0.4 solvent/water ratios. The K_D's obtained for toluene–pyridine were similar to those obtained in the wastewater. Hence, it is seen that phenol and pyridine appear to have a synergistic effect on the value of K_D for the toluene–pyridine system.

The distribution coefficients determined for phenol in the wastewater compare favorably with those reported in the literature for phenol in clean water. However, we should note that the K_D for phenol–toluene in the wastewater system does show an increase over that for phenol in clean water. Beychok (32) notes that an increase in K_D for phenol has been observed in the processing of petroleum for gasoline. He attributes the effect to base fraction organic compounds such as pyridine or quinoline present at concentrations greater than about 300 mg/L. Therefore, it appears that phenol and pyridine can form an interactive pair, probably through hydrogen bonding, that results in an increase in their respective K_D's. This effect should be more pronounced in hydrocarbon solvents, and it should be mentioned that synergistic/antagonistic effects between wastewater solutes could change for solutes at low concentrations.

Hydrogen Bonding

Hydrogen bonding (H bonding) occurs between solute and solvent molecules when one component acts as proton donor and the other as a proton acceptor. Following the notation of Pimentel and McClellan (33) we can refer to proton acceptors as B-type and proton donors as A-type molecules. Molecules that possess both donator and acceptor functional groups are termed AB type, and compounds exhibiting poor or no hydrogen-bonding characteristics can be classified as N type. Hence, H bonding can occur when A- and B-type, A- and AB-type, B- and AB-type, or AB- and AB-type molecules are mixed together. H bonding does not occur between solute and solvent molecules when two B-type or two A-type molecules are mixed together, or when one or both components are N type.

This scheme is complicated somewhat by the behavior of AB-type molecules. These compounds can self-associate
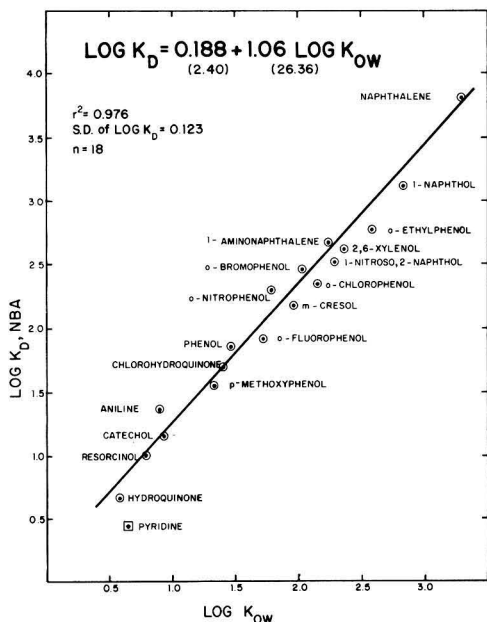
Figure 1. Correlation of distribution coefficients for various AB-type aromatic solutes in NBA–water and octanol–water systems. Pyridine was not included in the correlation; see text for explanation.

Figure 2. Correlation of distribution coefficients for various AB-type aromatic solutes in MIBK–water and octanol–water systems. Pyridine was not included in the correlation; see text for explanation.

to form dimers, trimers, etc., or form H bonds within a single molecule. The latter is termed intramolecular H bonding. Intramolecular H-bonded compounds are of particular interest because they may not behave like AB-type species; despite their having both acidic and basic groups, they tend to behave as N- or B-class molecules (33). The self-associating tendency of AB-class solutes, both polymer and intramolecular types, may be disrupted when these molecules are mixed with a strong donor or acceptor solvent. In this case H bonding between the solute and solvent can occur and displace the self-associated H bond.

A classification of the compounds of interest in this study shows that toluene and naphthalene are N-type molecules, although aromatic hydrocarbons do show some proton acceptor character (33). Pyridine, NBA, MIBK, and DIPE are B-type molecules; while phenolics, naphthol, aniline, aminonaphthalene, and quinolinols are AB-type molecules. Phenol is known to form dimers at sufficiently large concentrations (34), and it should be noted that ortho-substituted phenolics tend to form intramolecular H-bonds (33). The quinolinols and substituted naphthols shown in Figure 1–5 are believed to self-associate.

With the classification scheme described above we expect that all solutes considered here, except pyridine and naphthalene, should be able to form hydrogen bonds with NBA, MIBK, and DIPE. Furthermore, all solutes except naphthalene should be expected to form H bonds with octanol, while no solute is expected to form H bonds of significant strength with toluene. In hydrocarbon solvents like toluene, H bonding could occur between two solutes if they are present at sufficiently large concentrations (e.g., phenol–pyridine).

Modeling Results

The regular solution model of Helpinstill and Van Winkle (eq 3) was used to compute solute activity coefficients in the solvent phase; these values were then used
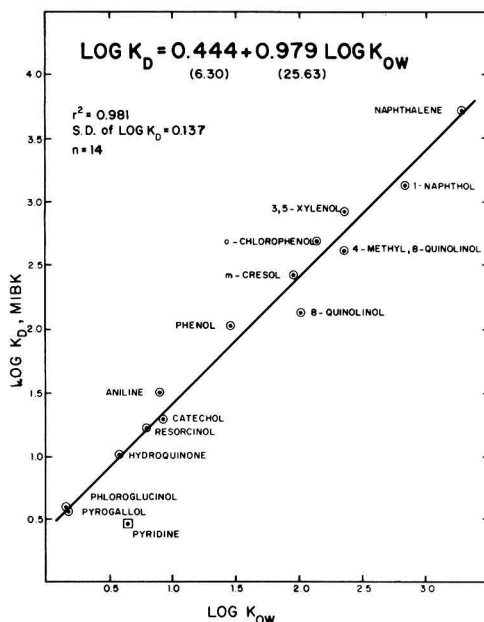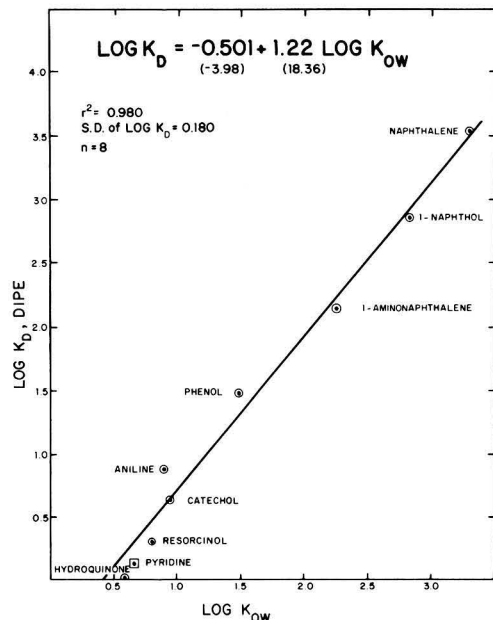
Figure 3. Correlation of distribution coefficients for various AB-type aromatic solutes in DIPE–water and octanol–water systems. Pyridine was not included in the correlation; see text for explanation.

in conjunction with literature values of solute activity coefficients in water (12) to predict distribution coefficients for several solvent–solute pairs. Thermodynamic data used in eq 3 were computed from 5–8 with data obtained from ref 35–37.

$$\text{LOG } K_D = -1.26 + 1.02 \text{ LOG } K_{OW}$$
$$(-7.32)\quad(13.53)$$

$r^2 = 0.938$
S.D. of LOG K_D = 0.154
$n = 13$
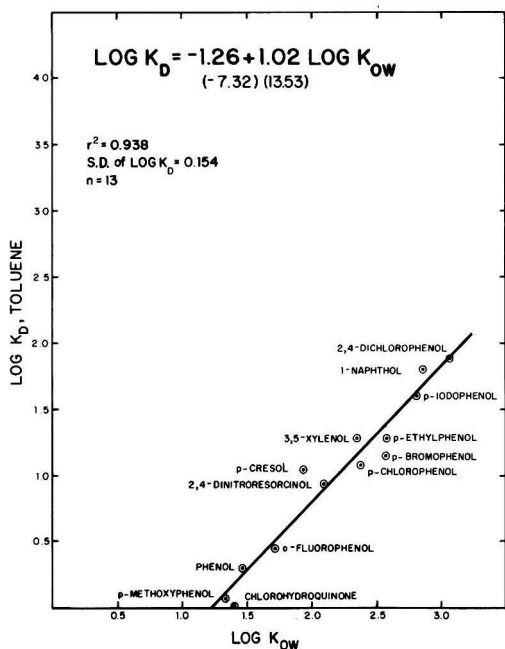
Figure 4. Correlation of distribution coefficients for various phenolic solutes, exhibiting primarily A-type character, in toluene–water and octanol–water systems.

$$\text{LOG } K_D = -0.348 + 1.30 \text{ LOG } K_{OW}$$
$$(-1.84)\quad(11.95)$$

$r^2 = 0.940$
S.D. of LOG K_D = 0.194
$n = 10$
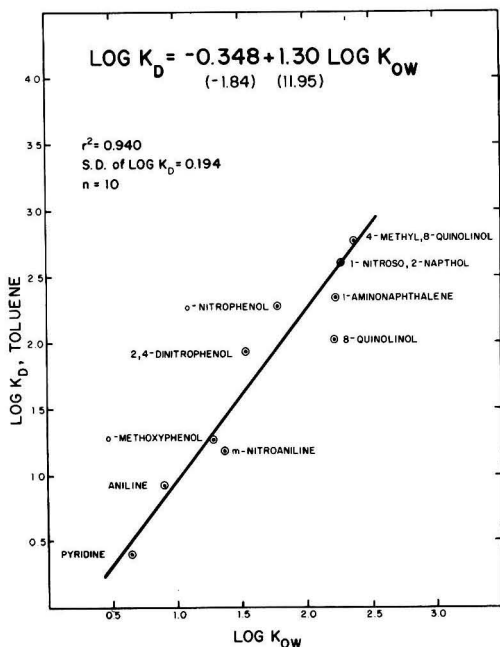
Figure 5. Correlation of distribution coefficients for various aromatic solutes, exhibiting primarily B-type character, in toluene–water and octanol–water systems.

Table IV compares the results of these calculations with experimental K_D values obtained in the present work, as well as with experimental values reported by ref 9 and 23. Two values of predicted K_D are reported in Table IV, depending on which expression was used to estimate the

Table IV. Comparison of Experimental and Predicted Distribution Coefficients, (mg/L)/(mg/L)

	MIBK			NBA			DIPE			toluene		
		eq 3			eq 3			eq 3			eq 3	
solute	exptl	$\psi_{12}*$	ψ_{12}	exptl	$\psi_{12}*$	ψ_{12}	exptl	$\psi_{12}*$	ψ_{12}	exptl	$\psi_{12}*$	ψ_{12}
aniline	31.4	5.2	231	23.1	5.4	73	7.6	3.4	3.3	8.4	17	13
catechol	19.5	0.05	6.88	13.2	0.06	0.99	4.9	0.03	0.01	0.05	0.19	0.03
o-chlorophenol	490	7.6	5.55	270	8.5	7.1				23	28	27
m-cresol	264	10	2132	153	10.3	223						
p-cresol				200	12	250						
hydroquinone	9.92	0.10	0.72	4.5	0.09	0.02	1.03	0.04	<0.01	11	26	1.7
phenol	102	3.04	274	71	3.0	36	30	1.8	0.3	2.0	0.27	<0.01
pyridine	2.9	0.76	46	2.8	0.76	8.2	1.34	0.51	0.15	2.5	6.6	0.65
resorcinol	16.6	0.03	0.63	9.9	0.03	0.03	2.06	0.01	<0.01	0.01	1.2	0.22
3,5-xylenol	814	23.32	5200	540	24	825				20	0.05	<0.01
naphthalene	5075	9460	5×10^6	6400	8740	2.3×10^5	3535	6630	245	63	74	46
naphthol	1370	134	19800	1360	143	4820	740	76	107		520	490

empirical correction term. Inspection of the data reveals that, in general, the regular solution model provides reasonable estimates of K_D for non-hydrogen-bonded systems. Data for the toluene–solute pairs show that range values of K_D can be predicted by using either correlation for the empirical correction term, ψ_{12} or $\psi_{12}*$. Predictions of K_D for naphthalene and pyridine in the polar solvents (MIBK, NBA, DIPE) are within range when the correction term is correlated with solute polarity (i.e., $\psi_{12}* = 0.477(\tau_1 - \tau_2)^2$). The magnitude of K_D values for the H-bonded systems considered here are not reliably predicted by the regular solution model. When evaluating the accuracy of predicted distribution coefficients, one should appreciate that K_D's can vary over many orders of magnitude, as evidenced by the range of experimental values shown in Table IV. While the regular solution model does not give reliable predictions for the magnitude of K_D for H-bonded systems, it is applicable for a relative ranking of several solvents for extraction of a particular solute when the correction term is correlated with solvent polarity ($\psi_{12} = 0.45\tau_1^2$). For example, K_D values for phenol show the ranking MIBK > NBA > DIPE > toluene, for aniline, MBIK > NBA > DIPE, etc. This observation has also been made by Kiezyk and Mackay (38) for phenol–solvent systems in which both polar and nonpolar solvents were evaluated.

Failure of the regular solution model to predict distribution coefficients for the phenolic solute–solvent systems is principally a result of the fact that the regular solution concept excludes systems that include specific interactions, notably, hydrogen bonding. Furthermore, there is an inherent error in the models owing to the correlations from which the empirical correction terms were predicted. These correlations were based on data from Deal and Derr (39) and Pierotti et al. (40). These compilations do not include data for polar solute–polar solvent systems. In addition, the data were from systems for which the solute organic phase mole fraction activity coefficients were greater than unity (i.e., positive deviations from ideality). Experimental results for the solute–polar solvent systems considered here reveal that, except for naphthalene, the organic phase mole fraction activity coefficients for the various solutes in MIBK, NBA, and DIPE were less than unity (i.e., negative deviations from ideality). H-bonded systems generally show negative deviations from ideality (33).

Linear Free Energy Relationships. The linear free energy approach of Leo and Hansch (21) was used to correlate distribution coefficients for aromatic solutes in NBA, MIBK, DIPE, and toluene with K_D values for the respective solutes in octanol. These correlations are shown in Figures 1–5, and experimental data were obtained from our own work, from the partition coefficient data base at Pomona College (23), and from Greminger and King (9). A least-squares analysis was used to obtain a best-fit straight line for the data, and the results are shown on the respective figures. Other statistical data shown include t statistics for the coefficients a and b, the r^2 values for the equations, the standard deviation of log K_D about the regression line, and the number of data points used in the correlations.

A review of Figures 1–5 shows a strong correlation between log K_D and log K_{ow} for the systems considered. Excellent correlation is obtained because compatible hydrogen-bonding systems are being compared. The procedure is not expected to work well when the solute set contains molecules which can H bond to both solvents along with those which can H bond to only one solvent (21). For a given solvent we expect solute sets with different H-bonding character to fit different correlations; hence, the correlation coefficients a and b depend upon the solute set. This is exemplified by the correlations for toluene–solute systems where molecules with predominately A-type character fit one correlation (Figure 4) and molecules with predominately B-type character fit another correlation (Figure 5). Alternatively, for a given solute set, the coefficients a and b are dependent upon the solvent being correlated with octanol. This is evidenced by Figures 1–4 where, for solute sets dominated by AB-type phenolic compounds, different values of a and b are obtained for NBA, MIBK, DIPE, and toluene. This is a result of the different H-bonding character of esters, ketones, ethers, and aromatic hydrocarbons.

A knowledge of compound structure and use of the solvent selectivity triangle of Snyder (41) is helpful in understanding differences in solvent character. Snyder gives the relative ranking of proton acceptor strength as NBA, MIBK, octanol, and DIPE. That NBA and MIBK are listed as having a stronger base strength is consistent with the double-bonded structure of the oxygen atom in esters and ketones (41). Snyder's classification scheme shows that NBA and MIBK have a similar chemical nature; this is also shown in Figures 1 and 2. Here we can see that the magnitude of the distribution coefficients for the compounds shown are similar in both solvents and that K_D values are consistently higher than respective K_{ow}'s. The chemical similarity of NBA and MIBK is also reflected by similar values of the slope of the correlation.

The data used in Figures 1 and 2 are for AB-class solutes, except naphthalene and pyridine. Naphthalene was included in these correlations because its distribution coefficient in NBA and MIBK is higher than its K_{ow} value, hence following the trend of the AB-type solutes, and because its attraction to NBA, MIBK, and octanol is dominated by nonspecific dispersion forces. Naphthalene does not H bond to an appreciable extent with these solvents and hence shows similar kinds of attractive energies. Pyridine was not included in these correlations because it can H bond with octanol but not with NBA and MIBK; note that the K_{ow} value for pyridine is higher than its K_D in either NBA or MIBK. We expect that a separate correlation for B-type solutes (e.g., pyridine) could be made if sufficient data were available. That the ortho-substituted phenolics are shown to behave like AB-type molecules suggests that the H-bonding strength of NBA and MIBK is sufficient to displace the intramolecular H bonds.

Snyder's selectivity triangle also suggests that DIPE has a chemical nature more like octanol than MIBK or NBA. A comparison of Figures 1–3 shows the DIPE correlation to have a steeper slope and a lower intercept value. The parity of K_D and K_{ow} values for aniline, aminonaphthalene, phenol, naphthalene, and naphthol in Figure 3 is evidence of the chemical similarity of DIPE and octanol. Naphthalene was included in the DIPE correlation because it follows the trend of the other data with a K_D value close to its K_{ow} value and because it does not H bond with either solvent. Pyridine was not included in the DIPE correlation because it can H bond with octanol and not with DIPE; note that pyridine has a higher value of K_{ow} than K_D. That pyridine appears to fall on the regression line is fortuitous.

Figures 4 and 5 show correlations between K_D and K_{ow} for toluene with acidic and basic solutes, respectively. It is interesting to note that these systems can be modeled by both the regular solution and linear free energy approaches. Figure 4 shows that the distribution coefficients for the phenolic solutes in toluene are lower than their respective K_{ow} values, as well as being lower than the K_D's

for these solutes in NBA, MIBK, or DIPE. This follows from the fact that toluene does not possess any significant hydrogen-bonding character. Figure 5 shows that intramolecularly H-bonded molecules fit the correlation for B-type solutes. This is in agreement with intramolecular H-bonded compounds behaving like N- or B-type molecules and shows that toluene does not disrupt intramolecular H bonds.

An interesting observation can be made for aniline and aminonaphthalene. These amino aromatic compounds fall into the AB class, but are dominated by B-type H-bonding strength. These solutes can H bond with NBA, MIBK, and DIPE through their A-type character but are correlated with B-type solutes in Figure 5. Hence, it is inferred that aniline and aminonaphthalene H bond with octanol by acting as proton acceptors. These compounds also fit the correlations shown in Figures 1–3 where the data are dominated by phenolic solutes. Phenolic solutes are also classified as AB-type molecules, but their H-bonding strength is dominated by A-type character. Therefore, we would expect that phenolics act as proton donors when H bonding with octanol. Hence, Figures 1–3 suggest that even though amino aromatic and phenolic solutes H bond with octanol through different mechanisms, the fact that H bonding takes place fulfills the requirement for compatible H-bonded systems.

Summary and Conclusions

Experimental data for aniline, phenol, and pyridine have shown that distribution coefficients for these compounds in clean water, single solute systems are not statistically different from distribution coefficients determined in a complex coal conversion wastewater. Hence, this offers the opportunity for simple laboratory experiments to evaluate the partitioning of principal organic solutes during solvent extraction processing of these wastewater streams. These data also suggest that pure component properties may be used for modeling partitioning behavior.

Our analysis has shown that the regular solution model for predicting distribution coefficients is accurate for systems which do not include hydrogen bonding. The approach is also suitable for a relative ranking of solvents for extraction of phenolic solutes (i.e., hydrogen-bonded systems). It appears that the model could be made more accurate by improving the correlations for the empirical correction term.

The linear free energy relationships appear to offer an acceptable method for prediction of distribution coefficients for various solutes and a particular solvent. The procedure holds for comparison of compatible hydrogen-bonding solute–solvent systems. The availability of octanol–water partition coefficient data and the simplicity of the correlation make this technique particularly attractive for engineering analysis and design.

Work is in progress to evaluate the applicability of the UNIFAC group contribution model for these systems.

Acknowledgments

Registry No. Aniline, 62-53-3; naphthalene, 91-20-3; 1-naphthol, 90-15-3; phenol, 108-95-2; pyridine, 110-86-1; methyl isobutyl ketone, 108-10-1; n-butyl acetate, 123-86-4; diisopropyl ether, 108-20-3; toluene, 108-88-3; tetradecane, 629-59-4; water, 7732-18-5.

Literature Cited

(1) Hicks, R. E.; Goldstein, D. J.; Seufert, F. B.; Wei, I. *U. S. Environ. Prot. Agency* **1979**, *EPA-600/79-133*.

(2) Seufert, F. B.; Hicks, R. E.; Wei, I. W.; Goldstein, D. J. March 1979, U.S. DOE Report FE-2635-T1.

(3) Continental Oil Company 1978, U.S. DOE, Report FE-2542-20, Vol. 2.

(4) Mohr, D. H., Jr.; King, C. J. "Identification of the Principal Organic Compounds in Reactor Condensate Water From a Coal-Gasification Process"; Lawrence Berkeley Laboratory and Department of Chemical Engineering, University of California: Berkeley, CA, 1982.

(5) Goldstein, D. J. paper presented at the 54th Annual Water Pollution Control Federation Conference, Detroit, MI, Oct 1981.

(6) Luthy, R. G.; Stamoudis, V. C.; Campbell J. R.; Harrison, W. *J. Water Pollut. Control Fed.* **1983**, *55*, 196–207.

(7) Stamoudis, V. C.; Luthy, R. G. *Water Res.* **1980**, *14*, 1143–1156.

(8) Guerin, M. R.; Ho, C.; Ran, T. K.; Clark, B. R.; Epler, J. L. *Environ. Res.* **1980**, *23*, 42–51.

(9) Greminger, D. C.; King, C. J. June 1979, Lawrence Berkeley Laboratory Report LBL-9177.

(10) Earhart, J. P.; Won, K. W.; Wong, H. Y.; Prausnitz, J. M.; King, C. J. *Chem. Eng. Prog.* **1977**, *73*, 67–73.

(11) Chiou, C. T.; Schmedding, D. W.; Manes, M. *Environ. Sci. Technol.* **1982**, *16*, 4–10.

(12) Tsonopoulos, C.; Prausnitz, J. M. *Ind. Eng. Chem. Fundam.* **1971**, *10*, 593–600.

(13) Grain, C. F. In "Handbook of Chemical Property Estimation Methods"; Lyman, W. J.; Reehl, W. F.; Rosenblatt, D. H., Eds.; McGraw-Hill: New York, 1982; Chapter 11.

(14) Hildebrand, J. H.; Prausnitz, J. M.; Scott, R. L. "Regular and Related Solutions"; Van Nostrand Reinhold: New York, 1970.

(15) Weimer, R. F.; Prausnitz, J. M. *Hydrocarbon Process. Pet. Refiner* **1965**, *44*, 237–242.

(16) Helpinstill, J. G.; Van Winkle, M. *Ind. Eng. Chem. Process Des. Dev.* **1968**, *7*, 213–220.

(17) Karger, B. L.; Snyder, L. R.; Eon, C. *Anal. Chem.* **1978**, *50*, 2126–2136.

(18) Karger, B. L.; Snyder, L. R.; Eon C. *J. Chromatogr.* **1976**, *125*, 71–88.

(19) Tijssen, R.; Billiet, H. A. H.; Schoenmakers, P. J. *J. Chromatogr.* **1976**, *122*, 185–203.

(20) Hildebrand, J. H.; Scott, R. L. "The Solubility of Nonelectrolytes", 3rd Ed.; Reinhold: New York, 1950.

(21) Leo, A.; Hansch, C. *J. Org. Chem.* **1971**, *36*, 1539–1544.

(22) Hansch, C.; Leo, A. "Substitutent Constants for Correlation Analysis in Chemistry and Biology"; Wiley: New York, 1979.

(23) Leo, A. Medchem Project, Pomona College, Claremont, CA.

(24) Hansch, C.; Quinlan, J. E.; Lawrence G. L. *J. Org. Chem.* **1968**, *33*, 347–350.

(25) Chiou, C. T.; Freed, U. H.; Schmedding, D. W.; Kohnert, R. L. *Environ. Sci. Technol.* **1977**, *11*, 475–478.

(26) Mackay, D. *Environ. Sci. Technol.* **1982**, *16*, 274–278.

(27) Karickhoff, S. W.; Brown, A. S.; Scott, T. A. *Water Res.* **1979**, *13*, 241–248.

(28) Luthy, R. G. *J. Water* Pollut. *Control Fed.* **1981**, *53*, 325–339.

(29) Greminger, D. C.; Burns, G. P.; Lynn, S.; Hanson, D. H.; King, C. J. *Ind. Eng. Chem. Process Des. Dev.* **1982**, *21*, 51–54.

(30) Leo, A.; Hansch, C.; Elkins, D. *Chem. Rev.* **1971**, *71*, 525–616.

(31) Bowker, A. H.; Lieberman, G. J. "Engineering Statistics"; 2nd Ed.; Prentice-Hall: Englewood Cliffs, NJ, 1972.

(32) Beychok, R. "Aqueous Wastes from Petroleum and Petrochemical Plants"; Wiley: New York, 1967.

(33) Pimentel, G. C.; McClellan, A. L. "The Hydrogen Bond"; Reinhold: New York, 1960.

(34) Won, K. W. Ph.D. Dissertation, University of California, Berkeley, CA, 1974.

(35) "CRC Handbook of Chemistry and Physics", 60th ed.; CRC Press Inc.: Boca Raton, FL 1979.

(36) Timmermans, J. "Physico-Chemical Constants of Pure Organic Compounds"; Elsevier: Amsterdam, 1950, 1965; Vol. I and II.

(37) Hoy, K. L. *J. Paint Technol.* **1970**, *42*, 76–118.

(38) Kiezyk, P. R.; Mackay, D. *Can. J. Chem. Eng.* **1973**, *51*, 741–745.

(39) Deal, C. H.; Derr, E. L. *Ind. Eng. Chem. Process Des. Dev.* **1964**, *3*, 394–399.

(40) Pierotti, G. L.; Deal, C. H.; Derr, E. L. *Ind. Eng. Chem.* **1959**, *51*, 95–102.

(41) Snyder, L. R. *J. Chromatogr. Sci.* **1978**, *16*, 223–234.

Evaluation of Models for Predicting Terrestrial Food Chain Behavior of Xenobiotics

Charles T. Garten, Jr.,* and John R. Trabalka

Environmental Sciences Division, Oak Ridge National Laboratory, Oak Ridge, Tennessee 37830

■ We evaluated the adequacy and capabilities of proposed univariate regression models for predicting the bioaccumulation of xenobiotic compounds in terrestrial vertebrates from physicochemical properties (structure–activity relationships) or from bioaccumulation by fish. Our findings raised doubts about the generic application of such statistical models, even for purposes of screening large numbers of compounds for potentially high bioaccumulation. We developed a "screening level" model based on lipophilic tendency of xenobiotic compounds which identified all compounds, but one, with a high bioaccumulation potential in fish, mammals, and birds, from large numbers of compounds. The one compound with a high bioaccumulation potential, which was not identified as such, represents an important class of toxic organic materials not accounted for in existing structure–activity relationships. Furthermore, our model incorrectly placed some compounds into the high bioaccumulation category when existing experimental data demonstrate low actual bioaccumulation. Problems such as those identified suggest that structure–activity relationships are not an adequate substitute for laboratory feeding trials in predicting the bioaccumulation potential of a xenobiotic compound.

Introduction

The ability to predict the bioaccumulation of new exotic organic chemicals (xenobiotics) in food chains solely on the basis of physicochemical and biochemical properties would be both convenient and economical. The current practice of toxicological testing on large vertebrates is under scrutiny because of economic considerations, scientific concerns over interpretation of so-called "animal models", and the rise of animal welfare activism (*1*). Two major alternatives that currently show promise for reducing the amount of testing on large animals are mathematical modeling and short-term in vitro tests. Another option is the substitution of invertebrates or fish for large vertebrates in testing. Feeding studies to test for bioaccumulation of xenobiotics in livestock are expensive and require large facilities for animal maintenance. Lower cost is a primary motive for trying to develop predictive relationships between xenobiotic bioaccumulation by terrestrial vertebrates and physicochemical data or bioaccumulation by fish.

One modeling approach that has received much attention in recent years is the application of structure–activity relationships to the process of bioaccumulation (*2–7*). Regression equations that relate some measure of biological activity to a physicochemical or biochemical property associated with chemical structure are called "structure–activity" relationships (SAR) (*1, 8*). For organic compounds in aquatic systems, a simple set of criteria involving only stability in water and hydrophobicity has been suggested to estimate the potential for high bioaccumulation by fish (*2, 5, 6*), although a variety of physicochemical characteristics have been used in simple univariate SAR (*9*). It has been further suggested that an estimate of hydrophobicity (e.g., octanol–water partition coefficient, P_{ow}) or bioaccumulation data derived entirely from aquatic test systems are adequate for making preliminary predictions of bioaccumulation by terrestrial vertebrates (*3, 4, 9*). Such proposed SAR models take the form of linear regressions with the logarithm of the bioaccumulation factor (BF) as the dependent variable and the logarithm of some chemical property (e.g., log P_{ow}) as the independent variable (*3, 4, 9*).

The use of SAR for predicting bioaccumulation of xenobiotics was first extended to terrestrial vertebrates by Kenaga (*4*). Average bioaccumulation of 23 organic chemicals from the diet into beef fat was correlated with P_{ow}, water solubility (SOL), and bioaccumulation factors in fish in either water-only exposure systems or model ecosystems. The correlations were biased by the use of questionable data for some independent variables (*9*). For example, some P_{ow} data deviate by more than an order of magnitude from measured values, and Kenaga has combined bioaccumulation data on fish derived by very different methods. Another complication is that 12 of the 23 values for BF in beef fat used to parameterize the models were obtained from unpublished reports (*4*). It is injudicious to accept such data that are not readily available for public evaluation of the methods used, analytical procedures, and associated statistical variability. Nonetheless, Kenaga's results show a correlation between hydrophobic tendency of organic chemicals and bioaccumulation in ruminant fat, suggesting a more general application of SAR for predicting bioaccumulation in all vertebrates (aquatic and terrestrial).

Although Kenaga (*4*) reported several statistically significant relationships between bioaccumulation and physicochemical factors, he found that the confidence intervals about predicted values are very large. When solubility was used as an independent variable, the 95% confidence interval about the SAR prediction for BF in beef fat at the mean of the SOL data (3.3 mg/L) contained 17 of the 23 measured bioaccumulation factors. For example, the average measured values of SOL and BF for chlorpyrifos were 0.3 mg/L and 0.02, respectively, com-

pared to a predicted BF equal to 0.06. However, the 95% confidence interval around the predicted BF for chlorphyrifos also contained the average measured bioaccumulation factors for dieldrin (2.3) and 2,4,5-T (0.0011). Thus, although the predicted value does not appear to deviate significantly from the measured bioaccumulation factor for chlorpyrifos, the confidence limits about the predicted bioaccumulation are quite large, covering nearly 4 orders of magnitude. The confidence interval would become even larger if observed variations about averaged bioaccumulation factors or physicochemical data were incorporated into the regression model.

Data Selection and Statistical Approach

The results obtained from an extensive literature review (9, 10) on potential modeling approaches, potentially usable physicochemical data, bioaccumulation by fish from water or by fish in model ecosystems (129 and 104 chemicals, respectively, from 96 studies), and lipid bioaccumulation, at subtoxic levels, by birds and mammals from the diet (107 chemicals from 144 studies) were used to evaluate the capabilities of existing simple empirical bioaccumulation models proposed for terrestrial vertebrates (4). Aquatic data were included for the purpose of comparison with previous studies.

We considered bioaccumulation into body lipids as the main measure of xenobiotic bioaccumulation in vertebrates for two reasons. First, there is the apparent association between increased tendency for lipophilicity and high bioaccumulation for many organic chemicals (4). Second, the data base for measurements of bioaccumulation in tissues and organs, other than on a fat basis, is limited (9). Our consideration of only lipid bioaccumulation is important because there are chemicals, not readily excreted from the vertebrate body, for which lipid partitioning is not the primary mechanism of bioaccumulation. These chemicals, for which methylmercury is one example, can bioaccumulate by lipid solubility as well as by covalent bonding to proteins (11-13). Organics that bind to proteins can become localized in a specific organ or tissue. Although the log P_{ow} for methylmercury compounds is <2, the bioaccumulation factors for body tissues other than fat are typically ≥1 (14, 15).

A summary of the data (9) available for development of generalized SAR for predicting bioaccumulation by terrestrial vertebrates is presented in Table I. A critical evaluation of published values for P_{ow} alone indicates the potential for errors in selection of data for independent variables in SAR (9). An example of this is shown in Table II. Published measurements range from reasonably uniform data sets, in the case of o-chlorophenol, to extremely erratic data, in the case of hexachlorobenzene, where variation is over 3 orders of magnitude (Table II). Reasons for these variations of P_{ow} and criteria for selection of optimum values for use in SAR have been discussed elsewhere (9). However, it should be recognized at the outset that such potential uncertainties in physicochemical data, in addition to uncertainties in bioaccumulation factors, have not been factored into existing SAR predictions based on average values.

In this study, mean log transformed bioaccumulation factors for the various xenobiotics in birds and mammals were regressed against their respective mean log transformed values for octanol-water partition coefficient, water solubility, and bioaccumulation factors in fish tests (Table I). The mammals were subdivided into ruminant and nonruminant groups for this analysis.

An analysis was also performed for both birds and mammals with the purpose of finding a "screening level"
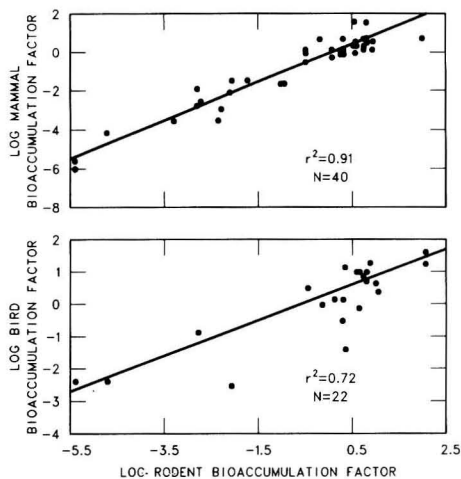
Figure 1. (Top) Correlation between dietary bioaccumulation of organic compounds in mammals other than rodents (cattle, dogs, swine, sheep, and primates) and bioaccumulation in rodents. (Bottom) Correlation between dietary bioaccumulation in birds and bioaccumulation in rodents.

in the physicochemical data. The screening level is a value of log P_{ow} below which (or in the case of log SOL, above which) no compound exhibits appreciable bioaccumulation. A log BF of -0.5 was arbitrarily chosen as the level above which bioaccumulation of xenobiotics was judged appreciable. A log BF of -0.5 means that for each milligram of xenobiotic ingested per kilogram of food, only 0.3 mg will be deposited per kg of fat. Furthermore, since the fat content of bird and animal tissues typically varies between 4 and 35%, a reduction of this concentration in fat to about 0.1 mg/kg of whole tissue, or less, can be expected. To find a screening level, values of log BF and log P_{ow}, or log SOL, for each chemical were matched and classified into discrete groups in a two-way cross-tabulation of log BF vs. log P_{ow} or log BF vs. log SOL. We then examined the cross-tabulation to find what portion of the table included compounds with appreciable bioaccumulation and how that portion corresponded to categories of the physicochemical data.

Results and Discussion

The bioaccumulation of xenobiotics by ruminants, nonruminants, and birds was significantly correlated (Table III) with log P_{ow} (positive association) and log SOL (negative association). In the case of ruminant bioaccumulation vs. log P_{ow}, the goodness of fit of the regression, as measured by the coefficient of determination (r^2), was lower for our data than for equations previously published by Kenaga (4) (Table III). Bioaccumulation factors in mammals showed higher correlations with water solubility data than with octanol-water partition coefficients in our study and Kenaga's. The amount of variance of bioaccumulation explained by log P_{ow} or log SOL in our regressions was low (r^2 < 0.55) which indicates limited usefulness of these equations for accurately predicting the bioaccumulation of a xenobiotic based only on the physicochemical data. By comparison, an r^2 of 0.9 for such an equation means that observed values are typically within ±1 order of magnitude of the predicted value (see Figure 1).

As noted earlier, Kenaga (4) reported significant correlations between bioaccumulation in beef fat and bioaccumulation by fish, as determined in flowing water tests or

Table I. Average log-Transformed Bioaccumulation Factors[a] for Xenobiotics in Sheep, Poultry, Small Birds, Rodents, Dogs, Cows, Swine, and Primates along with log-Transformed Average Bioaccumulation Factor[b] for Fish, Flowing Water (FW), or Microcosm (ME) Conditions, and Log-Transformed Octanol–Water Partition Coefficients (log P_{ow}) or Water Solubility (log SOL; µg/L) Data

compound	log bioaccumulation factor										log P_{ow}	log SOL
	sheep	poultry	small birds	rodents	dog	cow	swine	primate	fish (FW)	fish (ME)		
aldicarb	0.62	-1.44				-2.52	0.37			1.62	1.15	6.89
aldrin		1.09				0.51			4.03	3.50	5.52	1.11
Arochlor 1016	-0.11	0.13		0.15					4.63		5.88	
Arochlor 1242			-0.50	0.30			-0.27					
Arochlor 1248		0.82		0.72					4.85		6.11	
Arochlor 1254	0.18	0.77	0.98	0.79		0.53	0.03		4.70		6.47	
Arochlor 1262				1.50					5.29		6.91	
asulam			-2.40			-1.60						6.70
azinphos-methyl											2.45	3.58
benomyl		-2.40		-4.70							3.11	4.30
benzoylprop-ethyl					-4.22	-3.00					4.57	3.05
α-BHC		0.32							2.79	0.00	3.81	1.24
β-BHC		1.24				-0.04			2.86	2.97	3.96	3.27
γ-BHC		0.18		0.13	-0.32	-3.10			2.65	2.63	3.66	
buthidazole		-3.30									0.07	
carbaryl		-3.52								0.00	2.35	4.60
Cereclor-52				-0.03					1.69		7.05	1.00
chlordane	-0.05	0.52		-0.46		-0.50	-0.27		4.58	3.92	6.00	1.75
chlorobenzilate				-2.00		-1.64						3.90
chloroneb					-3.70	-2.00					3.46	
chlorpyrifos						-2.35			2.67	2.50	4.97	2.70
chlorpyrifos-methyl						-2.32				1.98	4.31	3.64
clopidol	-2.52					-2.96				-2.00	0.50	4.00
coumaphos		-3.30				-3.40					4.13	
Croneton				-2.05		-2.64					1.63	
cyhexatin				-2.70		-1.90					5.39	
dalapon		-0.89		-2.77	-2.70	-0.10					0.76c	
DDD			-0.11	0.65		0.50				0.20	6.02	8.70
DDE			0.65	1.03						4.92	5.83	0.50
DDMU			0.51					0.00	4.71	4.44	5.27	0.90
DDT	-0.23	1.09	-1.42	0.39		0.05	-0.13	0.53	4.53	4.49	5.76	0.30
Diazinon		-1.74		-1.80					2.49		4.20	5.00
dibutyl phthalate				-1.96					1.46	2.11	3.31	4.72
DEHP				-3.25							3.31c	5.60
dicamba						-3.52				-2.00		6.65
dieldrin	0.44	1.03	0.95	0.63	1.47	0.30	0.21		4.15	3.61	5.16	1.34
dimethoate		-1.38								0.00	-0.29	7.40
diquat		-3.70			-1.66						-3.05	8.85
diuron				-1.66							2.77	4.62
edifenphos	-5.70					-1.85				0.00	4.35	5.16
endosulfan	-0.38			-0.96		-0.35	-1.70				2.23	
endrin		0.77			-0.74		-0.21		3.42	3.13	5.16	1.38
ethion		-1.70										3.30
famphur	-3.43					-2.30					2.28	
fenoprop						-2.66			1.76		3.86c	5.15
fenthion						-2.70					3.16	4.74
flamprop						-2.40						4.26

Compound	1	2	3	4	5	6	7	8	9	10	11	12
flamprop-isopropyl		-2.70				-2.40	-2.70				4.41	4.23
flamprop-methyl						-2.22					3.48	4.54
HCB		1.29				0.46			4.09		5.45	0.78
heptachlor	-0.10	0.78	0.90			-0.25	-0.33		4.14	3.16	5.44	1.75
heptachlor epoxide		1.14		0.64		0.54		1.32	4.16	3.58	5.40	2.54
hexabromobenzene			-0.46						-0.82	3.69	6.51	
Kerb		-1.80				-2.89					3.18	4.18
malathion						-3.30				0.00	2.89	5.16
methazole		-1.77				-2.70					3.18	3.18
methoxychlor			2.09			-5.00	-5.00		3.92	3.19	4.40	2.79
mirex	-3.28	1.67			1.20	0.53			4.26	2.34	6.89	0.00
Nemacide		-2.15									5.14	
Nutriquinol			-2.22			-3.00					3.34	
OCDD			-1.10								8.31	
OP-DDT		0.02	-0.15								5.75	
oxadiazon					-1.66	-1.42			4.57	2.29	4.09	2.85
PBB (BP-6)		0.40	1.05									
PCNB		-2.38	-5.35	-5.65		-6.00					4.18	3.12
pentachlorobenzene						-2.82			3.84		4.94	4.15
pentachlorophenol		-0.78				-3.60			2.89	2.11	5.01	
Phosdrin (mevinphos)						-3.46					1.38	
phosphamidon			-2.30			-1.38					1.34	
picloram									1.49		0.26	5.63
ronnel											4.88	2.91
sulfamethoxazole		-3.00									0.89	
TCDD	-2.15	-0.61	-0.15			0.54				3.02	6.15	-0.70
TCNB	-1.34	-2.52	-2.05								4.76	
thidiazuron		1.03				-0.98					0.21	
toxaphene						-4.05			3.81	3.72	5.50	2.60
triclopyr						-4.52					2.09	5.63
trifluralin								0.06	3.03	2.45	5.33	1.70
2,2'-PCB		1.00	-1.35						2.05		4.52	2.95
2,3,4,2',3',4'-PCB		0.86									6.66	
2,3,6,2',3',6'-PCB											6.00	
2,4-D	-4.30					-3.37				0.00	2.81[c]	
2,4,5-T	-3.85					-3.05	-2.59			1.36	3.36[c]	5.95
2,4,5-T ester		0.99				-2.30				4.09	5.90	5.38
2,4,5,2',4'-PCB			0.32								6.11	
2,4,5,2',4',5'-PCB											6.72	
2,4,6,2',4'-PCB		1.02									5.89	
2,4,6,2',4',6'-PCB											6.10	
2,5,4'-PCB											5.56	
3,5,6-trichloropyridinol						-2.43					2.27	5.30
3,6-dichloropicolinic acid						-3.70					-0.68	6.00
5,5-DPH		-1.57									2.15	
6-chloropicolinic acid						-4.52					-1.36	

[a] Units: (mg/kg of fat)/(mg/kg of diet). [b] Units: (μg/kg fresh weight)/(μg/L of water). [c] Deletion of these values or reducing the log P_{ow} values appropriately as a correctio[n] for ionization did not significantly affect the regressions described in the text (9).

Table II. Summary of Literature Values for Octanol–Water Partition Coefficients (P_{ow}) for Selected Chemicals

chemical	log P_{ow}
hexachlorobenzene	$4.13^{a,b}$; 5.23^{b}; 5.47^{c}; 5.64^{c}; $6.18^{a,c}$; $6.44^{a,c}$; $7.42^{a,b}$
DDT	$3.98^{a,b}$; 5.57^{b}; 5.60^{b}; 5.75^{b}; 5.76^{c}; 5.76^{b}; 6.19^{b}
methoxychlor	$3.31^{a,b}$; 3.82^{b}; 4.30^{b}; 4.48^{c}; 5.08^{b}
naphthalene	3.01^{b}; 3.17^{b}; 3.30^{b}; 3.36^{b}; 3.36^{b}; 3.37^{b}; 3.45^{b}; 3.59^{b}; $4.70^{a,b}$
p-nitrophenol	$1.35^{a,b}$; 1.90^{b}; 1.91^{b}; 1.91^{b}; 1.95^{b}; 2.08^{b}; 2.91^{b}
o-chlorophenol	2.12^{b}; 2.15^{b}; 2.16^{b}; 2.17^{b}; 2.19^{b}

[a] Rejected as an outlier. [b] Data from references compiled by Trabalka and Garten (9). [c] Calculated as described by Trabalka and Garten (9).

Table III. Linear Regression of Bioaccumulation Factors in Ruminant Fat (RF), Nonruminant Fat (NRF), and Bird Fat (AF) with Octanol–Water Partition Coefficients (P_{ow}), Water Solubility (SOL), and Bioaccumulation Factors for Fish, under Flowing Water (FW) or Model Ecosystem (ME) Conditions

variables (log) y	x	study	N^{a}	regression equation	r^{2} [b]
RF	SOL	ref 4[c]	23	$y = -1.476 - 0.495x$	0.67
		present[d]	53	$y = 0.191 - 0.608x$	0.54
RF	P_{ow}	ref 4	23	$y = -3.457 + 0.500x$	0.62
		present	66	$y = -3.935 + 0.511x$	0.34
NRF	SOL	present[d]	37	$y = 0.527 - 0.538x$	0.49
NRF	P_{ow}	present	56	$y = -3.849 + 0.617x$	0.35
AF	SOL	present[d]	33	$y = 0.990 - 0.451x$	0.48
AF	P_{ow}	present	47	$y = -2.743 + 0.542x$	0.54
RF	FW	ref 4	23	$y = -3.839 + 0.869x$	0.59
		present	28	$y = 5.194 + 1.150x$	0.39
RF	ME	ref 4	18	$y = -2.842 + 0.674x$	0.77
		present	38	$y = -3.020 + 0.654x$	0.43
NRF	FW	present	31	$y = -1.147 + 0.311x$	0.09[e]
NRF	ME	present	28	$y = -2.227 + 0.626x$	0.39
AF	FW	present	24	$y = -1.180 + 0.464x$	0.20
AF	ME	present	44	$y = -1.573 + 0.587x$	0.35

[a] N = number of observations. [b] r^{2} = coefficient of determination. [c] Solubility in units of mg/L. [d] Solubility in units of μg/L. [e] Not significant ($\alpha \le 0.05$).

Table IV. Correlation Coefficients between log-Transformed Bioaccumulation Factors in Birds and Mammals

	sheep	poultry	rodents	dog	cow	swine
sheep	1.00 $(16)^{a}$	0.74^{b} (10)	0.93^{c} (6)		0.93^{c} (13)	0.88^{c} (10)
poultry		1.00 (51)	0.91^{c} (15)	0.96^{c} (7)	0.89^{c} (20)	0.98^{c} (9)
rodents			1.00 (40)	0.98^{c} (7)	0.95^{c} (18)	0.87^{b} (6)
dog				1.00 (9)	0.93^{c} (7)	
cow					1.00 (55)	0.98^{c} (11)
swine						1.00 (12)

[a] The number of compounds for each correlation is shown in parentheses. [b] Statistical significance: ≤0.05. [c] Statistical significance: ≤0.01.

Table V. Two-Way Cross-Tabulation for Bioaccumulation Factor in Mammals and log Octanol–Water Partition Coefficient (P_{ow}) Based on 122-Paired Observations for 68 Different Chemicals

log BF (±0.5)	log P_{ow} (±0.5)								
	−1	0	1	2	3	4	5	6	7
−5	1				1	6	1		
−4	1	1	1	5					
−3		2	6		8	5	3		
−2	2	2	6	6	3	1		1	
−1			1		1	3	3	1	
0						3	10	18	2
1							6	9	2
2									1

static water model ecosystem tests. In our study, bioaccumulation in mammals and birds was very weakly correlated or uncorrelated with xenobiotic bioaccumulation factors from fish tests (Table III). Expanding the number of compounds under consideration resulted in poorer predictability between ruminant bioaccumulation and fish bioaccumulation than previously indicated by Kenaga (4). The range in r^{2} values for our regressions between terrestrial vertebrate and fish bioaccumulation was 0.09–0.43, which indicated that these relationships cannot be used for accurate prediction of xenobiotic bioaccumulation in birds or mammals based on fish tests alone.

Xenobiotic bioaccumulation factors in sheep, poultry, rodents, dogs, cows, and swine were significantly correlated (Table IV) and have potential utility as an alternative to using data for bioaccumulation in fish for predicting bioaccumulation of xenobiotics in mammals and birds (Figure 1). Bioaccumulation factors for xenobiotics in rodents were highly correlated with bioaccumulation factors in poultry and cows. Such correlations indicate that continuous long-term feeding studies employing small laboratory rodents are more useful for forecasting food chain uptake of xenobiotics by larger livestock animals than bioaccumulation tests with fish.

For mammals (ruminants and nonruminants combined), Table V shows the results of classifying paired observations for log BF and log P_{ow} into a two-way cross-tabulation to find a physicochemical screening level. The outstanding feature of this frequency table is that, out of 68 different chemicals, compounds with log P_{ow} values ≤3.5 do not appreciably bioaccumulate in fat according to our criterion of log BF > −0.5. Since each compound with a log P_{ow} value < 3.5 has a log BF < −0.5, a log P_{ow} of 3.5 appears to be a useful physicochemical screening level for identifying xenobiotics that will potentially bioaccumulate in mammals.

A two-way cross-tabulation was also compiled based on paired observations of log BF and log SOL data in all mammals (9). From data for 47 compounds, none with a log SOL value greater than 4, corresponding to a water solubility of 10 mg/L, showed appreciable bioaccumulation. All compounds with a water solubility greater than 10 mg/L had bioaccumulation factors < 0.03, which is an order of magnitude less than our chosen criterion for bioaccumulation in fat.

Two-way cross-tabulations similar to those presented for mammals (Table V) were also prepared for birds by using the variables log BF vs. log P_{ow} and log BF vs. log SOL (9). Regression equations for these associations are presented in Table III. In birds, as in mammals, compounds with log P_{ow} < 3.5 did not have bioaccumulation factors in fat > 0.3. Birds also had the same water solubility screening level as found for mammals. Compounds with water solubility values > 10 mg/L did not bioaccumulate above a BF equal to 0.3 in birds.

For reasons previously discussed, a screening level of log P_{ow} equal to 3.5 will not successfully identify compounds such as methyl mercuric chloride which has a calculated

log P_{ow} of 1.48 (9) and an observed BF, derived from laboratory feeding studies, > 0.3 in body tissues (brain, liver, and kidneys) of birds and rodents (15). Methylmercury is an example of the problem of erroneously classifying a compound, based on physicochemical data, as not having a high potential for bioaccumulation (i.e., "false negative"). However, there is also the opposite problem of "false positive" errors, which means that a compound is wrongly classified, based on log P_{ow}, as having a high bioaccumulation potential. Approximately 25% of the 68 compounds used to make Table V were "false positive" classifications: for example, chlorpyrifos, cyhexatin, methoxychlor, oxadiazon, and pentachloronitrobenzene (PCNB) (Table I).

Bioaccumulation potential for many organics is frequently controlled by environmental conditions, physiological factors, and specific metabolic/steric interactions (e.g., covalent bonding) not adequately represented in SAR. For example, our review indicated a much greater potential for bioaccumulation by birds as compared to that by mammals. Thus, comparative relationships developed between bioaccumulation measurements in different taxa of terrestrial vertebrates become an important alternative or complement to the use of SAR. Such comparative relationships coupled with chronic feeding tests conducted with laboratory animals (e.g., time-honored rodent-testing protocols) appear superior to SAR for predicting bioaccumulation of xenobiotics in terrestrial vertebrates.

The present study has made several contributions over past studies in predicting xenobiotic bioaccumulation in terrestrial food chains. First, we have expanded the size of the data base for structure–activity relationships to predict bioaccumulation by terrestrial vertebrates and have developed "screening levels", based on physicochemical data, that are more appropriate, at this particular time, than regression equations for identifying chemicals that will bioaccumulate appreciably in mammals and birds. Second, we have, for the first time, included birds in the analysis of xenobiotic bioaccumulation vs. physicochemical data. Third, we have shown that fish tests of bioaccumulation are clearly inadequate for predicting bioaccumulation in birds and mammals, while correlations between bioaccumulation by livestock and rodents indicate the continuing usefulness of feeding studies in laboratory rodents to predict bioaccumulation in other vertebrates. Fourth, we reiterate that bioaccumulation of organics that can covalently bond or otherwise bind to proteins is not adequately predicted by existing SAR screening methods. Use of a laboratory feeding test is currently the only method for identifying such materials.

Registry No. Aldicarb, 116-06-3; aldrin, 309-00-2; Arochlor 1016, 12674-11-2; Arochlor 1242, 53469-21-9; Arochlor 1254, 11097-69-1; Arochlor 1262, 37324-23-5; asulam, 3337-71-1; azinphos-methyl, 86-50-0; benomyl, 17804-35-2; benzoylprop-ethyl, 22212-55-1; α-BHC, 319-84-6; β-BHC, 319-85-7; γ-BHC, 58-89-9; buthidazole, 55511-98-3; carbaryl, 63-25-2; chlordane, 12789-03-6; chlorbenzilate, 510-15-6; chloroneb, 2675-77-6; chlorpyrifos, 2921-88-2; chlorpyrifos-methyl, 5598-13-0; clopidol, 2971-90-6; coumaphos, 56-72-4; Croneton, 29973-13-5; cyhexatin, 13121-70-5; dalapon, 75-99-0; DDD, 72-54-8; DDE, 72-55-9; DDMU, 1022-22-6; DDT, 50-29-3; DEHP, 117-81-7; Diazinon, 333-41-5; dibutyl phthalate, 84-74-2; dicamba, 1918-00-9; dieldrin, 60-57-1; dimethoate, 60-51-5; diquat, 2764-72-9; diuron, 330-54-1; edifenphos,

17109-49-8; endosulfan, 115-29-7; endrin, 72-20-8; ethion, 563-12-2; famphur, 52-85-7; fenoprop, 93-72-1; fenthion, 55-38-9; flamprop, 58667-63-3; flamprop-isopropyl, 52756-22-6; flamprop-methyl, 52756-25-9; HCB, 118-74-1; heptachlor, 76-44-8; heptachlor epoxide, 1024-57-3; hexabromobenzene, 87-82-1; Kerb, 23950-58-5; malathion, 121-75-5; methazole, 20354-26-1; methoxychlor, 72-43-5; mirex, 2385-85-5; Nemacide, 97-17-6; Nutriquinol, 8067-69-4; OP-DDT, 789-02-6; oxadiazon, 19666-30-9; PBB, 52276-49-0; PCNB, 82-68-8; pentachlorobenzene, 608-93-5; pentachlorophenol, 87-86-5; Phosdrin, 7786-34-7; phosphamidon, 13171-21-6; picloram, 1918-02-1; ronnel, 299-84-3; sulfamethoxazole, 723-46-6; TCDD, 1746-01-6; TCNB, 117-18-0; thidiazuron, 51707-55-2; toxaphene, 8001-35-2; triclopyr, 55335-06-3; trifluralin, 1582-09-8; 2,2'-PCB, 13029-08-8; 2,3,4,2',3',4'-PCB, 38380-07-3; 2,3,6,2',3',6'-PCB, 38411-22-2; 2,4-D, 94-75-7; 2,4,5-T, 93-76-5; 2,4,5,2',4'-PCB, 38380-01-7; 2,4,5,2',4',5'-PCB, 35065-27-1; 2,4,6,2',4'-PCB, 39485-83-1; 2,4,6,2',4',6'-PCB, 33979-03-2; 2,5,4'-PCB, 16606-02-3; 3,5,6-trichloropyridinol, 1970-40-7; 3,6-dichloropicolinic acid, 1702-17-6; 5,5-DPH, 57-41-0; 6-chloropicolinic acid, 4684-94-0; hexachlorobenzene, 118-74-1; naphthalene, 91-20-3; p-nitrophenol, 100-02-7; o-chlorophenol, 95-57-8.

Literature Cited

(1) Holden, C. *Science (Washington, D.C.)* **1982**, *215*, 35–38.
(2) Veith, G. D.; Defoe, D. L.; Bergstedt, B. V. *J. Fish. Res. Board Can.* **1979**, *36*, 1040–1048.
(3) Kenaga, E. E.; Goring, C. A. I. In "Aquatic Toxicology, ASTM STP 707"; Eaton, J. G.; Parrish, P. R.; Hendricks, A. C., Eds.; American Society for Testing Material: Philadelphia, PA, 1980; pp 78–115.
(4) Kenaga, E. E. *Environ. Sci. Technol.* **1980**, *14*, 553–556.
(5) Veith, G. D.; Macek, K. J.; Petrocelli, S. R.; Carroll, J. In "Aquatic Toxicology, ASTM STP 707"; Eaton, J. G.; Parrish, P. R.; Hendricks, A. C., Eds.; American Society for Testing Material: Philadelphia, PA, 1980; pp 116–129.
(6) Mackay, D. *Environ. Sci. Technol.* **1982**, *16*, 274–278.
(7) Tulp, M. Th. M.; Hutzinger, O. *Chemosphere* **1978**, *7*, 849–860.
(8) Hansch, C. *Acc. Chem. Res.* **1969**, *2*, 232–239.
(9) Trabalka, J. R.; Garten, C. T., Jr. "Development of Predictive Models for Xenobiotic Bioaccumulation in Terrestrial Ecosystems"; National Technical Information Service: Springfield, VA, 1982; ORNL-5869.
(10) Trabalka, J. R.; Garten, C. T., Jr.; Uziel, M. S.; Opresko, D. M. "Xenobiotic Bioaccumulation by Terrestrial Vertebrates: A Bibliography for Food Chain Modeling"; National Technical Information Service: Springfield, VA, 1982; ORNL-5829.
(11) White, J. F.; Rothstein, A. *Toxicol. Appl. Pharmacol.* **1973**, *26*, 370–384.
(12) Takeda, Y.; Ukita, T. *Toxicol. App. Pharmacol.* **1970**, *17*, 181–188.
(13) Webb, J. L. "Enzyme and Metabolic Inhibitors: Malonate, Analogs, Dehydroacetate, Sulfhydryl Reagents, o-Iodosobenzoate, Mercurials"; Academic Press: New York, 1966; Vol. II.
(14) Heinz, G. H. *J. Wildl. Manage.* **1979**, *43*, 394–401.
(15) Soares, J. H., Jr.; Miller, D.; Lagally, H.; Stillings, B. R.; Bauersfeld, P.; Cuppett, S. *Poult. Sci.* **1973**, *52*, 452–458.

X-ray Diffraction Analysis of Airborne Particulates Collected by an Andersen Sampler. Compound Distribution vs. Particle Size

Tsutomu Fukasawa,* Masaaki Iwatsuki, and Sujith P. Tillekeratne

Department of Applied Chemistry, Faculty of Engineering, Yamanashi University, Takeda-4, Kofu-shi 400, Japan

■ Commercially available Nuclepore and Fuji microfilters were used as the collection media in an Andersen sampler. After sampling, the filter with the particulates was dissolved in dichloromethane, centrifuged to reduce the amount of the filter material, and formed to a suitably small film for X-ray diffraction analysis. Preparation of the small-film sample, sample mounting on the diffractometer, recovery, reproducibility in the X-ray diffraction intensity, identification of compounds in the particulates, and construction of a compound distribution vs. particle size curve are described. The distribution curves of the compounds are also given for the particulates collected in dry and wet seasons as examples.

Table I. Conditions of X-ray Diffraction Analysis

X-ray tube	Cu	r slit, mm	0.6
voltage, kV	35	time const, s	4
current, mA	14	scan speed, deg/min	1/2
filter	Ni	chart speed, mm/min	5
d and s slit, deg	1	sample spin	on

Table II. Conditions of X-ray Fluorescence Analysis

	heavy elements	light elements
X-ray tube	W	Cr
voltage, kV	45	40
current, mA	30	34
collimator	fine	coarse
detector	fc and sc	fc
analyzing cryst	LiF	EDDT
scan speed, deg/min	1	1
chart speed, mm/min	5	5
spinner	on	on
path	vacuum	vacuum

Introduction

The Andersen air sampler (*1*) is used as a device to obtain the aerodynamic particle size distribution of airborne particulates. Many papers and reports have been published on the distribution curves of element concentration vs. particle size, which were determined by atomic absorption (*2, 3*), neutron activation (*2, 4*), and spectrophotometric analyses (*3, 5*) of the particulates collected fractionally by the sampler. It has been reported (*6, 7*) that the X-ray diffraction analysis (XRD) of airborne particulates after heavy-liquid fractionation gave useful information for the study of air pollution. Also, the XRD has been carried out directly for the particulates collected by use of a dichotomous sampler (*8*) or for airborne heavy metals collected by a high-volume sampler in a zinc–lead smelter (*9*). No paper, however, has been published so far on the XRD of the particulates fractionated by the Andersen sampler or on compound distribution vs. particle size, although it is expected to provide more valuable information on the sources of pollutants, environmental chemistry, and others.

Membrane filters can be used as the collection media mounted on the aluminum or glass plates in the Andersen sampler (*14*). The particulates, however, are dispersed as many spots on the collection media of 80 mm diameter and cannot be analyzed directly by using a cut piece of the medium by a conventional X-ray diffractometer because of its poor sensitivity. Therefore, the membrane filters with the collected particulates must be reduced to small-size films with all the particulates for the XRD.

This paper describes the use of commercially available Nuclepore and Fuji microfilters (80 mm diameter) as the collection media, the preparation and reproducibility of small-size films (16 mm diameter) by using halogenated hydrocarbon, sample mounting on the goniometer, identification of compounds, construction of the distribution curves of compounds vs. particle size, etc. The identification of compounds was done by use of the JCPDS cards and the aid of the X-ray fluorescence analysis (XRF). The distribution curve of each compound vs. particle size was constructed by using its strongest diffraction line intensities from the film samples of all stages of the Andersen sampler and was compared with the distribution curves of the constituent elements vs. particle size obtained by using the results of the XRF of the same samples. Ex-

amples of the distribution curves of compounds vs. particle size are also given for the particulates collected in the dry winter and wet summer seasons. This method can be successfully applied to the analysis of any crystalline compound insoluble in the solvent, and the results obtained are very useful for environmental studies.

Experimental Section

Reagents, Filters, and Apparatus. All chemical reagents used were of analytical grade. An Andersen sampler, Koritsu Model KA 200, consisting of eight stages with aluminum plates as collection supports was used for sampling. Nuclepore filters (pore size: 1.0 μm, 80 mm diameter, 50 mg of polycarbonate, from Nuclepore Corp.) and Fuji microfilter FM-80 (pore size: 0.8 μm, 80 mm diameter, 210 mg of acetyl cellulose, from Fuji Photo Film Co. Ltd.) were used as collection media on the aluminum plates and backup filter, respectively.

A constant-humidity box (type C-3, from Doi Co. Ltd.) was used for keeping moisture of samples constant. The humidity of the box was adjusted at 50% with 43% sulfuric acid. Samples were weighed with a Sartorius semimicro balance or a Cahn 26 automatic ultramicro electrobalance.

A Rigaku X-ray diffractometer was used together with a standard rotating sample holder for the analysis of crystalline compounds, and the operating conditions are shown in Table I.

A Philips PW 1410 semiautomatic X-ray spectrometer was used for the elemental analysis. The sample was placed between two nylon nets set in a standard aluminum holder in the case of heavy-element determination and between a tungsten mask (aperture: 10 mm diameter) and a nylon net set in the holder in the case of light-element determination. The operating conditions are shown in Table II.

Intensity measurements in the XRD and XRF were done by chart recording.

Sampling. All filters were weighed after being kept in the 50% humidity box for 2 days before use (10). After the Nuclepore filters were mounted on the eight aluminum plates, they were arranged in order with a backup Fuji microfilter in the Andersen sampler. The sampling was done for around 10 days each, in a dry winter (Jan 12–23, 1982) and wet summer (July 2–13, 1982) at a constant flow rate of 28.3 L/min on the roof of Applied Chemistry Department building at Yamanashi University.

Calculation of Particle Size Distribution. After sampling, the filters were kept in the humidity box and weighed. Since the range of particle size varies on each stage, the simple histogram, with use of the weights of the particulates collected and their particle sizes, cannot clearly show the distribution of the particulates. Therefore, first the accumulated weight percentage in each stage was calculated from the lowest (finest) to the higher (coarser) stages. In the conventional method, then, the curve of the accumulated weight percentage vs. particle size has been constructed by plotting the accumulated weight percentages vs. logarithm values of their particle sizes, and the weight distribution curve has been constructed by differentiating manually the curve on the figure. This manual differentiating, however, gives an additional personal error to the distribution curve. In a previous paper by us (11), however, the accumulated weight curve was constructed by substituting all the accumulated weight percentages and the logarithms of the particle sizes into the Lagrange interpolation equation (eq 1), and the weight distribution

$$y = \sum_{i=1}^{n} y_i \prod_{\substack{j=1 \\ j \neq i}}^{n} {}' \frac{x - x_j}{x_i - x_j} \ldots \tag{1}$$

$$\frac{dy}{dx} = \sum_{i=1}^{n} y_i \frac{1}{\prod_{\substack{j=1 \\ j \neq i}}^{n} {}' (x_i - x_j)} \sum_{\substack{k=1 \\ k \neq i}}^{n} {}' \prod_{\substack{j=1 \\ j \neq i \\ j \neq k}}^{n} {}'' (x - x_j) \ldots \tag{2}$$

curve was also directly constructed by substituting the accumulated weight percentages and the logarithms of the particle sizes into the differentiated formula (eq 2) of eq 1, without any personal error, respectively. In the equations, x_i (x_j) is the logarithm of the particle size of the ith (jth) stage, y_i is the accumulated percentage of the ith stage, n is the number of sets of data used for the interpolation, and x and y represent the logarithm of the arbitrary particle size to be interpolated and the interpolated value of an arbitrary accumulated percentage, respectively. Therefore, in the present paper, eq 2 was used directly with the interpolation of the fourth order ($4 = n - 1$) which was recommended (11) for the construction of the distribution curves.

Sample Preparation and Mounting for XRD. Recommended procedure: Each filter with the particulates is dissolved in 10 mL of dichloromethane and centrifuged for 30 min at 2000 rpm in a 15-mL centrifuge tube with a cork stopper. After 9 mL is pipetted from the supernatant, the remainder is evaporated to obtain a deformed film with embedded particulates in the bottom of the centrifuge tube. The film is stripped off by use of a tweezer onto a 80-mm diameter watch glass that has a 16-mm diameter circle marked on the back-side, and a round homogeneous film of 16 mm diameter is made with the aid of a thin glass rod and a few drops of dichloromethane. Any filter material and particulates stuck onto the glass rod are transferred back to the sample by using a tweezer. The banks are also prepared in the same manner.

The sample film of 16 mm diameter is stuck onto a nondiffracting single-crystal quartz plate by using a drop of dichloromethane and mounted on the rotating sample holder of the diffractometer. This technique allowed to obtain a flat sample film suitable for the XRD and for sample rotation.

Experiment for Recovery of Compounds and Reproducibilities of Small-Film Sample and Diffraction Intensities. Crystalline ammonium sulfate and chloride were found by the XRD in the particulates on the collection media, and the finding was supported by a chemical microanalysis (12). Therefore, these compounds were used for the test of recovery, reproducibility, and preferred orientation effect. Since dichloromethane was used for filter dissolution, its effects on these compounds were also studied, i.e., dissolution of the compounds, any change in the crystal shape, recrystallization, and others.

Crystalline ammonium sulfate and chloride in powder form (<5 μm) of about 1 mg each were weighed precisely with the ultramicro balance and transferred into a centrifuge tube. A Nuclepore filter and 10 mL of dichloromethane were added to the tube, and the resulting solution was centrifuged. The supernatant of 9 mL was pipetted, and out of which 1 mL was transferred onto a watch glass and formed into a 16-mm diameter film (B). The remainder of 1 mL with particulates was evaporated to make a deformed film with the particulates, and the film was transferred onto a watch glass to reform into another 16-mm diameter film (A) with the particulates. For comparison, another 16-mm diameter film (C) was prepared by using about 1 mg each of ammonium sulfate and ammonium chloride, one-tenth (about 5 mg) of a Nuclepore filter, and a few drops of dichloromethane on a watch glass without centrifuging. A blank (D) was prepared by using one-tenth of a Nuclepore filter and a few drops of dichloromethane. These film samples were then subjected to the XRD to find the recovery, reproducibility, and other effects. The X-ray diffraction intensities of the compounds were corrected or normalized to 1-mg amounts for easy comparison.

Calculation for Distribution Curve of Compound or Element vs. Particle Size. It is known that the intensity of X-ray diffraction or fluorescence is proportional to minor amounts of a compound or element embedded in a film sample (13). Therefore, the distribution curve of the compound or element vs. particle size can be constructed by use of its strongest diffraction line or Kα line intensities obtained from the film samples of all stages. The accumulated intensity percentage up to each stage and the distribution curve were calculated by the same manner as the calculation of the accumulated weight percentage and weight distribution described before.

Results and Discussion

Particle Size Distribution. The total weights collected on the filters for around 10 days each in the winter (dry season) and summer (wet season) were 30.1 mg (68 μg/m³) and 16.6 mg (37 μg/m³), respectively, and the weight on each stage is shown in Figures 3–5 with the XRD data. Figure 1 shows the weight distribution curves vs. particle size. The distribution curve obtained for the dry season had two peaks around 0.6 and 4.5 μm, corresponding to fine and coarse particles. The curve for wet season, however, had one peak around 5 μm and also seems to have a peak in the submicron region. Similar observations have been made earlier (2, 4).

Preparation of Small-Film Sample for XRD. The filter with the particulates has to be dissolved and centrifuged in a solvent for eliminating the excess filter ma-
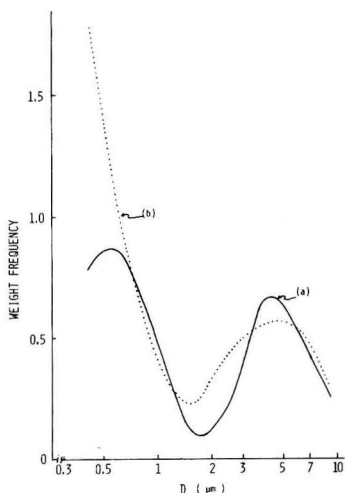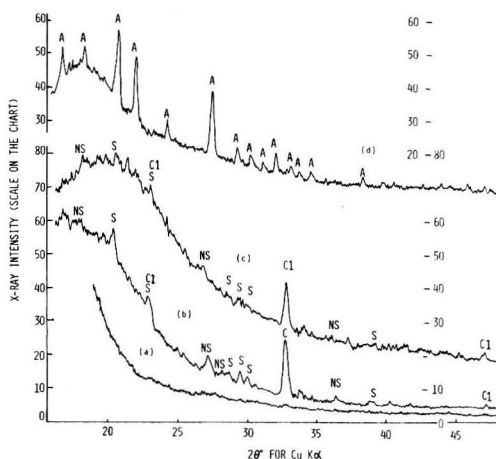
Figure 1. Distribution curves of weight vs. aerodynamic particle size: (a) particulates collected during Jan 12–23 1982 (dry season; 3 cloudy and the rest sunny days); (b) particulates collected during July 2–13, 1982 (wet season; 6 cloudy, 2 rainy, and 3 sunny days). D: particle size (aerodynamic diameter), $\log D = x$ in eq 2. Weight frequency: dy/dx in eq 2. Areas under the curves are equivalent to the total weights collected on all stages or concentrations in air, 30.1 mg or 68 $\mu g/m^3$ for a and 16.6 mg or 37 $\mu g/m^3$ for b, respectively.

Figure 2. X-ray diffraction patterns for a 25-mm diameter cut piece from a Nuclepore filter with particulates collected and 16-mm diameter film samples prepared: (a) 25-mm diameter cut piece from the Nuclepore filter with particulates of stage 8 (dry season); (b) 16-mm diameter film sample prepared by using the entire filter of stage 8 (dry season); (c) 16-mm diameter film sample prepared by using the backup Fuji microfilter (dry season); (d) 16-mm diameter film sample prepared by using the Nuclepore filter with particulates of stage 8 (wet season). Cl, NH_4Cl; S, $(NH_4)_2SO_4$; NS, $(NH_4)_4(NO_3)_2SO_4$; A, (NH_4,K)-$Al(SO_4)_2\cdot12H_2O$.

terial to make a small film. Therefore, solvents such as dichloromethane and chloroform were compared as to their rapidness, ease, and homogeneity in the formation of a small thin film on a watch glass (80 mm diameter) and in a Teflon mold (like a cup with a flat bottom of 16 mm diameter). A thin film was prepared easily in the Teflon mold but was undesirable for the XRD since it had vertical edges. Since dichloromethane has a lower boiling point and specific gravity than chloroform, dichloromethane allowed the easy and rapid formation of a homogeneous film on a watch glass, while chloroform gave a heterogeneous film with most of the particulates accumulating near the edge.

A thinner film sample, which is prepared by using a smaller volume of the remainder by pipetting more than 9 mL from the supernatant after centrifugation of the dissolved filter sample, would improve the sensitivity of the XRD due to lower absorption and background. However, the deformed film was difficult to remove from the centrifuge tube. The use of a larger volume, which contained more filter material, resulted in the opposite. It was found that the film of 16 mm diameter, containing one-tenth of the original filter material amount, was best from the view points of sensitivity and easy procedure.

Comparison of Diffraction Pattern between a Cut Piece of Filter Sample and Small-Film Samples Prepared. Figure 2 shows the comparison among the X-ray diffraction patterns observed on a cut piece of 25-mm diameter which was one-tenth of the original filter sample and on 16-mm diameter film samples prepared from the entire filter samples. The filter samples of the stage 8 and backup filter were taken as examples from the viewpoint of different substrate materials, larger quantity of particulates, and more compounds contained.

Figure 2a shows that no diffraction peak was observed on a cut piece of 25 mm diameter, on which about 0.4 mg of particulates were dispersed as many spots. Figure 2b, however, shows that distinct diffraction peaks were observed on the film sample consisting of about 4.0 mg of

particulates and 5 mg of polycarbonate, which was prepared by using the same entire filter sample described above. Figure 2d is another example of a diffraction pattern observed on the film prepared by using the entire filter of the stage 8, on which 3.9 mg of the particulates was collected in the wet season at the same sampling location. These examples show that forming a small film increased the X-ray diffraction intensities to allow for the identification of compounds in the particulates collected by the Andersen sampler. This is obviously due to the reduction of substrate amount and the concentration of all the particulates into a suitably small area.

Differences between the background intensities of Figure 2a and 2b or 2d are due to the differences between the irradiated amounts of polycarbonate and the particulates. The X-ray diffraction pattern of the backup filter was also improved significantly by preparing its small film, which exhibited many distinct peaks as shown in Figure 2c, though it still showed a high background, which could be reduced by further elimination of the acetyl cellulose amount in the centrifugation process.

Identification of Compounds. Figures 3–5 show the results of the XRD of the particulates collected on each stage in the dry (Figure 3) and wet (Figures 4 and 5) seasons, together with the data of JCPDS cards.

Ammonium sulfate, ammonium chloride, ammonium nitrate sulfate, α-quartz, plagioclase, and probably calcite were found in the samples collected in the dry winter. Though potassium and iron were also found as the main constituents by the XRF, their respective compounds were not found; plagioclase may contain potassium and iron partially. The identification of ammonium compounds was further supported by a microspectrophotometric determination (12).

α-Quartz, plagioclase (albite and anorthite), alum, ammonium sulfate, and calcite were found in the samples collected in the wet season. Some strong and weak diffraction peaks, which appeared in the samples of each stage, could not be designated. Though iron, titanium,

Table III. Recovery and Reproducibility of Compounds on the Film Sample Prepared

		A		B	C		D	
sample prep		mixture of filter[a] (50 mg), CH$_2$Cl$_2$ (10 mL), NH$_4$Cl (1.11 mg), and (NH$_4$)$_2$SO$_4$ (1.11 mg) was centrifuged			cut piece of $^1/_{10}$ filter[a] and CH$_2$Cl$_2$ (0.2 mL) was used directly without centrifuging			
		1 mL of remainder in the centrifuge tube, intensity, cps		1 mL (from 9 mL) of super-natant, inten-sity, cps,	with NH$_4$Cl (1.04 mg) and (NH$_4$)$_2$SO$_4$ (1.12 mg), intensity, cps		without compd, inten-sity, cps,	differ-ence[c] of A and C,
X-ray diffraction		measd	corrd[b]	measd	measd	corrd[b]	measd	%
(NH$_4$)$_2$SO$_4$	(111)	334	301	0	330	295	0	+2
	(202, 211)	118	106	0	121	108	0	−2
	(013)	114	103	0	121	108	0	−5
	(200)[d]							
NH$_4$Cl	(100)[d]	369	332	0	348	328	0	+1
	(110)	904	814	0	870	837	0	−3

[a] Nuclepore.   [b] Corrected for 1 mg of each compound.   [c] For corrected intensities.   [d] Overlap peak.
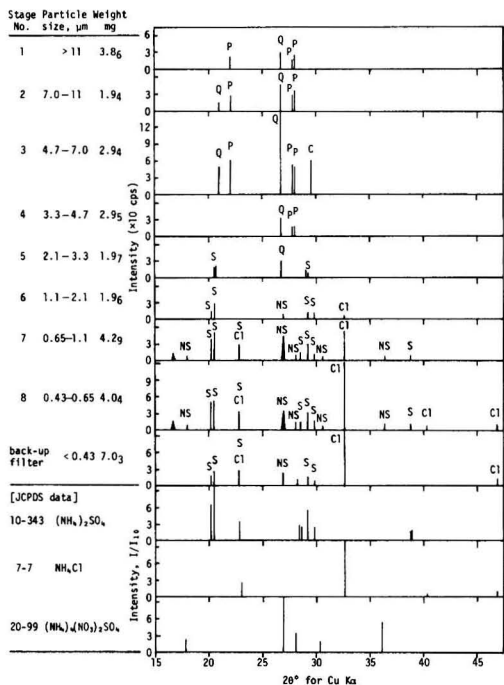
Figure 3. X-ray diffraction patterns of particulates collected in dry season: Q, α-quartz; P, plagioclase (albite and anorthite); C, calcite; S, (NH$_4$)$_2$SO$_4$ mascagnite; Cl, NH$_4$Cl salammoniac; NS, (NH$_4$)$_4$(NO$_3$)$_2$SO$_4$; cf. the JCPDS patterns in Figure 4.

Figure 4. X-ray diffraction patterns of particulates collected in the wet season (1): Q, α-quartz; P, plagioclase (albite and anorthite); C, calcite. No mark peaks: unidentified.

potassium, and zinc were also found as major constituents, any corresponding compound was not found.

Relationships between compounds and their constituent elements will be discussed again later with their distribution curves.

Recovery of Compounds and Reproducibilities of Small-Film Sample and Diffraction Intensities. Table III shows the results of the recovery test and the reproducibility test of the film samples prepared. No diffraction peak was shown in sample B, prepared with 1 mL of the supernatant after the centrifugation, or in sample D (blank

test). Samples A and C, however, gave many strong diffraction peaks of both ammonium sulfate and ammonium chloride, and the differences between the corrected intensities were insignificant being less than 5% for the same plane of the same compound in both samples. These results show that the recommended procedure gave a very good recovery of both compounds in the prepared film, a good reproducibility of small-film samples for the XRD and also very little orientation effect. Microscopic ob-
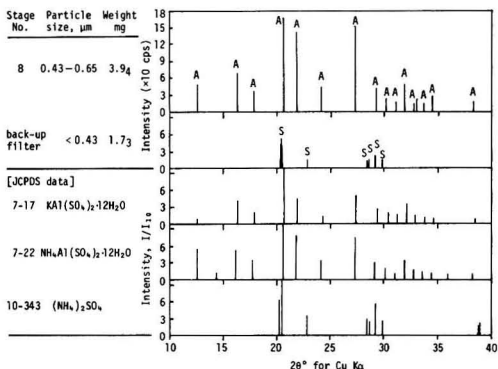
Figure 5. X-ray diffraction patterns for particulates collected in the wet season (2): A, $(NH_4,K)Al(SO_4)_2 \cdot 12H_2O$; S, $(NH_4)_2SO_4$.
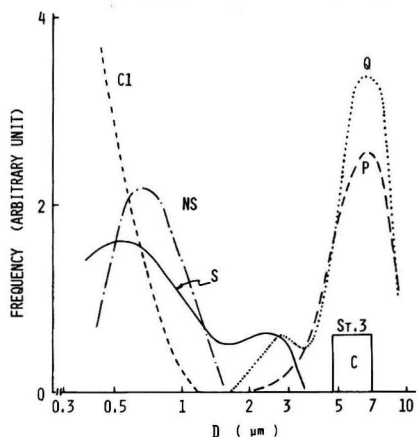
Figure 6. Distribution curves of compounds vs. particle size for particulates collected in the dry season: Cl, NH_4Cl; NS, $(NH_4)_4(NO_3)_2SO_4$; S, $(NH_4)_2SO_4$; Q, α-quartz; C, calcite; P, plagioclase. For D and frequency, refer to Figure 1. St. 3: found only in stage 3.
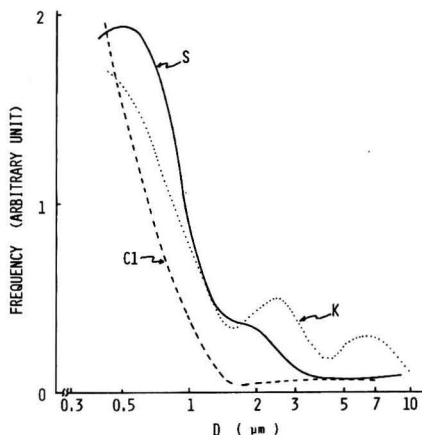
Figure 7. Distribution curves of S, Cl, and K vs. particle size for particles collected in dry season. For D and frequency, refer to Figure 1.

Figure 8. Distribution curves of Si, Ca, and Fe vs. particle size for particulates collected in dry season. For D and frequency, refer to Figure 1.

Figure 9. Distribution curves of compounds vs. particle size for particulates collected in wet season: (—) α-quartz; (⋯) plagioclase; (- - -) calcite. For D and frequency, refer to Figure 1.

servation also showed no change between the crystal shapes of both compounds before and after treatment with dichloromethane. These conclusions must be identical for any other insoluble compounds found in the particulates.

Distribution Curves of Compounds vs. Particle Size. The distribution curves of the identified compounds are shown in Figures 6 and 9 for the dry and wet seasons, respectively. The distribution curves of major elements vs. particle size are shown in Figures 7 and 8 for the dry season and in Figures 10 and 11 for the wet season for the comparison with the related compound curve and for verification of the identification of compounds done before.

Figure 6 shows that ammonium chloride, ammonium sulfate, and ammonium nitrate sulfate identified in the particulates collected in the dry season were mainly concentrated in the fine-particle region, while α-quartz, plagioclase, and calcite were in the coarse-particle region with their peaks at around 6.5 μm. The summation of distribution curves of the compounds resembled the weight distribution curve a shown in Figure 1. The distribution curves of chlorine and sulfur shown in Figure 7 were in

Figure 10. Distribution curves of Si (—), Ca (- - -), Fe (-·-), and Ti (···) vs. particle size for particulates collected in wet season. For D and frequency, refer to Figure 1.
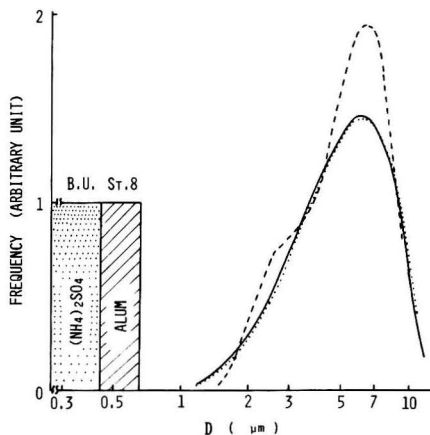

Figure 11. Distribution curves of S, Al, K, and Zn vs. particle size for particulates collected in wet season. For D and frequency, refer to Figure 1.
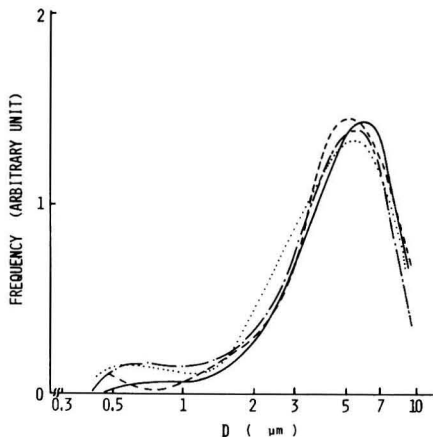

Figure 12. Distribution curves for unidentified compounds in particulates collected in wet season: (—) drawn by use of the line intensities of 2.71-Å spacing; (···) drawn by use of the line intensities of 5.4-Å spacing. For D and frequency, refer to Figure 1.

the backup filter. Therefore, their existence was represented in Figure 9 by shadowed and dotted areas, respectively. The curves for silicon and calcium in Figure 10 resembled the curves of α-quartz, plagioclase, and calcite and supported their identification by the XRD as described earlier. The curves of aluminum and potassium in Figure 11 resembled the summation of both the curves of plagioclase (which may contain partially potassium) and alum, and supported the identification of the compounds. The distribution curve of sulfur in Figure 11 showed high concentration toward the fine-particle region with a maximum at 0.43 μm or below and supported the detections of ammonium sulfate and alum in the backup filter and the stage 8 shown in Figure 9.

The distribution curves of α-quartz, plagioclase, and calcite resembled each other for the particulates collected in both seasons and were shifted little from the weight distribution curves shown in Figure 1. It seems to show that such compounds are the main crystalline substances in the coarse-particle region and contained steadily as air pollutants. Ammonium salts and alum were found as the main crystalline substances in the fine-particle region, while their distributions or existence depended on the season, weather conditions, or others. The curves for the unidentified compound(s) in Figure 4 (wet season) were constructed by using the strong diffraction line intensities of 5.4- and 2.71-Å spacings and are shown in Figure 12 for future study, though both lines may belong to a common compound.

Acknowledgments

The assistance of Noaki Hiramatsu in some of the initial experimental work is gratefully acknowledged.

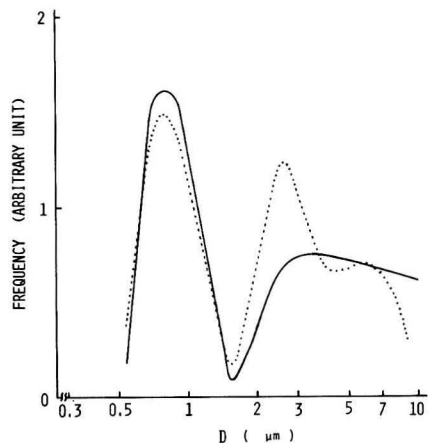accordance with the curves of ammonium chloride, ammonium sulfate, and ammonium nitrate sulfate, while the curves of silicon and calcium in Figure 8 were also in accordance with the curves of quartz, plagioclase, and calcite. These results support the identification of their compounds by the XRD described before. Other major elements such as iron and potassium may be partially contained in compounds like plagioclase, and potassium may be partially contained in place of ammonium ion of its salts as a substituting element, though their main compounds were not found.

Figure 9 shows that, for the particulates collected in the wet season, the distribution curves of α-quartz and plagioclase almost overlapped each other and had their peaks at 6.0 μm of the coarse-particle region similarly to the calcite peak. The distribution curves of alum and ammonium sulfate were not calculated, because alum was found only in the stage 8 and ammonium sulfate only in

Literature Cited

(1) Andersen, A. A. *Am. Ind. Hyg. Assoc. J.* **1966**, *27*, 160–165.
(2) Fujimura, M.; Hashimoto, Y. *J. Chem. Soc. Jpn.* **1977**, 902–906.
(3) Kadowaki, S. *J. Chem. Soc. Jpn.* **1980**, 141–146.
(4) Mizohata, A.; Matsunami, T.; Mamuro, T. *Annu. Rep. Radiat. Cent. Osaka Prefect.* **1975**, *16*, 1–7.
(5) Walker, M. V.; Weschler, C. J. *Environ. Sci. Technol.* **1980**, *14*, 594–597.
(6) Henry, W. H. EPA Contract EPA-70-159, final report July 23, 1971.

(7) Fukasawa, T.; Iwatsuki, M.; Kawakubo, S.; Miyazaki, K. *Anal. Chem.* 1980, *52*, 1784–1787.

(8) O'Connor, B. H.; Jaklevic, J. M. *Atmos. Environ.* 1981, *15*, 1681–1690.

(9) Harrison, R. M.; Williams, C. R.; O'Neill, I. K. *Environ. Sci. Technol.* 1981, *15*, 1197–1204.

(10) Fukasawa, T.; Iwatsuki, M.; Kawana, K. *Bunseki Kagaku* 1981, *30*, T55–T60.

(11) Fukasawa, T.; Iwatsuki, M.; Ito, J.; Hayashi, E.; Kamiyanagi, T. *J. Chem. Soc. Jpn.* 1982, 1940–1945.

(12) Fukasawa, T.; Kawakubo, S.; Mizuike, A. *Anal. Chim. Acta* 1983, *149*, 363–367.

(13) Maruyama, H.; Nakayama, M.; Amemiya, M.; Kimura, I.; Ito, I. *Adv. X-ray Chem. Anal., Jpn.* 1979, *11*, 61–68.

(14) The paper is being arranged by the authors.

Catalysis of the Autoxidation of Aquated Sulfur Dioxide by Homogeneous Metal–Phthalocyanine Complexes

Scott D. Boyce, Michael R. Hoffmann,* P. Andrew Hong, and Lorraine M. Moberly

Department of Environmental Engineering Science, W. M. Keck Laboratories, California Institute of Technology, Pasadena, California 91125

■ The autoxidation of sulfur dioxide to sulfate in aqueous solution has been examined in the pH range 4–13 in the presence of water-soluble transition metal-4,4′,4′′,4′′′-tetrasulfophthalocyanine complexes, MTSP (where M = Fe^{II}, Mn^{II}, Co^{II}, Ni^{II}, Cu^{II}, and V^{IV}). Experimental rate data have been analyzed in terms of a Michaelis–Menten kinetic expression derived from a bisubstrate kinetic model. The rate law and spectroscopic measurements indicate that the reaction proceeds via the formation of an activated complex in which O$_2$ and two molecules of SO$_3^{2-}$ are reversibly bonded to the catalytic center. Relative reactivity is determined by the ability of the central metal atom to reversibly bind molecular oxygen. Analysis of the spectroscopic data suggests that photoassisted catalysis arises from the absorption of light by a ternary activated complex.

Introduction

Numerous attempts have been made to characterize the kinetics and mechanisms of the metal-catalyzed autoxidation of sulfur dioxide in aqueous solution (*1–20*). Results obtained from previous studies show considerable disagreement as to the rate, rate law, and pH dependence of this reaction (*21–24*). The reaction rate is sensitive to catalysis by a wide variety of transition-metal ions such as Mn^{2+}, Fe^{3+}, Co^{2+}/Co^{3+}, and Cu^{2+}. The catalytic autoxidation of SO$_2$ dissolved in atmospheric water droplets represents a viable pathway for the formation of sulfate (*25*), while oxygenation of S^{IV} in aquatic environments plays a fundamental role in the natural sulfur cycle (*26, 27*).

Hoffmann and Jacob (*28*) describe in detail inconsistencies reported by other investigators. There is general agreement that the homogeneous reaction rate exhibits a zero-order dependence on [O$_2$], but observed kinetic orders in substrate and metal-ion concentration vary from zero to two for reactions carried out under similar concentration conditions. The majority of experimental data indicates that the kinetics of sulfite oxidation conform to a simple empirical rate law which is first order in both [S^{IV}] and [M^{n+}]. However, Barron and co-workers (*2, 5*), Bengtsson and Bjerle (*3*), and Mishra and Srivastava (*17, 18*) have each reported a nonintegral dependence on reductant (three-halves order) and catalyst (half order) concentration.

Three types of reaction mechanisms have been proposed to account for the catalytic activity of transition metals in solution. These mechanisms include free-radical chain processes involving a sequence of one-electron transfer steps following thermal initiation (*29*), heterolytic mechanisms in which metal–sulfite complexation precedes the inner-sphere transfer of two electrons from S^{IV} to oxygen (*30*), and photoassisted pathways whereby homolytic oxidation of sulfite is promoted through the absorption of light by either the substrate, the metal catalyst, or a metal–substrate adduct (*31–34*).

In order to investigate the reaction of aquated SO$_2$ with molecular oxygen in a well-defined catalytic system, water-soluble metal–phthalocyanine, M(PC), complexes were employed. Phthalocyanines are macrocyclic tetrapyrrole compounds that readily form square-planar complexes in which the metal center is bonded to the four pyrrole nitrogen atoms of the ligand as depicted in Figure 1. Cobalt(II)-4,4′,4′′,4′′′-tetrasulfophthalocyanine, Co^{II}-TSP, has been shown to be an effective catalyst for the autoxiation of hydrogen sulfide (*23*), cysteine (*35, 36*), hydrazine (*37*), and hydroxylamine (*38*). The properties of M(PC) derivatives have been compared to those of catalase, oxidase, and oxygenase enzymes (*36, 39–46*). The results of the current investigation should clarify several fundamental aspects of the mechanism for the catalytic autoxidation of S^{IV} in aqueous media. From a commerical standpoint, the oxidation of SO$_2$ and other S-containing reductants in the presence of either homogeneous or heterogeneous transition-metal complexes may provide convenient and economical methods for sulfur pollution control (*23, 47*).

Experimental Procedures

Materials. The monosodium salt of 4-sulfophthalic acid was obtained by neutralization of a 50% aqueous solution of 4-sulfophthalic acid (Eastman) with 15 N NaOH and purified by recrystallization from absolute ethanol. All other chemicals utilized in the preparation of the metal–phthalocyanine catalysts were of reagent grade.

Analyses. Microanalyses were performed by Galbraith Microanalytical Laboratories, Inc., of Knoxville, TN. ^{1}H NMR spectra were recorded on a Varian Model EM 390 nuclear magnetic resonance spectrometer.

Synthesis of Catalysts. The tetrasodium salt of cobalt(II)-4,4′,4′′,4′′′-tetrasulfophthalocyanine dihydrate, Co^{II}TSP, was synthesized from sodium 4-sulfophthalate, ammonium chloride, urea, ammonium molybdate, and cobalt(II) sulfate heptahydrate according to the procedure

$$2SO_3^{2-} + O_2 \xrightarrow{\text{catalyst}} SO_4^{2-}$$

catalyst = M—4,4',4'',4''' — tetrasulfophthalocyanine

$$M \equiv Fe^{II}, Mu^{II}, Co^{II}, Ni^{II}, Cu^{II}, V^{IV}$$
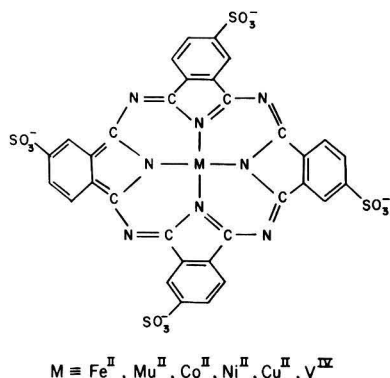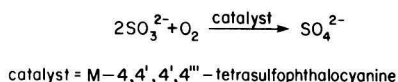
Figure 1. Generalized stoichiometric relationship for the aqueous phase autoxidation of sulfite as catalyzed by homogeneous transition metal–phthalocyanine complexes.

described by Weber and Busch (48). The initial product was treated successively with NaCl, 0.1 N NaOH, and 80% aqueous ethanol in the prescribed manner. Pure $Co^{II}TSP$ was obtained by extracting the solid with absolute ethanol for 4 h in a Soxhlet apparatus. The blue crystalline complex was then dried in vacuo over P_2O_5 prior to analysis.

Tetrasulfophthalocyanine complexes containing manganese(II), iron(II), nickel(II), copper(II), and vanadium-(IV) were prepared from appropriate metal salts by using analogous procedures. The structure of each catalyst was characterized by elemental analysis and through a comparison of ^1H NMR and UV/VIS spectra with published reference data (38, 48).

Buffers. Tris(hydroxymethyl)aminomethane hydrochloride (TRIS-HCl) (Sigma), 2-[[tris(hydroxymethyl)-methyl]amino]ethanesulfonic acid (TES) (Sigma), monobasic sodium phosphate (Mallinckrodt), dibasic sodium phosphate (Mallinckrodt), tribasic sodium phosphate (Mallinckrodt), sodium borate (Mallinckrodt), sodium chloride (Mallinckrodt), and sodium hydroxide (Mallinckrodt) were used to prepare the pH buffer solutions. Sodium perchlorate (G. Frederick Smith) was employed to maintain the ionic strength constant at $\mu = 0.4$ M. Deionized water (18 $M\Omega$ cm resistivity) obtained from a Milli RO-4/Milli Q purification system (Millipore) was utilized in the preparation of all reagent solutions. The water was deoxygenated by purging with N_2 prior to the preparation of the Na_2SO_3 solutions.

Kinetic Data. Kinetic data were obtained from two different analytical procedures. In one set of experiments $[S^{IV}]$ was determined by monitoring the UV absorption spectrum (λ_{max} 212 nm) of the reaction solution as a function of time. Optical absorption data were collected with a Hewlett-Packard Model 8450A UV/vis spectrophotometer. The reactions were performed at 25 ± 1 °C directly in Teflon-stoppered quartz spectrophotometer cells (2- or 10-cm pathlength).

In another set of experiments, the oxidation of S^{IV} was followed by continuous measurement of changes in O_2 concentration as a function of time. Dissolved oxygen was determined potentiometrically by using an Orion Model 97-08-00 O_2 electrode coupled to an Orion Model 901 Ionanalyzer/Model 951 digital printer system. The pH

of the reaction mixture was monitored simultaneously with an Orion Model 91-62 combination pH electrode. The dissolved oxygen and pH electrodes were interfaced to the Ionanalyzer through an Orion Model 605 electrode switch.

These reactions were conducted in a water-jacketed, glass and Teflon reactor with a total volume of 2.0 L. The design and operation of the batch reactor system have been described previously by Hoffmann and Lim (47). To minimize the potential catalytic effect of trace-metal contaminants, all glassware was washed with phosphate-free detergent (Alconox), soaked in 5.2 N HNO_3, and then rinsed several times with deionized water.

In a typical experiment, a 2.0 L volume of buffer solution containing the appropriate catalyst was transferred to the reactor system. Air (Matheson), oxygen (Matheson), or a controlled N_2/O_2 mixture was purged through the solution with constant stirring for 30 min. After saturation, the reaction was sealed from the atmosphere. A constant temperature of 25 (±0.1) °C was maintained by using a Haake Model FK-2 water circulation system and temperature controller.

To initiate the reaction, a known volume of a stock sulfite solution was added to the buffer/catalyst mixture. Sulfite concentrations, $[S^{IV}]$, ranged from 5×10^{-5} to 5×10^{-3} M. Dissolved oxygen varied from 2.5×10^{-4} to 1.2×10^{-3} M. Addition of the disodium salt of ethylenediaminetetraacetic acid (EDTA) (Sigma) reduced the potential catalytic effect of residual trace-metal contaminants during control reactions (49). Mannitol, sodium cyanide (NaCN), and EDTA were used selectively as free-radical and trace-metal inhibitors.

Analyses for sulfate were conducted by using the standard $BaCl_2$ turbidimetric procedure (50). Hydrogen peroxide was detected as a kinetic intermediate by measuring the decrease in the fluorescence intensity of scopoletin dye (6-methoxy-7-hydroxy-2H-1-benzopyran-2-one) in the presence of horseradish peroxidase as described by Perschke and Broda (51). Aliquots of the reaction solution were collected during the course of experiments for analysis of SO_4^{2-} and H_2O_2. Fluorescence spectra were recorded with an Aminco-Bowman spectrofluorometer.

Results

The reaction of sulfur dioxide with oxygen in aqueous solution proceeds according to the following stoichiometry:

$$2S^{IV} + O_2 \rightarrow 2S^{VI} \tag{1}$$
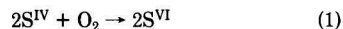
where $[S^{IV}] = [SO_2 \cdot H_2O] + [HSO_3^-] + [SO_3^{2-}]$ and $[S^{VI}] = [H_2SO_4] + [HSO_4^-] + [SO_4^{2-}]$. Addition of water-soluble cobalt(II)-, iron(II)-, and manganese(II)-tetrasulfophthalocyanine complexes accelerated reaction 1 under neutral and alkaline pH conditions. Another frequently observed, but low-yield reaction product, is dithionate, $S_2O_6^{2-}$ (52). However, dithionate was not detected in any of the reaction solutions containing $M^{II}TSP$ catalysts.

Reaction kinetics were studied under pseudo-order conditions with respect to substrate concentration (i.e., $[O_2]_0 \gg [S^{IV}]_0$) at constant pH and ionic strength. The observed rate constant, k_{obsd}, for each reaction was calculated from linear least-squares analyses of sulfite concentration $[\ln ([S^{IV}]_t/[S^{IV}]_0)]$ vs. time plots.

Reaction Orders. The kinetic data obtained from a typical series of experiments are summarized in Figure 2. At the principal wavelength for light absorption due to SO_3^{2-} (λ_{max} 212 nm), Beer's law ($A = \epsilon l c$) was found to be valid over a broad range in $[S^{IV}]$ as reported by Hayon and co-workers (31). Under the reaction conditions specified in Figure 2, the observed pseudo-first-order rate constants
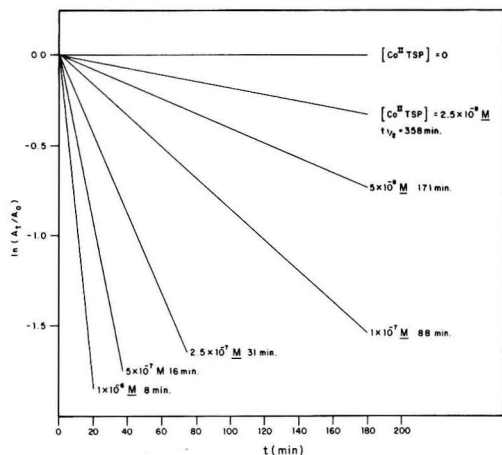
Figure 2. Pseudo-first-order plots of ln (A_t/A_0) (λ 212 nm) for the reaction of S^{IV} with O_2. $[S^{IV}]_0 = 1 \times 10^{-4}$ M, $[O_2]_0 = 1.2 \times 10^{-3}$ M, and $[Co^{II}TSP]_0 = 2.5 \times 10^{-8}$–$2.5 \times 10^{-6}$ M, pH 9.2 (borate buffer); $\mu = 0.4$ M, $T = 25 \pm 1$ °C.

ranged from 3.3×10^{-5} s^{-1} at $[Co^{II}TSP]_0 = 2.5 \times 10^{-8}$ M to 5.2×10^{-3} s^{-1} at $[Co^{II}TSP]_0 = 2.5 \times 10^{-6}$ M ($0.985 \le R^2 \le 0.999$). No decrease in $[S^{IV}]$ was observed after 12 h in the absence of catalyst. First-order kinetic behavior in total sulfite concentration was also observed for reactions carried out at pH 6.7 and over the entire pH range under study.

The linearity of ln (A_t/A_0) vs. time can be accepted as evidence of a first-order rate dependence on $[S^{IV}]$. Additional support for this conclusion was obtained from a series of experiments in which the rate of change of $[O_2]$ was monitored potentiometrically at different initial values of $[S^{IV}]$. The amperometric response of the O_2 electrode is a linear function of the dissolved oxygen concentration (53). Analysis of this data by the van't Hoff method of initial rates (54) confirmed that the reaction was nearly first order in reductant. For example, the slopes of linear plots of $-d[O_2]_0/dt$ vs. $[S^{IV}]_0$ were equal to 1.18 ($R^2 = 0.9893$) at pH 6.7 and 1.25 $R^2 = 0.9580$) at pH 9.2. A moderate degree of scatter in the experimental data could account for the values of greater than one. These results suggest that a potential source of variability in previously reported empirical rate laws for the oxidation of SO_2 may originate from the selective fitting of experimental measurements to a narrow range of concentration conditions.

The dissolved oxygen electrode response ($i_\infty \alpha [O_2]$) decreased linearly with time during reactions in which $[O_2]_0 \gg [S^{IV}]_0$. This observation indicated that the apparent reaction order in oxygen concentration was zero. Additional evidence of zero-order kinetic behavior was acquired through the spectrophotometric determination of k_{obsd} at a variety of initial oxidant concentrations (2.5×10^{-4} M $\le [O_2]_0 \le 1.2 \times 10^{-3}$ M). In this case, the observed first-order rate constants remained unchanged within the limits of experimental error ($\pm 5\%$). When the initial pseudo-order reaction conditions were adjusted in a fashion such that $[S^{IV}]_0 \gg [O_2]_0$, an apparent exponential decay in $[O_2]$ was observed. This result suggests a shift to a first-order rate dependence on oxygen when sulfite is in excess.

From a least-squares regression analysis of the rate data presented in Figure 2, the rate of oxidation of S^{IV} was determined to be first order in cobalt(II)–phthalocyanine over the concentration range 2.5×10^{-8} M $\le [Co^{II}TSP]_0 \le 2.5 \times 10^{-6}$ M. In contrast, the kinetic measurements

Table I. Effect of pH on k_{obsd}[a]

pH	buffer system	k_{obsd} (s^{-1})
4.1	0.1 M NaH$_2$PO$_4$ 0.3 M NaClO$_4$	no reaction
6.7	0.1 M NaH$_2$PO$_4$ 0.1 M Na$_2$HPO$_4$	2.56×10^{-4}
7.7	0.2 M TES 0.1 M NaOH 0.3 M NaClO$_4$	3.22×10^{-5}
8.4	0.1 M TRIS 0.1 M TRIS-HCl 0.3 M NaClO$_4$	4.53×10^{-5}
9.2	0.1 M NaB$_4$O$_7$ 0.1 M NaClO$_4$	5.27×10^{-5}
10.1	0.1 M Na$_2$CO$_3$ 0.1 M NaHCO$_3$	3.47×10^{-5}
11.5	0.044 M Na$_2$HPO$_4$ 0.044 M Na$_3$PO$_4$	4.17×10^{-5}
12.9	0.1 M NaCl 0.1 M NaOH 0.2 M NaClO$_4$	7.03×10^{-5}

[a] $[S(IV)]_0 = 5 \times 10^{-5}$ M, $[O_2]_0 = 2.5 \times 10^{-4}$ M, and $[Co^{II}TSP]_0 = 1 \times 10^{-6}$ M; $\mu = 0.4$ M, $T = 25.0 \pm 0.1$ °C.

collected from reactions occurring in phosphate buffer or neutral pH showed a nonintegral rate dependence on $[Co^{II}TSP]_0$.

pH Dependency. A summary of the experimental rate data presented in Table I shows a complex pH dependency for the kinetics of S^{IV} oxidation. In general, the rate of reaction appeared to increase with increasing hydroxide concentration over the pH range 4–13. However, the observed trend is obscured by a number of secondary factors such as general-base catalysis and inhibition due to competitive complexation of buffering reagents such as TRIS and TES to cobalt(II). The increase in the reaction rate between pH 4.1 and 6.7 corresponds approximately to the acid dissociation of bisulfite ion to form SO_3^{2-} ($pK_a = 6.7$ at $T = 20$ °C and $\mu = 0.1$ M) (55). As the fraction of S^{IV} present as sulfite increases, the rate of reaction is enhanced. This behavior suggests that SO_3^{2-} is the principal reactant species in aqueous solution.

In a related study, Hoffmann and Lim (47) reported that the rate of the autoxidation of HS^- in the presence of $Co^{II}TSP$ increased significantly under strongly alkaline conditions (pH 9–12). Acceleration of the reaction was attributed to the enhanced catalytic efficiency of the dioxygen complex $Co^{III}TSP(O_2^-\cdot)^{3-}$ [relative to $Co^{III}TSP$-$(O_2^-\cdot)^{2-}$] formed by deprotonation of a pyrrole N atom of the phthalocyanine ligand. Boucher (56) recently suggested that coordination of O_2 by $Co^{II}TSP$ at high pH may be controlled by the acid dissociation of a water molecule attached to the metal center. With an increase in the pH of the reaction medium, the remaining solvent molecules within the coordination sphere of the cobalt–phthalocyanine complex are replaced by hydroxyl groups resulting in an enhancement of the stability of monomeric species such as $(HO)Co^{II}TSP^{3-}$ and $(HO)Co^{III}TSP(O_2^-\cdot)^{3-}$. From ligand field theory, the bonding of OH^-, a strong σ-electron donor, in an axial coordination site would raise the energy of the $3d_{z^2}$ $3d_{xz}$, and $3d_{yz}$ atomic orbitals on Co^{II} to a level which would promote stronger bonding with the π^*-molecular orbitals of appropriate symmetry on O_2 (57). This change in catalyst speciation may account for a further increase in the rate of sulfite oxidation by O_2 between pH 10 and 13.

Relative Reactivity of MTSP Complexes. The reactivity of $Co^{II}TSP$ is significantly greater than that of the other homogeneous phthalocyanine catalysts. According to the data presented in Table II, the order of catalytic

Table II. Effect of a Variation in the Central Metal Atom on the Rate of Autoxidation of S^{IV} [a]

metal-tetrasulfophthalocyanine	k_{obsd} $(s^{-1}) \times 10^4$
Co^{II}	18.30
Fe^{II}	2.23
Mn^{II}	0.24
Cu^{II}	~0
Ni^{II}	~0
V^{IV}	~0

[a] $[S^{IV}]_0 = 1 \times 10^{-4}$ M, $[O_2]_0 = 1.2 \times 10^{-3}$ M, and $[MTSP]_0 = 1 \times 10^{-6}$ M, pH 9.2 (borate buffer); $\mu = 0.4$ M, $T = 25 \pm 1$ °C.
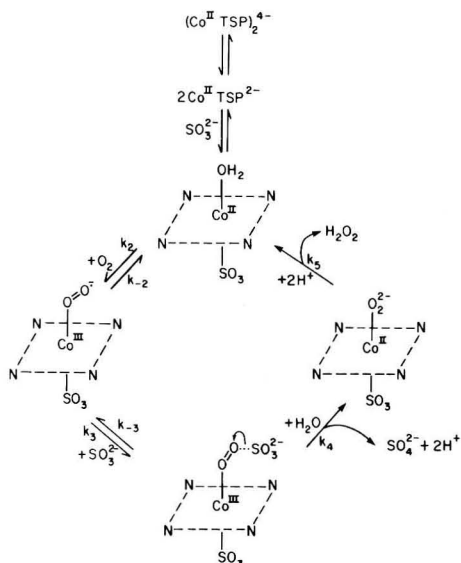

Figure 3. Schematic representation of the proposed bisubstrate complexation reaction mechanism for the catalytic autoxidation of sulfite in aqueous solution.

activity, $Co^{II} > Fe^{II} > Mn^{II} > V^{IV} \simeq Ni^{II} \simeq Cu^{II}$, follows a general sequence that reflects the relative capacity of each square-planar transition-metal complex to reversibly coordinate O_2 (56). Tetra- and pentacoordinate low-spin complexes of cobalt(II), iron(II), and manganese(II) have been shown to function as dioxygen carriers in organic and aqueous solvent systems (58, 59), whereas square-planar nickel(II) ($3d^8$ low spin) and copper(II) ($3d^{10}$) derivatives do not form stable dioxygen adducts. Similar trends in the catalytic properties of metal–phthalocyanines have been reported previously by Kropf et al. (60, 61) for the liquid-phase autoxidation of aromatic hydrocarbons and by Kothari and Tazuma (62) for the oxygenation of phenols.

Discussion

The catalytic activity of transition metal–phthalocyanine complexes in aqueous solution was documented initially by Cook (39, 40) for the decomposition of H_2O_2 and the oxidation of HI, later by Wagnerova and co-workers (35, 37, 38) for the autoxidation of hydrazine, hydroxylamine, and cysteine, and by Hoffmann and Lim (47) for the oxidation of H_2S. These investigators suggested that the catalytic properties of metal–phthalocyanines were characteristic of an oxidase. Wagnernova et al. (37) reported that the kinetics of oxidation reactions catalyzed by
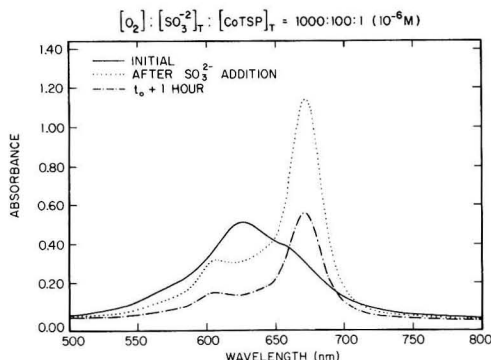
Figure 4. Changes in the visible absorption spectrum of $Co^{II}TSP$ during the catalytic autoxidation of sulfite. $[S^{IV}]_0 = 1 \times 10^{-4}$ M, $[O_2]_0 = 1.2 \times 10^{-3}$ M, and $[Co^{II}TSP]_0 = 1 \times 10^{-6}$ M, pH 6.7; $\mu = 0.4$ M, $T = 25 \pm 1$ °C.

$Co^{II}TSP$ conformed to a Michaelis–Menten rate law. The experimental evidence obtained in this study is indicative of enzymelike kinetics for the catalytic autoxidation of S^{IV}. A well-known characteristic of enzymatic reactions is the variability of reaction order with respect to the concentrations of substrate and catalyst (63). For example, the order in substrate can vary between zero and one. In order to interpret the observed reaction kinetics of sulfite oxidation within this framework, a bisubstrate complexation model has been proposed.

The mechanism proposed for the kinetics of the autoxidation of S^{IV} between pH 6.7 and pH 9.2 is an ordered-ternary complex pathway (64) which is depicted schematically in Figure 3 and consists of the following elementary steps:

$$(Co^{II}TSP)_2^{4-} \underset{}{\overset{K_d}{\rightleftharpoons}} 2Co^{II}TSP^{2-} \qquad (2)$$

$$Co^{II}TSP^{2-} + SO_3^{2-} \overset{K_1}{\rightleftharpoons} (SO_3)Co^{II}TSP^{4-} \qquad (3)$$

$$(SO_3)Co^{II}TSP^{4-} + O_2 \underset{k_{-2}}{\overset{k_2}{\rightleftharpoons}} (SO_3)Co^{III}TSP(O_2^-\cdot)^{4-} \quad (4)$$

$$(SO_3)Co^{III}TSP(O_2^-\cdot)^{4-} +$$
$$SO_3^{2-} \underset{k_{-3}}{\overset{k_3}{\rightleftharpoons}} (SO_3)Co^{III}TSP(O_2^-\cdot)(SO_3)^{6-} \quad (5)$$

$$(SO_3)Co^{III}TSP(O_2^-\cdot)(SO_3)^{6-} + H_2O \overset{k_4}{\underset{slow}{\longrightarrow}}$$
$$(SO_3)Co^{II}TSP(O_2^{2-})^{6-} + SO_4^{2-} + 2H^+ \quad (6)$$

$$(SO_3)Co^{II}TSP(O_2^{2-})^{6-} + 2H^+ \overset{k_5}{\underset{rapid}{\longrightarrow}}$$
$$(SO_3)Co^{II}TSP^{4-} + H_2O_2 \quad (7)$$

$$H_2O_2 + SO_3^{2-} \overset{k_6}{\underset{rapid}{\longrightarrow}} SO_4^{2-} + H_2O \qquad (8)$$
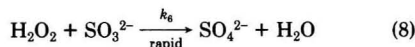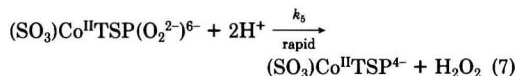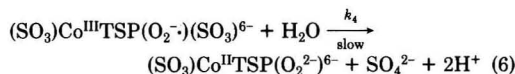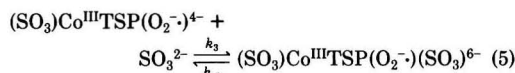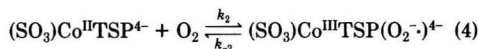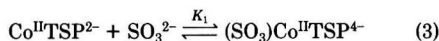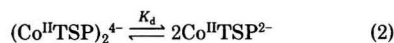
The theoretical rate expression for this mechanism was derived by using the method of King and Altman (65), which is based on a standard determinant procedure for solving a system of nonhomogeneous linear equations. Reactions 2 and 3 represent the formation of the active catalytic center $(SO_3)Co^{II}TSP^{4-}$, from the dimer of cobalt(II)–phthalocyanine (66, 67). This sequence of reactions is consistent with the observed changes in the spectrum of $Co^{II}TSP$ (Figure 4) that indicate a shift in the position of the monomer/dimer equilibrium, monomer (λ_{max} 636 nm)/dimer (λ_{max} 670 nm), upon coordination of a substrate molecule to the metal center at an axial pos-

ition either above or below the plane of the macrocyclic ring. Complexation of sulfite by $Co^{II}TSP$ in an axial coordination site enhances the subsequent uptake of molecular oxygen as written in eq 4. Carter et al. (68) have studied the reversible binding of dioxygen to cobalt(II) chelates of the general form $Co^{II}(L)(B)$ where L refers to a quadridentate Schiff base or porphyrin ligand and B designates an axial base. The authors concluded that as the π-electron-donating ability of B increased, the electron density on the cobalt atom would be enhanced and that this would, in turn, strengthen the "π-back-bonding" interaction between Co and O_2. Rollman and Chan (69) reported that the imidazole complex of $Co^{II}TSP$ underwent rapid reaction with O_2, whereas the corresponding pyridine derivative did not. Similar trends in the bonding of dioxygen to $Co^{II}TSP$ have been observed previously by Cookson and co-workers (70) and Przywarska-Boniecka and Fried (71). In addition, studies of the catalytic properties of Co^{II}-substituted heme have demonstrated that the electronic properties of B affect both the formation constant and reversibility of oxygen transfer (59).

Electron spin resonance spectroscopic studies on 1:1 $Co^{II}TSP$–dioxygen adducts have been shown to be consistent with the formulation of the structure of the oxygenated complex as cobalt(III)–superoxide (69, 70). Consequently, the intermediate that is produced by reaction 4 is considered to be a mixed ligand superoxo–$Co^{III}TSP$ complex in which O_2^- and SO_3^{2-} are bonded to the metal center at opposite axial coordination sites. Subsequently, this O_2 adduct reacts with an additional molecule of substrate to form the ternary activated complex $(SO_3)Co^{III}TSP(O_2^-)(SO_3)^{6-}$. The rate-limiting step of the reaction involves photoassisted electron transfer from SO_3^{2-} to the sulfito–cobalt–phthalocyanine–dioxygen system and hydrolysis of the bound SO_3 to yield SO_4^{2-} and a $Co^{II}TSP$–peroxide complex as shown in Figure 3. After protonation, O_2^{2-} is released to solution as hydrogen peroxide which either disproportionates to water and oxygen under the catalytic influence of $Co^{II}TSP$ (44, 45) or reacts directly with additional sulfite by means of a two-electron redox process (eq 8) (57). Hydrogen peroxide was detected at a steady-state concentration of $\leq 10^{-7}$ M as an intermediate reduction product of oxygen.

In the proposed mechanism, the active catalytic center is the complex $(SO_3)Co^{II}TSP^{4-}$. The catalytic cycle begins and ends with this species. The initial steps leading to the formation of $(SO_3)Co^{II}TSP^{4-}$ (reactions 2 and 3) are assumed to be in rapid equilibrium and are ignored in the preliminary development of a theoretical rate expression. In the catalytic cycle, there are three intermediates, $(SO_3)Co^{III}TSP(O_2^-)^{4-}$, $(SO_3)Co^{III}TSP(O_2^-)(SO_3)^{6-}$, and $(SO_3)Co^{III}TSP(O_2^{2-})^{6-}$. According to the method of King and Altman (65), $[(SO_3)Co^{II}TSP^{4-}]$, $[(SO_3)(Co^{III}TSP(O_2^-)^{4-}]$, $[(SO_3)Co^{III}TSP(O_2^-)(SO_3)^{6-}]$, and $[(SO_3)Co^{III}TSP(O_2^{2-})^{6-}]$ can be shown to be proportional to the sums of terms that are obtained from the reaction steps which either individually or sequentially lead to the formation of a particular species. Given these conditions, the concentrations of the various forms of the catalyst are expressed as follows:

$$[(SO_3)Co^{II}TSP^{4-}] \propto k_3 k_4 k_5 [SO_3^{2-}] + k_{-2}k_{-3}k_5 + k_{-2}k_4 k_5 \tag{9}$$

$$[(SO_3)Co^{III}TSP(O_2^-)^{4-}] \propto k_1 k_4 k_5 [O_2] + k_2 k_{-3}k_5[O_2] \tag{10}$$

$$[(SO_3)Co^{III}TSP(O_2^-)(SO_3)^{6-}] \propto k_2 k_3 k_5 [O_2][SO_3^{2-}] \tag{11}$$

$$[(SO)_3Co^{II}TSP(O_2^{2-})^{6-}] \propto k_2 k_3 k_4 [O_2][SO_3^{2-}] \tag{12}$$

where the proportionality constant for each equation is

$[(SO_3)Co^{II}TSP]^{1}_{total}$. The mass-balance condition for the total catalyst concentration is given by eq 13:

$$[(SO_3)Co^{II}TSP]_{total} = [(SO_3)Co^{II}TSP^{4-}] + [(SO_3)Co^{III}TSP(O_2^-)^{4-}] + [(SO_3)Co^{III}TSP(O_2^-)(SO_3)^{6-}] + [(SO_3)Co^{II}TSP(O_2^{2-})^{6-}] \tag{13}$$

From steady-state considerations

$$[(SO_3)Co^{III}TSP(O_2^-)(SO_3)^{6-}] = [k_2 k_3 k_5 [(SO_3)Co^{II}TSP]_{total}[O_2] \times [SO_3^{2-}]]/[k_5(k_{-2}k_{-3} + k_{-2}k_4) + k_2 k_5(k_{-3} + k_4)[O_2] + k_3 k_4 k_5 [SO_3^{2-}] + k_2 k_3(k_4 + k_5)[O_2][SO_3^{2-}]] \tag{14}$$

By use of this expression and the rate-limiting step of the reaction as defined by eq 6, the rate law for the production of sulfate can be written as

$$\nu = \frac{d[SO_4^{2-}]}{dt} = \frac{k'[(SO_3)Co^{II}TSP]_{total}[O_2][SO_3^{2-}]}{K_A + K_B[O_2] + K_C[SO_3^{2-}] + [O_2][SO_3^{2-}]} \tag{15}$$

where

$$k' = \frac{k_4 k_5}{k_4 + k_5}$$

$$K_A = \frac{k_5(k_{-2}k_{-3} + k_{-2}k_4)}{k_2 k_3(k_4 + k_5)}$$

$$K_B = \frac{k_5(k_{-3} + k_4)}{k_3(k_4 + k_5)}$$

and

$$K_C = \frac{k_4 k_5}{k_2(k_4 + k_5)}$$

Equation 15 can be modified to account for the rapid equilibria preceding the catalytic cycle involving (SO_3)-$Co^{II}TSP^{4-}$ as the reactive center. The concentration of the active center can be defined in terms of the dimer dissociation constant, K_d, and the formation constant, K_1, for the initial metal–sulfite complex:

$$K_d = \frac{[Co^{II}TSP^{2-}]^2}{[(Co^{II}TSP)_2^{4-}]} \tag{16}$$

$$K_1 = \frac{[(SO_3)Co^{II}TSP^{4-}]_{total}}{[Co^{II}TSP^{2-}][SO_3^{2-}]} \tag{17}$$

Equations 16 and 17 are combined to yield

$$[(SO_3)Co^{II}TSP^{4-}]_{total} = K_1 K_d^{1/2}[(Co^{II}TSP)_2^{4-}]^{1/2}[SO_3^{2-}] \tag{18}$$

when $[SO_3^{2-}]_0 \gg [(Co^{II}TSP)_2^{4-}]_0$. This condition allows the approximation that the concentration of SO_3^{2-} in solution remains relatively constant with respect to the amount of substrate bound in the complex $(SO_3)Co^{II}TSP^{4-}$ to become valid such that

$$[(SO_3)Co^{II}TSP^{4-}]_{total} = K'[(Co^{II}TSP)_2^{4-}]^{1/2} \tag{19}$$

where $K' = K_1 K_d^{1/2}[SO_3^{2-}]$ (i.e., K' is a conditional equilibrium constant). Substitution of eq 19 into eq 15 gives an approximate form of the final rate law:

$$\nu = \frac{k'K'[(Co^{II}TSP)_2^{4-}]^{1/2}[O_2][SO_3^{2-}]}{K_A + K_B[O_2] + K_C[SO_3^{2-}] + [O_2][SO_3^{2-}]} \tag{20}$$

The theoretical rate expression can be simplified for the pseudo-order experimental conditions used in the current study. When $[O_2]_0 \gg [SO_3^{2-}]_0$ and $[SO_3^{2-}]_0$ is sufficiently low such that $K_B[O_2] \gg K_A$ and $K_C[SO_3^{2-}]$, eq 20 is reduced to the form

$$\nu \simeq \frac{k'K'[(Co^{II}TSP)_2{}^{4-}]^{1/2}[SO_3^{2-}]}{K_B + [SO_3^{2-}]} \quad (21)$$

Two sets of limiting conditions for eq 21 can be considered. If $K_B \gg [SO_3^{2-}]$, then

$$\nu \simeq k'K_1K_d{}^{1/2}[(Co^{II}TSP)_2{}^{4-}]^{1/2}[SO_3^{2-}]^2/K_B \quad (22)$$

whereas if $[SO_3^{2-}] \gg K_B$, then

$$\nu \simeq k'K_1K_d{}^{1/2}[(Co^{II}TSP)_2{}^{4-}]^{1/2}[SO_3^{2-}] \quad (23)$$

Each limiting case can be compared with the experimentally determined rate laws for the autoxidation of S^{IV} at pH 6.7 and 9.2. According to eq 23, the rate of reaction is zero order in $[O_2]$ and approximately first order in $[SO_3^{2-}]$ which is in agreement with observation. Under neutral pH conditions, the catalytic reaction rate exhibited a fractional-order dependence of 0.3 on the concentration of total added catalyst. However, eq 23 predicts a half-order rate dependence on $[(Co^{II}TSP)_2{}^{4-}]$. Schelly and co-workers (67) have reported that phthalocyanine complexes of cobalt(II) and copper(II) tend to form higher order polymers in aqueous solution, especially at high ionic strength ($\mu > 0.01$ M). Consideration of the equilibria between aggregate species and $Co^{II}TSP^{2-}$ in the derivation of the theoretical rate law would further reduce the apparent kinetic order in catalyst concentration. Evaluation of k_{obsd} as a function of $[Co^{II}TSP]$ for reactions conducted in the presence of EDTA yielded a reaction order of approximately 0.5. Since the dimer and polymers of $Co^{II}TSP$ are the dominant catalyst species in water at pH 6.7, a nonintegral rate dependence on phthalocyanine is consistent with the conclusion that the monomer is the active form. Nonintegral reaction orders arise frequently in polar reactions when the principal reactive species is formed through the dissociation of a polymer (54). At pH 9.2, a first-order dependence in catalyst concentration is observed. This result would be consistent with the postulated kinetic formulation if $(Co^{II}TSP)_2{}^{4-}$ is no longer the dominant species in solution. Cookson et al. (70) obtained ESR spectra that were indicative of a shift in the monomer/dimer equilibrium toward the monomer as pH increased from 7 to 10. In this case eq 2 can be neglected, and the theoretical rate expression would show a first-order dependence on total catalyst concentration.

Equation 20 can be simplified in a similar fashion for the case in which the oxidation of sulfite proceeds under pseudo-order concentration conditions in oxidant. When $[SO_3^{2-}]_0 \gg [O_2]_0$ and $K_C[SO_3^{2-}] \gg K_A$ and K_B, the approximate rate equation

$$\nu \simeq \frac{k'K'[(Co^{II}TSP)_2{}^{4-}]^{1/2}[O_2]}{K_C + [O_2]} \quad (24)$$

can be expressed in the simplified form

$$\nu \simeq k'K_1K_d{}^{1/2}[(Co^{II}TSP)_2{}^{4-}]^{1/2}[O_2][SO_3^{2-}]/K_C \quad (25)$$

if the value of $K_C \gg [O_2]$. For the opposite extreme, i.e., $[O_2] \gg K_C$, eq 24 will be reduced to yield eq 23. The limiting rate law given in eq 25 is consistent with the apparent first-order $[O_2]$ dependence observed in reactions carried out in the presence of excess S^{IV}.

A variant of the proposed mechanism occurs when sulfite ion reacts with the SO_3-bound cobalt(II)–dioxygen adduct without the formation of a ternary activated complex of sufficiently long life to be kinetically significant. This type of reaction pathway was originally suggested by Theorell and Chance (72). The resulting form of the theoretical rate expression is identical with eq 15, except that K_A, K_B, and K_C are specified by different combinations of individual rate constants:

$$K_A = \frac{k_{-2}k_4k_5}{k_2k_3(k_4 + k_5)}$$

$$K_B = \frac{k_4k_5}{k_3(k_4 + k_5)}$$

$$K_C = \frac{k_4k_5}{k_2(k_4 + k_5)}$$

in accordance with the assumption that $k_4 \gg k_{-3}$. Support for this mechanistic scheme was obtained through an assessment of the influence of ionic strength on the rate of sulfite autoxidation. If $k_4 \gg k_{-3}$, then the rate-determining step would be defined by reaction 5 in which two negatively charged ions, SO_3^{2-} and $(SO_3)Co^{III}TSP(O_2^-)^{4-}$, combine to form an intermediate complex bearing an overall negative charge. The primary salt effect predicts that a reaction between ions of similar charge would proceed at a faster rate upon an increase in the ionic strength of the solvent medium (54). Even though the experimental conditions ($\mu > 0.1$ M) exceed the upper boundary for strict applicability of the Debye–Hückel theory ($\mu = 0.01$ M), a positive slope was observed for plots of $\log k_{obsd}$ vs. $\mu^{1/2}$ at pH 6.7 ($m = 0.425$, $b = -3.42$, and $R^2 = 0.9972$) and pH 9.2 ($m = 1.47$, $b = -3.54$, and $R^2 = 0.9973$). In general, the reaction rate increases with increasing values of μ. Hoffmann and Lim (47) reported a positive ionic strength effect for the $Co^{II}TSP$-catalyzed autoxidation of HS^- in aqueous solution.

In order to verify the applicability of eq 20, the experimental data were analyzed in terms of double-reciprocal plots of $1/\nu_0$ vs. $1/[SO_3^{2-}]_0$ where ν_0 and $[SO_3^{2-}]_0$ are the initial reaction rate and initial substrate concentrations (69). Rearrangement of eq 20 yields

$1/\nu_0 =$
$$[1 + K_A/([O_2][SO_3^{2-}]) + K_B/[SO_3^{2-}] + K_C/[O_2]]/V_0 \quad (26)$$

where $V_0 = k'K'[(Co^{II}TSP)_2{}^{4-}]^{1/2}$. A plot of $1/\nu_0$ vs. $1/[SO_3^{2-}]_0$ at constant $[O_2]$ should be linear with a slope of

$$(K_A/[O_2] + K_B)/V_0 \quad (27)$$

and an intercept on the $1/\nu_0$ axis of

$$(1 + K_C/[O_2])/V_0 \quad (28)$$

Shown in Figure 5 are the double-reciprocal plots for pH 6.7 and 9.2. Linearity of these functions is consistent with the proposed bisubstrate ternary complex mechanism.

Direct spectrophotometric evidence for complexation of SO_3^{2-} and dioxygen by cobalt(II)–phthalocyanine as a prelude to electron transfer was obtained as shown in Figure 4. The absorption spectrum of $Co^{II}TSP$ (denoted by the solid line) in the 600–700-nm wavelength range has two characteristic bands which are attributed to an equilibrium mixture of the dimeric complex (λ_{max} 636 nm) and a combination of an oxygen-free monomer and a $Co^{III}TSP(O_2^-)$ adduct (λ_{max} 670 nm) (66, 67, 73, 74). Addition of sulfite caused a rapid increase in A_{670} in proportion to a decrease in absorbance at 636 nm. This change corresponds to a shift in the equilibrium speciation of the catalyst due to the formation of intermediates such
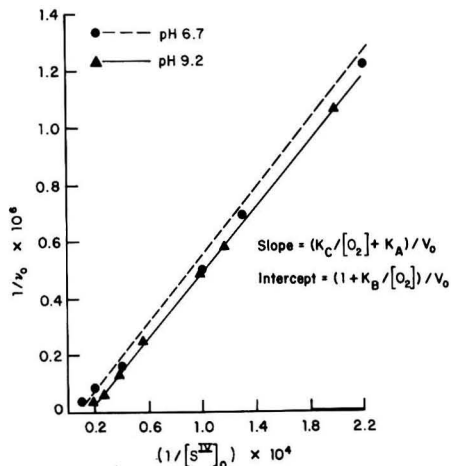
Figure 5. Lineweaver–Burk plots for the rate of the catalytic autoxidation of sulfite as a function of $[S^{IV}]_0$. $[S^{IV}]_0 = 2.5 \times 10^{-5}$–$1 \times 10^{-3}$ M, $[O_2]_0 = 2.5 \times 10^{-4}$ M, and $[Co^{II}TSP]_0 = 1 \times 10^{-6}$ M; $\mu = 0.4$ M, $T = 25 \pm 0.1$ °C.

as $(SO_3)Co^{II}TSP^{4-}$, $(SO_3)Co^{III}TSP(O_2^{-}\cdot)^{4-}$, and (SO_3)-$Co^{III}TSP(O_2^{-}\cdot)(SO_3)^{6-}$. Preliminary stopped-flow experiments have shown that the equilibrium between $Co^{II}TSP^{2-}$ and $(SO_3)Co^{II}TSP^{4-}$ is attained rapidly (in the absence of O_2) in comparison to the rate of conversion of S^{IV} to sulfate. The value of A_{670} decreases with time as the oxidation of sulfite proceeds. At the conclusion of the reaction, the absorbance at 670 nm is approximately equivalent to the initial intensity of the 636-nm peak. Subsequent introduction of substrate results in the reemergence and decline in the 670-nm absorption maximum as a second catalytic cycle unfolds. In subsequent reactions the oscillation in peak height at 670 nm is repeated. These data confirm that $Co^{II}TSP$ participates in a closed-sequence catalytic cycle. There appears to be only a minor loss in catalytic activity upon successive additions of substrate as indicated by a net 25% decrease in k_{obsd} after five consecutive catalytic runs.

Results obtained from a series of experiments in which strong complexing reagents such as EDTA and cyanide were added to reaction solutions containing $Co^{II}TSP$ lend further support to the hypothesis that inner-sphere coordination of sulfite and molecular oxygen to cobalt(II) plays an important role in the catalytic autoxidation of S^{IV}. Addition of EDTA and CN^- reduced significantly the measured values of k_{obsd} at pH 9.2 as shown in Table III. The inhibitory effect of EDTA on reactions conducted under neutral pH conditions seems to be associated primarily with the complexation of background levels of trace-metal contaminants. For example, the half-life for the "uncatalyzed" oxidation of sulfite increased from 333 min to approximately 60 h upon the introduction of EDTA at 10^{-5} M. Cyanide did not inhibit the reaction of sulfur(IV) with O_2 at pH 6.7 because it exists almost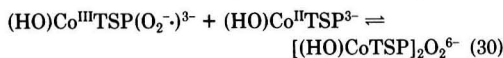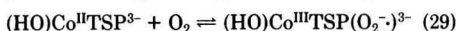 entirely as HCN ($pK_a = 9.2$) which is a much weaker ligand than CN^- for the binding of transition-metal ions (55).

Under strongly alkaline conditions (pH $\geq$12), $Co^{II}TSP$ undergoes reversible oxygenation as shown in eq 29 and 30 to produce a dioxygen-bridged dicobalt complex which

$$(HO)Co^{II}TSP^{3-} + O_2 \rightleftharpoons (HO)Co^{III}TSP(O_2^{-}\cdot)^{3-} \quad (29)$$

$$(HO)Co^{III}TSP(O_2^{-}\cdot)^{3-} + (HO)Co^{II}TSP^{3-} \rightleftharpoons$$
$$[(HO)CoTSP]_2O_2^{6-} \quad (30)$$

Table III. Effect of Inhibitors on $k_{obsd}{}^a$

[inhibitor] $\times 10^6$, M	k_{obsd} (s^{-1}) $\times 10^3$ at	
	pH 6.7	pH 9.2
none, 0	1.62	1.83
EDTA, 1	1.52	
EDTA, 2.5	1.45	
EDTA, 5.0	0.94	
EDTA, 10.0	0.78	0.33
mannitol, 10.0	1.25	0.85
NaCN, 10.0	1.61	0.29

^{a} $[S^{IV}]_0 = 1 \times 10^{-4}$ M, $[O_2]_0 = 1.2 \times 10^{-3}$ M, and $[Co^{II}TSP]_0 = 1 \times 10^{-6}$ M; $\mu = 0.4$ M, $T = 25 \pm 1$ °C.

may also exhibit catalytic properties for the autoxidation of S^{IV}. The μ-superoxo dimer of $Co^{II}TSP$ may participate in either a one-electron-transfer or two-electron-transfer redox process as proposed by Davies et al. (7) for $(NH_3)_5Co^{III}-O_2^{-}-Co^{II}(NH_3)_5{}^{5+}$ and by Yatsimirskii et al. (75) for $(L$-histidine$)_2Co^{III}-O_2^{-}-Co^{II}(L$-histidine$)_2$. According to this hypothesis, the active catalytic center $[(HO)CoTSP]_2O_2^{6-}$ reacts with sulfite in one of the following ways as shown in either Scheme I or Scheme II.

Scheme I

$$[(HO)CoTSP]_2O_2^{6-} + SO_3^{2-} \xrightarrow{\text{slow}}$$
$$SO_4^{2-} + (HO)Co^{III}TSP^{3-} + (HO)Co^{IV}TSP(O^{2-})^{3-} \quad (31)$$

$$(HO)Co^{IV}TSP(O^{2-})^{3-} + SO_3^{2-} \rightarrow$$
$$SO_4^{2-} + (HO)Co^{II}TSP^{3-} \quad (32)$$

Scheme II

$$[(HO)CoTSP]_2O_2^{6-} + SO_3^{2-} \xrightarrow{\text{slow}}$$
$$SO_3^{-}\cdot + (HO)Co^{III}TSP-O_2^{-}-Co^{II}TSP(OH)^{7-} \quad (33)$$

$$(HO)Co^{III}TSP-O_2^{-}-Co^{II}TSP(OH)^{7-} + SO_3^{-}\cdot \rightarrow$$
$$SO_3 + (HO)Co^{II}TSP(O_2^{2-})^{5-} + (HO)Co^{II}TSP^{3-} \quad (34)$$

$$SO_3 + H_2O \rightarrow SO_4^{2-} + 2H^+ \quad (35)$$

$$(HO)Co^{II}TSP(O_2^{2-})^{5-} + 2H^+ \rightarrow (HO)Co^{II}TSP^{3-} + H_2O_2 \quad (36)$$
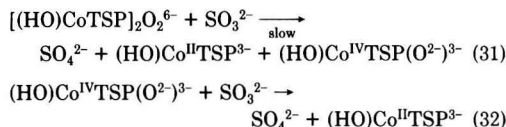
In Scheme I, production of sulfate through an O–O bond cleavage would be hindered by formation of a highly unstable cobalt(IV) oxide intermediate (76). While the second pathway is chemically viable, it seems to be less consistent with the reported kinetic data than is the proposed bisubstrate complexation pathway. For example, Scheme II predicts a second-order reaction rate dependence on the concentration of the $Co^{II}TSP$ monomer. This condition was not observed in the present study.

The relative efficiency of $Co^{II}TSP$, $Fe^{II}TSP$, and $Mn^{II}TSP$ as homogeneous catalysts for the autoxidation of SO_3^{2-} appears to be directly related to the stability of the corresponding 1:1 metal–dioxygen adduct of each complex in aqueous solution. In organic as well as water-based solvent systems, macrocyclic complexes of iron(II) and manganese(II) react with O_2 to yield oxygen-bridged dinuclear species of the general form $M^{III}-O_2^{2-}-M^{III}$ (59). These products then decompose irreversibly to μ-oxo dimers as shown in eq 37 and 38. In

$$M^{III}-O_2^{2-}-M^{III} \rightarrow 2M^{IV}(O^{2-}) \quad (37)$$

$$M^{IV}(O^{2-}) + M^{II} \rightarrow M^{III}-O-M^{III} \quad (38)$$

contrast, the oxygenation of most cobalt(II) complexes is reversible under a majority of reaction conditions. Ochiai (76) has attributed this contrasting behavior to the rela-
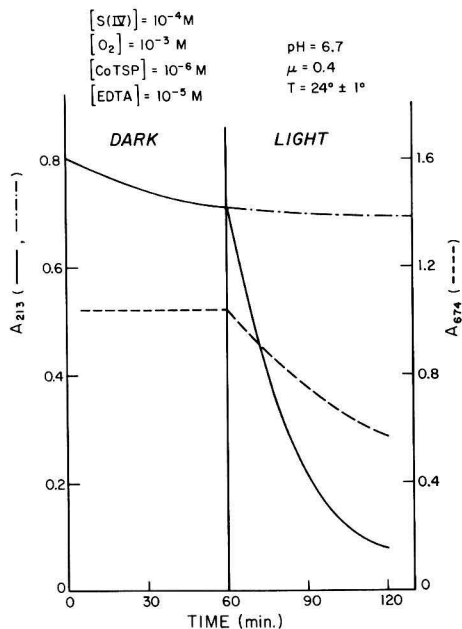
Figure 6. Effect of fluorescent room light on the catalytic autoxidation of sulfite. $[S^{IV}]_0 = 1 \times 10^{-4}$ M, $[O_2]_0 = 1.2 \times 10^{-3}$ M, and $[Co^{II}TSP]_0 = 1 \times 10^{-6}$ M, pH 6.7; $\mu = 0.4$ M, $T = 25 \pm 1$ °C.
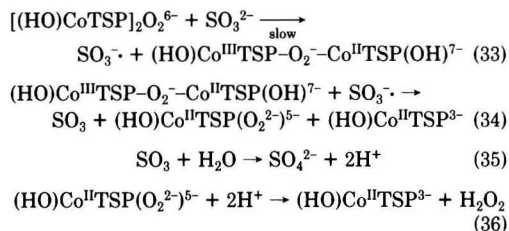
tively high stability of the $Fe^{IV}-$ and $Mn^{IV}-$oxides in comparison to $Co^{IV}(O^{2-})$. Both $Fe^{II}TSP$ and $Mn^{II}TSP$ have been shown to undergo irreversible oxidation upon dissolution in water at neutral or alkaline pH (56).

Photoassisted Catalysis. A noteworthy result of the current investigation involves the apparent photochemical reactivity of $Co^{II}TSP$ (Figure 6). Since a wide variety of transition metal–phthalocyanine complexes and structurally related metalloporphyrins are known to function as photosensitizers for the production of singlet oxygen ($^1O_2$) and/or superoxide ($O_2^-\cdot$), catalysis of the autoxidation of S^{IV} by $Co^{II}TSP$ may be light dependent (77, 78). To test this hypothesis, a series of experiments was conducted in the presence and absence of conventional fluorescent room light. It should be noted that the kinetic measurements discussed in previous sections of this paper were obtained from reactions that occurred under background illumination. In the dark, the oxidation of SO_3^{2-} proceeded very slowly following rapid formation of the $Co^{II}TSP-$dioxygen complex as shown in Figure 6. However, the decline in the concentration of sulfite and the ternary intermediate was accelerated significantly upon exposure of the reaction solution to light. Addition of specific inhibitors for superoxide ion (superoxide dismutase) (79) and singlet molecular oxygen (1,4-diazabicyclo[2.2.2]octane) (80) did not have any perceptible effect on the rate of reaction. Reactions catalyzed by $Fe^{II}TSP$, $Mn^{II}TSP$, $Ni^{II}TSP$, $Cu^{II}TSP$, and $V^{IV}TSP$ were insensitive to irradiation.

Beelen and co-workers (81) observed that irradiation with visible light in the 600–700-nm wavelength range enhanced the catalytic activity of $Co^{II}TSP$ for the aqueous-phase autoxidation of 2-mercaptoethanol. These authors suggested that the increased rate of disulfide formation resulted from a light-induced shift in the $Co^{II}TSP$ dimer dissociation equilibrium (eq 2) in favor of the catalytically reactive monomer. In an earlier study, Ferraudi

and Srisankar (82) demonstrated that $(Co^{II}TSP)_2^{4-}$ undergoes photochemical dissociation to form metastable $Co^{I}-$ and $Co^{III}-TSP$ ligand radical species upon ultraviolet photolysis under anoxic conditions. However, photochemical redox activity did not occur at excitation energies of less than 105 kcal/mol (i.e., $\lambda > 260$ nm).

An alternative explanation for the observed photocatalytic effect on the autoxidation of sulfite may involve the absorption of light by the ternary intermediate $(SO_3)Co^{II}TSP$ $(O_2^-\cdot)(SO_3)^{6-}$ to form a cobalt(II)–singlet oxygen complex, $(SO_3)Co^{II}TSP(^1O_2)(SO_3)^{6-}$, in the excited state. This species would possess more favorable spin-state symmetry for two-electron transfer during the rate-limiting step (reaction 6). The electronic spectra of numerous μ-superoxo–dicobalt complexes have been shown to contain O_2 $(\pi_\nu^*) \rightarrow Co^{II}(d\sigma^*)$ ligand-to-metal charge-transfer transitions (log $\epsilon \simeq 3.3$–3.5) in the visible wavelength region at 300–400 nm (83). Electron transfer from SO_3^{2-} to the $Co^{II}TSP-$dioxygen system would be enhanced further by the potential delocalization of excess electron density from the metal center to the conjugated π-orbital system of the phthalocyanine ligand. Many porphyrin complexes of cobalt(II) undergo intramolecular redox transformations in solution (84). Further details concerning photoassisted catalysis by $Co^{II}TSP$ will be presented in a subsequent communication.

Conclusion

The heterolytic mechanism summarized in Figure 5 and eq 2–8 appears to explain the kinetic and spectral data for a broad range of experimental conditions. The simplified kinetic expressions of eq 22, 23, and 25 account for both the apparent shift in the reaction order of sulfite to values of greater than one as reported by some investigators and the observed zero-order rate dependence on $[O_2]$. The current results do not necessarily preclude a homolytic pathway; but if free-radical intermediates were significantly involved in the oxidation of S^{IV}, than a considerable yield of dithionate should be formed as a chain termination product. Since $S_2O_6^{2-}$ was not detected and sulfate was the only observed product, the contribution of a free-radical chain process to the overall reaction seems unlikely. Furthermore, the addition of free-radical scavengers such as mannitol did not inhibit the autoxidation of sulfite in the presence of $Co^{II}TSP$.

Summary

Cobalt(II)–4,4′,4″,4‴-tetrasulfophthalocyanine is an effective homogeneous catalyst for the quantitative conversion of sulfur(IV) to sulfate in aqueous solution. Addition of $Co^{II}TSP^{2-}$ at concentrations of 10^{-8}–10^{-6} M can result in dramatic increases in the rate of autoxidation. Other water-soluble phthalocyanine complexes are less effective.

The catalytic properties of $Co^{II}TSP$, $Fe^{II}TSP$, $Mn^{II}TSP$, $Ni^{II}TSP$, $Cu^{II}TSP$, and $V^{IV}TSP$ have been determined, and differences in activity have been evaluated in terms of the relative capacity of the square-planar complexes to reversibly bind molecular oxygen. The kinetics of the autoxidation of SO_3^{2-} in the presence of $Co^{II}TSP^{2-}$ have been interpreted in terms of a bisubstrate Michaelis–Menten rate expression. The empirical rate law and spectral data indicate that the reaction proceeds through the formation of an activated complex in which two sulfite ions and O_2 are reversibly bonded to $Co^{II}TSP^{2-}$, followed by hydrolysis under the influence of light to yield SO_4^{2-} and hydrogen peroxide. The pH dependence of the reaction rate has been attributed to the acid dissociation of HSO_3^- and the

deprotonation of a coordinated water molecule at high pH.

Literature Cited

(1) Aubuchon, C. Ph.D. Thesis, Johns Hopkins University, Baltimore, MD, 1976.
(2) Barron, C. H.; O'Hern, H. A. *Chem. Eng. Sci.* **1966**, *21*, 397–404.
(3) Bengtsson, S.; Bjerle, I. *Chem. Eng. Sci.* **1975**, *30*, 1429–1435.
(4) Brimblecombe, P.; Spedding, D. J. *Atmos. Environ.* **1974**, *8*, 937–345.
(5) Chen, I. H.; Barron, C. H. *Ind. Eng. Chem. Fundam.* **1972**, *11*, 466–470.
(6) Coughanowr, D. R.; Krause, F. E. *Ind. Eng. Chem. Fundam.* **1965**, *48* 61–66.
(7) Davies, R.; Hagopian, A. K. E.; Sykes, A. G. *J. Chem. Soc. A* **1969**, 623–629.
(8) Freiberg, J. *Environ. Sci. Technol.* **1974**, *8*, 731–734.
(9) Fuller, E. C.; Crist, R. H. *J. Am. Chem. Soc.* **1941**, *63*, 1644–1650.
(10) Fuzzi, S. *Atmos. Environ.* **1978**, *12*, 1439–1442.
(11) Ibusuki, T. *Atmos. Environ.*, in press.
(12) Kaplan, D. J.; Himmelblau, D. M.; Kanaoka, C. *Atmos. Environ.* **1981**, *15*, 763–773.
(13) Linek, V.; Mayrhoferova, J. *Chem. Eng. Sci.* **1970**, *25*, 787–800.
(14) Lunak, S.; El-Wakil, A.; Veprek-Siska, J. *Collect. Czech. Chem. Commun.* **1978**, *43*, 3306–3316.
(15) Martin, L. R. In "Acid Precipitation: SO$_2$, NO, NO$_2$ Oxidation Mechanisms: Atmospheric Considerations"; Calvert, J. G., Ed.; Ann Arbor Science Publishers: Ann Arbor, MI, 1982, in press.
(16) Matteson, J. J.; Stöber, W.; Luther, H. *Ind. Eng. Chem. Fundam.* **1969**, *8*, 677–684.
(17) Mishra, G. C.; Srivastava, R. D. *Chem. Eng. Sci.* **1975**, *30*, 1387–1390.
(18) Mishra, G. C.; Srivastava, R. D. *Chem. Eng. Sci.* **1976**, *31*, 969–971.
(19) Sawicki, J. E.; Barron, C. H. *Chem. Eng. J* **1973**, *5*, 153–159.
(20) Yagi, S.; Inoue, H. *Chem. Eng. Sci.* **1962**, *17*, 411–421.
(21) Hegg, D. A.; Hobbs, P. V. *Atmos. Environ.* **1978**, *12*, 241–253.
(22) Hoffmann, M. R.; Boyce, S. D. *Adv. Environ. Sci. Technol.* **1983**, *12*, 147–189.
(23) Hoffman, M. R. *Environ. Sci. Technol.* **1980**, *14*, 1061–1066.
(24) Beilke, S.; Gravenhorst, G. *Atmos. Environ.* **1978**, *12*, 231–239.
(25) Larson, T. V.; Horike, N. R.; Halstead, H. *Atmos. Environ.* **1978**, *12*, 1597–1611.
(26) Meyer, B. "Sulfur, Energy and the Environment"; Elsevier: Amsterdam, The Netherlands, 1977.
(27) Nriagu, J. O. Ed. "Sulfur in the Environment"; Wiley-Interscience: New York, 1978.
(28) Hoffmann, M. R.; Jacob, D. J. In "SO$_2$, NO, NO$_2$ Oxidation Mechanisms: Atmospheric Considerations"; Calvert, J. G., Ed.; Ann Arbor Science Publishers: Ann Arbor, MI, 1983, in press.
(29) Backström, H. *Z. Phys. Chem., Abt. B* **1934**, *25B*, 122–138.
(30) Bassett, H.; Parker, W. G. *J. Chem. Soc.* **1951**, 1540–1560.
(31) Hayon, E.; Treinin, A.; Wilf, J. *J. Am. Chem. Soc.* **1972**, *94*, 47–57.
(32) Lunak, S.; Veprek-Siska, J. *Collect. Czech. Chem. Commun.* **1976**, *41*, 3495–3503.
(33) Lunak, S.; Veprek-Siska, J. *J. React. Kinet. Catal. Lett.* **1976**, *5*, 157–161.
(34) Veprek-Siska, J.; Lunak, S.; El-Wakil, A. *Z. Naturforsch. B: Anorg. Chem., Org. Chem.* **1974**, *29B*, 812–813.
(35) Dolansky, J.; Wagnerova, D. M.; Veprek-Siska, J. *Collect. Czech. Chem. Commun.* **1976**, *41*, 2326–2332.
(36) Kundo, N. N.; Keier, N. P. *Russ. J. Phys. Chem., (Engl. Transl.)* **1968**, *42*, 707–711.
(37) Wagnerova, D. M.; Schwertnerova, E.; Veprek-Siska, J. *Collect. Czech. Chem. Commun.* **1973**, *38*, 756–768.
(38) Wagnerova, D. M.; Schwertnerova, E.; Veprek-Siska, J. *Collect. Czech. Chem. Commun.* **1974**, *39*, 3036–3047.
(39) Cook, A. H. *J. Chem. Soc.* **1938**, 1761–1768.
(40) Cook, A. H. *J. Chem. Soc.* **1938**, 1768–1774.
(41) Dufour, M. N.; Crumbliss, A. L.; Johnston, G.; Gaudemer, A. *J. Mol. Catal.* **1980**, *7*, 277–287.
(42) Dufour-Ricroch, M. N.; Gaudemer, A. *Tetrahedron Lett.* **1976**, 4079–4082.
(43) Uchida, K.; Soma, M.; Naito, S.; Oriski, T.; Tamaru, K. *Chem. Lett.* **1978**, 471–474.
(44) Waldmeier, P.; Prijs, B.; Sigel, H. *Z. Naturforsch., B: Anorg. Chem., Org. Chem., Biochem., Biophys., Biol.* **1972**, *27B*, 95–100.
(45) Waldmeier, P.; Sigel, H. *Inorg. Chim. Acta* **1971**, *5*, 659–666.
(46) Hajibrahim, S. K.; Tibbetts, P. J. C.; Watts, C. D.; Maxwell, J. R.; Eglington, C.; Colin, H.; Guiochon, G. *Anal. Chem.* **1978**, *50*, 549–553.
(47) Hoffmann, M. R.; Lim, B. C. *Environ. Sci. Technol.* **1979**, *13*, 1406–1413.
(48) Weber, J. H.; Busch, D. H. *Inorg. Chem.* **1965**, *48* 469–471.
(49) Huss, A., Jr.; Lim, P. K. Eckert, C. A. *J. Am. Chem. Soc.* **1978**, *100*, 6252–6253.
(50) "Standard Methods for the Examination of Water and Wastewater", 15th ed.; American Public Health Association: Washington, DC, 1981; pp 439–440.
(51) Perschke, H.; Broda, E. *Nature (London)* **1961**, *190*, 257–258.
(52) Higginson, W. C. E.; Marshall, J. W. *J. Chem. Soc.* **1957**, 447–458.
(53) Mancy, K. H.; Westgarth, W. C. *J. Water Pollut. Control Fed.* **1962**, *34*, 1037–1051.
(54) Frost, A. A.; Pearson, R. G. "Kinetics and Mechanism", 2nd ed.; Wiley-Interscience: New York, 1961.
(55) Smith, R. M.; Martell, A. E. "Critical Stability Constants Inorganic Complexes"; Plenum Press: New York, 1976; Vol. 4.
(56) Boucher, L. J. In "Coordination Chemistry of Macrocyclic Compounds"; Melson, G. A. Ed.; Plenum Press: New York, 1979; pp 461–516.
(57) Hoffmann, M. R.; Edwards, J. O. *J. Phys. Chem.* **1975**, *79*, 2096–2098.
(58) Collman, J. P.; Halpert, T. R.; Suslick, K. S. In "Metal Ion Activation of Dioxygen"; Spiro, T. G., Ed.; Wiley-Interscience: New York, 1980; pp 1–72.
(59) Jones, R. D.; Sommerivlle, D. A.; Basolo, F. *Chem. Rev.* **1979**, *79*, 139–179.
(60) Kropf, H.; Hoffmann, Hd. *Tetrahedron Lett.* **1967**, 659–663.
(61) Kropf, H.; Knaack, K. *Tetrahedron* **1972**, *28*, 1143–1151.
(62) Kothari, V. M.; Tazuma, J. J. *J. Catal.* **1976**, *41*, 180–189.
(63) Mahler, H. R.; Cordes, E. H. "Biological Chemistry"; Harper and Row: New York, 1966.
(64) Laidler, K. J.; Bunting, S. J. "The Chemical Kinetics of Enzyme Action"; Clarendon Press: Oxford, England, 1973.
(65) King, E. L.; Altman, C. *J. Phys. Chem.* **1956**, *60*, 1375–1378.
(66) Gruen, L. C.; Blagrove, R. J. *Aust. J. Chem.* **1973**, *26*, 319–323.
(67) Schelly, Z. A.; Farina, R. D.; Eyring, E. M. *J. Phys. Chem.* **1970**, *74*, 617–620.
(68) Carter, M. J.; Rillema, D. P.; Basolo, F. *J. Am. Chem. Soc.* **1974**, *96*, 392–400.
(69) Rollmann, L. D.; Chan, S. I. *Inorg. Chem.* **1971**, *10*, 1978–1982.
(70) Cookson, D. J.; Smith, T. D.; Boas, J. F.; Hicks, P. R.; Pilbrow, J. R. *J. Chem. Soc.* **1977**, 109–114.
(71) Przywarska-Boniecka, H.; Fried, K. *Pol. J. Chem.* **1976**, *50*, 43–52.
(72) Theorell, H.; Chance, B. *Acta Chem. Scand.* **1951**, *5*, 1127–1144.
(73) Bernauer, K.; Fallab, S. *Helv. Chim. Acta* **1961**, *44*, 1287–1292.
(74) Wagnerova, D. M.; Schwertnerova, E.; Veprek-Siska, J. *Collect. Czech. Chem. Commun.* **1974**, *39*, 1980–1988.
(75) Yatsimirskii, K. B.; Bratushko, I. Y.; Zatsny, I. L. *Zh. Neorg. Khim.* **1977**, *22*, 1611–1666.

(76) Ochiai, E. *Inorg. Nucl. Chem. Lett.* **1974**, *10*, 453–457.
(77) Cox, G. S.; Whitten, D. G.; Gianotti, G. *Chem. Phys. Lett.* **1979**, *67*, 511–515.
(78) Harbour, J. R.; Hair, M. L. *Photochem. Photobiol.* **1978**, *28*, 721–727.
(79) McCord J. M.; Fridovich, I. *J. Biol. Chem.* **1969**, *244*, 6056–6063.
(80) Wasserman, H. H.; Murray, R. W.; Eds. "Singlet Oxygen"; Academic Press: New York, 1979.
(81) Beelen, T. P. M.; de Costa Gomez, C. O.; Kuijer, M. *Recl. Trav. Chim. Pays-Bas* **1979**, *98*, 521–522.

(82) Ferraudi, G.; Srisanskar, E. V. *Inorg. Chem.* **1978**, *17*, 3164–3168.
(83) Lever, A. B. P.; Gray, H. B. *Acc. Chem. Res.* **1978**, *11*, 348–355.
(84) Berezin, B. D. "Coordination Compounds of Porphyrins and Phthalocyanines"; Wiley-Interscience: New York, 1981.

Mesocosm Experiments To Determine the Fate and Persistence of Volatile Organic Compounds in Coastal Seawater[†]

Stuart G. Wakeham,* **Alan C. Davis, and Jennifer L. Karas**

Chemistry Department, Woods Hole Oceanographic Institution, Woods Hole, Massachusetts 02543

■ Studies were carried out in experimental marine ecosystems to determine the fate and persistence of a series of volatile organic compounds in coastal seawater. A suite of aliphatic hydrocarbons, aromatic hydrocarbons, chlorinated C_2-hydrocarbons, and chlorinated aromatic hydrocarbons, covering a wide range of water solubilities, volatilities, and susceptibilities to biological degradation, was added to the water column of the mesocosms at concentrations typical of a moderately polluted estuary (0.2–4 $\mu g/L$). Concentrations in the water column were followed for up to 2 months, under experimental conditions simulating winter, spring, and summer. Water column half-lives of the same compounds ranged from ~1 day to up to 4 weeks, depending on season and compound class. Volatilization appears to be the major process removing aromatic hydrocarbons, chlorinated C_2-hydrocarbons, and chlorinated aromatic hydrocarbons during all seasons, with biodegradation also important for aromatic hydrocarbons in summer. Aliphatic hydrocarbons are quickly sorbed onto particulate matter and thus removed from the "volatile" pool; biodegradation also affects the alkanes.

Introduction

Several recent studies have characterized the spatial and temporal distributions of volatile organic compounds (VOCs) in coastal and open ocean waters (*1–9*). Field studies are important in unravelling the complex interaction of several processes, including evaporation, microbial degradation, photochemical degradation, and sorption onto particulate matter, which control VOC distributions in seawater. On the other hand, laboratory studies (e.g., ref *10–15*) provide a high degree of control over one or two processes that then can be studied in detail, but extrapolating laboratory results to the natural environment is difficult. One partial solution to this problem is to conduct scaled-up experiments in controlled ecosystems (microcosms or mesocosms depending on relative size) with the hope that the experimental ecosystem reasonably mimics the environment being simulated. One such system is the Marine Ecosystems Research Laboratory (MERL) (*16, 17*), located on Narragansett Bay, RI. MERL mesocosms have been successfully used to study the fate of petroleum hydrocarbons (*18–21*), polycyclic aromatic hydrocarbons (*22, 23*), trace metals (*24, 25*), and natural radionuclides (*26*).

Our approach to studying VOC in the coastal marine environment combines field measurements with mesocosm

experiments. Distributions and postulated fates of VOC in Narragansett Bay have been described in detail elsewhere (*6, 27*). On the basis of Bay data, we conducted a series of experiments in MERL mesocosms to evaluate better the fates and persistence of VOC in the estuary. In this paper we present results obtained from experiments under varied experimental conditions over a period of 2 years.

Methods

Volatile organic compound experiments were performed in MERL mesocosms (*16, 17*), each a 5.5 m high and 1.8 m diameter Fiberglass tank containing 13 m^3 of Narragansett Bay seawater and associated planktonic and microbial communities. Tanks were mixed four times a day for 2 h to simulate tidal currents and the turbulence regime in the bay; thus, the tanks did not stratify. Experiments were run in a batch mode, that is, without seawater flow-through as is normally used in MERL experiments and without the usual 30-cm sediment bed. Water levels were 10–15 cm below the top of the tank wall. Four VOC experiments comprised this investigation: (1) Mar 15 to June 18, 1980, with water column temperatures ranging between 8 and 16 °C to simulate "spring" conditions; (2) Aug 19 to Sept 8, 1980, 20–22 °C as "summer"; (3) Mar 4 to May 4, 1982, 3–7 °C, as "winter"; (4) Sept 9–15 1980, 22 °C, in which the water column of one of a pair of mesocosms was poisoned with $HgCl_2$ (2 mg/L) to retard biological activity. Tanks were filled with fresh Narragansett Bay seawater prior to initiating each experiment.

A mixture of VOC covering a range of compound classes (Tables I and II) was spiked into the water column of the mesocosm by mixing 10–15 mL of an acetone solution of the compounds into 2 L of seawater and then adding this seawater via Teflon tubing to about middepth in the tank during mixing. The tank mixer was operated for several hours after spiking to ensure uniform dispersal of the VOC throughout the water column before sampling was begun. Initial VOC concentrations ranged from 0.2 to 4 $\mu g/L$ (Tables I and II) and were comparable to levels measured in moderately polluted upper Narragansett Bay (*6, 27*). For two experiments (spring and winter) difluorodichloromethane (Freon 12) was also added to the water column as a gas-exchange tracer (see ref *28* for details of the Freon spiking and analysis). In the first two experiments, four C_2-benzene, eight C_3-benzene, three dichlorobenzene, and three trichlorobenzene isomers were included; subsequent experiments used only the isomers given in

---

[†] Woods Hole Oceanographic Institution Contribution No. 5309.

Table I. Experimental Results for VOC Experiments

	spring, Apr 15–June 18, 1980, 8–16 °C			summer, Aug 19–Sept 8, 1980, 20–22 °C			winter, Mar 4–May 4, 1982, 3–7 °C		
compound	C_0,[a] μg/L	λ,[b] days^{-1}	$t_{1/2}$,[b] days	C_0,[a] μg/L	λ,[b] days^{-1}	$t_{1/2}$,[b] days	C_0,[a] μg/L	λ,[b] days^{-1}	$t_{1/2}$,[b] days
benzene	1.4	−0.030	23	2.7	−0.220	3.1	3.0	−0.054	13
toluene	3.6	−0.043	16	3.1	−0.463	1.5	3.1	−0.053	13
ethylbenzene	3.3	−0.035	20	2.4	0.331	2.1	2.5	−0.054	13
n-propylbenzene	0.8	−0.037	19	1.8	−0.539	1.3	2.5	−0.065	11
naphthalene	c			c			1.2	−0.058	12
2-methylnaphthalene	0.6	−0.064	11	0.5	−0.687	1.0	0.9	−0.054	13
1,1,1-trichloroethane	4.3	−0.029	24	3.5	−0.058	12	2.7	−0.063	11
trichloroethylene	3.2	−0.025	28	2.4	−0.052	13	3.8	−0.045	15
tetrachloroethylene	3.2	−0.028	25	1.4	−0.051	14	4.5	−0.056	12
chlorobenzene	1.0	−0.033	21	0.6	−0.152	4.6	2.8	−0.053	13
1,4-dichlorobenzene	1.5	−0.040	18	0.3	−0.068	10	2.2	−0.054	13
1,2,4-trichlorobenzene	0.5	−0.032	22	0.2	−0.066	11	2.2	−0.058	12
1-chloro-2-methylbenzene	d			d			2.3	−0.059	12
n-dodecane	0.3	−0.60	1.1	0.2	−0.97	0.7	0.9	−0.20	3.6
n-pentadecane	0.9	−0.69	1.0	0.2	−0.85	0.8	1.1	−0.16	4.3
n-heptadecane	1.3	−1.23	0.6	0.2	−0.79	0.9	1.7	−0.14	5.0
dichlorodifluoromethane (F-12)		−0.035	20	d				−0.053	13

[a] Initial concentrations measured by stripping at the beginning of each experiment. [b] Rate constants (λ) and half-lives ($t_{1/2}$) are for periods during the experiments when volatilization appears to dominate. [c] Interference from n-C_{14} in gas chromatogram. [d] Not spiked.

Tables I and II since we could not distinguish major discriminations between isomers.

VOC concentrations in the water column were monitored over the time course of the experiments. Water samples were collected during mixing of the tank by siphoning through a Teflon tube from ~1 m below the water surface and filling 2-L glass stoppered bottles without headspace. Mercuric chloride was used as preservative. The volatile organic compounds in unfiltered water samples (100–1000 mL depending on VOC concentration) were determined by using the closed-loop stripping and glass capillary gas chromatography procedures described in Wakeham et al. (6). Unfiltered water samples were purged for 1.5 h with recycled headspace air and the stripped compounds adsorbed from the gas stream onto 1.5 mg of activated charcoal. The charcoal was extracted with ~20 μL of CS_2 and the VOC thus preconcentrated were analyzed with a Carlo Erba Model 2150 gas chromatograph with flame ionization and a 40 m × 0.3 mm i.d. Pluronics 121 column. Injections were made without stream splitting at room temperatures, followed by temperature programming of the column over up to 180 °C at 2 °C/min. Compound concentrations were calculated relative to internal standards added to samples prior to analysis which corrected for differential stripping efficiencies. Precision (including both sampling and analysis) was about ±15%. VOC levels in prespike tank water and in blanks were generally at least an order of magnitude below levels of the spiked compounds.

Results and Discussion

Concentrations of volatile organic compounds in the MERL mesocosm water column decreased at rates that depended on season and on molecular structure of the model compounds (Figures 1–3). Concentration decreases were generally exponential, although in the spring and summer studies, there are major concentration breaks for aromatic hydrocarbons and chlorobenzene (Figure 2). VOC loss rate constants (λ, days^{-1}) and half-lives ($t_{1/2}$, days; Table I) were calculated according to an exponential decay ($C_t = C_0 \exp(\lambda t)$). For aromatic hydrocarbons and chlorobenzene, rate constants and half-lives were calculated by using data obtained prior to the concentration breaks;
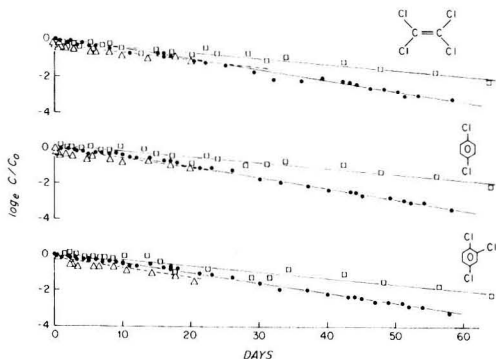

Figure 1. Concentration changes with time for tetrachloroethylene, 1,4-dichlorobenzene, and 1,2,4-trichlorobenzene in MERL experiments: "winter" (●), "spring" (□), "summer" (△).
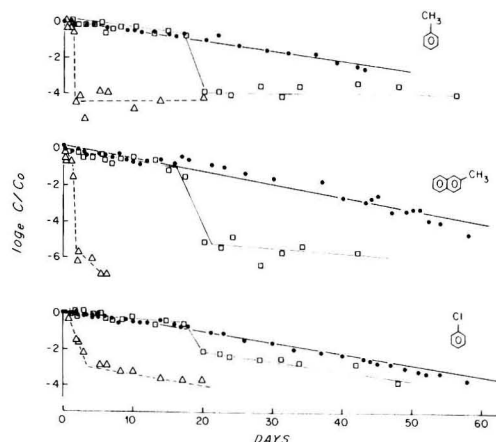

Figure 2. Concentration changes with time for toluene, 2-methylnaphthalene, and chlorobenzene in MERL experiments: winter (●), spring (□), and summer (△).

compound	tank 12, with HgCl$_2$			tank 0, without HgCl$_2$		
	C_o,[a] μg/L	λ, days^{-1}	$t_{1/2}$, days	C_o,[a] μg/L	λ, days^{-1}	$t_{1/2}$, days
benzene	3.4	-0.101	6.9	3.6	[b]	
toluene	3.4	-0.088	7.9	3.1		
ethylbenzene	3.0	0.097	7.1	3.6		
n-propylbenzene	2.5	-0.086	8.1	3.4		
tetrahydronaphthalene	1.1	-0.082	8.5	1.7		
naphthalene	0.3	-0.061	11.3	0.4	-0.896	0.8
2-methylnaphthalene	0.2	-0.046	15.1	0.4	-0.954	0.7
1,1,1-trichloroethane	3.6	-0.60	11.5	3.1	-0.072	9.6
trichloroethylene	3.2	-0.064	10.7	3.6	-0.081	8.6
tetrachloroethylene	1.8	-0.057	12.1	2.7	-0.058	12.0
chlorobenzene	0.5	-0.080	8.9	0.7		
1,4-dichlorobenzene	0.4	-0.066	10.6	0.6	-0.063	11.0
1,2,4-trichlorobenzene	0.2	-0.073	9.5	0.3	-0.066	10.6
n-dodecane	0.3	-0.377	1.8	0.4	-1.085	0.64
n-pentadecane	0.2	-0.343	2.0	0.3	-1.241	0.56
n-pentadecene	0.2	-0.383	1.8	0.4	-0.998	0.69
n-heptadecane	0.3	-0.359	1.9	0.6	-1.362	0.51
pristane	0.3	-0.400	1.8	0.4	-0.899	0.77

[a] Initial concentrations measured by stripping at the beginning of the experiments. [b] Half-lives cannot be calculated from the data.
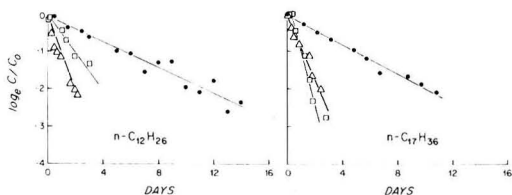

Figure 3. Concentration changes with time for n-dodecane and n-heptadecane in MERL experiments: winter (●), spring (□), summer (△).

however, in the summer experiment few measurements were made before the break so that calculated results are only rough estimates. As will be shown below, the rate constants and half-lives represent conditions under which volatilization dominates; biodegradation rates in spring and summer appear to be much faster.

Behavior of the volatile organic compounds grouped the compounds into three categories: (1) compounds that had loss rates with half-lives of 2-3 weeks regardless of season (e.g., chlorinated C$_2$-hydrocarbons and di- and trichlorobenzenes); (2) those compounds that had 2-3-week half-lives in winter and for the first half of the spring experiment but that were very rapidly lost in summer (aromatic hydrocarbons and chlorobenzene); (3) compounds that had half-lives of only a few days in all seasons (aliphatic hydrocarbons). These groupings demonstrate that molecular structure and environmental conditions are both important parameters in determining the fate and persistence of VOC in coastal seawater.

Chlorinated C$_2$-Hydrocarbons and Dichloro- and Trichlorobenzenes. Half-lives for the chlorinated C$_2$-hydrocarbons and the di- and trichlorobenzenes were similar to the measured F-12 half-lives in the spring and winter experiments for which F-12 data are available. The utility of the Freon is that it is not subject to biodegradation or sorption onto particulate matter and thus is thought to be lost from the water column only via gas exchange (28). The F-12 therefore provides a maximum volatilization rate that can be compared to loss rates for other VOC. A favorable comparison is taken as indicating that volatilization may be the primary control on the fate of these chlorinated VOC. However, even if the model VOC had a loss rate less than F-12, volatilization, at a slower rate, may still be the dominant removal process. It

is interesting to note that the half-lives for these VOC and F-12 measured in spring were about twice the winter and summer values. This relationship is the reverse of what might be predicted on the basis of diffusion coefficients alone, assuming that diffusion across a stagnant boundary layer as proposed by Broecker and Peng (29) and Liss and Slater (30) is a realistic model for volatilization, since diffusion coefficients are an inverse function of temperature. Thus for the F-12, a diffusion coefficient of 0.6 × 10^{-5} cm^2/s at about 0 °C and 30‰ salinity vs. 0.9 × 10^{-5} cm^2/s at 20 °C and 30‰ salinity (28) would lead to a faster gas-exchange rate at the higher temperature, if the theoretical stagnant boundary layer were the same in both cases. However, since we observed the opposite behavior, we conclude that in fact the stagnant boundary layer during the spring experiment was actually thicker than at the other times. The boundary layer thickness may be calculated from the freon data where

$$C_t = C_0 \exp(-D/hz)t \qquad (1)$$

and D is the diffusion coefficient (dependent on temperature), h is the height of the water column (500 cm for a MERL tank), and z is the stagnant boundary layer film thickness (dependent on turbulence (29)) and yields ~400 μm in spring and ~200 μm in winter. The boundary layer thickness is itself a function of the hydrodynamics of the water body, so that a thinner boundary layer in winter can be attributed to greater turbulence in the tank at that time. Because the water in the tanks was stirred to the same degree in all experiments, changes in hydrodynamics are attributed to variations in wind stress regimes, and in fact, windspeeds in winter generally are higher than the rest of the year. Thus differential hydrodynamics in the mesocosms alone can account for the seasonal difference in persistence for the chlorinated C$_2$-hydrocarbons and the di- and trichlorobenzenes.

How do half-lives and rate constants with respect to volatilization measured in mesocosm experiments compare with predictions based on laboratory experiments, and how can one extrapolate from the mesocosms to the natural environment? Laboratory and model studies (10-14) have suggested that volatile organic compounds should evaporate from natural waters with mass transfer coefficients (K_L (cm/h) = $0.693h/t_{1/2}$ = D/z) of ~10 cm/h. These studies are based on rapidly stirred solutions and may apply directly to highly turbulent streams. However, the
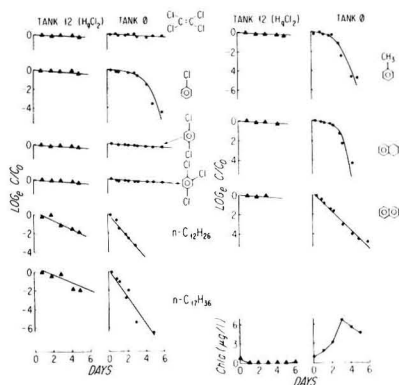
Figure 4. Concentration changes with time for several volatile organic compounds in the HgCl$_2$ poisoned (▲; tank 12) and nonpoisoned (●; tank 0) experiments. Chlorophyll a data are also shown as a rough indicator of biological activity.

MERL results give K_L of 0.5–1.5 cm/h, compared with field estimates in a lake (31) and in coastal seawater (4) of ~1 cm/h. The difference between laboratory and mesocosm/field estimates of K_L likely is related to very different hydrodynamic regimes in operation. On the other hand, turbulence at MERL is substantially less than in either Narragansett Bay or in the open ocean, where stagnant boundary layers range from 60 to 180 μm (32) and 50 ± 30 μm (29), respectively. Thus volatilization in the bay or in the ocean should be significantly faster (perhaps up to an order of magnitude) than in MERL tanks. In any event, in nature it may be catastrophic events such as severe storms that act as the dominant control on volatilization rates, not some type of "average" hydrodynamic conditions.

That the half-lives for the chlorinated hydrocarbons are similar to that of the F-12 further suggests that other removal processes such as biodegradation and sorption onto particles probably are not very important for these VOC, since a contribution from some other process should lower the observed half-lives. Microbial degradation of trichloroethylene and tetrachloroethylene was found to be slow in the laboratory, even when bacterial inocula from sewage (33) was used, and dichloro- and trichlorobenzenes were only slowly degraded by soil microbes (34, 35). In seawater, degradation should be even slower, due to lower microbial population densities and, sometimes, lower water temperatures. Further evidence of resistance to microbial degradation comes from the HgCl$_2$ poisoned/nonpoisoned experiment (Figure 4 and Table II), which gave similar behaviors in both cases. With regard to sorption of this group of compounds, laboratory studies (36, 37) yielded partition coefficients (K_p ~20–70) for a suite of sediments, including suspended particulate matter from Narragansett Bay (37), showing particle association to be minimal. Calculations based on theoretical considerations for distributions of several VOC between seawater and Narragansett Bay suspended particulate matter suggest that <0.1% of these compounds should be particle bound (6).

Alkylbenzenes and Chlorobenzene. The overall behavior of the alkylbenzenes (C$_0$–C$_3$) and of chlorobenzene differs significantly from that of the chlorinated C$_2$-hydrocarbons and the dichloro- and trichlorobenzenes, and there also was a strong seasonal effect. In the winter experiment (Figure 2), loss rates for the alkylbenzenes and chlorobenzene were comparable to rates for the chlorinated C$_2$-hydrocarbons and the dichloro- and trichlorobenzenes,

indicating the importance of volatilization under these experimental conditions. In spring similar trends were observed for the first 2 weeks of the experiment, but there was a sudden concentration break during which alkylbenzenes decreased by more than an order of magnitude, reaching background concentrations in less than 2 days. For chlorobenzene, the concentration drop was less dramatic, and concentrations continued to decrease slowly throughout the remainder of the experiment. The summer results were even more striking, with the concentration break occurring after only 2 days.

We interpret these concentration breaks as evidence of rapid biodegradation of the alkylbenzenes and of chlorobenzene under the relatively warm spring and summer water temperatures, when microbial activities are greater than in winter. A lag period was observed for both spring and summer experiments, with the lag being longer in the former. A possible explanation for the lag is that the microbial populations present in the water column at the time of spiking must become acclimated to the spike before degradation can proceed, and the acclimation period is shorter at warmer temperatures. Field data (6) suggest that Narragansett Bay water in summer contains a microbial community capable of degrading alkylbenzenes so that this community probably is present in the water of the summer MERL experiment. While we do not have bacterial activity and VOC respiration data for this series of experiments, such measurements are being made in conjunction with ongoing experiments using ^{14}C model VOC (38). In these experiments, there is a strong correlation between the concentration break, an increase in microbial activity and uptake of the ^{14}C model compound, and production of ^{14}CO$_2$.

The HgCl$_2$ poisoned/nonpoisoned experiment supports the suggestion that the concentration breaks observed in the other experiments are indeed related to biological activity. In similar HgCl$_2$-poisoned experiments, oxygen production and respiration fell to zero during the course of the experiments (21). Half-lives for alkylbenzenes and chlorobenzenes in the poisoned tank are similar to half-lives observed for the presumed "recalcitrant" chlorinated C$_2$-hydrocarbons and dichloro- and trichlorobenzenes (Table II), indicating loss by volatilization. However, loss rates for the alkylbenzenes were actually about 50% faster than for the other group of compounds, possibly indicating that the HgCl$_2$ did not really stop all degradation. On the other hand, alkylbenzenes and chlorobenzenes were quickly lost from the unpoisoned tank, although again with a lag of a couple of days. It is interesting to note that tetrahydronaphthalene (Figure 4) behaved more like an aromatic hydrocarbon than like an aliphatic hydrocarbon (as discussed below).

Biodegradation of aromatic hydrocarbons in seawater and freshwater has recently been reviewed by Jordan and Payne (39), and degradation rates can be fast but vary greatly depending on environmental conditions, especially temperature and the abundance of hydrocarbon-degrading (acclimated) populations. Our results clearly support these generalizations. Mechanisms of degradation by soil bacteria, leading to catechols, have been studied for aromatic hydrocarbons (40–42) and for monochlorobenzene (43). It is significant that the inclusion of one chlorine atom on the aromatic ring gives a degradable substrate (if other carbon sources, such as aromatic hydrocarbons, are present) (43) while two or more halogens tend to inhibit, but not eliminate, the degradation (34, 35). Since biodegradation is dependent on molecular structure (as we and Alexander (44) have observed), isomeric discriminations

might be expected. Indeed, Grob and Grob (45) in a lake and Gschwend et al. (4) in coastal seawater reported preferential loss of n-propylbenzene and ethylbenzene relative to other isomers; these depletions were attributed to preferential microbial attack of the C ≥ 2 alkyl side chains. We had hoped to make a similar observation in the first two experiments, in which the spike mixture contained all four C_2- and all eight C_3-alkylbenzene isomers. However, we could detect no preferential loss of n-propylbenzene or ethylbenzene; perhaps the initial concentrations were simply too high to observe an effect that was observed in field samples at considerably lower concentrations.

Apparent degradation rates for alkylbenzenes in our mesocosm experiments are comparable to rates reported for aromatics in earlier MERL experiments involving no. 2 fuel oil (21). However, the lag periods and concentration breaks we observed were not seen in the earlier study, which may reflect the very different spiking mixtures (the oil experiment was dosed with an oil–seawater dispersion giving initial oil concentrations of 150–300 µg/L). Turnover times with respect to biodegradation determined in smaller scale laboratory incubation experiments using a series of ^{14}C-labeled aromatic hydrocarbons (benzene, toluene, and naphthalene and other nonvolatile compounds) and estuarine, coastal, and open ocean water ranged from 30 to 130 days, depending to a certain extent on season, compound, and previous exposure to the water to petroleum hydrocarbons (46). In comparison, turnover times (calculated as C_0/λ) for toluene in our experiments were as follows: winter, 58 days; spring, 85 days prior to the concentration break vs. <2 days after the concentration break; summer, 7 days before break vs. 0.7 day after. We stress that the longer turnover times in our study are thought to represent primarily volatilization-controlled loss, whereas the very short times are due to biological degradation. We believe that the seasonal variations between winter and spring are largely due to changes in hydrodynamic conditions due to changes in wind-driven turbulence (mechanical mixing of the water in the tanks remained constant through each experiment). For the summer experiment, it is likely that the increased turnover time is also due in part to biodegradation.

Aliphatic Hydrocarbons. Loss rates for the aliphatic hydrocarbons (Figures 3 and 4; Tables I and II) were the highest for all of the VOC we examined. A comparison of the HgCl$_2$-poisoned and -unpoisoned runs (Figure 4 and Table II) suggests that some of this difference probably is due to microbial degradation of the alkanes, as half-lives in the poisoned tank were about 3 times longer than in the unpoisoned system. Indeed, our present ^{14}C experiments (38) show rapid remineralization of alkanes that can account for a large part of the concentration changes observed here. Nevertheless, even in the poisoned run half-lives were very short, certainly much too short to be accounted for by volatilization. Moreover, the relatively low vapor pressures and water solubilities (Henry's law constants) of the alkanes, compared, for example, to the aromatic hydrocarbons, would tend to argue against enhanced volatilization. Nor did half-lives correlate with variations in Freon half-lives, which are related to tank hydrodynamics. For example, the longest half-lives for the alkanes were observed in the winter experiment, when the Freon half-lives were shorter. Estimated residence times with respect to volatilization for alkanes have been calculated for Narragansett Bay and are somewhat greater than for chlorinated C_2-hydrocarbons, most chlorobenzenes, and most aromatic hydrocarbons (e.g., 11 days

for n-C_{12}, 13 days for n-C_{17}, 7 days for tetrachloroethylene and toluene, 9 days for 1,2,4-trichlorobenzene and 1,2,4-trimethylbenzene (6)).

Association of the alkanes with suspended particulate matter in the water column ("sorption") is the probable reason for the short half-lives for the alkanes. Several investigations (e.g., ref 15 and references therein) have shown that partitioning of nonpolar organic compounds between aqueous and particulate phases can be reliably estimated from the organic content of the particles and the octanol/water partition of the sorbate, according to eq 2 (see ref 15), where $K_p^z(s)$ is the equilibrium partition

$$\log K_p^z(s) = 0.72 \log K_{ow}^z + \log f_{oc}(s) + 0.5 \quad (2)$$

coefficient of compound z ($K_p^z(s)$ cm^3_l/g$_s$ = $S(z)$ (micrograms of sorbate (z) per gram sorbent)/$C(z)$ (microgram of z per cubic centimeter of liquid phase)), K_{ow}^z the octanol/water partition coefficient for z, and $f_{oc}(s)$ the fractional organic carbon content of the sorbent. For dodecane and heptadecane, as examples, $K_p^z(s)$'s of 4×10^3 and 2.5 $\times 10^5$ are estimated by assuming suspended particulate matter in the MERL tank to be 6% organic carbon and $\log K_{ow}^z$ of 6.0 and 8.5, respectively (extrapolated from ref 47). Of greater interest, however, is the distribution of the alkanes between particulate and aqueous phases under realistic suspended particle concentrations; about 6 mg/L is typical for the mesocosms and Narragansett Bay. The fraction of the alkanes sorbed onto suspended particles ($f(s)$) may be calculated by

$$f(s) = \frac{(K_p^z)\rho}{1 + (K_p^z(s))\rho} \quad (3)$$

where ρ is the grams of suspended particles per milliliter of water. Thus for alkanes dodecane and heptadecane, calculated $f(s)$ indicate that some 2.4% and 60% of these alkanes should be associated with particles. Similar calculations have been made for a series of volatile organic compounds in Narragansett Bay (6); for comparison, $f(s)$ for tetrachloroethylene was 0.013% and for toluene 0.008%, showing that these compounds are essentially nonparticle associative.

Thus we can make a case for sorption of alkanes onto suspended particles, especially for the higher molecular weight/lower water solubility compounds (e.g., heptadecane vs. dodecane). Sorption onto particles would make these compounds appear to be less volatile, hence our stripping recoveries would be poor (recoveries for dodecane and heptadecane are about 85% and 40% respectively vs. 94% and 96% for toluene and tetrachloroethylene; low alkane recoveries are not due to irreversible adsorption on the charcoal traps, based on experimental data). Sorption, of course, will not actually remove the alkanes from the water column unless the particles are sedimented, but in any event sorption will lower the activity of the alkanes so as to lower their volatilities. While the results of the no. 2 fuel oil experiment (21) may not be completely applicable to our VOC studies, it should be pointed out that >90% of the oil saturated hydrocarbons were in a particulate (collected on 0.3-µm filters, and possibly including micelles) form, but <20% of the aromatics were particle associated.

Gearing and Gearing (21) also reported significant biodegradation of the oil alkanes, probably on the same order of magnitude as the aromatics, and clearly more rapid in warm water. Our winter vs. summer alkane half-lives tend to agree, although we cannot rule out the difference being in part due to variations in suspended particle concen-

trations for the several experiments. Nevertheless, concentration trends for alkanes and aromatic hydrocarbons in the poisoned/nonpoisoned experiment are very different, suggesting differing biodegradative processes are involved for the two compound classes. We attempted to see if n-alkanes, isoprenoids, and n-alkenes behaved differently in our experiments; however, no significant differences could be observed within out study (Table II). This result was surprising since hydrocarbons generally have been shown to degrade alkenes > alkanes > isoprenoids in both laboratory and field studies (e.g., ref 21 and 37). Aromatic hydrocarbons may tend to be less rapidly degraded then aliphatic hydrocarbons, or there may be a lag period before the onset of aromatic degradation during which the aliphatics are being degraded. This is also our observation (e.g., Figure 4).

Naphthalenes. Results for naphthalene and 2-methylnaphthalene indicate behaviors intermediate between that of the alkylbenzenes and that of the aliphatic hydrocarbons. That is, the naphthalenes in the "winter" experiment have long half-lives like the alkylbenzenes, suggesting the importance of volatilization and the relative absence of major biodegradation. But in the spring and summer experiments, the naphthalenes are subjected to rapid degradation after the lag. On the other hand, half-lives for the naphthalenes in the spring, summer, and $HgCl_2$/non-$HgCl_2$ experiments approach values obtained for the aliphatic hydrocarbons, and in fact the concentration trend in the poison/nonpoison experiment is more similar to the aliphatics than the alkylbenzenes (Figure 4). Thus, relatively lower seawater solubilities of the naphthalenes compared to alkylbenzenes, but considerably higher than the alkanes, means that particle association should be intermediate for the naphthalenes. Likewise, biodegradation rates for naphthalenes are generally slower than for alkylbenzenes (46).

Conclusions

The fates and persistence of volatile organic compounds in coastal seawater depend on several competing removal processes: volatilization, biodegradation, and sorption onto particulate matter. The extent to which each process acts on a given compound is a function of chemical and physical properties of the compound as well as the physical and biological state of the ecosystem. Controlled ecosystem (mesocosm) experiments have aided in unravelling how these several processes affect different volatile organic compounds.

Volatilization plays a major role in the removal of many VOC from the water column. For chlorinated C_2-hydrocarbons, dichlorobenzenes, and trichlorobenzenes, volatilization appears to be the dominant removal process during each of the three experiments. Volatilization also plays the major role in controlling the fate of alkylbenzenes, and to a certain extent naphthalenes, in cold water conditions, where microbial activity is low. On the other hand, in warm/high biological activity situations, microbial degradation also becomes important. The fate of aliphatic hydrocarbons seems to be controlled to a large extent by sorption onto particulate matter, although biodegradation also plays a significant role in warm water. The molecular structure (and hence the physical and chemical/biochemical properties) of VOC also has a major influence in the fate of these compounds in seawater.

Acknowledgments

Registry No. Benzene, 71-43-2; toluene, 108-88-3; ethylbenzene, 100-41-4; n-propylbenzene, 103-65-1; naphthalene, 91-20-3; 2-methylnaphthalene, 91-57-6; 1,1,1-trichloroethane, 71-55-6; trichloroethylene, 79-01-6; tetrachloroethylene, 127-18-4; chlorobenzene, 108-90-7; 1,4-dichlorobenzene, 106-46-7; 1,2,4-trichlorobenzene, 120-82-1; 1-chloro-2-methylbenzene, 95-49-8; n-dodecane, 112-40-3; n-pentadecane, 629-62-9; n-heptadecane, 629-78-7; pristane, 1921-70-6; F-12, 75-71-8.

Literature Cited

(1) Schwarzenbach, R. P.; Bromund, R. H.; Gschwend, P. M.; Zafiriou, O. C. Org. Geochem. 1978, 1, 93–107.
(2) Gschwend, P. M., Ph.D. Dissertation, Woods Hole Oceanographic Institution, Woods Hole, MA; Feb 1979.
(3) Gschwend, P. M.; Zafiriou, O. C.; Gagosian, R. B. Limnol. Oceanogr. 1980, 25, 1044–53.
(4) Gschwend, P. M.; Zafiriou, O. C.; Mantoura, R. F. C.; Schwarzenbach, R. P.; Gagosian, R. B. Environ. Sci. Technol. 1982, 16, 31–38.
(5) Mantoura, R. F. C.; Gschwend, P. M.; Zafiriou, O. C.; Clarke, K. R. Environ. Sci. Technol. 1982, 16, 38–45.
(6) Wakeham, S. G.; Davis, A. C.; Goodwin, J. T. Can. J. Fish. Aquat. Sci., in press.
(7) Sauer, T. C., Jr.; Sackett, W. M.; Jeffrey, L. M. Mar. Chem. 1978, 7, 1–16.
(8) Sauer, T. C. Limnol. Oceanogr. 1980, 25, 338–351.
(9) Sauer, T. C. Org. Geochem. 1981, 3, 91–101.
(10) Mackay, D. M.; Wolkoff, A. W. Environ. Sci. Technol. 1973, 7, 611–614.
(11) Mackay, D. M.; Leinonen, P. J. Environ. Sci. Technol. 1975, 9, 1178–1180.
(12) Dilling, W. L.; Tefertiller, N. B.; Kallos, G. J. Environ. Sci. Technol. 1975, 9, 833–838; 1976, 10, 1275.
(13) Dilling, W. L.; Bredeweg, C. I.; Tefertiller, N. B. Environ. Sci. Technol. 1976, 10, 351–356.
(14) Dilling, W. L. Environ. Sci. Technol. 1977, 11, 405–409.
(15) Schwarzenbach, R. P.; Westall, J. C. Environ. Sci. Technol. 1981, 15, 1360–1367.
(16) Pilson, M. E. Q.; Vargo, G. A.; Gearing, P.; Gearing, J. N. In "Proceedings of the 2nd National Conference, Interagency Energy, Environment RGD Program"; U.S. Environmental Protection Agency Report 600/9-77-012: Washington, D.C., 1977; pp 513–516.
(17) Santschi, P. H. In "Marine Mesocosms: Biological and Chemical Research in Experimental Ecosystems"; Grice, G. D., Reeve, M. R., Eds.; Springer Verlag: New York, 1982; pp 63–80.
(18) Gearing, J. N.; Gearing, P. J.; Wade, T.; Quinn, J. G.; McCarty, H. B.; Farrington, J.; Lee, R. F. In "Proceedings of the 1979 Oil Spill Conference (Prevention, Behavior, Control, Cleanup)"; American Petroleum Institute Publication No. 4308: Washington, D.C.; 1979; pp 555–564.
(19) Gearing, P. J.; Gearing, J. N.; Pruell, R. J.; Wade, T. L.; Quinn, J. G. Environ. Sci. Technol. 1980, 14, 1129–1136.
(20) Wade, T. L.; Quinn, J. G. Mar. Environ. Res. 1980, 3, 15–33.
(21) Gearing, P. J.; Gearing, J. N. Mar. Environ. Res. 1982, 6, 115–132, 133–143.
(22) Hinga, K. R.; Pilson, M. E. Q.; Lee, R. F.; Farrington, J. W.; Tjessem, K.; Davis, A. C. Environ. Sci. Technol. 1980, 14, 1136–1143.
(23) Lee, R. F.; Hinga, K. R.; Almquist, G. In "Marine Mesocosms: Biological and Chemical Research in Experimental Ecosystems"; Grice, G. D., Reeve, M. R., Eds.; Springer Verlag: New York, 1982; pp 123–135.
(24) Hunt, C. D.; Smith, D. L. In "Marine Mesocosms: Biological and Chemical Research in Experimental Ecosystems"; Grice, G. D., Reeve, M. R., Eds.; Springer Verlag: New York, 1982; pp 111–122.
(25) Amdurer, M.; Adler, D. M.; Santschi, P. H. In "Marine Mesocosms: Biological and Chemical Research in Exper-

imental Ecosystems"; Grice, G. D. Reeve, M. R., Eds.; Springer Verlag: New York, 1982; pp 81–95.

(26) Santschi, P. H.; Carson, S.; Li, Y.-H. In "Marine Mesocosms: Biological and Chemical Research in Experimental Ecosystems"; Grice, G. D., Reeve, M. R., Eds.; Springer Verlag: New York, 1982; pp 98–109.

(27) Wakeham, S. G.; Goodwin, J. T.; Davis, A. C. Woods Hole Oceanographic Institution Technical Report 82-36, 1982; p 62.

(28) Bopp, R. F.; Santschi, P. H.; Li, Y.-H.; Deck, B. L. *Org. Geochem.* 1981, 3, 9–14.

(29) Broecker, W. S.; Peng, T.-H. *Tellus* 1974, 26, 21–35.

(30) Liss, P. S.; Slater, P. G. *Nature (London)* 1974, 247, 181–184.

(31) Schwarzenbach, R. P.; Molnar-Kubica, E.; Giger, W.; Wakeham, S. G. *Environ. Sci. Technol.* 1979, 13, 1367–1373.

(32) Nixon, S. W.; Alonso, D.; Pilson, M. E. Q.; Buckley, B. A. In "Microcosms in Ecological Research"; Glessey, Ed.; DOE Symposium Series CONF-F81101, National Technical Information Service: Washington, D.C., 1980; pp 818–849.

(33) Bouwer, E. J.; Rittmann, B. E.; McCarty, P. L. *Environ. Sci. Technol.* 1981, 15, 596–599.

(34) Ballschmitter, K.; Scholz, C. *Chemosphere* 1980, 9, 457–467.

(35) Marinucci, A. C.; Bartha, R. *Appl. Environ. Microbiol.* 1979, 38, 811–817.

(36) Schwarzenbach, R. P.; Westall, J. C. *Environ. Sci. Technol.* 1981, 15, 1360–1367.

(37) Schwarzenbach, R. P. Swiss Federal Institute for Water Resources and Water Pollution Control (EAWAG), private communication, 1982.

(38) Wakeham, S. G. Woods Hole Oceanographic Institution, Woods Hole, Massachusetts, unpublished data, 1983.

(39) Jordan, R. E.; Payne, J. R. In "Fate and Weathering of Petroleum Spills in the Marine Environment"; Ann Arbor Science Publishers: Ann Arbor, MI, 1980; p 174.

(40) Claus, D.; Walker, N. *J. Gen. Microbiol.* 1964, 36, 107–122.

(41) Gibson, D. T.; Koch, J. R.; Kallio, R. E. *Biochemistry* 1968, 7, 2653–2662.

(42) Gibson, D. T.; Gschwendt, B.; Yeh, W. K.; Kobal, V. M. *Biochemistry* 1973, 12, 1520–1528.

(43) Gibson, D. T.; Koch, J. R.; Kallio, R. E. *Biochemistry* 1968, 7, 3795–3802.

(44) Alexander, M. *Adv. Appl. Microbiol.* 1965, 7, 35–80.

(45) Grob, K.; Grob, G. *J. Chromatogr.* 1974, 90, 303–313.

(46) Lee, R. F. In "Proceedings, 1977 Oil Spill Conference (Prevention, Behavior, Control, Cleanup)"; American Petroleum Institute Publication 4284: Washington, D.C., 1977; pp 611–616.

(47) Leo, A.; Hansch, C.; Elkins, D. *Chem. Rev.* 1971, 71, 525–616.

Biodegradation of the Monochlorobiphenyls and Biphenyl in River Water

Robert E. Bailey,* Stanley J. Gonsior, and Wayne L. Rhinehart

Environmental Sciences Research Laboratory, Dow Chemical U.S.A., Midland, Michigan 48640

■ The rates of primary biodegradation, as well as mineralization, of the three isomers of monochlorobiphenyl (MCB), biphenyl (BP), and 2,2′,4,4′-tetrachlorobiphenyl (TCB) have been determined by using a river water dieaway test. Analysis of river water extracts by high-performance liquid chromatography showed the times for 50% degradation of parent MCBs were 2–3 days and 1.5 days for BP at initial concentrations of about 1 μg/L. The unchlorinated ring degraded initially and after a 50-day incubation, approximately 50% of the theoretical $^{14}CO_2$ was recovered from the subsequent degradation of the chlorinated ring of the MCBs. The rate of biodegradation of higher concentrations was somewhat slower. No degradation of TCB was observed over 98 days under conditions of this test.

Introduction

The biodegradation of the monochlorobiphenyls (MCBs) has been reported by several groups in studies conducted both with pure cultures (1, 2) and by mixed populations (3–8). A comparison of the rate of MCB biodegradation with the rates of biphenyl (BP) and 2,2′,4,4′-tetrachlorobiphenyl (TCB) allows an estimation of the environmental importance of their biodegradation. TCB is a typical component of the polychlorinated biphenyls (PCBs) found in environmental samples. TCB has been observed to not degrade under conditions where other PCB congeners were degraded (1, 9). In contrast, BP is widely distributed in the environment as a component of petroleum and as an article of commerce but was observed only at concentra-

tions of 0.1–0.5 μg/L in natural waters (10).

The production of chlorobenzoic acid (CBA) from MCB biodegradation has been reported several times (1, 2, 11). Recently, (2-chlorobenzoyl)formic acid was reported as a metabolite of 2-MCB (5). The CBAs are well-known to be biodegradable, although often slowly or with a lag period depending on the bacterial inoculum used (12–21).

The purpose of this study was to determine the rate of primary biodegradation as well as mineralization of all the MCB isomers for use in predicting their environmental removal rate. Each of the three MCB isomers was studied separately to observe any isomer effects and compared with BP and TCB.

Experimental Procedures

Chemicals. Radioactively labeled MCBs (uniformly ^{14}C labeled on the chlorinated ring) were synthesized by Pathfinder Laboratories (St. Louis, MO). The radiochemical purity was determined by reverse-phase high-performance liquid chromatography (HPLC) and liquid scintillation counting. The radiochemical purity and specific activity of the products were the following: 2-MCB, 94%, 11.84 mCi/mmol; 3-MCB, 91%, 14.28 mCi/mmol; 4-MCB, 87%, 18.05 mCi/mmol. BP (The Dow Chemical Co.) and TCB (Pathfinder Laboratories) were uniformly ^{14}C labeled with radiochemical purities and specific activities of 99%, 6.647 mCi/mmol and 99%, 11.46 mCi/mmol, respectively.

River Die-Away Studies. River water was obtained from the Tittabawassee River, Midland, MI. The sampling site was upstream from any significant industrial activity

or municipal discharge. The Tittabawassee River drains primarily farm and forest land north of Midland. Tests began within 4 h of collection after filtration through coarse paper to remove large solids. The biphenyl compounds were added to the river water without a carrier solvent by evaporating a hexane solution of the material on the inside surface of a glass jar. Rolling the jar after filling with river water gave approximately 100 μg/L solution of the MCBs. These solutions were diluted with river water to approximately 10 and 1 μg/L. The TCB was set at 10 and 1 μg/L due to its low water solubility. Aliquots (100 mL) of these river water solutions were transferred to 160-mL serum bottles and sealed with aluminum foil faced Teflon-coated silicone rubber septa. The foil was found necessary to prevent loss of the parent compounds due to volatilization and apparent absorption by the septum.

Control samples were treated with 100 mg/L HgCl$_2$ to enable detection of any abiotic loss of material. All samples were incubated in the dark at 20 °C on a rotary shaker at 100 rpm. Bottles were sacrificed at each time point for analysis. Mineralization of the compounds was observed by trapping ^{14}CO$_2$ in ethanolamine and 2-methoxyethanol after addition of 0.1 mmol of NaHCO$_3$, acidification by the addition of 2.3 mmol of H$_2$SO$_4$, and purging with nitrogen. The amount of ^{14}CO$_2$ trapped was determined by subtracting the amount of ^{14}C-labeled parent compound calculated to have been volatilized from the total radioactivity trapped. The remaining parent compound was determined by extraction of the acidified water solution with methylene chloride followed by concentration and HPLC analysis. The results presented in the figures have been corrected for volatilization of the parent compound.

The MCBs were separated from the corresponding benzoic acid metabolites by using a Waters C$_{18}$ μBondapak reverse-phase column. The solvent system used for elution was composed of 74% methanol, 25% water, and 1% acetic acid at a flow rate of 2 mL/min. Fractions of the HPLC eluent were collected for liquid scintillation counting to determine the parent compound and metabolite concentrations. Aquasol liquid scintillation cocktail (New England Nuclear, Boston, MA) was used throughout this study for ^{14}C determinations. The retention times of the parent compounds under the above conditions were about 6.5, 7.3, 7.3, 5.3, and 13.3 min for 2-MCB, 3-MCB, 4-MCB, BP, and TCB, respectively.

The HPLC retention time of the CBA under the above conditions was about 3.5 min, close to the solvent front. Consequently, a Lichrosorb RP-8 column with a solvent system composed of 59.75% (volume) H$_2$O, 39.75% methanol, and 0.5% acetic acid was used to isolate CBAs. This allowed a retention time of about 7.5 min for 2-CBA. A 6-min retention time for 4-CBA was observed when the solvent system was composed of 44.75% H$_2$O, 54.75% methanol, and 0.5% acetic acid.

Millipore Total Count paddles (Millipore Corp. Bedford, MA) were used to estimate the bacterial population of the river water. They are reported to be equivalent to standard plate counts (22) in number of colony forming unit (CFU). Dilutions are prepared by using Millipore dilution kits. The paddles were incubated at 20 °C for 3 days prior to counting. Colonies were counted visually. An average of 6900 CFU/mL in the river water was observed on March 10, 1980.

Results

Rapid biodegradation of each of the three isomers of MCB and BP was observed in Tittabawassee River water. The disappearance of the parent compounds, appearance of a metabolite(s) in the methylene chloride extract, and
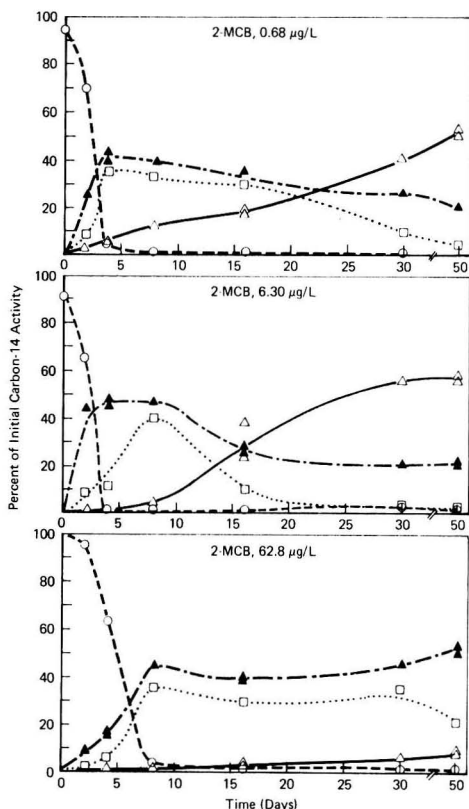
Figure 1. Distribution of radioactivity in biodegradation of 2-MCB: (O) parent 2-MCB, (△) ^{14}CO$_2$ recovered, (□) metabolite observed, and (▲) activity remaining in the river water raffinate.

Table 1. Times for Biodegradation of 50% of Initial Concentrations of Biphenyl, 2-, 3-, and 4-Monochlorobiphenyl, and 2,2′,4,4′-Tetrachlorobiphenyl at 20 °C

compound	starting date	time, days, at initial concentration, μg/L, of		
		1	10	100
biphenyl	5/19/80	1.5	2	3
biphenyl	3/10/80	2.5	not set	not set
2-MCB	3/10/80	2.5	2	3.5
3-MCB	3/10/80	3	3.5	4
4-MCB	3/10/80	2	3	5
TCB	3/10/80	a	a	a

^{a} No degradation observed over 98 days.

the evolution of ^{14}CO$_2$ are shown in Figures 1–4. The unextracted activity, that which is associated with the cells or very water soluble, is in the raffinate. A comparison of the yields of ^{14}CO$_2$ from the chlorinated ring of the MCBs and biphenyl at initial concentrations of about 1μg/L is shown in Figure 5.

The three MCB isomers biodegraded at approximately the same rate at all concentrations, although an apparent lag period was noted at the higher concentrations. Biphenyl was observed to biodegrade somewhat faster than the MCBs. No degradation was observed for TCB, a less than 1% yield of ^{14}CO$_2$. No metabolites were observed by HPLC analysis of the TCB extract after a 98-day incubation. The approximate elapsed times for 50% removal
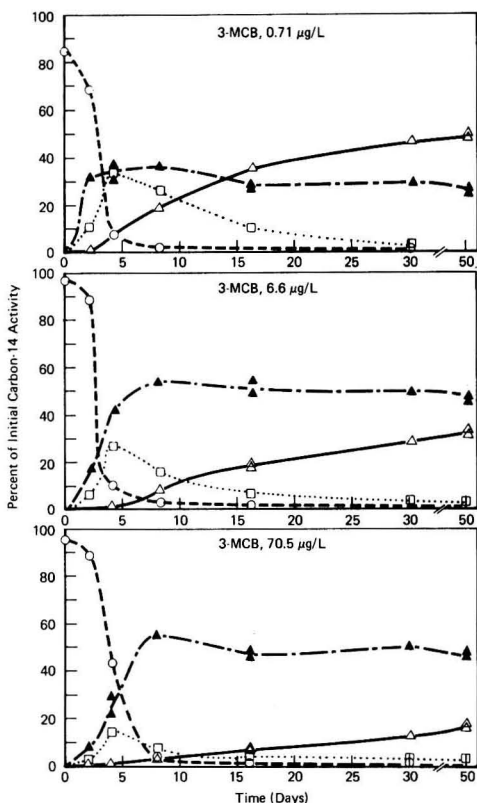
Figure 2. Distribution of radioactivity in biodegradation of 3-MCB: (O) parent 3-MCB, (△) $^{14}CO_2$ recovered, (□) metabolite observed, and (▲) activity remaining in the river water raffinate.

Figure 3. Distribution of radioactivity in biodegradation of 4-MCB: (O) parent 4-MCB, (△) $^{14}CO_2$ recovered, (□) metabolite observed, and (▲) activity remaining in the river water raffinate.
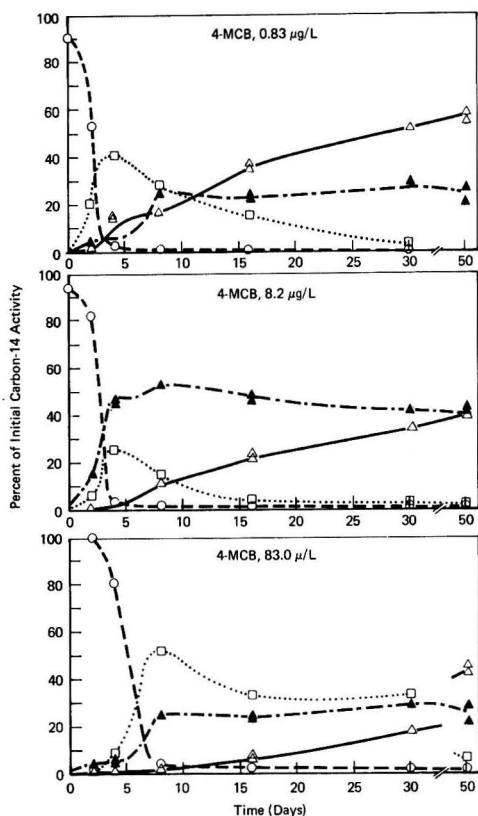
of the parent compounds are listed in Table I.

A metabolite, believed to be the corresponding chlorobenzoic acid based on the HPLC retention time, was observed from degradation of each of the MCBs. Up to 50% of the initial radioactivity was found as metabolite. The metabolite was observed to degrade more slowly than the parent compound with release of $^{14}CO_2$. No appreciable amount of an extractable metabolite was observed from biphenyl. In addition, a portion of the radioactivity initially added was apparently incorporated in the cell mass or present in some other form which was not extracted by methylene chloride.

A material balance was determined for each sample by summing the $^{14}CO_2$ trapped, radioactivity extracted, and that remaining in the river water raffinate. The mean accountability of ^{14}C was 92.2% with a standard deviation of 12.6 and a range of 58–128%. The mean recovery of parent compound from all control samples was 94.7%. A mean of 5.4% of the radioactivity was apparently volatilized during purging and recovered in the ethanolamine traps in the initial sample workup. This amount of volatilization is approximately what is predicted from the air/water partition coefficients for MCBs, BP, and TCB (23).

Discussion

Visual inspection of the results, Figures 1–4, clearly show that the rate of MCB degradation increases with time. The increased rate can be attributed to either an increase in
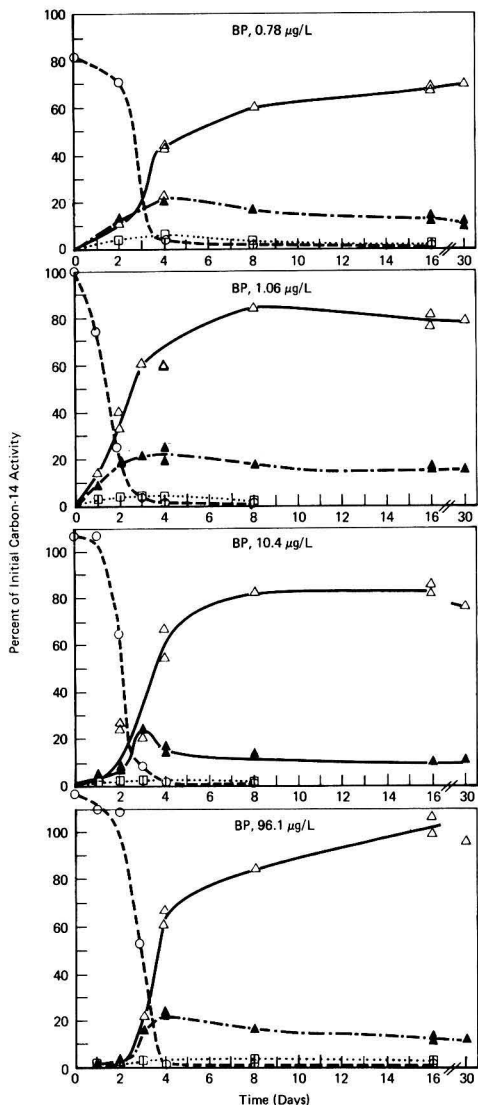
the population of MCB or BP degrading species or an increase in activity due to increased concentrations of the appropriate enzymes. In this study, the low concentration of added chemical relative to the background TOC in the river water was not expected to cause an appreciable increase in the total bacterial population.
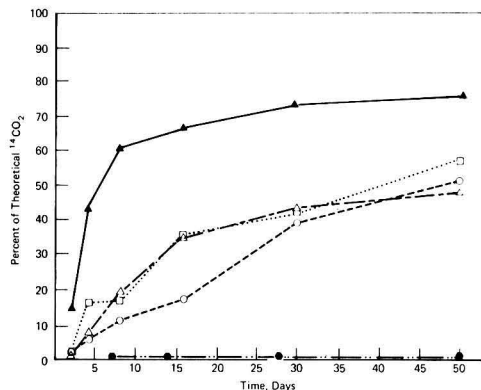
All three isomers of MCB were degraded in river water samples at similar rates. The effect of concentration from about 1 to 100 $\mu g/L$ was greater than the effects of chlorine position on the time for 50% degradation. Previous investigators have examined degradation rates for the MCBs and found essentially the same thing—the degradation rates for the three MCBs vary by only a factor of 2 and are about half that observed for biphenyl (2–4). The similarity of rates of primary degradation for the different compounds is also consistent with the calculations and observations of Kennedy et al. (24) on in vitro metabolism of MCBs by hepatic microsomal cytochrome P-450. They found no differences in the reactivity of the nonchlorinated ring of the different isomers. In addition, extended Hückel molecular orbital calculations by Kennedy et al. (24) indicated the net electronic changes on the unchlorinated ring of the MCBs are close to those calculated for BP. Thus, electrophilic attack on the unchlorinated ring would also be expected to occur at similar rates during bacterial metabolism.

The yield of $^{14}CO_2$ from mineralization of the chlorinated ring was similar for all three isomers of MCB. A lag period of about one week was observed before appreciable $^{14}CO_2$

Figure 4. Distribution of radioactivity in biodegradation of BP: (O) parent BP, (△) $^{14}CO_2$ recovered, (□) metabolite observed, and (▲) activity remaining in river water raffinate. The set at 0.78 µg/L was concurrent with the MCBs, March 10, 1980. The remaining samples were set May 18, 1980.

Figure 5. Comparison of $^{14}CO_2$ released on biodegradation of approximately 1 µg/L solutions of (▲) BP, (O) 2-MCB, (△) 3-MCB, (□) 4-MCB, and (●) TCB.

phase after extraction. BP yielded no appreciable amounts of extractable metabolites. Apparently benzoic acid and its related metabolites were rapidly metabolized to CO_2 and cell mass.

Acknowledgments

We thank C. G. Mendoza for excellent analytical advice, W. J. Maier and W. B. Neely for stimulating discussions, and H. T. Bell for assistance in preparing the manuscript.

Literature Cited

(1) Furukawa, K.; Tonomura, K.; Kamibayashi, A. *Appl. Environ. Microbiol.* **1978**, *35*, 223–227.
(2) Ahmed, M.; Focht, D. *Can. J. Microbiol.* **1973**, *19*, 47–52.
(3) Wong, P. T. S.; Kaiser, K. L. E. *Bull. Environ. Contam. Toxicol.* **1975**, *13*, 249–255.
(4) Reichardt, P. B.; Chadwick, B. L.; Cole, M. A.; Robertson, B. R.; Button, D. K. *Environ. Sci. Technol.* **1981**, *15*, 75–79.
(5) Shiaris, M. P.; Sayler, G. S. *Environ. Sci. Technol.* **1982**, *16*, 367–369.
(6) Clark, R. R.; Chian, E. S. K.; Griffin, R. A. *App. Environ. Microbiol.* **1979**, *37*, 680–685.
(7) Branson, D. R., The Dow Chemical Co., Midland, MI, personal communication, 1979.
(8) Tucker, E. S.; Saeger, V. W.; Hicks, O. *Bull. Environ. Contam. Tox.* **1975**, *14*, 705–713.
(9) Baxter, R. A.; Gilbert, P. E.; Lidgett, R. A.; Mainprize, J. H.; Vodden, H. A. *Sci. Total Environ.* **1975**, *4*, 53–61.
(10) Hites, R. A. *J. Chromatogr. Sci.* **1973**, *11*, 570–574.
(11) Ballschmiter, K.; Unglert, Ch.; Neu, H. *J. Chemosphere* **1977**, *6*, 51–56.
(12) Boethling, R. S.; Alexander, M. *Appl. Environ. Microbiol.* **1979**, *37*, 1211–1216.
(13) Haller, H. D. *J. Water Pollut. Control Fed.* **1978**, *49*, 2771–2777.
(14) Reineke, W.; Knackmuss, H.-J. *Biochim. Biophys. Acta* **1978**, *542*, 412.
(15) DiGeronimo, M. J.; Nikaido, M.; Alexander, M. *Appl. Environ. Microbiol.* **1979**, *37*, 619–625.
(16) Knackmuss, H.-J.; Reineke, W. *Chemosphere* **1973**, *2*, 225–230.
(17) Spokes, J. R.; Walker, N. *Arch. Microbiol.* **1974**, *96*, 125–134.
(18) Hartmann, J.; Reineke, W.; Knackmuss, H.-J. *Appl. Environ. Microbiol.* **1979**, *37*, 421–428.
(19) Ruisinger, S.; Klages, U.; Lingens, F. *Arch. Microbiol.* **1976**, *110*, 253–256.
(20) Haller, H. D.; Finn, R. K. *Eur. J. Appl. Microbiol. Biotechnol.* **1979**, *8*, 191–205.

was recovered. Apparently, the growth of the microorganisms degrading the chlorinated ring is significantly slower than the growth of microorganisms that degrade the parent MCB. The slow growth rate after a lag period is consistent with literature reports on the biodegradation of chlorobenzoates (*19, 20*). The mineralization rates observed in this study are qualitatively the same as those reported by Boethling and Alexander (*12*) for 4-chlorobenzoic acid (4-CBA). They recovered 48% of theoretical $^{14}CO_2$ in 8 days from a stream water sample treated with 4.7 µg/L 4-CBA with slower mineralization at higher concentrations. We observed metabolites that were consistent with the corresponding CBA in all of the experiments with additional carbon-14 remaining in the water

(21) Shamat, N.; Maier, W. J. *J. Water Pollut. Control Fed.* 1980, 52, 2158.

(22) Cotton, R. A.; Sladek, K. J.; Sohn, B. I., World Congress of Environmental Medicine and Bioloy, Paris, France, July 1974.

(23) Bailey, R. E.; Rhinehart, W. L.; Gonsior, S. J.; Batchelder, T. L.; Mendoza, C. G.; Neely, W. B., Second Annual Meeting

of the Society for Environmental Toxicology and Chemistry, Arlington, VA, Nov 1981.

(24) Kennedy, M. W.; Carpentier, N. K.; Dymerski, P. P.; Adams, S. M.; Kaminsky, L. S. *Biochem. Pharmacol.* 1980, 29, 727–736.

NOTES

Is the Direct Mutagenic Activity of Diesel Particulate Matter a Sampling Artifact?

Terence H. Risby*

Division of Environmental Chemistry, Department of Environmental Health Sciences, The Johns Hopkins University School of Hygiene and Public Health, Baltimore, Maryland 21205

Samuel S. Lestz

Department of Mechanical Engineering, The Pennsylvania State University, University Park, Pennsylvania 16802

■ Some of the direct microbial mutagenic activity of diesel particulate matter has been assigned to the presence of nitro derivatives of polynuclear aromatic hydrocarbons. A number of researchers have suggested that these compounds may be produced during sample collection. This paper discusses their formation on the basis of simple chemical kinetic and collision phenomena.

Introduction

Many reports have recently appeared in the literature that demonstrate, by in vitro microbial assays, the direct mutagenic activity of extracts of diesel particulate matter: examples of this work are contained in three books, published during the past two years (*1–3*). The observation that these samples do not require mammalian enzymes for activation of mutagenic activity was interesting since engine combustion sources are known to produce polynuclear aromatic hydrocarbons (PAHs) that require microsomal activation (*4*). It was therefore apparent that the diesel sorbate contains additional classes of mutagens. One such class of direct mutagens is nitroaromatics, and some of these compounds have been identified on diesel particles [1-nitropyrene, nitromethylanthracene, hydroxynitrofluorene, nitrodehydropyrene, and 2-nitrofluorene (*5*)]. These rapid predictive microbial assays have been confirmed with mammalian cell culture assays, skin painting, and intratracheal instillations (*1–3*). However, these results have not been confirmed by studies in which various types of laboratory animals were exposed to diluted total diesel exhaust; no increased incidence of carcinomas was demonstrated (*1–3*). There was morphological and biochemical evidence of lung tissue injury and adaption or repair after inhalation of very high levels of diesel exhaust (*6*). While this difference between the results obtained with in vitro and in vivo assays and with animal exposure studies is not without precedent, it has served to cloud the understanding of the potential health effects of diesel exhaust.

There are many possible explanations for these differences in results such as relative bioavailability of the adsorbates on the diesel particle (*7*), detoxification mecha-

nisms (*3*), number of animals exposed (*3*), lack of typical atmospheric interactions (*2*), and long-term retention of particles (*2*). However, a simpler explanation may be that there is a chemical difference between the agents of exposure in in vitro and in vivo assays and in inhalation exposure. This chemical difference may arise during sampling, and if so, the direct mutagenic activity of diesel particles is therefore an artifact. Theoretically it should be possible to investigate whether sampling artifactual processes are causing the problem by performing exposure studies using reaerosolized diesel particles; in practice these studies have not proved successful. Diesel particles have a mean particle diameter of 0.027 μm (*8*), and the mean diameter of reaerosolized diesel particles in the only study reporting such exposure was 2.8 μm (*9*). It is therefore difficult to use such data to support conclusive arguments for or against the premise that the activity is produced as a sampling artifact. Collection of diesel particles by different sampling methods (e.g., electrostatic precipitation) represents an alternative approach. The direct microbial mutagenic activity of the extract from electrostatically precipitated diesel particles was found to be not significantly different from the direct activity of filtered particles (*10*). These results suggest that the direct microbial mutagenic activity is not due to sampling artifactual reactions. Alternatively, the reduction in direct mutagenic activity from sampling artifactual reactions could be compensated by reactions with ozone: ozone is produced by the corona discharge in electrostatic precipitators. Pitts et al. have shown that both ozone and nitric acid react with polynuclear aromatic hydrocarbons to produce strong direct microbial mutagens (*11, 12*). The direct microbial activities of an oxide and a nitro derivative of benzo[*a*]pyrene have been shown to be comparable [1- or 3-nitrobenzo[*a*]pyrene, 3600–5300 revertants/μg (*11, 13*); benzo[*a*]pyrene 4,5-oxide, 1600 revertants/μg (*12*)]. In addition ozone will rapidly oxidize nitric oxide to nitrogen dioxide, which has been postulated as the reactant, in the presence of small amounts of water vapor, for the formation of direct mutagens (nitropolynuclear aromatic compounds). Therefore the direct microbial mutagenic activities of electrostatically

Table I. Exhaust Emissions from the Model Diesel Engine

compound	composition by vol	total exhaust emission rates	
		g/s	molecule/s
oxygen	9.9%	7.5×10^{-1}	1.4×10^{22}
carbon dioxide	8.0%	8.3×10^{-1}	1.1×10^{22}
water	9.0%	3.8×10^{-1}	1.3×10^{22}
nitrogen	73.1%	4.8	1.0×10^{23}
carbon monoxide	390 ppm	2.6×10^{-3}	5.6×10^{19}
hydrocarbons	643 ppm	2.4×10^{-3}	9.0×10^{19} [a]
nitric oxide	395 ppm	2.8×10^{-3}	5.6×10^{19}
nitrogen dioxide	73 ppm	7.9×10^{-4}	1.0×10^{19}
nitric acid[b]	0.7 ppm	7.9×10^{-6}	7.5×10^{16}
pyrene		5.3×10^{-7}	1.6×10^{15}
1-nitropyrene		6.0×10^{-9} [c]	1.5×10^{13}
particulate matter		1.7×10^{-3}	5.6×10^{13} [d] particles/s
total exhaust	100%	5.3 L/s	

[a] The hydrocarbons are assumed to be emitted as methane since the hot flame ionization detector is a carbon counting device. [b] The concentration of nitric acid is assumed to be 1% of the concentration of nitrogen dioxide (11). [c] This emission rate accounts for 10% of the observed direct mutagenic activity. [d] The particles are assumed to be spherical with a diameter of 360 Å and a density of 1.65 g/cm³.

precipitated particles and filtered particles may not be significant since no detailed chemical analyses of the extracts were performed (10).

In view of the difficulties associated with the design of an experiment to investigate the sampling artifactual contributions to the direct mutagenic activity of diesel particles, a theoretical study has been performed. Since diesel exhaust is extremely complex, we have based our study on published data from our laboratory augmented with measurements made for pyrene (14, 15). Since a simple kinetic study can be very complicated if every possible reaction is investigated, we have limited our discussion to formation of direct mutagens. Many studies have suggested that 1-nitropyrene is the major direct mutagen (93 μg/g in the particles) accounting for approximately 20% of the mutagenic activity present in diesel emissions (16). We have therefore based our discussion on formation of 1-nitropyrene.

Experimental Section

The experimental data used in this study have been published previously (14, 15). The particles were collected from the undiluted exhaust of a single-cylinder direct-injection diesel engine operated with a constant speed (2400 rpm) and full load. A pure hydrocarbon fuel (1:1 mixture of *n*-tetradecane and 2,2,4-trimethylpentane) and synthetic lubricant (UCON LB 525 poly(alkylene glycol)) were used in an attempt to simplify the chemistry and increase the reproducibility of the exhaust. The total exhaust emissions from this engine are presented in Table I.

Results and Discussion

Various studies have shown that polynuclear aromatic hydrocarbons are readily nitrated by nitric acid, and eq 1 is an overall reaction using pyrene as an example (11,

$$\text{pyrene} + HNO_3 \longrightarrow \text{1-nitropyrene} + H_2O \quad (1)$$
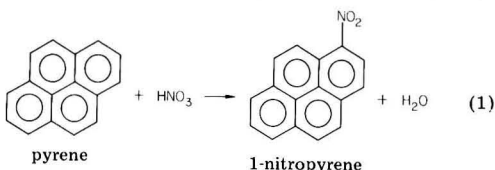
15). Other reaction products are possible, but these have been ignored. Also, it has been assumed that nitric acid is the nitrating species responsible for the formation of 1-nitropyrene from pyrene (eq 1), which is 1% of the concentration of nitrogen dioxide (11). If this type of reaction is responsible for the formation of the nitrated polynuclear aromatic hydrocarbons, it is possible to predict their rate of formation on the basis of collision theory kinetics. There are four distinct time periods when the nitrated polynuclear aromatic hydrocarbons can be produced: during the expansion and exhaust strokes; during the passage through the exhaust manifold and tailpipe; during dilution and cooling; during sampling on the collection media.

(a) Expansion and Exhaust Strokes. The single-cylinder four-cycle diesel engine was operated at a constant load (full rack) and speed (2400 rpm), and the peak cylinder pressure was found to be 54 atm (15). Since the expansion stroke and the exhaust stroke each occur in 0.0125 s, the maximum time for the reaction of pyrene with nitric acid is 0.025 s. For the purpose of this discussion, it has been assumed that 1-nitropyrene can be produced only by collision between pyrene and nitric acid, the pyrene being synthesized prior to this reaction. The synthesis of pyrene has been postulated to involve the free-radical polymerization of short-chain hydrocarbon species; this involves a number of successive collisions (17-22). Therefore, most of the available reaction time will be spent in the synthesis of the pyrene molecule. The rate of formation of 1-nitropyrene will be small since the concentration of pyrene is low. However, the assumption that nitrated polynuclear aromatic hydrocarbons are formed only after the PAHs have been synthesized may not be valid, since the free-radical intermediates could be nitrated prior to ring closure. It is difficult to determine the probability of the latter reactions, hence they have been ignored in the subsequent discussion. Their contribution may be significant since a number of free-radical intermediates are involved and the probability of nitration during the synthesis will be large.

(b) Manifold and Tailpipe. The temperature of the exhaust decreases after it leaves the cylinder prior to its emission via the tailpipe into the ambient air. During this time the gas-phase molecules will collide, and the collision frequency will be dependent upon their relative velocities (i.e., exhaust temperature). Therefore, by use of simple bimolecular collision theory, it is possible to obtain the rate of the formation of 1-nitropyrene from the collision of pyrene with nitric acid.

(c) Dilution and Cooling. Similarly, the simple bimolecular collision theory can be used to obtain the rate of the formation of 1-nitropyrene during dilution and cooling, providing that the dilution factor is known.

(d) Collection on the Filter Media. The rate of formation of 1-nitropyrene increases as a function of time since the pyrene molecules sorbed on the surface of particles are collected by the filter: this reaction can also be considered by the simple bimolecular collision theory.

Bimolecular Collision Theory

Manifold and Tailpipe Reactions. (i) Gas-Phase Reaction of Nitric Acid and Pyrene in the Exhaust Manifold and Tailpipe. The rate of formation of 1-nitropyrene ($d[N]/dt$) equals the number of collisions per second (Z_g) multiplied by the chance of the collision having energy greater than or equal to the activation energy of the reaction (E_g).

The calculation and assumptions are summarized in the Appendix. If every collision produces a molecule ($E_g = 0$),

then the maximum rate of production for 1-nitropyrene by gaseous reaction of pyrene with nitric acid is 1×10^{15} molecule/(cm³ s).

In addition to collisions between gas-phase molecules, pyrene molecules are expected to collide with particles and condense or sorb onto their surfaces. The surface areas and activities of diesel particles have been reported recently, and these studies have shown that diesel particles collect gas-phase molecules efficiently (8, 23). This process will have the effect of decreasing the rate of formation of 1-nitropyrene since the effective velocity of pyrene molecules sorbed on particles is equal to the exhaust gas flow rate and is not dependent upon the gas temperature. Although there is a much greater probability of pyrene colliding with a nitric acid molecule than with a particle (1000:1), this is compensated for by the particle cross section being greater than the collision cross section of the nitric acid molecule (23:1). In addition, the collision between a gas-phase molecule of nitric acid and a particle-bound pyrene molecule will have a lower probability since it requires two separate collisions or a three-body collision.

(ii) Gas-Phase Collision between Pyrene and a Particle. Rate of formation of a particle-adsorbed pyrene molecule (d[Pa]/(dt) equals number of collisions per second (Z_p) multiplied by the chance of the collision having energy less than or equal to the adsorption energy of pyrene onto the particle (E_p); (see Appendix).

Similarly, if every collision produces a sorbed pyrene molecule, then the maximum rate with which pyrene is sorbed onto the surface of the particles by gas phase collision is 2×10^{-5} molecule/(cm³ s), and its magnitude suggests it is not important. However, this result is extremely significant for other reasons since it suggests that some of the gas-phase molecules are not sorbed onto the surface of the particle by gas-phase collisions: sorption occurs as a result of sampling (25).

(iii) Gas-Phase Reaction of Nitric Acid and Pyrene after Dilution and Cooling. A similar approach can be used to estimate the rate of formation of 1-nitropyrene by the gaseous collision of pyrene and nitric acid after dilution and cooling (Appendix).

Similarly, the maximum rate of production for 1-nitropyrene by gaseous reaction of pyrene and nitric acid after dilution is 1×10^{13} molecule/(cm³ s).

Collection on the Filter Media

Gas-Phase Reaction of Nitric Acid with Pyrene Sorbed on Particles Deposited on a Filter. Rate of formation of 1-nitropyrene equals the number of collisions per second multiplied by chance of the collision having energy greater than or equal to the activation energy of the reaction. This rate is given by

$$d[N]/dt = Z_{HPA} \exp(-E_a/RT) \tag{2}$$

and

$$Z_{HPA} = DHQ_F X \tag{3}$$

where Q_F is the flow rate of exhaust passing through the filter (cubic centimeters per second), X is the probability of a collision between nitric acid and pyrene molecules, E_a is the activation energy of this reaction, and T is the temperature of the filter (K).

If P is the concentration of pyrene in the exhaust (molecules per cubic centimeter) and G is the probability that a pyrene molecule will collide with the filter or a collected particle, then p_t is the quantity of pyrene collected by the filter at time t or

$$p_t = \int_0^t PQ_F DG \, dt \tag{4}$$

If we assume that the particles are collected with 100% efficiency by the filtering medium and that pyrene molecules are collected if they collide with the filter or a collected particle, then the probability that a pyrene molecule is collected at time t, $G(t)$, is

$$G(t) = (Y + SDVtQ_F)/F \tag{5}$$

where Y is the projected area of the filter responsible for collection (square centimeters), V is the cross section of a particle (square centimeters per particle), and F is the cross-sectional area of the filter (square centimeters). Equation 5 is valid since the vapor pressure of pyrene is low and its heat of adsorption is high. It is possible to determine how rapidly $G(t)$ approaches unity by using the following experimental data: $Y = 14.2 \text{ cm}^2$ (24), $S = 1.1 \times 10^{10}$ particles/cm³, $D = 0.1$, $Q_F = 9.0 \times 10^2 \text{ cm}^3/\text{s}$, $V = 1.0 \times 10^{-11} \text{ cm}^2/\text{particle}$, $F = 158 \text{ cm}^2$.

$G(t)$ approaches unity when $t = 15$ s. Therefore after 15 s pyrene is collected with approximately 100% efficiency.

On the basis of this result it is possible to evaluate eq 4 since P and Q_F are constant:

$$p_t = PQ_F D(t - 15) \tag{6}$$

If A is the cross section of a pyrene molecule (square centimeters per molecule) and A_t is the total cross section of pyrene at time t (square centimeters per filter), then

$$A_t = \int_0^t DAPQ_F \, dt = DPAQ_F(t - 15) \tag{7}$$

Therefore, it is possible to obtain an expression for the probability of a collision between nitric acid and pyrene molecules (X):

$$X = A_t/F \tag{8}$$

Substituting eq 7 and 8 into eq 3 provides the rate equation for the formation of 1-nitropyrene on the filter:

$$d[N]/dt = [D^2HPA(Q_F)^2(t - 15)/F] \exp(-E_a/RT) \tag{9}$$

It is possible to evaluate eq 9 by using parameters already used and $t = 9.00 \times 10^2$ s (maximum sampling time) and $A = 6.1 \times 10^{-15} \text{ cm}^2/\text{molecule}$:

$$d[N]/dt = 8 \times 10^{14} \exp(-E_a/RT) \text{ molecule/(filter s)}$$

Similarly, the maximum rate for the formation of 1-nitropyrene by the reaction of gaseous nitric acid with pyrene adsorbed on the particle collected by the filter is 8×10^{14} molecule/(filter s).

If the magnitudes of the activation energies for the formation of 1-nitropyrene are ignored, then the maximum rates for gas-phase and adsorbed-phase reactions are comparable. However, the activation energy for some surface reactions is much lower than for comparable gas-phase reactions (26); therefore, the 1-nitropyrene may be a sampling artifact.

Equation 2 has also assumed that, if a nitric acid molecule does not collide with a pyrene molecule, it passes through the filter unreacted. This is probably not valid since the adsorption of nitric oxide and nitrogen dioxide were found to be irreversible in the Henry's law region of the adsorption isotherm (27). These results suggest that nitric acid will also be adsorbed and may diffuse on the particle surface to react with adsorbed pyrene molecules. This could increase the rate of reaction on the filter by as much as $10^6(Q_F t)$.

Conclusions

This simple collision kinetic approach suggests that some of the direct microbial mutagenic activity of diesel particles

could be a sampling artifact. The experimental rate of emission of 1-nitropyrene is 1.5×10^{13} molecules/s, which is 10^2 less than the predicted maximum rates.

Acknowledgments

We thank the following people for their helpful comments: Julian P. Heicklen, James N. Pitts, Jr., Dennis Schuetzle, and David L. Swift.

Appendix. Calculations Based on Simple Collision Theory

General Equation:

$$d[N]/dt = Z \exp(-E/RT)$$

(i) Gas-Phase Reaction of Nitric Acid and Pyrene in the Exhaust Manifold and Tailpipe:

$$Z_g = \pi P H d^2 (8kT/\mu\pi)^{1/2}$$

where P is the concentration of pyrene (molecules per cubic centimeter), H is the concentration of nitric acid (molecules per cubic centimeter), d is the mean molecular diameter, $(dH + dp)/2$ (5.3×10^{-8} cm), T is the exhaust gas temperature (535 K), and μ is the reduced mass, $M_H M_P/(M_H + M_P)$ (8.34×10^{-23} g/molecule).
Therefore

$$d[N]/dt = 1.2 \times 10^{15} \exp(-E_g/RT) \text{ molecules}/(\text{cm}^3 \text{ s})$$

(ii) Gas-Phase Collision between Pyrene and a Particle:

$$Z_p = PS(9\pi^3 kT)^{1/2} (dP)^2 (dD)^3$$

where S is the concentration of particles (particles per cubic centimeter) and dD is the average diameter of a particle (centimeters).
Therefore

$$d[Pa]/dt = 2 \times 10^{-5} \exp(-E_p/RT) \text{ molecules}/(\text{cm}^3 \text{ s})$$

(iii) Gas-Phase Reaction of Nitric Acid and Pyrene after Dilution and Cooling. This is similar to (i) with the exception that P and H have been decreased by the dilution factor (1:10) and T is 325 K.
Therefore

$$d[N]/dt = 1 \times 10^{13} \exp(-E_g/RT) \text{ molecules}/(\text{cm}^3 \text{ s})$$

Registry No. 1-Nitropyrene, 5522-43-0; pyrene, 129-00-0; nitric acid, 7697-37-2; nitrogen dioxide, 10102-44-0; nitric oxide, 10102-43-9.

Literature Cited

(1) "Health Effects of Exposure to Diesel Exhaust"; National Research Council, National Academy of Sciences Press: Washington, D.C., 1981, and references cited therein.
(2) "Health Effects of Diesel Engine Emission: Proceedings of an International Symposium"; EPA-600/9-80-057 a and b; U.S. Environmental Protection Agency; 1980; Vol. 1, 2, and references cited therein.
(3) Lewtas, J., Ed. "Toxicological Effects of Emissions from Diesel Engines"; Elsevier: New York, 1982, and references cited therein.
(4) McCann, J.; Choi, E.; Yamasaki, E.; Ames, B. N. *Proc. Natl. Acad. Sci. U.S.A.* **1975**, *72*, 5135–5139.
(5) Schuetzle, D.; Riley, T.; Prater, T. J.; Harvey, T. M.; Hunt, D. F. *Anal. Chem.* **1982**, *54*, 265–271.
(6) Cuddihy, R. G.; McClellan, R. O.; Griffith, W. C.; Seiler, F. H.; Scott, B. R. In "Toxicological Effects of Emissions from Diesel Engines", Lewtas, J., Ed.; Elsevier: New York, 1982, p 353–367.
(7) Vostal, J. J. *Bull. N.Y. Acad. Med.* **1980**, *56*, 914–934.
(8) Ross, M. M.; Risby, T. H.; Steele, W. A.; Lestz, S. S.; Yasbin, R. E. *Colloids Surf.* **1982**, *5*, 17–31.
(9) Abraham, N. M.; Kim, C. S.; Januszkiewics, A. J.; Welker, M.; Mingle, M.; Schreck, R. *Arch. Environ. Health* **1980**, *35*, 77–80.
(10) Chan, T. L.; Lee, P. S.; Siak, J.-S. *Environ. Sci. Technol.* **1981**, *15*, 89–93.
(11) Pitts, J. N., Jr.; Cauwenberghe, K. A. V.; Grosjean, D.; Schmid, J. P.; Fritz, D. R.; Belser, W. L.; Knudson, G. B.; Knudson, P. M. *Science (Washington, D.C.)* **1978**, *202* 515–519.
(12) Pitts, J. N., Jr.; Lokensgard, D. M.; Ripley, P. S.; Cauwenberghe, K. A. V.; Vaeck, L. V.; Schaffer, S. D.; Thill, A. J.; Belser, W. L., Jr. *Science (Washington, D.C.)* **1980**, *210*, 1347–1349.
(13) Pitts, J. N., Jr.; Lokensgard, D. M.; Harger, W.; Fisher, T. S.; Mejia, V.; Schular, J. J.; Scorziell, G. M.; Katzenstein, Y. A.; *Mutat. Res.* **1982**, *103*, 241–249.
(14) Yergey, J. A.; Risby, T. H.; Lestz, S. S. *Anal. Chem.* **1982**, *54*, 354–357.
(15) Herr, J. D.; Dukovich, M.; Yergey, J. A.; Tejada, S. B.; Lestz, S. S.; Risby, T. H. In "Diesel Engine Combustion, Emissions and Particulates"; Society of Automobile Engineers P-107: Warrendale, PA, 1982, pp 311–321.
(16) Rosenkranz, H. S. *Mutat Res.* **1982**, *101*, 1–10.
(17) Badger, G. M.; Kimber, R. W. L.; Spotswood, T. M. *Nature (London)* **1960**, *187*, 663–665.
(18) Badger, G. M. *Natl. Cancer Inst. Monogr.* **1962**, *9*, 1–16.
(19) Ray, S. K.; Long, R. *Combust. Flame* **1964**, *8*, 139–151.
(20) Thomas, A. *Combust. Flame* **1962**, *6*, 46–62.
(21) Porter, G. *Symp. (Int.) Combust., [Proc.]* **1952**, *4*, 248–252.
(22) Latlaye, J.; Prado, G. *Water Air Soil Pollut.* **1974**, *3*, 473–481.
(23) Ross, M. M.; Risby, T. H.; Lestz, S. S.; Yasbin, R. E. *Environ. Sci. Technol.* **1982**, *16*, 75–78.
(24) Adiletta, J. G., Pallfex Products Corp., Putnam, CT, private communication, 1982.
(25) Risby, T. H.; Yasbin, R. E.; Lestz, S. S. *Environ. Int.* **1981**, *5*, 267–279.
(26) "Particulate Polycyclic Organic Matter"; National Academy of Sciences: Washington, D.C., 1972, and references cited therein.
(27) Ross, M. M.; Risby, T. H. Johns Hopkins University, Baltimore, MD, unpublished results, 1981.

Identity and Yields of Major Halogenated Products of Aquatic Fulvic Acid Chlorination

Russell F. Christman,* Daniel L. Norwood, David S. Millington, and J. Donald Johnson

Department of Environmental Sciences and Engineering, School of Public Health, University of North Carolina, Chapel Hill, North Carolina 27514

Alan A. Stevens

Municipal Environmental Research Laboratory, U.S. Environmental Protection Agency, Cincinnati, Ohio 45268

■ Chlorination of fulvic acid isolated from a natural surface water produces a variety of C_1 to C_4 aliphatic acids in addition to chloroform. Yields of the four principal reaction products, trichloroacetic acid, chloroform, dichloroacetic acid, and dichlorosuccinic acid are approximately 14 wt % of starting organic material and account for 53% of the total organic halogen. No halogenated aromatic products were identified. This appears to be the first reported quantitation of unambiguously identified major chlorination products, which accounts for the majority of the total organic halogen. An isotope dilution GC/MS method for the determination of aqueous trichloroacetic acid is also described.

Introduction

More than 150 million people in the U.S. ingest approximately 2 L/day of chlorinated drinking water derived from surface water or groundwater sources. Concern over possible adverse health effects of chlorination was heightened when the U.S. Environmental Protection Agency (USEPA) published the results of a national survey (1) that established that chloroform was ubiquitous in chlorinated drinking water, and the National Cancer Institute declared chloroform an animal carcinogen under the conditions of their bioassay (2). Prompted by these concerns, the USEPA issued a new regulation limiting the concentration of chloroform and its sister trihalomethanes to 100 μg/L (3). The intent of the regulation was to control not only trihalomethanes but also other associated byproducts as well (3, 4).

Various research reports have supported the hypothesis that natural product organic material (fulvic and humic acids) is the most common reaction precursor to trihalomethanes in natural water systems (5–7), although measured values for total chlorine demand and total organic halogen formed in water exposed to chlorine are greater than can be accounted for by the amounts of trihalomethanes formed (4, 8). These findings strongly suggest the presence of chlorinated reaction products other than chloroform and that some of the chlorine demand is exerted via oxidative reactions which do not covalently bind chlorine into reaction products. We have reported the qualitative identification of halogenated and nonhalogenated chlorination products of aquatic humic acid at high pH (9, 10) and of aquatic fulvic acid at neutral pH (11). Havlicek et al. (21) have reported numerous oxygenated and chlorinated products of chlorination of aquatic humic material. Quimby et al. (12) have also reported the tentative identification of several halogenated aliphatic and aromatic compounds after laboratory chlorination of soil humic and fulvic acids. Similar materials were tentatively identified in a local tapwater sample by these authors. Most recently, Miller and Uden (13) have shown that the relative composition of chloroform, di- and trichloroacetic acids, and chloral hydrate in chlorinated reaction mixtures

of soil fulvic acid is a function of pH, Cl_2/C molar ratio, and time.

We report here the unambiguous identification of those halogenated products we have found to be common in laboratory chlorinated solutions of humic and fulvic acid fractions of the organic material isolated from a natural surface water. Since fulvic acid is more abundant, we also report the yields of the four principal products found for this acid and the fraction of total organic halogen represented by these four products.

Experimental Procedures

Humic and fulvic acids utilized in this study were isolated from an eastern North Carolina surface water (Black Lake) by using methods previously reported (14, 15). Reaction conditions and experimental procedures for the qualitative analysis of chlorination byproducts from aquatic humic acid (high pH) and aquatic fulvic acid (neutral pH) have also been documented, along with the criteria utilized for component identification (10, 11). We wish to emphasize that although reaction times, pH (for fulvic acid), and temperature were similar to water treatment conditions, the chlorine to carbon molar ratios were significantly higher (4 vs. ~0.4) and total concentrations were very much higher than normal treatment conditions.

The strategy for the quantitative analysis of the principal chlorination products of the fulvic acid/neutral pH reaction took the following form: (1) quantify amounts in ether extracts of aqueous reaction mixtures; (2) measure the absolute amounts of the two most abundant components (chloroform and trichloroacetic acid) in the aqueous reaction mixtures; (3) compare these amounts with initial total organic carbon (TOC) and final total organic halogen (TOX). To carry out step 1, reactions were performed in a head-space free condition according to the parameters listed in Table IA. Table IB documents the generalized experimental sequence. Quantities of various components extracted were determined by adding known amounts of an internal standard (methyl p-chlorobenzoate) to ether extracts and measuring GC/MS peak area ratios derived from selected mass chromatograms (e.g., m/z 117/139 for methyl trichloroacetate). Actual weights were then calculated from standard curves. All chemical standards were of the highest purity commercially available and were used without further purification.

In step 2 the chloroform was determined by the method of Bellar and Lichtenburg (16). In order to determine the total trichloroacetic acid produced, an isotope dilution GC/MS method was developed which utilized trichloro-[^{13}C]acetic acid (KOR, Inc., Cambridge, MA) of 99% isotope purity as an internal standard. After reaction and quenching of excess chlorine, measured quantities of this material were added to 100-mL aliquots of aqueous reaction mixture to give a concentration of approximately 50 mg/L, and 30 min was allowed for equilibration with the

Table I. Summary of Relevant Experimental Parameters

(A) reaction conditions	(B) experimental sequence	(C) GC/MS conditions for quantification
fulvic acid, 900 mg/L HOCl/C, 4 pH, 7 time, 24 h temperature, ambient	(1) chlorination (24-h reaction time) (2) excess HOCl removed by sodium arsenite addition (3) aliquot (350 mL) acidified (pH 0.7 with HCl) (4) extracted (3 × 100 mL ether) (5) ether dried (liquid N_2, $MgSO_4$ equilibration overnight) (6) concentrated (9 mL, Kuderna-Danish apparatus) (7) aliquot methylated (ethereal CH_2N_2) (8) analyzed (GC/MS)	mode, EI (full scan), 70 eV electrons, 200-μA trap current, 4-kV accelerating voltage resolution, 1000 scan rate, 0.7 s/decade mass range, 350–50 cycle time, 1.1 s samples per peak, 8 injection, on column (1–1.5 μL) relative standard deviation (triplicate area ratios), 5% or less (generally)

sample matrix. The aqueous solutions were then extracted with one 100 mL volume of ether, and an aliquot of this extract was methylated and analyzed by GC/MS. Since so much trichloroacetic acid was produced, the drying and other concentration steps were eliminated (see Table IB). Peak area ratios from selected mass chromatograms were again utilized for standard curve generation and unknown measurement. In this case the ratio m/z 59/60 was chosen.

The GC/MS system consists of a VG Micromass 7070F double-focusing sector mass spectrometer of Nier-Johnson geometry (VG Analytical, Altrincham, Cheshire, U.K.) interfaced to an HP 5710A capillary gas chromatograph (Hewlett-Packard, Inc., Avondale, PA). The GC is equipped with an SGE OCI-2 on-column injector (Scientific Glass and Engineering, Austin, TX) and a 30-m DB-1 fused silica capillary column (J & W Scientific, Rancho Cordova, CA). Instrumental conditions for the qualitative studies have been previously reported (10, 11). Conditions employed for all quantitative experiments are listed in Table IC.

In step 3 total organic carbon measurements were derived from an elemental analysis of the solid fulvic acid (17). Total organic halogen was determined with an activated carbon adsorption procedure (18) and a Dohrmann microcoulometer system (Dohrmann, Inc., Santa Clara, CA).

Results and Discussion

More than 100 different reaction products were identified after independent chlorination of the humic and fulvic acid fractions, and significant differences were observed in the composition of the product mixtures of these fractions. The most notable difference was that most of the products of fulvic acid chlorination contained chlorine whereas most of the humic acid chlorination products did not. In both cases, however, chlorinated products were the most concentrated, and these were dominated by tri- and dichloroacetic acid, chloroform, and dichlorosuccinic and dichloromalonic acids. Chlorine-containing products common to both fulvic and humic acids are shown in Table II. Non-chlorine-containing products of each acid were similar to the polybasic aromatic and aliphatic acids we have reported from $KMnO_4$ oxidation (15).

It is evident from the data in Table II that a variety of nonvolatile aliphatic halogenated products result from the exposure of aquatic humic and fulvic acids to chlorine. The apparent dominance of the C_2 chlorinated acids is in agreement with the findings of Quimby et al. (12), who reported the tentative identification of trichloroacetic acid and halogenated phenols after soil extract chlorination, and Rook (19), who found that di- and trichloroacetic acids were the principal constituents in methylene chloride extracts of Rotterdam drinking water after breakpoint

Table II. Short-Chain Chlorination Products of Aquatic Humic and Fulvic Acids

$CHCl_3$	trichloromethane (chloroform)	a
$CHBrCl_2$	bromodichloromethane	a
CCl_3CHO	trichloroethanal (chloral)	a
H_2CClCO_2H	chloroethanoic acid (chloroacetic acid)	a
$HCCl_2CO_2H$	dichloroethanoic acid (dichloroacetic acid, DCA)	a
CCl_3CO_2H	trichloroethanoic acid (trichloroacetic acid, TCA)	a
$CH_3CCl_2CO_2H$	2,2-dichloropropanoic acid	a
$CCl_2=CHCO_2H$	3,3-dichloropropenoic acid	b
$CCl_2=CClCO_2H$	2,3,3-trichloropropenoic acid	c, d
$HO_2CCCl_2CO_2H$	dichloropropanedioic acid (dichloromalonic acid, DCM)	b
$HO_2C(CH_2)_2CO_2H$	butanedioic acid (succinic acid)	a
$HO_2CCH_2CHClCO_2H$	chlorobutanedioic acid (chlorosuccinic acid)	b
$HO_2CCCl_2CH_2CO_2H$	2,2-dichlorobutanedioic acid (α,α-dichlorosuccinic acid, DCS)	b
$HO_2CCH=CClCO_2H$	cis-chlorobutenedioic acid (chloromaleic acid)	a
$HO_2CCCl=CClCO_2H$	cis-dichlorobutenedioic acid (dichloromaleic acid)	a
$HO_2CCCl=CClCO_2H$	$trans$-dichlorobutenedioic acid (dichlorofumaric acid)	b

[a] Confirmed; EI spectrum, CI spectrum, accurate mass measurements, and GC retention time comparison with authentic specimen. [b] Confident; EI spectrum, CI spectrum, accurate mass measurements, no authentic specimen available. [c] Tentative; data relatively incomplete in some respect. [d] Observed only in fulvic acid samples.

Table III. Yields of Chlorination Products from Extracted Fulvic Acid (Black Lake)

| product	mg/g of FA	mg of C/g of FA	original TOC, %	final TOX, %
trichloroacetic acid[b]	90.3	13.3	3.0	32.1
$CHCl_3$[c]	38.2	3.8	0.8	17.3
dichloroacetic acid[d]	10.2	1.9	0.4	3.6[a]
dichlorosuccinic acid[d]	3.4	0.9	0.2	
total	142.1	19.9	4.4	53.0

[a] Sum of dichloroacetic and dichlorosuccinic acids. [b] As determined by isotope dilution GC/MS. [c] As determined by the method of Bellar and Lichtenburg (16). [d] Amounts recovered in the ether extract.

chlorination. Our results, however, do not show the presence of any halogenated aromatic products from chlorination of actual aquatic humic or fulvic acid.

Yield values resulting from quantitative measurements on the fulvic acid/neutral pH reaction are shown in Table
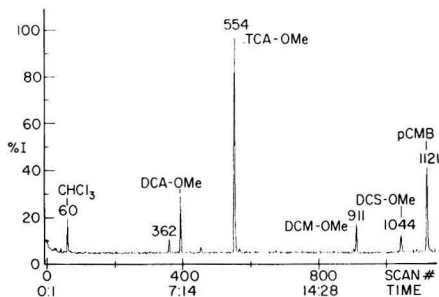
Figure 1. Reconstructed total ion chromatogram of a methylated ether extract derived from a neutral pH fulvic acid chlorination reaction (chloroform, CHCl₃; methyl dichloroacetate, DCA-OMe; methyl trichloroacetate, TCA-OMe; dimethyl dichloromalonate, DCM-OMe; dimethyl dichlorosuccinate, DCS-OMe; methyl p-chlorobenzoate, pCMB).
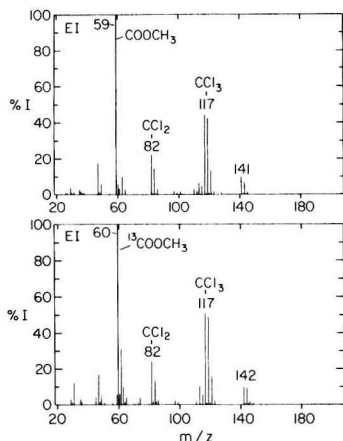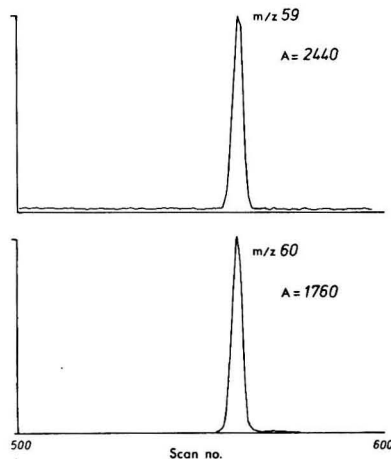

Figure 2. Electron ionization mass spectra of methyl trichloroacetate and methyl trichloro[¹³C]acetate.

Figure 3. Selected mass chromatograms of m/z 59 (methyl trichloroacetate) and m/z 60 (methyl trichloro[¹³C]acetate) derived from a total ion chromatogram such as that shown in Figure 1.

III and constitute the first report of the relative magnitudes of the four principal chlorination products of aquatic fulvic acid. These measurements are derived from reconstructed total ion chromatograms such as that shown in Figure 1. The confirmed dominance of trichloroacetic acid is in agreement with the findings of Quimby et al. (12), who utilized a somewhat different method for quantitative analysis (20). The yield values for the two minor products in Table III may be underestimated since they were determined only in the ether extract. Note that dichloromalonic acid was also present in reasonable amounts, but this structure was not confirmed, and no standard was available for quantitative analysis.

It is appropriate to comment on the relative merits of the isotope dilution GC/MS method vs. the Miller method (20). The latter involves the extraction, concentration, and recovery of 100% of the trichloroacetic acid in an aqueous sample with subsequent analysis by GC/microwave plasma emission. The microwave emission detector (MED) is operated in a chlorine-specific mode. Experiments were done to demonstrate that 100% recovery could be achieved for various amount of trichloroacetic acid spiked into laboratory water. Therefore, no true internal standard was utilized in the procedure.

In the isotope dilution method the internal standard is a stable isotopically labeled analogue of the compound of interest (Figure 2). Therefore, its chemical behavior through the extraction and concentration procedure should be the same as that of the unknown. Meticulous procedures necessary to ensure 100% recovery are not needed since any losses during workup are compensated for and the unknown/internal standard ratio remains constant. The use of isotopically labeled internal standards has not been demonstrated with the MED, and such demonstration is necessary since the two components (methyl trichloroacetate and methyl trichloro[¹³C]acetate) coelute on the capillary column (Figure 3).

If proper equilibration time is allowed, the internal standard should interact with the matrix to the same extent as the unknown, thus correcting for losses through adsorption to macromolecular material etc. Although Miller et al. have demonstrated 100% recovery of trichloroacetic acid from laboratory water, they report no recovery values from a true sample matrix.

We have determined for our sample matrix that there is no difference in recovery between trichloro[¹³C]acetic acid and unlabeled trichloroacetic acid by reverse isotope dilution. In this sense, the procedure we report here has been validated.

Total organic halogen values were independently obtained on the quenched chlorinated fulvic acid solutions, and the concentrations of the four reaction products shown in Table III account for 53% of this value. However, only 4.4% of the original fulvic acid carbon can be accounted for. It may be presumptive to conclude that the total organic halogen method is responding to these same compounds.

Conclusions

It appears that aqueous chlorine is an effective degrader of natural product organic materials present in terrestrial water systems. If it can be shown that these results apply to normal water chlorination conditions, consumers of chlorinated drinking water may be ingesting a much wider range of halogenated organic molecules than heretofore imagined, and at least one of these (trichloroacetic acid) may be significantly more concentrated than chloroform.

Acknowledgments

thank Ronald Dressman, U.S. EPA, Cincinnati, OH, for performing the total organic halogen measurements.

Literature Cited

(1) Symons, J. M.; Bellar, T. A.; Carswell, J. K.; De Marco, J.; Kropp, K. L.; Robeck, G. G.; Seeger, D. R.; Slocum, C. J.; Smith, B. L.; Stevens, A. A. *J.—Am. Water Works Assoc.* **1975**, *67*, 634-647.

(2) "Report on Carcinogenesis Bioassay of Chloroform"; National Cancer Institute: Washington, DC, 1976.

(3) National Interim Primary Drinking Water Regulations. *Fed. Regist.* **1979**, *44*, 68624–68707.

(4) Cotruvo, J. *Environ. Sci. Technol.* **1981**, *15*, 268.

(5) Rook, J. J. *Water Treat. Exam.* **1974**, *23*, 234–243.

(6) Stevens, A. A.; Slocum, C. J.; Seeger, D. R.; Robeck, G. G. *J.—Am. Water Works Assoc.* **1976**, *68*, 615.

(7) Babcock, D. B.; Singer, P. C. *J.—Am. Water Works Assoc.* **1979**, *71*, 149.

(8) Morris, J. C.; Baum, B. In "Water Chlorination: Environmental Impact and Health Effects"; Jolley, R. L., et al., Eds.; Ann Arbor Science: Ann Arbor, MI, 1978; Vol. 2, pp 29–48.

(9) Christman, R. F.; Johnson, J. D.; Pfaender, F. K.; Norwood, D. L.; Webb, M. R.; Hass, J. R.; Bobenrieth, M. J. In "Water Chlorination: Environmental Impact and Health Effects"; Jolley, R. L., et al., Eds.; Ann Arbor Science: Ann Arbor, MI, 1980; Vol. 3, Chapter 7.

(10) Johnson, J. D.; Christman, R. F.; Norwood, D. L.; Millington, D. S. *Environ. Health Perspect.* **1982**, *46*, 63–71.

(11) Norwood, D. L.; Johnson, J. D.; Christman, R. F.; Millington, D. S. In "Water Chlorination: Environmental Impact and Health Effects"; Jolley, R. L., et al., Eds.; Ann Arbor Science: Ann Arbor, MI, 1983; Vol. 4, Chapter 13.

(12) Quimby, B. D.; Delaney, M. F.; Uden, P. C.; Barnes, R. M. *Anal. Chem.* **1980**, *52*, 259–263.

(13) Miller, J. W.; Uden, P. C. *Environ. Sci. Technol.* **1983**, *17*, 150–157.

(14) Christman, R. F.; Liao, W. T.; Millington, D. S.; Johnson, J. D. In "Advances in the Identification and Analysis of Organic Pollutants in Water"; Keith, L. H., Ed.; Ann Arbor Science: Ann Arbor, MI, 1981; Vol. 2, Chapter 49.

(15) Liao, W. T.; Christman, R. F.; Johnson, J. D.; Millington, D. S.; Hass, J. R. *Environ. Sci. Technol.* **1982**, *16*, 403–410.

(16) Bellar, T. A.; Lichtenberg, J. J. *J.—Am. Water Works Assoc.* **1974**, *66*, 739–744.

(17) Liao, W. T. Ph.D. Dissertation, University of North Carolina, 1981.

(18) "Total Organic Halide. Interim Method 450.1"; Environmental Monitoring and Support Laboratory, U.S. Environmental Protection Agency: Cincinnati, OH, 1980.

(19) Rook, J. J. In "Water Chlorination: Environmental Impact and Health Effects"; Jolley, R. L., et al., Eds.; Ann Arbor Science: Ann Arbor, MI, 1980; Vol. 3, Chapter 8.

(20) Miller, J. W.; Uden, P. C.; Barnes, R. M. *Anal. Chem.* **1982**, *54*, 485–488.

(21) Havlicek, S. C.; Reuter, J. H.; Ingols, R. S.; Ghosal, M.; Lupton, J. D.; Stratton, L. W.; Rolls, J. W. "Identification of major and minor Classes of Natural Organic Substances Found in Drinking Water". Final progress report submitted to the U.S. Environmental Protection Agency, 1980.

Degradation of Chloroform by Photoassisted Heterogeneous Catalysis in Dilute Aqueous Suspensions of Titanium Dioxide

Ann Lorette Pruden† and **David F. Ollis*‡**

Department of Chemical Engineering, Princeton University, Princeton, New Jersey 08544

■ The complete mineralization of trichloromethane (chloroform) to inorganic products is demonstrated with heterogeneous photoassisted catalysis by using near-UV-illuminated TiO₂ aqueous slurries.

Introduction

Chloroform was studied because it is the major haloform produced from organic matter during the disinfection of municipal waters by chlorination (*1–3*) and because it is a suspected carcinogen (*4*). Disappearance of polychlorinated biphenyl (*5*) and of *p*-dichlorobenzene (*6*) from aqueous solutions of UV-illuminated TiO₂ slurries has been reported; in neither case was a chlorine mass balance or product identification established. In this paper, we report the *complete* degradation of chloroform (CHCl₃) to hydrogen chloride ion and carbon dioxide by dilute aqueous suspensions (0.1 wt %) of a heterogeneous photoassisted catalyst, titanium dioxide.

Experimental Procedures

The reactions were carried out in a batch reactor (Figure 1) constructed of glass and Teflon (*7*). A 0.1 wt % aqueous slurry of titanium dioxide was recirculated with a polypropylene/ceramic pump. The catalyst was Fisher certified grade TiO₂ (Lot no. 745547) with a surface area of 7 m²/g, as determined from B.E.T. nitrogen adsorption (*8*). The catalyst loading and illumination intensity were held constant at 0.1 wt % TiO₂ and 6.6×10^{-4} einstein/min, respectively. The illumination wavelength range of the "black light" fluorescent bulbs (GE BLB-15W) was predominantly 320–440 nm, with virtually no emission below 300 nm or above 500 nm. Freshly boiled distilled deionized water was stripped with helium in the reactors to diminish CO₂ and O₂ before the catalyst and chloroform were added.

Chloroform was Baker analyzed reagent grade, supplied with ~0.6 wt % ethanol as stabilizer (weight percent was estimated by gas chromatography (GC) analysis, assuming detector response factor for ethanol and methanol is equal). Its solubility in water at 20–25 °C and 1 atm total pressure is 8.2×10^3 mg/L, about 8200 ppm (*9*). In 150 ppm aqueous CHCl₃ solution, only trace ethanol, CHCl₃, and

† Present address: Mobil Research and Development Laboratory, Pennington, Princeton, NJ 08540.

‡ Present address: Chemical Engineering Department, University of California, Davis, CA 95616.
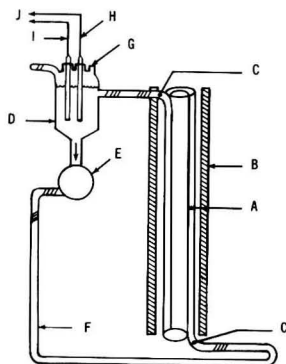
Figure 1. Recirculating, differential conversion photoreactor. (A) Quartz annular photoreactor; (B) black lights parallel to reactor axis (7 GE BLB (15 W each)); (C) thermocouple; (D) pyrex sampling vessel; (E) centrifugal recirculation pump; (F) Teflon tubing; (G) sampling port with Teflon-faced septum; (H) chloride ion electrode; (I) reference electrode; (J) millivoltmeter.
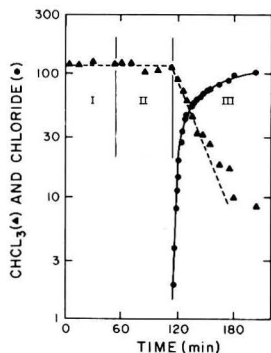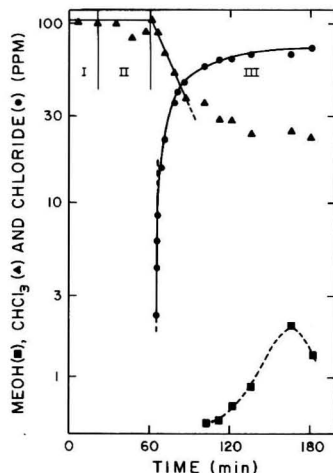

Figure 2. Photocatalyzed degradation of chloroform (run A1, initial [Cl⁻] < 2 ppm; initial [CHCl₃] = 122 ppm). Regions: I, illumination, no TiO₂ catalyst; II, TiO₂ catalyst, no illumination; III, illumination and TiO₂ catalyst present simultaneously. Chloroform (▲) and chloride (●).

an unidentified contaminant eluting at ~7 min (120 °C isothermal operation, 15 cm³/min He carrier gas) appeared as new peaks in the GC trace compared to analyses of distilled water and laboratory air (7). A small peak appeared during reaction, as noted by GC-FID; it was identified by retention time comparison (0.53 min) with a known sample such as methanol, and the identification was confirmed in the final reaction mixture of run A by purge and trap analysis with gas chromatography–mass spectrometry (GC–MS). (The liquid sample was purged with an inert gas and the resultant effluent passed through a Tenax/silica gel column. The trapped organics were then desorbed into the GC–MS by heating the trap.) The maximum methanol concentration was about 3.5 ppm.

Chloride ion was determined by in situ specific chloride electrode analysis (HNU Systems) and by silver nitrate titrations (9, 10), and carbon dioxide by barium carbonate precipitation. Chloroform does not absorb near-UV light as shown by its 100% transmission between 300 and 500 nm (7).

Results

In the presence of both TiO₂ slurries and near-UV illumination, CHCl₃ was rapidly dehalogenated (region III, Figures 2 and 3), while in the presence of either illumination (region I) or TiO₂ (region II) alone, no CHCl₃ dis-

Figure 3. Photocatalyzed degradation of chloroform (run B1, initial [Cl⁻] < 2 ppm; initial [CHCl₃] = 104 ppm). Regions I, II, and III as in Figure 2. Chloroform (▲), chloride (●), and methanol (■).

Table 1. Chloroform Conversion to Chloride

run no.	initial concn of CHCl₃, ppm	fraction of CHCl₃ converted	chlorine in CHCl₃ converted	chloride obsd, ppm	chlorine[a] recovery, %
A1	122	0.931	101	104	103.0
A2	112	0.445	45	46	102.2
B1	104	0.774	72	72	100.0
B2	135	0.874	105	109	103.8
				av:	102.3

[a] Chlorine recovery ≡ (chlorine contained in converted CHCl₃ × 100)/chloride observed in solution.

appearance or chloride production was observed.

For the CHCl₃ reactions with catalyst and illumination, complete dechlorination of converted chloroform was evident from the chlorine mass balances (Table I). The 3–5% uncertainty in chloride recovery was within the experimental error of the chloroform determinations.

Carbon dioxide product was confirmed by precipitate formation in the barium hydroxide trap. The only organic product noted by GC-FID or GC-MS in either the liquid or vapor phases of the reactor was methanol, which appeared and disappeared during illumination with TiO₂. The lower detection limit for methanol was estimated as ~0.05 ppm by assuming that the calibration curve was linear between 0 and 100 ppm. This estimate provides a lower bound of at least 99% on the ultimate conversion of organic carbon to carbon dioxide.

The total chlorine mass balances, the production of barium carbonate precipitate, and the disappearance of the trace methanol product observed show the complete degradation of chloroform to CO₂ and Cl⁻ at 34–44 °C in illumination aqueous suspensions of titanium dioxide.

Initial reaction rates for both chloroform degradation and chloride production were first order, as shown by the initial straight line behavior of the semilog plots (Figures 2 and 3); this apparent order changed with reaction extent. Trace methanol was detected by GC-FID in Figure 3 but was observed only by GC-MS (at ~100 ppb) for Figure 2. The reaction could be continued by adding chloroform (to 120 ppm) to the final reaction mixture of Figure 3, after overnight shutdown (lamps off, continuous recirculation).

Table II. Initial Conditions and Rates of Chloroform Degradation

run no.	initial concn, ppm		temp, °C	specific rate,[a] μmol·cm^{-2}·min^{-1}	turnover no.,[b] molecules· site^{-1}·s^{-1}	specific rate/ photon absorbed,[c] μmol·cm^{-2}· min^{-1}·(μmol of photon)$^{-1}$	app first-order rate constant, k_{CHCl_3}, min^{-1}[d]
	CHCl$_3$	Cl					
A1	122	<2	36 ± 2	6.2×10^{-4}	1.3×10^{-2}	9.5×10^{-7}	0.044
B1	104	<2	35 ± 5	5.2×10^{-4}	1.1×10^{-2}	7.9×10^{-7}	0.041
B2	135	58	38 ± 1	0.6×10^{-4}	0.1×10^{-2}	0.9×10^{-7}	0.004
B3	99	7	45 ± 1	1.4×10^{-4}	0.3×10^{-2}	2.1×10^{-7}	0.012

[a] Based on measured surface are, 7 m^2/g. [b] Based on assumed surface site concentration of 5×10^{14}/cm^2. [c] Based on photons absorbed by actinometer solution 660 μmol/min. [d] CHCl$_3$ disappearance.
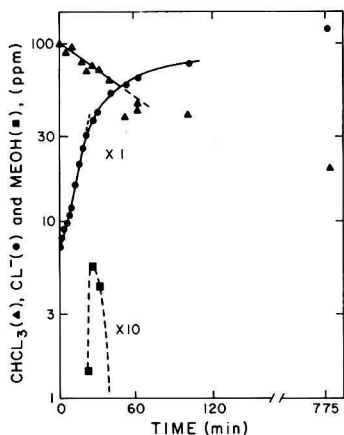

Figure 4. Photocatalyzed degradation of chloroform (run B3, initial [Cl$^-$] = 7 ppm; initial [CHCl$_3$] = 99 ppm). Catalyst from run B2 filtered and placed in distilled water for 2 h, prior to commencing reaction. Data: Chloroform (▲), chloride (●), and methanol (■). (Catalyst and illumination present at all times.)

The subsequent final pH achieved was 3.48. The half-life of chloroform in solution with 58 ppm initial chloride was 170 min, while in the absence of initial chloride the half-life was 16 min (Figure 3).

The catalyst from Figure 3 andd the subsequent 120 ppm experiment described above was filtered and replaced in the reactor with distilled water. Two hours was allowed for equilibrium to be established for chlorine adsorption and desorption, to give 7 ppm Cl$^-$ at a temperature of 46 ± 1 °C in the slurry. Figure 4 indicated a higher rate of subsequent reaction. It appears from these experiments of Figures 3 and 4 that the H$^+$ or Cl$^-$ products in solution inhibit the chloroform degradation reaction.

The kinetic parameters evaluated from Figures 2–4 and the 120 ppm addition experiment are collected in Table II. The specific rates and estimated turnover numbers are shown, as well as the specific rates referreds to unit photon absorption. (Turnover number equals molecules converted per surface atom (Ti or O) per second.) The apparent first-order rate constants were calculated from the initial slopes of these figures.

The turnover numbers are typical of those calculated for other photoassisted reactions in the literature and those measured for trichloroethylene in this study (7, 11, 12): near 10^{-2} molecules·site^{-1}·s^{-1} in chloride-free solutions. The specific rates per photon absorbed by the actinometer are ($\sim$1–10) $\times$ 10^{-7} μmol·cm^{-2}·min^{-1}·(μmol of photon)$^{-1}$. Total turnovers of $\sim$36 and $\sim$98 were demonstrated for chloroform and chloride, respectively, indicating that the reaction is catalytic (13).

Quantum efficiencies ((molecules of CHCl$_3$ converted/photon entering slurry-free reactor) $\times$ 100) obtained from the initial rates of Figures 2 and 3 were 3.9 and 3.3%, respectively.

The initial deaeration with helium stripping removes most but not all dissolved O$_2$. Moreover, addition of the TiO$_2$ catalyst adds O$_2$ to the system in two ways: as O$_2$ (gas) when the reactor (Figure 1) is opened and as O (adsorbed) on the TiO$_2$ surface. A subsequent study with CHCl$_3$ and other halomethanes (14) indicates unequivocally a requirement for O$_2$ in order that CHCl$_3$ conversion occur. A useful stoichiometry for this novel heterogeneous photocatalytic conversion may therefore be written as

$$CHCl_3 + H_2O + {}^1/_2O_2 \rightarrow CO_2 + 3HCl \qquad (1)$$
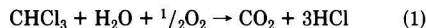
Discussion

The complete dehalogenation of chloroform to chloride and the appearance of carbon dioxide together with ultimate disappearance of the trace methanol noted during reaction indicate the *complete mineralization* of this haloform by photoassisted heterogeneous catalysis with TiO$_2$. We note that the chloride balance achieved by considering only chloride ion product (eq 1) precludes the production of significant amounts of any other chlorine-containing products, e.g., Cl$_2$ or HOCl. Chloride ion oxidation is not observed in UV-illuminated slurries of TiO$_2$, even in the presence of molecular oxygen (15). Significant conversion of CHCl$_3$ to carbon monoxide would have resulted in evolution of permanent gas, which was not observed.

Kinetics. The kinetics of chloromethane conversions, including trichloromethane, dichloromethane, and carbon tetrachloride, are discussed elsewhere (11).

Potential Applications

A recent bibliography (16) of degradation methods for carcinogenic chemicals including aliphatic halides and vinyl chloride cites pyrolysis, oxidation, microbial action, natural hydrolysis, ozonation, and homogeneous photodecomposition as possibilities. Application of these methods to water treatment seems impractical. High-temperature pyrolysis and oxidation (thermal or catalytic) are not suited for the low concentrations (<100 ppb) of chlorinated hydrocarbons permitted in drinking water. Both microbial degradation and natural hydrolysis are typically very slow, occurring over months to years. The major disadvantage of homogeneous photodecomposition, aside from the high energy photons required (typically <300 nm), is the lack of total degradation of the pollutant (17). Ozonation does not always lead to complete organic degradation, as noted in the ozonation of phenol in wastewaters (18) and in a review of ozone treatment in drinking water (19). Ozonation in combination with UV treatment (20, 21) has been suggested; the obvious disadvantages there lies in the use

of two energy intensive sources, neither of which effect the complete degradation desired.

In addition to halomethane formation in water chlorination, we note that a recent groundwater and surface water analysis (22) published in this journal reported routine detection of trace quantities of chloromethanes (chloroform, carbon tetrachloride) and a chloroethylene (trichloroethylene). Given the photocatalyzed mineralization of trichloroethylene (7, 11, 12), of $CHCl_3$ (this paper), and of other chloromethanes a (14), a potential exists for the application of heterogeneous photoassisted catalysis in removal of these trace chlorinated hydrocarbons from water. The reaction conditions are mild, and the reaction times may be modest compared to other schemes. The questions raised in this study concerning pH effects and chloride ion influences require further study before the full potential of such a process for water treatment can be assessed.

Acknowledgments

Literature Cited

(1) Rook, J. J. *Water Treat. Exam.* **1974**, *23*, 234–243.
(2) Bellar, T. A.; Lichtenberg, J. J.; Kroner, R. D. *J.—Am. Water Works Assoc.* **1974**, *66*, 703.
(3) Oliver, B. G.; Lawrence, J. *J.—Am. Water Works Assoc.* **1979**, *71*, 161–163.
(4) *Annual Report on Carcinogenesis Bioassy of Chloroform*"; National Cancer Institute: Bethesda, MD, 1976.
(5) Carey, J. H.; Lawrence, J.; Tosine, H. M. *Bull. Environ. Contam. Toxicol.* **1976**, *16*, 697.
(6) Oliver, B. G.; Cosgrove, E. G.; Carey, J. H. *Environ. Sci. Technol.* **1979**, *13*, 1075.
(7) Pruden, A. L. Ph.D. Thesis, Princeton University, Princeton, NJ, 1981.
(8) Strier, M. P. *Environ. Sci. Technol.* **1980**, *14*, 28–31.
(9) Kolthoff, I. M.; Sandell, E. B. "Textbook of Quantitative Analysis", 3rd ed.; Macmillian: New York, 1952; p 542ff.
(10) "Standard Methods for the Examination of Water and Wastewater", 13th ed.; Taras, M. J. Ed.; American Public Health Association: New York, 1971; p 96ff.
(11) Pruden, A. L.; Ollis, D. F. *J. Catal.*, in press.
(12) Ollis, D. F.; Pruden, A. L., Conference Heterogeneous Catalysis in Atmospheric Chemistry, Albany, NY, June 1981.
(13) Childs, A. L.; Ollis, D. F. *J. Catal.* **1981**, *67*, 35.
(14) Hsiao, C.-Y.; Lee, C.-L.; Ollis, D. F. *J. Catal.*, in press.
(15) Herrman, J. M.; Pichat, P. *J. Chem. Soc., Faraday Trans. 1* **1980**, *76*, 1138.
(16) Stein, M. W.; Sansone, E. B. "Degradation of Chemical Carcinogens"; Van Nostrand Reinhold: New York, 1980; pp 47–87, 113–126, 158–170.
(17) Faust, S. D. Adv. *Environ. Sci. Technol.* **1977**, *8*, 65.
(18) Li, K. Y.; Kao, C. H.; Weeks, J. L., Jr. *AIChE J.* **1979**, *25*, 583–591.
(19) Lawrence, J.; Cappelli, F. P. *Sci. Total Environ.* **1977**, *7*, 99–108.
(20) *Chem. Eng.* [*Int. Ed.*] **1977**, *84*, 18.
(21) Prengle, H. W., Jr.; Hank, C. E.; Payne, J. E. *Proc—Forum Ozone Disinfect.* **1977**, 286–295.
(22) Page, G. W. *Environ. Sci. Technol.* **1981**, *15*, 1475.

Interactions of Poliovirus with Montmorillonite Clay in Phosphate-Buffered Saline

Vincent L. Vilker, * **Gerald C. Meronek, and Paul C. Butler**

Chemical Engineering Department, University of California, Los Angeles, California 90024

■ The interaction of poliovirus 1 (Sabin strain) with montmorillonite clay in phosphate-buffered saline (0.15 M, pH 7.3) at 20 °C has been investigated. Clay aggregation is shown to accompany adsorption in certain ranges of clay/virus/electrolyte concentration ratios. This may have important implications on the use of isotherms determined in agitated batch electrolyte solutions for predicting virus movement in percolating soil beds where clay particles are restrained from forming aggregates. Scanning electron micrographs suggests that poliovirus adsorbs to the edges of 1-μm montmorillonite clay particles.

Introduction

The interactions of enteric viruses with soil clay minerals has important implications for the public health aspects associated with land application of municipal wastewater and sludges (1, 2). Adsorption of single virus particles to clay effectively detains the movement of these particles through soil beds. In addition, clay content has an essential role in determining soil hydraulic permeability which also significantly affects virus particle movement (3). It is also important to understand the extent of virus adsorption with clay minerals since these adsorbed viruses are thought to experience a lower rate of inactivation relative to the rate for unadsorbed virus (4, 5).

Previously, we have shown that an adsorption mass transfer model can lead to a prediction of the amount of virus which percolates through a soil bed and the amount which is adsorbed to the soil matrix (3). The analysis requires knowledge of soil permeability, soil composition, and the virus equilibrium distribution, that is, the adsorption isotherms between the percolating water and those components of the soil matrix which serve as adsorbents. This report describes the interaction between single particles of poliovirus 1 (Sabin) and montmorillonite clay in phosphate-buffered saline near neutral pH. The initial experiments were designed to obtain the first reported adsorption isotherm between an enteric virus and this prevalent soil–clay mineral. The large scatter in the measurements of adsorbed virus per mass of clay vs. virus concentration suggested that more detailed investigations of the virus–clay particle interactions were needed. These were performed with purified monodisperse poliovirus and chemically purified preparations of Na^+–montmorillonite which were fractionated to give monodisperse suspensions of 1–2 μm clay particles. Bright-field photomicroscopy and scanning electron microscopy were used to examine clay-virus interactions in agitated suspensions at adsorption equilibrium.

Isotherm Measurements

Virus adsorption isotherms are usually presented as graphs of log virus adsorbed per unit mass of solid sorbent (q) vs. log virus liquid-phase concentration (C_e) at ad-

0013-936X/83/0917-0631$01.50/0   © 1983 American Chemical Society

Environ. Sci. Technol., Vol. 17, No. 10, **1983** **631**

sorption equilibrium. In many studies of measured adsorption to whole soils, measurement precision suffers owing to the variability in adsorbent surface area for a mass of soil consisting of varying particle sizes (3).

Carlson et al. (6) investigated the uptake of poliovirus 1 (Sabin) and T2 bacteriophage by montmorillonite, kaolinite, and illite in electrolyte solutions of varying concentrations of either sodium chloride or calcium chloride. Clay particle size was controlled (but not measured) by isolating particles remaining in the supernatants after gravity settling of suspensions containing ground clay. Adsorption isotherms (q vs. C_e) were not obtained although a dependence of adsorption capacity on clay concentration was observed in the range 0.005–0.100 mg of clay/mL. This dependence, as well as observations of clay aggregation above certain minimum ionic strength, suggests that clay–clay particle interactions influenced their measurements of virus adsorption.

In our initial work to find the virus adsorption isotherm, dry montmorillonite clay powder (Wards Natural Science Establishment, catalog no. 46W0435 PAC) was suspended and agitated for 15 min in phosphate-buffered saline (PBS; ionic strength of 0.15 and pH 7.3 ± 0.1). Fine clay particles were obtained in supernatants remaining in 2–L graduated cylinders after settling times of 1, 4, or 15 h. These settling times are estimated to give particles of 5.6-, 2.8-, and 1.4-μm equivalent spherical diameters, respectively (7a). Poliovirus 1 (Sabin) suspensions in comparable PBS buffer were prepared from purified virus supplied by the UCLA Virology Department at 10^8 PFU/mL initial concentration.

Concentration of infective virus particles was determined by the plaque assay method which gives virus concentration in plaque-forming units (PFU). Primary tissue cultures of African green monkey kidney (AGMK) cells were used in the assay. Further details on the tissue culture and plaquing methods used here can be found in Hoskins (8) and Lennette and Schmidt (9).

Clay and virus solutions were diluted with additional PBS to attain desired initial concentrations. The solutions were mixed in a constant temperature (20 °C) gyrotary bath for 1 h to ensure adsorption equilibrium. Preliminary experiments showed that the rate of adsorption at these conditions was sufficiently rapid that equilibrium was achieved in about 30 min. After equilibration, clay particles were separated from the suspension by centrifugation at 25000g for 10 min. Control solutions containing virus in PBS without clay were run in parallel with each experiment in order to determine inactivation and centrifugation losses of virus infectivity. These losses averaged 30% of initial virus concentration for all experiments.

The adsorption isotherm shown with the measured results in Figure 1 was derived by linear regression analysis of the equation

$$\log q = n \log C_e + b$$

The regression coefficients were found to be $n = 1.0 \pm 0.2$ and $b = 2.3 \pm 0.6$. The large variability of these coefficients and the low value for the correlation coefficient ($r^2 = 0.71$) reflect the obvious wide scatter in the data of adsorption capacity. No correlation was found between adsorption capacity and the nominal clay particle sizes obtained by varying clay suspension settling time. A weak negative dependence of capacity on increasing clay concentration was found over the range 0.001–1.7 mg of clay/mL. This effect did not significantly improve the correlation between q and C_e and was much less significant than the decreasing adsorption capacity with increasing solid concentration which we have previously observed for poliovirus virus adsorption to activated sludge solids (10). The decreased
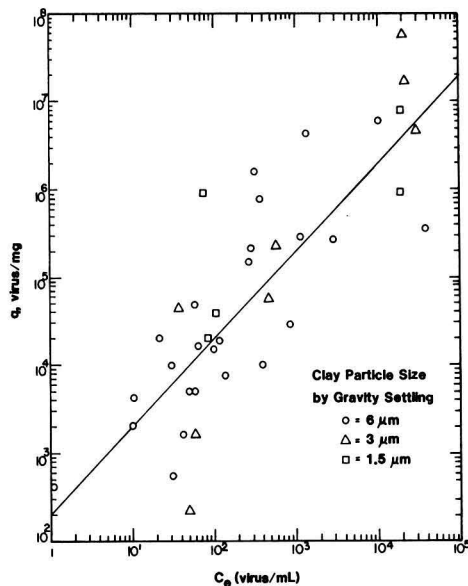

Figure 1. Poliovirus 1 (Sabin) adsorption to montmorillonite clay particles at 20 °C in 0.15 M phosphate-buffered saline solution, pH 7.3.

capacity of the sludge solids is thought to be caused by self-aggregation of the solids, thereby decreasing the available adsorption surface area per unit mass solids. Reasons for the large variability in adsorption capacity by clay were investigated in the experiments described in the next section.

Interaction with 1-μm Clay Particles

We sought to improve our understanding of particle interactions in clay–virus–PBS suspensions by examining individual clay particles isolated from solutions at adsorption equilibrium. Raw clay was suspended in water, dispersed in an ultrasonic bath, and fractionated by gravity sedimentation to eliminate agglomerates larger than 20 μm from the suspension. Clay particles in the supernatant were centrifuged, and the pellet was washed in a series of sodium acetate, hydrogen peroxide, and sodium citrate/ sodium bicarbonate solutions in order to remove soluble ions, trace organic material, and free iron oxides, respectively (7b). The 1–2-μm size fraction of the chemically treated clay was isolated by a series of centrifugation steps by using 50-mL polycarbonate centrifuge tubes in a Damon IEC HT centrifuge followed by sonication for pellet redispersion (7c). Final yield of the 1–2-μm particles was estimated to be about 1% of the initial bentonite mass. Clay particles were sterilized and stored in sodium carbonate solution at pH 9.5 and 4 °C. Monodisperse, uniformly sized particles were readily obtained from this preparation by mild sonication before an aliquot was withdrawn for adsorption or coagulation studies. Clay particle size in the monodisperse suspension was confirmed by microscopy at 640X magnification by using a calibrated eyepiece micrometer.

Solutions of monodisperse single virus particles were prepared from the purified preparations used in the adsorption studies by propagating new virus in secondary African green monkey kidney (AGMK) cell cultures (grown as monolayers on 57-cm^2 culture flasks) in Eagle' MEM (in Earle's BSS) supplemented with 10% heat-inactivated
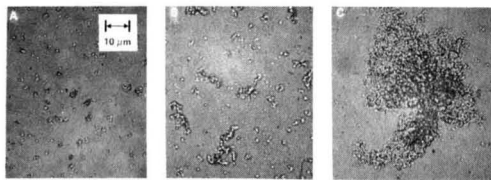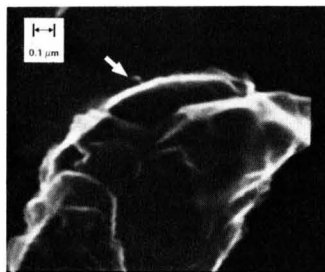
Figure 2. Photomicrographs of 1–2-μm montmorillonite clay particles [single particle size in (A)] suspended in solutions of phosphate-buffered saline (0.026 M, pH 7) and poliovirus (8 × 10^7 virus/mL) showing increasing aggregation with increasing clay concentration: (A) 0.028 mg of clay/mL; (B) 0.055 mg of clay/mL; (C) 0.080 mg of clay/mL.

Figure 3. Scanning electron micrograph (40000×) of spherical particle adsorbed to edge of probable clay particle. Particles were isolated from solution of 1-μm clay particles (0.31 mg/mL), 0.078 M NH$_4$HCO$_3$ (pH 8), and purified poliovirus (3.2 × 10^4 virus/mL). Carbon-coating thickness was estimated to be 65 Å from other electron micrographs of coated latex spheres of known diameter. Spherical particle diameter is 308 ± 128 Å, and clay particle width is 0.9 μm, after correction for carbon coating.

newborn calf serum, 1% L-glutamine, and 1% penicillin-streptomycin solution. Harvesting of virus after incubation for 2 days at 37 °C was done by the freeze/thaw method at the 3$^+$ CPE (cytopathic effect) stage as recommended by Hoskins (8). Cell debris was removed by centrifugation at 5000 rpm for 10 min at 4 °C on a Sorvall RC2-3 centrifuge by using a GSA rotor. The supernatant volume was about 2 L and had a virus titer of about 1.2 × 10^8 PFU/mL. Viral material was pelleted by centrifugation at 60 000 rpm for 1.5 h at 4 °C on a Beckman L5-65 ultracentrifuge by using a Ti type 70 rotor. The pellet was resuspended and washed by repeated pipetting in 1–2 mL of PBS. Residual cell debris and pellet material were removed by repeating the earlier low-speed centrifugation step. About 10 mL of recovered supernatant had an approximate titer of 10^{10} PFU/mL. This supernatant was further purified by isopycnic sedimentation in a cesium chloride gradient (11) on a Beckman L5-65 ultracentrifuge with a SW-27 rotor at 25 000 rpm and 4 °C for 72 h. The recovered virus band yielded 25 mL at about 3.5 × 10^9 PFU/mL. The purified virus was dialyzed against PBS for 24 h at 4 °C to remove the cesium ions. The final preparation, 28 mL at 2 × 10^9 PFU/mL titer, was stored at –20 °C. Poliovirus solutions prepared in this manner have been found to consist of mostly monodisperse single virus particles (12).

The interactions between clay and virus particles were first investigated by mixing solutions of clay, virus, and PBS in various ratios and examining small drops of the suspensions at 640× magnification with bright-field illumination. The result of the study in which poliovirus concentration at 8 × 10^7 PFU/mL and PBS concentration at 0.026 M were held constant is shown in Figure 2. A transition from nearly monodisperse clay particles to aggregates occurs as clay concentration is increased from 0.028 to 0.080 mg/mL. In the absence of virus, the clay particles remain unaggregated to at least 0.08 mg/mL at these conditions. Lowering virus concentration or raising PBS concentration relative to the conditions for Figure 2B also produced greater aggregation. In other studies at 0.15 M PBS, we have found that 1–2-μm clay particle suspensions remain monodisperse to concentrations of 0.4 mg of clay/mL with no virus present.

Our second investigation involved the use of scanning electron microscopy (SEM) to inspect single clay particles that were isolated from equilibrium virus–clay suspensions under conditions where clay aggregation was absent. Jakubowski reported an earlier unsuccessful attempt to examine poliovirus 1 adsorption to clay minerals in seawater by electron microscopy (13). We eliminated the problem of salt crystal interference in SEM sample preparation by sedimenting the poliovirus from PBS electrolyte and resuspending it in a solution of the volatile salt ammonium bicarbonate (NH$_4$HCO$_3$) (14). A small drop of an equilibrium mixture of virus and clay in NH$_4$HCO$_3$ solution

(0.078 M, pH 8.0) was placed on a prepared SEM sample holder and dried overnight in a vacuum desiccator. The samples were next coated with thin conductive layers of either gold, gold–palladium, or carbon. Electron micrograph quality varied with the several different coating materials. Gold and gold–palladium coatings gave the brightest images but the least reproducible coating thickness. Carbon coating gave darker images but more reproducible coating thickness as determined by coating and subsequent measurement of the images of polystyrene latex spheres of known diameter (850 ± 55 Å). The scanning electron micrograph of Figure 3 shows a carbon-coated image of a spherical particle attached to the edge of one or more overlapping platelike particles. Examination of the shape and size of these particles (by estimation of the thickness of carbon coating from measured coating thicknesses applied at the same time to polystyrene latex particles) gives strong indication that these are images of the virus adsorbed to the edge of a clay particle. The width of the clay particle is 0.9 μm, and the diameter of the spherical particle is 308 ± 128 Å. This diameter of the spherical particle agrees closely with the diameter of poliovirus, 280–300 Å (15). Similar inspections of 144 platelike particles from three different clay–virus–electrolyte preparations showed an average of one virus-sized spherical particle adsorbed for every 6$^1/_2$ clay particles. In each case the spherical particle was attached to an edge and in only one case was more than one spherical particle found on a clay particle. This adsorbed virus-to-clay particle ratio gives an estimate of $q = 3 × 10^7$ virus/mg which is within the range of the data shown in Figure 1 for the comparable value of C_e (~3 × 10^4 PFU/mL).

Conclusions

Montmorillonite clay is an important adsorbent for organic and biological substances found in many soils. The interactions between clay and virus particles in agitated electrolyte solutions can include aggregation of clay particles as well as simple adsorption of virus on clay surfaces. Such aggregation effects are likely to be absent when virus is adsorbed from solutions percolating through a soil matrix in which the clay particles are not free to form aggregates.

Both clay aggregation and virus adsorption to clay surfaces may be considered to result from electrostatic interactions among the two types of particles in electrolyte solutions near neutral pH. Mandel (16) has reported po-

liovirus isoelectric points at pHs 4.5 and 7.0 which indicate that the virus has a neutral or slightly negative charge at our experimental conditions. The net charge of montmorillonite particles is dominated by the negative charge of their silica surfaces, but regions of positive charges are located along edge surfaces due to the presence of aluminum ions (17a). Adsorption of negatively charged virus particles would be expected along these edge surfaces as suggested in our SEM observations. The use of aluminum ions for the precipitation of poliovirus from natural and treated waters (pH ~7) is well-known (18–20).

The destabilizing influence of long-chain polymer adsorption to particles of a clay suspension has been well-known for a long time (21). One way in which the adsorbed polymer is thought to affect colloid stability is by alteration of the electrical double layer structure. Aggregation of platelet particles will occur when the adsorbed layer is thicker than that of the electrical double layer, thereby permitting adjacent particles to approach one another at distances close enough for attractive van der Waals forces to dominate interparticle interactions (22). The compact poliovirus may exert a similar influence on the stability of our clay suspensions. It has also been observed that destabilization of montmorillonite sols passes through a maximum in the concentration of a second electrolyte when the anion of the second electrolyte is polyvalent (17b). This could be the explanation for our observation of increasing clay aggregation with decreasing poliovirus concentration. Our current research is directed to finding the range of concentrations for which aggregation is absent and to determining the poliovirus–clay adsorption isotherm at these conditions.

Registry No. Montmorillonite, 1318-93-0.

Literature Cited

(1) Vilker, V. L. In "Modeling Wastewater Renovation: Landtreatment"; Iskandar, I. K., Ed.; Wiley: New York, 1981; Chapter 9.
(2) Keswick, B. H.; Gerba, C. P. *Environ. Sci. Technol.* **1980**, *14*, 1290.
(3) Vilker, V. L.; Burge, W. D. *Water Res.* **1980**, *14*, 783.
(4) Stotzky, G. In "Microbial Adhesion to Surfaces"; Berkely, R. C. W., et al., Eds.; Society of Chemical Industry: London; Ellis Harwood Ltd.: Chichester, England, 1980; Chapter 13.
(5) Hurst, C. J.; Gerba, C. P.; Cech, I. *Appl. Environ. Microboil.* **1980**, *40*, 1067.
(6) Carlson, G. F., Jr.; Woodard, F. E.; Wentworth, D. F.; Sproul, O. J. *J. Water Pollut. Control Fed.* **1968**, *40*, R89.
(7) Jackson, M. L. "Soil Chemical Analysis—Advanced Course", 2nd ed.; Soils Science Department: University of Wisconsin, Madison, WI, 1965; (a) p 115, (b) Chapter 2, (c) p 152.
(8) Hoskins, J. M. "Virological Procedures"; Butterworths: London, 1967; 31.
(9) Lennette, E.; Schmidt, N., Eds. "Procedure for Viral and Rickettsial Infections", 4th ed.; American Public Health Association: New York, 1969; p 115.
(10) Vilker, V. L.; Kamdar, R. S.; Frommhagen, L. H. *Chem. Eng. Commun.* **1980**, *4*, 569.
(11) Frommhagen, L. H.; Martins, M. J. *Virology* **1961**, *15*, 30.
(12) Floyd, R.; Sharp, D. G. *Appl. Environ. Microbiol.* **1977**, *33*, 159.
(13) Jakubowski, W. *Bacteriol. Proc.* **1969**, V198.
(14) Schwerdt, C. E.; Fogh, F. *Virology* **1957**, *4*, 41.
(15) Davis, B. D. "Microbiology", 2nd ed.; Harper and Row: New York, 1973; p 1283.
(16) Mandel, B. *Virology* **1971**, *44*, 554.
(17) van Olphen, H. "An Introduction to Clay Colloid Chemistry", 2nd ed.; Wiley: New York, 1977; (a) pp 92–95, (b) pp 111–113.
(18) Wallis, C.; Henderson, M.; Melnick, J. L. *Appl. Microbiol.* **1972**, *23*, 476.
(19) Farrah, S. R.; Goyal, S. M.; Gerba, C. P.; Conklin, R. H.; Smith, E. H. *Appl. Environ. Microbiol.* **1978**, *35*, 360.
(20) Nielsen, A. L.; Lydholm, B. *Water Res.* **1980**, *14*, 175.
(21) Black, A. P.; Birkner, F. B.; Morgan, J. J. *J. Colloid Interface Sci.* **1966**, *21*, 626.
(22) Furusawa, K.; Tezuka, Y.; Watanabe, N. *J. Colloid Interface Sci.* **1980**, *73*, 21.
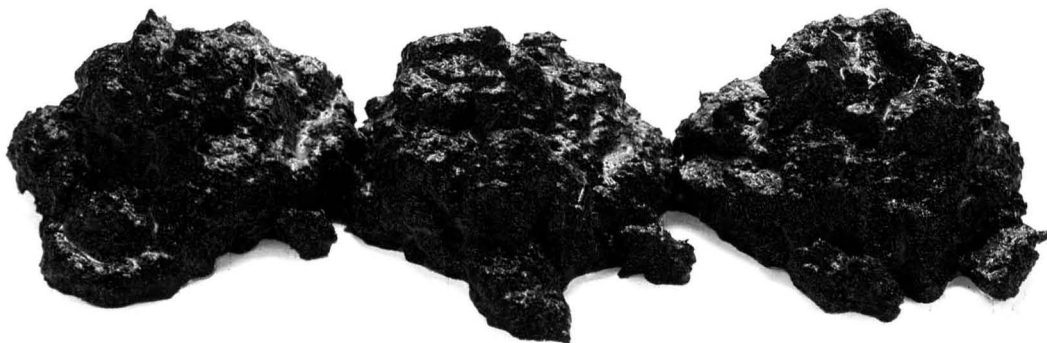
WILL THE REAL
2,3,7,8-TETRACHLORO-DIBENZO-P-DIOXIN SLUDGE
PLEASE STAND UP?

To tell the truth, if dioxins and other organic compounds just stood up and identified themselves, you wouldn't need analytical laboratories. But you do. Because you not only need to know *what* you're dealing with, but *what else* and *how much*.

That's where we come in. We're Mead CompuChem® Laboratories. We're here to tell you the truth about the constituents in every sample you send us.

Not only do we have one of the few laboratories willing to look at dioxins, but we can discriminate among *75 different* dioxins.

It's just a routine part of the wide range of analytical

services we offer. For example, our *Disposal Site Screening* can economically identify a wide variety of priority and other pollutants in wastes.

For air monitoring we offer *Diagnostic Air Screening* to confirm and quantify volatile organic compounds.

For permits and other purposes we test ground, surface, influent, effluent, point source, non-point waste and other waters.

And we back all those services with *Library Search*, to match the mass spectra of mystery compounds with choices from over 31,000 mass spectra from the National Bureau of Standards.

We also do *ICAP* analysis for heavy metals and other inorganics.

The truth is, no other analytical laboratory comes close to matching our capabilities at Mead CompuChem.® We have 24 GC/MS instruments — more than any other laboratory in the world. Our staff of experienced and degreed spectroscopists work around the clock, seven days a week, guided by quality assurance programs that set standards for the industry.

For the last word in compliance monitoring, get the truth from Mead CompuChem® Laboratories. The first name in environmental analysis.
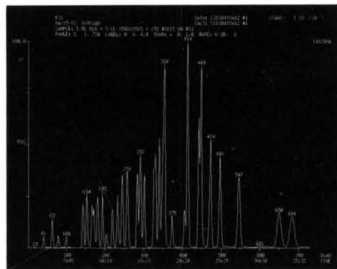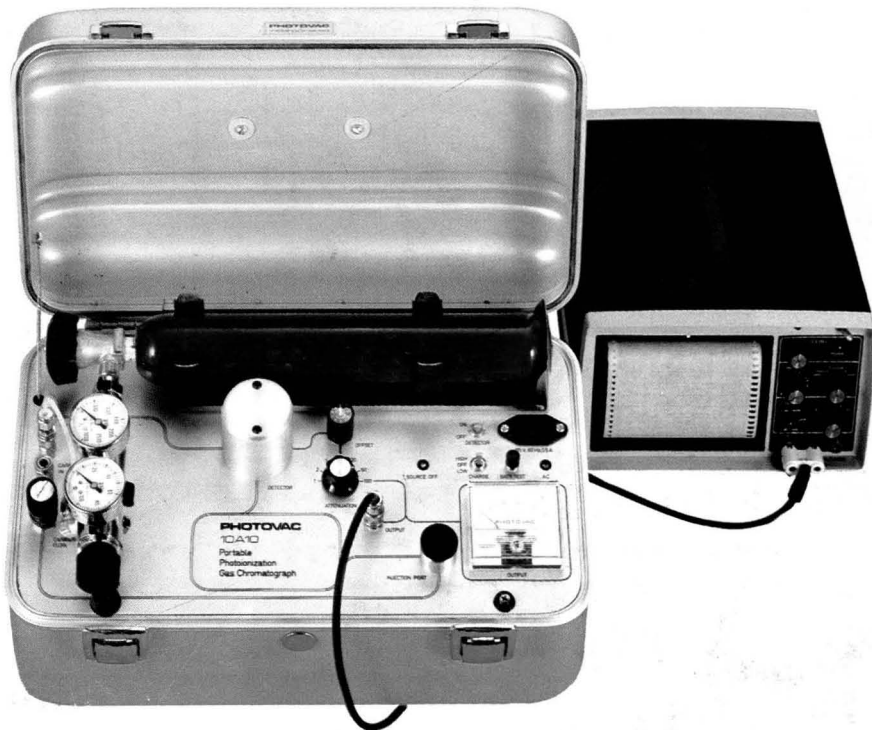

MeadCompuChem®
LABORATORIES

Absolute, Uncompromising Dedication to Quality Data

Call now at **800-334-8525** (in North Carolina call **919-549-8263**) or write
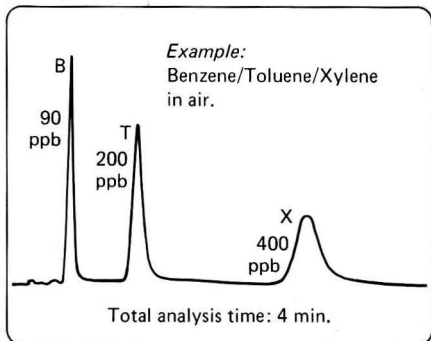**P.O. Box 12652, Research Triangle Park, NC 27709**
Regional Offices in Chicago, Illinois • Cleveland, Ohio • Dallas, Texas • New York, New York • Richmond, Virginia

CIRCLE 6 ON READER SERVICE CARD